Process Data Rectification and Process Optimization with Uncertainty

by

Yuan Yuan

A thesis submitted in partial fulfillment of the requirements for the degree of

Doctor of Philosophy

in

Process Control

Department of Chemical and Material Engineering

University of Alberta

Abstract

Process measurements collected from daily industrial plant operations are essential for process control and optimization. However, due to various reasons, the process data are always corrupted by errors, so that process model constraints representing the mass balance and energy balance are not satisfied with measured data. If the data with errors are used in process control or optimization, the results may not be appropriate for the system, and cannot achieve the desired target, or even worse, it may be hazardous to the system and even cause damage and break-down. Random errors and gross errors are two major sources of errors, and techniques are needed to detect and eliminate the errors from the measurements to obtain clean data for further use.

Even after the processing of the data, there remain some uncertainties in the data. After passing the data to optimization problems, due to the existence of uncertainty in the data, the deterministic optimization formulation can no longer be utilized in order to avoid suboptimal or infeasible solutions. Optimization with uncertainty becomes an important topic in both research and applications.

In this thesis, a technique is first developed to detect the gross errors and reconcile the data simultaneously to remove the errors from the data. A hierarchical Bayesian algorithm is used to formulate a unified framework to detect the gross errors, estimate the magnitude of the gross errors, determine the covariance matrix of the random errors, and reconcile the data.

Among various approaches for optimization with uncertainty, chance constraint problem

is a natural way to quantify the reliability of the solutions by setting a restriction on the level of the probability that the constraints are satisfied. In the case that multiple constraints should be satisfied simultaneously, joint chance constraint is appropriate to model the uncertainties. However, joint chance constraint problem is generally intractable and a variety of methods are available to approximate it into tractable forms. Robust optimization with the distribution-free property is an approach with computational advantage. In this thesis, a novel framework is proposed to approximate the joint chance constraints using robust optimization and improve the approximation results using a two-layer algorithm to optimize two types of important variables. There are always correlations between different measurements or data. It is necessary to consider the correlations in the data uncertainty. In this thesis, the robust optimization formulation based on the uncertainty set incorporating correlations of uncertainties is studied. Furthermore, nonlinearity is commonly seen in practical process models. This thesis develops a novel robust optimization framework to consider the uncertain nonlinear optimization problems. The thesis provides practical applications as well. An economic optimization problem is investigated for steam generation and water distribution for SAGD (steam-assisted-gravity-drainage) process. The uncertainty in oil production capacity is considered and the proposed robust optimization algorithms are utilized to solve the optimization problems that contain uncertainty.

Preface

This thesis is an original work by Yuan Yuan. The materials in this thesis are part of the research project under the supervision of Dr. Biao Huang and Dr. Zukui Li, and are funded by Alberta Innovates Technology Futures (AITF) and Natural Sciences and Engineering Research Council (NSERC) of Canada.

Chapter 2 of this work has been published as Y. Yuan, S. Khatibisepehr, B. Huang, Z. Li, "Bayesian method for simultaneous gross error detection and data reconciliation", AIChE Journal (2015).

Chapter 3 has been published as Y. Yuan, Z. Li, B. Huang, "Robust optimization approximation for joint chance constrained optimization problem", Journal of Global Optimization (2017).

Chapter 4, except Section 4.5 has been published as Y. Yuan, Z. Li, B. Huang, "Robust optimization under correlated uncertainty: Formulations and computational study", Computers & Chemical Engineering (2016).

Chapter 5 has been briefly presented and published as Y. Yuan, Z. Li, and B. Huang, "Nonlinear robust optimization with uncertain equality constraints", FOCAPO/ CPC conference (2017) as a short version. And it is submitted to AIChE Journal in 2017 as Y. Yuan, Z. Li, and B. Huang, "Nonlinear robust optimization for optimal process design", which is a complete version.

For all the materials listed above, I am responsible for the theory development, numerical simulation and analysis, as well as the manuscript composition. Dr. Biao Huang and Dr.

Zukui Li are the supervisory authors and are involved with the guidance of concept formation and manuscript composition. And in Chapter 2, the publication is also completed with the help of Dr. Shima Khatibisepehr, who provides valuable advice to construct and improve the manuscript.

To my family, for their support and encouragement.

Acknowledgements

It is my great pleasure to acknowledge with sincere gratitude to those people who have assisted and accompanied with me in my doctoral journey.

First and foremost, I would like to express my sincere appreciation to Prof. Biao Huang and Prof. Zukui Li, who acted as my research supervisors and life mentors, and provided their inspiration, support and patience throughout my research and my overall professional development. I would like to thank Prof. Li for the constant discussion on my research works and showing me the big picture view of my research during the meetings we had on campus. I would like to thank Prof. Huang for giving me consistent motivation and providing me financial support and excellent opportunities for attending prestigious international conferences so that I was able to interact with external research group members. In addition, I sincerely acknowledge for the financial support provided by Prof. Huang throughout my graduate studies. I am grateful to them not only for their scholarly guidance and valuable critiques for my doctoral studies, but also for their infinite patience and continuous encouragement.

I would like to thank the Alberta Innovates Technology Futures (AITF) and National Science and Engineering Research Council (NSERC) of Canada for the financial support, and the department of Chemical and Materials Engineering at the University of Alberta for providing a pleasant environment to pursue my PhD.

I would like to thank my group of friends on Campus for making my graduate student life a wonderful experience, both personally and professionally. Also I should thank all CPC group members, especially Shima Khatibisepehr, who knowingly supported me during my studies.

Last but not the least, I would like to gratefully thank my parents who always gave me selfless and infinite courage and support to pursue my education and handle difficulties. In the end, I would like to thank my lovely companion Xiaodong Xu who has stayed beside me in every step of this difficult journey. Without his wholehearted support, I really doubt if I could even complete a chapter of this thesis.

Contents

List of Figures

List of Tables

List of Abbreviations and Notations

Abbreviations

ARO	Adjustable robust optimization.
BFW	Boiler feed water.
CSOR	Cumulative steam to oil ratio.
FGE	Final gross errors.
GA	Genetic algorithm.
GEC	Gross error candidates.
HRSG	Heat recovery steam generator.
ICC	Individual chance constraint.
IE	Interval+ellipsoidal.
IP	Interval+polyhedral.
JCC	Joint chance constraint.
LP	Linear programming.
MAP	Maximum *a posteriori*.
MAD	Median absolute deviation.
MILP	Mixed integer linear programming.
MLE	Maximum likelihood estimation.
NLP	Nonlinear programming.
OTSG	One through steam generator.

PW	Produced water.
RO	Robust optimization.
SAGD	Steam assisted gravity drainage process.
SG	Steam generator.
SOCP	Second order conic programming.
SOR	Steam-to-oil-ratio.
SVM	Support vector machine.
TDS	Total dissolved solid.
WAC	Weak Acid Cation.
WLS	Warm lime softening.
WOR	Water-to-oil-ratio.
WP	Water treatment plant.

Notations

μ	Mean.
σ	Standard deviation.
P	Probability.
R	Real number set.
$\mathcal{N}$	Normal distribution.
χ^2_d	Chi-square distribution.
$F_{\chi^2_d}$	Cumulative distribution function of χ^2_d.
$t_{1-(\alpha/2),n-p}$	Value of the Student-t distribution.
$F_{1-\alpha,n-p}$	Value of the F-distribution.
$1_{(0,+\infty)}$	Indicator function.
E	Expectation operator.
$[\cdot]^+$	Maximum operator.
$[\cdot]^T$	Transpose.
$Diag\{\cdot\}$	Diagonal.
D	Matrix of measured data.
Y^C_j	jth column of D.
Y^R_i	ith row of D.
Σ	Covariance matrix.
$\Gamma(.)$	Gamma function.
I	Indentity matrix.
U_{box}	Box type uncertainty set.
$U_{ellipsoid}$	Ellipsoidal type uncertainty set.
$U_{polyhedral}$	Polyhedral type uncertainty set.
$U_{in+poly}$	Interval+polyhedral uncertainty set.
$U_{in+ellip}$	Interval+ellipsoidal uncertainty set.
$S_{intersect}$	Intersected uncertainty set.
Δ	Uncertainty set size.
$\boldsymbol{\xi}$	Basic uncertainty.

exp	Exponential.
log	Logarithm.
det	Determinant.
$\|\cdot\|_1$	1-norm.
$\|\cdot\|_2$	2-norm.
$\|\cdot\|_\infty$	$\infty-$norm.
∇	Gradient operator.
H	Total time horizon
U_{PW}	Set of produced water tanks
U_{BFW}	Set of BFW tanks
U_{WP}	Set of water treatment plants
U_{SG}	Set of steam generators
U_{Well}	Set of well pads
$Pair$	Set of unit pairs representing connection from unit i to unit j
η_i^{WP}	Water plant efficiency, $i \in U_{WP}$
η_i^{SG}	Steam quality, $i \in U_{SG}$
Ca_i^{lo}	Lower capacity limitation of unit i
Ca_i^{up}	Upper capacity limitation of unit i
$Oil_i^{lo,t}$	Oil production lower capability of well pad i at time t
$Oil_i^{up,t}$	Oil production upper capability of well pad i at time t
SOR_i^t	Steam to oil ratio of well pad i at time t
$Water_i^t$	Water produced from well pad i at time t
WOR_i^t	Water to oil ratio of well pad i at time t
Co_i	Capital cost per Sm^3 steam generated, $i \in U_{SG}$
$F_{i,j}^t$	Flow rates from unit i to unit j at time t
M_i^t	Make-up water flow rate to unit i at time t
P_i^t	Produced water flow rate to unit i at time t
$Steam_i^t$	Steam generated by steam generator i at time t
V_i^t	Volume of tank i at time t

Oil_i^t	Oil production rate of well pad i at time t
ST_i^t	Status of steam generator i at time t
SW_i^t	Switch of steam generator i at time t

Chapter 1

Introduction

1.1 Motivation

In the process industry, a typical plant usually consists of a large number of process units such as reaction vessels, distillation columns, storage tanks, etc. These units are interconnected by a complicated network of streams. There are hundreds and even thousands of variables, such as flow rates, temperatures, pressures, levels, and compositions. Process variables are routinely measured and automatically recorded for the purpose of process control, optimization, and process monitoring. The large amount of information can be exploited from the process data, and applied in various practical fields. Figure 1.1 shows a summary of the industrial applications associated with data.

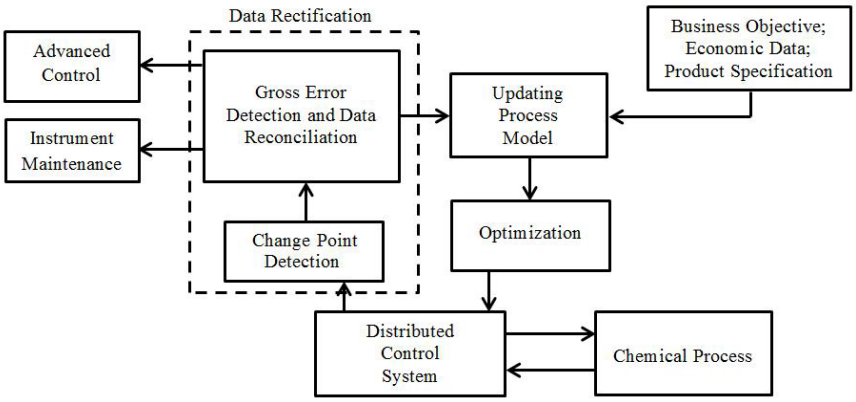

Figure 1.1: Summary of the industrial applications associated with data

However, process measurements are inevitably contaminated by errors. There are two types of errors that contribute to the total error in a measurement: random errors can be referred to as noise and they exist in any measurements; gross errors are nonrandom errors caused by malfunctioning, miscalibration, fault of sensors, etc. To obtain reliable process data, it is necessary to remove the errors from the measurements. Usually, random errors and gross errors are addressed separately by data reconciliation and gross error detection.

Data reconciliation is used to enhance the accuracy of measurements by reducing the influence of random errors. Its objective is to estimate the true value of the measurements that satisfy the process models. In general, data reconciliation is based on the assumption that there are only random errors in the measurements. The data reconciliation problem can be formulated as an optimization problem [1]. Mah[2] provided an overview of the basis of data reconciliation.

The existence of gross errors will invalidate the statistical basis of data reconciliation. Hence, gross errors must be detected and removed/compensated before data reconciliation. In practice, we are not only interested in detecting the presence of gross errors but also want to identify the locations of gross errors as well as to estimate the sizes of them. Generally, the gross error detection and data reconciliation technique are taken in separate steps, and few methods can deal with the two problems simultaneously, which motivates the work in this thesis to implement gross error detection and data reconciliation simultaneously in a unified framework. When component balance or energy balance is included in the process model, nonlinear data reconciliation problem needs to be addressed. In this thesis, both linear and nonlinear formulations are considered in the simultaneous gross error detection and data reconciliation framework.

From Figure 1.1, it can be observed that in chemical process, optimization also plays an important role. The optimization technique is widely used to achieve business objectives, for example, it can be utilized to determine how to design or operate the process to obtain more products with lower cost. In the optimization framework, the process is modeled using

equality constraints to represent the process model and inequality constraints for operation conditions and other requirements. There are a lot of parameters in the optimization model and in many optimization applications, it is assumed that the data are known and certain. However, due to the random nature of process data, measurement noise or other reasons, uncertainties are commonly observed in parameters. There are plenty of sources of the uncertainties; for instance, for a chemical process, the amount of the raw materials as well as the price may contain uncertainty depending on the availability of the suppliers. Similarly, uncertainties may arise in the demand and the price of the products according to the market. Also, uncertainties exist in the process itself. For instance, in a blending process, the concentration of the inputs may have uncertainty due to the measurement noise or the operation of the process which is not completely removed from the data rectification step. Furthermore, as shown in Figure 1.1, the models used in optimization may be obtained by learning from the process data. The estimated parameters in the model always contain uncertainty. If we ignore the uncertainties while solving the optimization problem, it may lead to solutions which are suboptimal or even infeasible for practical applications. Thus, it is of great importance to deal with the uncertainty in parameters.

Many process design problems can be formulated as nonlinear optimization problems involving system parameters. It is common to see uncertain parameters in those models due to the errors or noise in the data used for estimation of the parameters.

In this thesis, the main focuses are on both the data rectification and the optimization with uncertainty. In the first part, a unified framework is utilized for simultaneous gross error detection and data reconciliation. In the second part, the optimization problem with uncertainty for both linear and nonlinear systems are studied. The correlations in uncertainties are also considered in the formulation to incorporate more information from the available process data.

Another important target of this thesis is to consider economic optimization of water flow network in steam-assisted-gravity-drainage (SAGD) process. The proposed algorithms

are also demonstrated on the steam-assisted-gravity-drainage (SAGD) process in oil sands industry. SAGD is an important technique to extract the oil buried deep underground. Steam is used in SAGD to heat the bitumen and then the oil can be extracted out in a mixture with water from the production well. The strategy of steam generation and water distribution should be optimally determined to avoid waste and high production cost.

1.2 Literature Review

1.2.1 Data Rectification

In this thesis, gross error detection and data reconciliation are implemented simultaneously. However, in the literature, most of the methods treated the two problems separately.

Several statistical tests have been utilized for gross error detection by linear model under steady state, such as global test [3], measurement test [4, 5], nodal test [3, 6], generalized likelihood ratios [7], Bonferroni tests [8], and principle component tests [9], etc.

In practice, identifying the locations of gross errors as well as estimating the sizes of them is also an important task. These targets can be fulfilled by different strategies combined with statistical tests. Serial elimination strategy [10, 11, 12] detects each measurement one by one, recomputes the statistical tests and then finally eliminates the gross error candidates. Serial compensation strategy [7] can be used to estimate the sizes of gross errors. In this strategy, gross errors are estimated and the measurements are compensated in turn. It is applicable to all kinds of gross errors but its results rely on the accuracy of estimated size of gross errors [8]. Collective compensation strategy [8, 13, 14] has also been proposed to estimate all gross errors simultaneously. This method is more accurate than others [14, 15]. However, it is computationally expensive.

Some researchers have proposed methods to combine the gross error detection and data reconciliation and address them simultaneously [16, 17]. The objective is to remove the random errors as well as the gross errors and to obtain clean data.

When nonlinearity exists in the gross error detection and data reconciliation framework, the usual procedure is to first perform a linearization of the process model. Sequential quadratic programming technique solves a nonlinear optimization problem by successively solving a series of quadratic programming problems [18, 19, 20]. Tjoa and Biegler used a new distribution function considering both contributions from random errors and gross errors and proposed a hybrid sequential quadratic programming method to solve the nonlinear gross error detection and data reconciliation problem simultaneously [16].

1.2.2 Optimization with Uncertainty

In this thesis, optimization with uncertainty is also considered and a critical issue in the problem is how to quantify or model the uncertainty in the optimization problems. Various approaches have been proposed in the past to address uncertainty in optimization problems, such as robust optimization, stochastic programming with recourse, and chance constraints.

A natural way to quantify the solution reliability under parameter uncertainty is to place a restriction on the probability of constraint satisfaction. Such a constraint is known as chance/probabilistic constraint [21]. According to the number of constraints on which we enforce for constraint satisfaction, the chance constraint can be classified as individual chance constraint (ICC) and joint chance constraint (JCC). General challenges of chance constrained problem include the difficulty in checking the feasibility of the probabilistic constraint and the non-convexity of the feasible region determined by the distributions. There are merely a few cases that a deterministic equivalent model can be obtained. Specially, for multivariate normal distribution, individual chance constrained problem can be formulated as a second-order cone optimization problem, which is computationally tractable [22]. Furthermore, if the random parameters follow uniform distributions over a convex symmetric set, the individual chance-constrained problem is convex and tractable as shown by Lagoa [23]. In addition, Calafiore and El Ghaoui [24] presented that the individual chance constrained problem can be converted to a second-order cone optimization problem under the condition that the

random parameters follow radial distributions. However, chance constrained problems are computationally intractable under general distributions [25][26].

It is even more complicated to handle the joint chance constrained optimization problem because it enforces that several constraints are satisfied simultaneously under parameter uncertainty and it models the uncertainty correlation in different constraints. Prekopa [27] showed that a joint chance constrained problem is convex only when the distributions are log-concave. Due to the intractability of joint chance constrained problem, it is generally solved through approximations. There are mainly two ways to approximate the chance constrained problem: sampling based approach and analytical approximation approach.

Sampling approximations are based on the assumption that it is possible to draw observations from the given distribution of the uncertain parameters. These observations are then used to approximate the probability of constraint satisfaction or violation. Important contributions in the area of sampling based approximation methods have been made by Calafiore and Campi [24], Leudtke [28], Nemirovski and Shapiro [29] and Pagnoncelli et al. [30]. Sampling based approximation methods include scenario approximation and sample average approximation. The main idea of scenario approximation is to generate a set of samples of the random parameters and approximate the chance constraint with a set of constraints corresponding to each sample. However, the approximation itself is random and it may be infeasible or the solution may not satisfy the chance constraint. Sample average approximation generalizes the scenario approximation and only requires that constraints are satisfied under part of the samples. Such kind of approximation method can be found in Luedtke [31], Ahmed et al. [32], and Pagnoncelli et al. [30]. However, sampling based approximation methods requires the size of the samples to be large enough to ensure the quality of the approximation. It may take more computational efforts to solve the resulting problems with a large sample size and the effectiveness of the sampling based approximation is limited.

Other than the sampling based approximation, analytical approximation methods try to

approximate the chance constrained problem with a deterministic optimization formulation. There are various ways to achieve the approximation. For example, probabilistic inequalities (e.g., Chebyshev [33], Bernstein [34] and Hoeffding [35]) were applied to provide deterministic approximation to the individual chance constraint. In addition, Nemirovski and Shapiro [29] and Hong et al. [36] studied convex approximations of chance constraint. Among all the analytical approximation methods, robust optimization has received an increasing attention recently. The advantage of the robust optimization approximation is that it is a distribution-free approach and the data uncertainties are described using uncertainty sets.

Besides the chance constraints, robust optimization is also a method to deal with optimization problem with uncertainty. Robust optimization addresses the parameter uncertainty based on an uncertainty set which covers part or the whole region of the uncertainty space. The target of robust optimization is to select the best solution that remains feasible for any realizations of the uncertain parameters in the uncertainty set. Compared to other methods for addressing uncertainty in optimization problems, one of the significant advantages of robust optimization is the computational tractability. The robust counterpart generally does not increase much in model size compared to the deterministic model, and the convexity of the constraint can also be preserved.

The uncertainty set induced robust optimization framework has been investigated by many studies in past decades and it has been applied to various decision making problems. One of the earliest work by Soyster [37] studying robust optimization considered simple perturbations in the data and reformulated the original linear programming problem so that the solution would be feasible under all possible perturbations. However, the approach is very conservative since it ensures feasibility for all potential realizations of the uncertainty. Robust optimization received more attention since the 1990s. El-Ghaoui and Lebret [38] studied least-squares problems with uncertainty. El-Ghaoui et al. [39] investigated uncertain semidefinite problems with robust optimization framework. A number of valuable formulations and applications in linear programming and general convex programming have

been proposed by [40], [41], [42] and [43]. Ben-Tal and Nemirovski [40][41] pointed out that robust formulation becomes a conic quadratic problem for a linear constraint with ellipsoidal uncertainty set. Ben-Tal et al. [44] proposed an approach for linear programming problems where some of the decision variables must be determined before the realization of uncertain data, while the other decision variables can be set after realization. Bertsimas and Sim [45] derived a robust formulation for uncertain linear programming problems using budget parameter which can control the degree of conservatism of the solution. Bertsimas et al. [46] studied the robust counterpart of linear programming problems based on the uncertainty set defined by a general norm. By generalizing the symmetric uncertainty sets, Chen et al. [47] investigated asymmetrical set induced robust optimization.

Li et al. [48] conducted an extensive study on different types of uncertainty set and studied the robust counterpart optimization techniques for linear optimization and mixed integer linear optimization problems. Chen et al. [49] [50] developed different tractable approximations to individual chance constrained problems via robust optimization and extended the idea to joint chance constrained problems.

Besides the above contributions made by the operations research community, robust optimization also received attention by the process systems engineering researchers. Li and Ierapetritou [51] studied the application of various robust optimization formulations to process scheduling problem under uncertainty. Lin et al. [52] and Janak et al. [53] studied robust optimization for mixed integer linear optimization problems with uncertainty under both bounded and several known probability distributions. Verderame and Floudas [54] applied the robust optimization framework to operational planning problems.

The issue of robust solution quality also received attention in several recent works. To improve the solution quality of a robust optimization problem, the main issue is to find an appropriate uncertainty set size. To be more specific, a small set size is preferred while the solution reliability is met, because it leads to less conservative solution. The traditional way of determining the set size is based on the a *priori* probability bound, which is a

function of the set size. Li et al. [55] proposed various a *priori* and a *posteriori* probability bounds. Based on that, Li and Floudas [56] proposed an iterative method to improve the robust solution quality by iteratively adjusting the set size until the probability of constraint satisfaction reaches the desired level. In another work, Li and Li [57] proposed a method to identify the smallest set size with the least conservative solution through an optimal set size identification algorithm.

Most of the robust optimization algorithms mentioned above are for linear optimization problems [41, 45, 48], second-order cone programming [38, 58], and semi-definite programming [59, 39]. On the other hand, general nonlinear robust optimization has received less attention in the past. In the literature, a linearization of the uncertainty set was employed to approximate robust formulation [60]. A general robust optimization method has been studied based on linearization around nominal value of the uncertain parameter [61]. However, both of the papers used linearization around a single point, so the methods are only effective for the optimization problem under uncertainty with small perturbation. A sequential convex bilevel programming algorithm was proposed to numerically solve the min-max problems in the robust optimization framework [62], but this method can only deal with the inequality constrained nonlinear optimization problem. Recently, robust counterparts of nonlinear uncertain inequalities have been derived based on convex analysis including support function, conjugate functions, Fenchel duality and conic duality, and in this paper, both simple and complex types of uncertainty set have been studied[63].

1.3 Thesis Outline

After reviewing background on previous developed algorithms for gross error detection and data reconciliation as well as optimization with uncertainty, the remainder of this thesis is organized as follows:

In Chapter 2, gross error detection and data reconciliation are implemented simultaneously in a unified framework using the hierarchical Bayesian inference technique. The

framework fulfilled multiple targets: First, it detects which measurements contain gross errors, i.e., it can locate the gross errors. Second, the magnitudes of the gross errors are estimated. Third, the covariance matrix of the random errors is also determined. Finally, data reconciliation is performed using the maximum *a posteriori* estimation. Chapter 2 considers the linear and nonlinear systems working at steady state. Serial identification technique is modified to combine with the proposed hierarchical Bayesian framework to improve the gross error detection results. The conditional probability ratio of a measurement containing gross error and not containing gross error is compared to identify a list of suspect gross error candidates. Numerical examples representing both linear and nonlinear cases are provided to demonstrate the effectiveness of the proposed approach.

In Chapter 3, joint chance constraint problem is studied and approximated by robust optimization. First, the joint chance constraint is divided into individual chance constraint using the maximization operator. Second, the individual chance constraints are approximated by the robust optimization formulation through a series of probability inequalities. Finally, different robust optimization formulations are derived based on box, ellipsoid, polyhedral, interval+polyhedral and interval+ellipsoid types of uncertainty set. A two-layer optimization algorithm is proposed to further improve the solution. In the inner layer, the set size of the uncertainty set is optimized to meet the probability of constraints satisfaction and in the outer layer, the variable that controls the upper bound of the approximation is optimized to improve the objective value. The proposed formulation and algorithm are tested using multiple examples.

In Chapter 4, correlations in uncertainties are taken into consideration. The information contained in the correlation is incorporated into the design of the uncertainty set with different types. Robust optimization formulations are derived based on the different types of uncertainty set with correlation information. In the numerical examples, different levels of the correlations are considered and the corresponding results are compared to verify the necessity of considering uncertainty correlations into the traditional robust optimiza-

tion method. Other than the numerical examples, a production planning example is used to test the proposed formulations. A brief study for the correlated uncertainty in multiple constraints is taken in Section 4.5. Two types of uncertainty set named "constraint-wise" and "global" according to the uncertainty set construction idea are compared in the aspect of objective values. Different correlation structures are considered in the comparison, and the conclusion obtained from the robust optimization formulation is tested using numerical examples.

In Chapter 5, a novel nonlinear robust optimization framework is proposed to address general nonlinear problems with uncertain parameters. The proposed method is based on piecewise linearization with respect to the uncertain parameters around multiple realizations of the uncertainty. The points used for piecewise linearization are selected using an iterative algorithm. Three cases of problems are considered. In the first case, the uncertainty only exists in inequality constraints. In the second case, design variables and state variables are coupled by equality constraints, and both inequality and equality constraints contain uncertain parameters. In the third case, some of the variables called control variables can be adjusted after the realizations of the uncertainties are available. The proposed algorithm is applied to different optimal design problems representing the three cases.

In Chapter 6, the economic optimization of steam generation and water distribution is studied for the SAGD process operation under steady state. A long term planning problem is studied for distribution of steam to well pads which start working at different years. First, the deterministic formulation is solved and then, the uncertainty in oil production rate capacity is considered and modeled by JCC. The proposed robust optimization framework in Chapter 3 is used to approximate JCC and the two-layer algorithm is implemented to improve the approximation results.

Chapter 7 concludes the thesis and presents the future works. Some theoretical and practical improvements which can be further considered in further studies are introduced.

1.4 Main Contributions

The main contributions in this thesis can be summarized as follows:

1. Developing a unified framework for gross error detection and data reconciliation and estimating the magnitudes of the gross errors and the covariance matrix of the random errors.

2. Providing a robust optimization framework to approximate the joint chance constraints problem and further improving the approximation results by a proposed two-layer algorithm.

3. Considering correlations in uncertainties and incorporating the correlation information into the definition of the uncertainty set for the robust optimization derivation.

4. Addressing the general nonlinear uncertain optimization problem using robust optimization and "piecewise" linearization technique and applying the algorithm into optimal design problems.

5. Applying the proposed algorithms into economic optimization of steam generation and water distribution for SAGD process.

Chapter 2

Bayesian Method for Simultaneous Gross Error Detection and Data Reconciliation

2.1 Introduction

Process measurements collected from daily industrial plant operations are essential for process control and optimization. However, those measurements are generally corrupted by errors, and the measured data cannot satisfy the mass balance and energy balance which represent the process model. If the data with errors are used in process control or optimization, the results may not be appropriate for the system and the final target cannot be reached, or even worse, it may be hazardous to the system and cause damage and breakdown. Thus, it is of great importance to process the data and reduce or eliminate the errors in the data. Random errors and gross errors are two major types of errors existing in the measured data. Neither the magnitude nor the sign of the random errors can be predicted or known with certainty and the only possible way to characterize them is to use probability distributions. Random errors can also be regarded as noise in the measurements. Data reconciliation is a powerful way to reduce or remove the random errors in the data. However,

data reconciliation is effective based on the assumption that the gross errors are already removed from the data. Gross errors are caused by nonrandom events, which implies that at any given time they have certain magnitude and sign. Gross error detection is a companion technique to data reconciliation which has been developed to identify and eliminate gross errors in process data.

Generally, gross error detection and data reconciliation are implemented in different steps, i.e., gross error detection technique is taken in the first place followed by data reconciliation. This chapter is devoted to the issue of combining gross error detection and identification problem with data reconciliation problem within a hierarchical Bayesian framework to detect and eliminate the gross errors and reconcile the data simultaneously. Hierarchical Bayesian framework has been applied to various problems. For instance, MacKay[64] first proposed the heuristic Bayesian evidence framework and this framework was applied to neural network modeling by MacKay[65]. The hierarchical Bayesian procedure was used to address the image modeling and restoration problem by Molina et al.[66] and Galatsanos et al. [67]. Kwok [68] and Suykens et al. [69] derived the probabilistic formulation of the least squares support vector machine (SVM) within a hierarchical Bayesian evidence framework. The hierarchical Bayesian framework was utilized for process identification with outliers in the data-set by Khatibisepehr and Huang[70].

The final goal of gross error detection and data reconciliation is to obtain the clean data which satisfy the process model, e.g., mass balance and energy balance. Generally, mass balances have simple linear form, while if energy balances are also involved in the problem, nonlinearity will be introduced. This chapter focuses on the system working at steady state which can be both linear and nonlinear. New strategies based on hierarchical Bayesian combining with serial identification and collective estimation of gross errors are proposed. Instead of using statistical tests method, (e.g., Sáchez et al. [14], Jiang and Bagajewicz [71]), the proposed approach compares the conditional probability ratio of containing gross error and not containing gross error, so as to identify a list of suspect gross error candidates. The

proposed algorithm performs gross error detection and data reconciliation simultaneously, and also estimates the magnitudes of the gross errors. Furthermore, the proposed approach does not assume that the covariance matrix of random errors is known. Instead, the proposed approach estimates the covariance matrix.

The rest of the chapter is organized as follows. Section 2.2 provides the problem statement. Then, in Section 2.3, the simultaneous gross error detection and data reconciliation problem is formulated in a hierarchical Bayesian framework, where different variables are estimated in different layers. In Section 2.4, the gross error exact detectability issue will be discussed and a serial strategy is adopted for gross error identification to improve the results. Numerical examples are provided to demonstrate the effectiveness of the proposed approach for both linear and nonlinear cases in Section 2.5, which is followed by conclusion in the final section.

2.2 Problem Statement

The objective of simultaneous gross error detection and data reconciliation can be stated as follows. First, detect which measurements contain gross errors; second, estimate the magnitudes of gross errors as well as the covariance matrix of the random errors; finally, apply data reconciliation to estimate the correct value of the data.

In this chapter, the system under consideration is assumed to be time invariant and operating under steady state. According to mass balance or energy balance the system model can be expressed as

$$f(x, u) = 0$$

where x is an $n \times 1$ vector of true values of measured variables, n is the number of measured variables, and u is a vector of unmeasured variables.

In the real process, the process data are automatically sampled and recorded at regular time intervals. It is assumed that a gross error persists in a measurement (if it exists) during

a measurement period consisting of m sampling points. According to the above assumptions, the measurement data is organized as follows

$$D = \begin{pmatrix} y_{11} & y_{12} & \cdots & y_{1m} \\ y_{21} & y_{22} & \cdots & y_{2m} \\ \cdots & \cdots & \cdots & \cdots \\ y_{n1} & y_{n2} & \cdots & y_{nm} \end{pmatrix} = \begin{pmatrix} {Y_1}^C & {Y_2}^C & \cdots & {Y_m}^C \end{pmatrix} = \begin{pmatrix} Y_1^R \\ Y_2^R \\ \cdots \\ Y_n^R \end{pmatrix}$$

where Y_j^C, $j = 1, ..., m$, is the data at each sampling point and Y_i^R, $i = 1, ..., n$, is the data for each variable. The data are assumed to be mutually independent.

At each sampling point, the measurement model can be described as

$$Y_j^C = x + \eta\delta + \varepsilon, \qquad j = 1, ..., m$$

where η is an $n \times n$ matrix which indicates whether there is a gross error in the measurement or not (0 means no gross error and 1 means gross error), δ is an $n \times 1$ vector which denotes the magnitudes of the biases, ε is the random error vector which follows a multivariate normal distribution, i.e., $\varepsilon \sim \mathcal{N}(0, \Sigma)$, and Σ is the $n \times n$ covariance matrix. Notice that η is constructed as a diagonal matrix with the elements on the diagonal to be the gross error indicators for each measurements:

$$\eta = \begin{pmatrix} \eta_1 & 0 & ... & 0 \\ 0 & \eta_2 & ... & 0 \\ ... & ... & ... & ... \\ 0 & 0 & ... & \eta_n \end{pmatrix}$$

Since the measurements are obtained from different instruments it can be assumed that

the measurement noise is mutually independent. Then Σ is a diagonal matrix:

$$\Sigma = \begin{pmatrix} \sigma_{11}^2 & 0 & ... & 0 \\ 0 & \sigma_{22}^2 & ... & 0 \\ ... & ... & ... & ... \\ 0 & 0 & ... & \sigma_{nn}^2 \end{pmatrix}$$

For the purpose of simplification, the precision is introduced as $\alpha_i = \sigma_{ii}^{-2}$.

It is known that finding estimates of parameters using maximum likelihood estimation (MLE) may lead to an ill-posed problem since the estimation can be underdetermined and is also sensitive to the noise in the data[64]. A useful way to avoid that is to combine the information from the data with some additional knowledge concerning the distribution of the parameters called prior distribution. In this chapter, the priors for the magnitudes of biases δ and the correct values of measurements x are considered. Specifically, a uniform distribution is introduced as the prior distribution of δ. A normal distribution is introduced as the prior distribution of x, i.e., $x \sim \mathcal{N}(\mu_0, \Sigma_0)$, where hyperparameter μ_0 is a $n \times 1$ vector and Σ_0 is the covariance matrix. If any hyperparameter of those prior distributions is not known *a priori*, its value can be estimated by an intermediate step of the whole process. For instance, the hyperparameters μ_0 and Σ_0 are not known a *priori* in this chapter. The estimation of x in the current iteration is taken as the estimation of μ_0 in the next step and Σ_0 is estimated by maximizing the posterior distribution over it. In this chapter, it is assumed that the correct values of x are independent and Σ_0 is a diagonal matrix:

$$\Sigma_0 = \begin{pmatrix} \sigma_{11,0}^2 & 0 & ... & 0 \\ 0 & \sigma_{22,0}^2 & ... & 0 \\ ... & ... & ... & ... \\ 0 & 0 & ... & \sigma_{nn,0}^2 \end{pmatrix}$$

and the precision for $\sigma_{ii,0}$ is introduced as $\alpha_{i0} = \sigma_{ii,0}^{-2}$.

2.3 Proposed Hierarchical Bayesian Framework

In the simultaneous gross error detection and data reconciliation problem, five different parameters (x, δ, η, Σ, Σ_0) are considered. In the proposed Bayesian framework, maximum *a posteriori* (MAP) is used to estimate the parameters. To obtain MAP estimates for the five parameters simultaneously, the joint probability density function $P(x, \delta, \Sigma, \Sigma_0, \eta|D)$ should be maximized. However, maximizing such a posterior probability density functions is complex. The corresponding optimization problem is difficult to solve directly. To avoid the difficulties in direct maximization of $P(x, \delta, \Sigma, \Sigma_0, \eta|D)$, a layered solution framework is proposed. Based on the chain rule, the joint probability density function is factorized into three parts

$$P(x, \delta, \Sigma, \Sigma_0, \eta|D) = P(x, \delta|\Sigma, \Sigma_0, \eta, D)P(\Sigma, \Sigma_0|\eta, D)P(\eta|D)$$

The proposed method includes three levels according to the above factorization. The correct values of the measurements x and the magnitudes of gross errors δ are estimated at Level 1. The covariance matrix Σ of the random error and the hyperparamter Σ_0 are estimated at Level 2 and the gross error indicator matrix η is addressed at Level 3. The overall procedure of the Bayesian algorithm is summarized as follows:

Level 1: Inference of x and δ

$$\max_{x,\delta} P(x, \delta|\Sigma, \Sigma_0, \eta, D) = \max_{x,\delta} \frac{P(D|x, \delta, \Sigma, \Sigma_0, \eta)P(x, \delta|\Sigma, \Sigma_0, \eta)}{P(D|\Sigma, \Sigma_0, \eta)}$$

Level 2: Inference of Σ and Σ_0

$$\max_{\Sigma,\Sigma_0} P(\Sigma, \Sigma_0|\eta, D) = \max_{\Sigma,\Sigma_0} \frac{P(D|\Sigma, \Sigma_0, \eta)P(\Sigma, \Sigma_0|\eta)}{P(D|\eta)}$$

Level 3: Inference of η

$$\max_{\eta} P(\eta_i|D) = \max_{\eta} \frac{P(D|\eta)P(\eta)}{P(D)} = \max_{\eta} P(D|\eta)P(\eta)$$

Each level of the above Bayesian framework has the following form

$$Posterior = \frac{Likelihood}{Evidence} \times Prior$$

It is easy to see that the likelihood at a certain level is equal to the evidence at the previous level. In this way, the three levels are connected to each other. The procedure is iterated until convergence.

2.3.1 First Layer: Inference of x and δ

Given the collected data D, the hyperparameters Σ and Σ_0, and the matrix of gross error indicators η, the MAP estimates of the correct values of measurements x and the magnitudes of the biases δ are obtained by maximizing the posterior density function $P(x, \delta|\Sigma, \Sigma_0, \eta, D)$. Using Bayes rule, the formulation in the first layer of the hierarchical framework is:

$$P(x, \delta|\Sigma, \Sigma_0, \eta, D) = \frac{P(D|x, \delta, \Sigma, \Sigma_0, \eta)P(x, \delta|\Sigma, \Sigma_0, \eta)}{P(D|\Sigma, \Sigma_0, \eta)} \tag{2.1}$$

As stated in the above section, the following prior distributions for x and δ are slected: a normal distribution is introduced for x and a uniform distribution is set for δ. It is also assumed that x and δ are independent. For the correct value of x, it can be considered to be independent of Σ and η, and dependent on its hyperparameter Σ_0. The magnitudes δ of the gross errors can be considered to be independent of Σ, η and Σ_0.

$$\begin{aligned} &P(x, \delta|\Sigma, \Sigma_0, \eta) = P(x|\Sigma_0)P(\delta) \\ &= (2\pi)^{-n/2}|\Sigma_0|^{-1/2} \exp\{-\tfrac{1}{2}(x - \mu_0)^T {\Sigma_0}^{-1}(x - \mu_0)\} \end{aligned} \tag{2.2}$$

Given x and δ, the sampled data D would be independent of hyperparameter Σ_0, and the likelihood can be directly obtained from the measurement model, i.e. $P(D|x, \delta, \Sigma, \Sigma_0, \eta) =$

$P(D|x,\delta,\Sigma,\eta)$

$$
\begin{aligned}
&P(D|x,\delta,\Sigma,\Sigma_0,\eta) = P(D|x,\delta,\Sigma,\eta) = \prod_{j=1}^{m} P(Y_j^C|x,\delta,\Sigma,\eta) \\
&= (2\pi)^{-mn/2}|\Sigma|^{-m/2} \exp\left\{ -\tfrac{1}{2} \sum_{j=1}^{m} (Y_j^C - x - \eta\delta)^T \Sigma^{-1} (Y_j^C - x - \eta\delta) \right\}
\end{aligned} \tag{2.3}
$$

The posterior probability of x and δ can be calculated by combining Equations (2.2) and (2.3):

$$
\begin{aligned}
&P(x,\delta|\Sigma,\Sigma_0,\eta,D) \propto P(D|x,\delta,\Sigma,\Sigma_0,\eta) P(x,\delta|\Sigma,\Sigma_0,\eta) \\
&= (2\pi)^{-(m+1)n/2}|\Sigma|^{-m/2}|\Sigma_0|^{-1/2} \\
&\times \exp\left\{ -\tfrac{1}{2} \left[\sum_{j=1}^{m} (Y_j^C - x - \eta\delta)^T \Sigma^{-1} (Y_j^C - x - \eta\delta) + (x-\mu_0)^T \Sigma_0^{-1} (x-\mu_0) \right] \right\} \\
&\propto \exp\{-J_1(x,\delta)\}
\end{aligned} \tag{2.4}
$$

where

$$
J_1(x,\delta) = \frac{1}{2} \sum_{j=1}^{m} (Y_j^C - x - \eta\delta)^T \Sigma^{-1} (Y_j^C - x - \eta\delta) + (x-\mu_0)^T {\Sigma_0}^{-1} (x-\mu_0) \tag{2.5}
$$

All positive constants in Equation (2.4) are neglected, since they do not affect the optimal solution of MAP problem. To estimate the most probable values of x and δ, denoted as x^{MP} and δ^{MP}, the posterior probability should be maximized, or equivalently, the negative logarithm of Equation (2.4) should be minimized:

$$
\max_{x,\delta} P(x,\delta|\Sigma,\Sigma_0,\eta,D) = \min_{x,\delta} J_1(x,\delta) \tag{2.6}
$$

Since the correct value of the measurement x must satisfy the material or/and energy balances, constraints $f(x,u) = 0$ are added to this optimization problem. Then the opti-

mization problem for estimating x and δ becomes:

$$\begin{aligned} \min_{x,\delta} \quad & J_1(x,\delta) \\ s.t. \quad & f(x,u) = 0 \end{aligned} \tag{2.7}$$

2.3.1.1 Linear Case

Assume the system model with only measured variables is represented as $A_x x = 0$ (matrix A_x is obtained by decomposing the measured and unmeasured parts). Lagrange multipliers can be introduced to the above optimization problem. The observable unmeasured variables can be calculated through the system model after the gross error detection and the redundant measured variables are reconciled.

$$L = J_1(x,\delta) + \lambda^T A_x x \tag{2.8}$$

Based on the following optimality condition:

$$\frac{\partial L}{\partial x} = (x-\mu_0)^T {\Sigma_0}^{-1} - \sum_{j=1}^{m} (Y_j - x - \eta\delta)^T \Sigma^{-1} + \lambda^T A_x = 0 \tag{2.9}$$

$$\frac{\partial L}{\partial \delta} = -\sum_{j=1}^{m} (Y_j - x - \eta\delta)^T \Sigma^{-1} = 0 \tag{2.10}$$

$$\frac{\partial L}{\partial \lambda} = A_x x = 0 \tag{2.11}$$

The analytical expression for the estimations, x^{MP} and δ^{MP}, can be derived:

$$x^{MP} = (I - mR(I-W)\Sigma^{-1}\eta)^{-1} R(I-W)({\Sigma_0}^{-1}\mu_0 + \Sigma^{-1}\sum_{j=1}^{m} Y_j^C - \Sigma^{-1}\eta\sum_{j=1}^{m} Y_j^C) \tag{2.12}$$

$$\delta^{MP} = \eta(\frac{1}{m}\sum_{j=1}^{m} Y_j^C - x) \tag{2.13}$$

where $R = ({\Sigma_0}^{-1} + m\Sigma^{-1})^{-1}$ and $W = A_x^T[A_x R A_x^T]^{-1} A_x R$.

2.3.1.2 Nonlinear Case

If component balance and energy balance are considered, nonliear model can be obtained. If analytical solutions for the optimization problem in Equation (2.7) cannot be derived, numerical methods can be used to solve the nonlinear optimization problem to get solution for x^{MP} and δ^{MP}. The unmeasured variables can be calculated through the system model $f(x, u) = 0$ with the values of x^{MP}.

2.3.2 Second Layer: Inference of Hyperparameters Σ and Σ_0

Hyperparameters Σ and Σ_0 can be estimated in the second layer. The posterior distribution of the hyperparameters is expressed as

$$P(\Sigma, \Sigma_0|\eta, D) = \frac{P(D|\Sigma, \Sigma_0, \eta)P(\Sigma, \Sigma_0|\eta)}{P(D|\eta)} \tag{2.14}$$

Based on the assumption that the measurements are independent of each other, the likelihood can be separated and the posterior distribution corresponding to each measurement can be written as

$$P(\sigma_{ii}^2, \sigma_{ii,0}^2|\eta_i, Y_i^R) = \frac{P(Y_i^R|\sigma_{ii}^2, \sigma_{ii,0}^2, \eta_i)P(\sigma_{ii}^2, \sigma_{ii,0}^2|\eta_i)}{P(Y_i^R|\eta_i)} \tag{2.15}$$

For prior distributions, it is assumed that σ_{ii}^2 and $\sigma_{ii,0}^2$ are independent, so $P(\sigma_{ii}^2, \sigma_{ii,0}^2|\eta_i) = P(\sigma_{ii}^2|\eta_i) \times P(\sigma_{ii,0}^2|\eta_i)$. Using the precisions defined for σ_{ii}^2 and $\sigma_{ii,0}^2$, it can be written that $P(\sigma_{ii}^2, \sigma_{ii,0}^2|\eta_i) = P(\alpha_i, \alpha_{i0}|\eta_i) = P(\alpha_i|\eta_i)P(\alpha_{i0}|\eta_i)$. If there is no a *priori* information for the hyperparameters, a uniform distribution can be used to describe appropriate non-informative priors. To incorporate the prior knowledge, conjugate priors are commonly assigned so that the resulting posterior distribution can be conveniently evaluated and an analytical solution

can be obtained. In this layer, gamma distributions are considered as hyperpriors:

$$P(\alpha_i|\eta_i) = \frac{{s_i}^{k_i}{\alpha_i}^{k_i-1}}{\Gamma(k_i)}\exp(-s_i\alpha_i) \propto {\alpha_i}^{k_i-1}\exp(-s_i\alpha_i) \tag{2.16}$$

$$P(\alpha_{i0}|\eta_i) = \frac{{s_{i0}}^{k_{i0}}{\alpha_{i0}}^{k_{i0}-1}}{\Gamma(k_{i0})}\exp(-s_{i0}\alpha_{i0}) \propto {\alpha_{i0}}^{k_{i0}-1}\exp(-s_{i0}\alpha_{i0}) \tag{2.17}$$

$$P(\alpha_i, \alpha_{i0}|\eta_i) = P(\alpha_i|\eta_i)P(\alpha_{i0}|\eta_i) \propto {\alpha_i}^{k_i-1}\exp(-s_i\alpha_i){\alpha_{i0}}^{k_{i0}-1}\exp(-s_{i0}\alpha_{i0}) \tag{2.18}$$

where k_j is the shape parameter and s_j is the inverse scale parameter. Both parameters are positive real numbers. The reason that gamma distribution is selected as hyperpriors is that the gamma distribution is the conjugate prior to the likelihood.

The likelihood $P(Y_i^R|\sigma_{ii}^2, \sigma_{ii,0}^2, \eta_i)$ is actually the evidence separated according to each measurement in the first layer in Equation (2.1). To get the expression of the evidence in the first layer, the joint probability (which is the product of likelihood and priors in the first layer) can be integrated over the unknown parameters x and δ. According to whether there is a gross error or not, the problem can be addressed in two different cases:

$$\begin{aligned} &P(Y_i^R|\alpha_i, \alpha_{i0}, \eta_i) = P(Y_i^R|\sigma_{ii}^2, \sigma_{ii,0}^2, \eta_i) \\ &= \begin{cases} (2\pi)^{(-m+1)/2}(\alpha_i)^{(m-1)/2}m^{-1/2}\exp\left\{-\frac{\alpha_i}{2}\left(\sum_{j=1}^{m}y_{ij}^2 - \frac{1}{m}\left(\sum_{j=1}^{m}y_{ij}\right)^2\right)\right\}, \\ \text{if } \eta_i = 1 \\ (2\pi)^{-m/2}(\alpha_i)^{m/2}\alpha_{i0}^{1/2}(\alpha_{i0}+m\alpha_i)^{-1/2}\exp\left\{\left(\frac{\mu_{i0}^2\alpha_{i0}}{-2} + \frac{\alpha_i\sum_{j=1}^{m}y_{ij}^2}{-2}\right) - \frac{\left(\mu_{i0}\alpha_{i0}+\alpha_i\sum_{j=1}^{m}y_{ij}\right)^2}{-2(\alpha_{i0}+m\alpha_i)}\right\}, \\ \text{if } \eta_i = 0 \end{cases} \end{aligned} \tag{2.19}$$

Substituting Equation (2.18) and Equation (2.19) into Equation (2.15), the posterior

probability of the hyperparameters can be written as

$$
\begin{aligned}
&P(\alpha_i, \alpha_{i0}|\eta_i, Y_i^R) = P(\sigma_{ii}^2, \sigma_{ii,0}^2|\eta_i, Y_i^R) \propto P(Y_i^R|\sigma_{ii}^2, \sigma_{ii,0}^2, \eta_i) P(\sigma_{ii}^2, \sigma_{ii,0}^2|\eta_i) \\
&= \begin{cases}
{\alpha_i}^{(m-1)/2} \exp\left\{ \frac{\sum_{j=1}^{m} y_{ij}^2 - \frac{1}{m}\left(\sum_{j=1}^{m} y_{ij}\right)^2}{-2} \alpha_i \right\} {\alpha_i}^{k_i - 1} \exp(-s_i \alpha_i) {\alpha_{i0}}^{k_{i0}-1} \exp(-s_{i0}\alpha_{i0}), \\
\text{if } \eta_i = 1 \\
{\alpha_i}^{m/2} {\alpha_{i0}}^{1/2} (\alpha_{i0} + m\alpha_i)^{-1/2} \exp\left\{ -\frac{1}{2} \left(\mu_{i0}^2 \alpha_{i0} + \alpha_i \sum_{j=1}^{m} y_{ij}^2 - \frac{\left(\mu_{i0}\alpha_{i0} + \alpha_i \sum_{j=1}^{m} y_{ij}\right)^2}{\alpha_{i0} + m\alpha_i} \right) \right\} \\
\times {\alpha_i}^{k_i - 1} \exp(-s_i \alpha_i) {\alpha_{i0}}^{k_{i0}-1} \exp(-s_{i0}\alpha_{i0}), \text{ if } \eta_i = 0
\end{cases}
\end{aligned} \tag{2.20}
$$

In order to find the posterior mode, the above posterior distribution can be maximized, or equivalently, the negative logarithm of the posterior probability can be minimized. It leads to the following optimization problem:

$$
\max_{\alpha_i, \alpha_{i0}} P(\alpha_i, \alpha_{i0}|\eta_i, Y_i^R) = \min_{\alpha_i, \alpha_{i0}} J_2(\alpha_i, \alpha_{i0}) \tag{2.21}
$$

where

$$
\begin{aligned}
&J_2(\alpha_i, \alpha_{i0}) \\
&= \begin{cases}
-\frac{m-1}{2} \log \alpha_i + \frac{\sum_{j=1}^{m} y_{ij}^2 - \frac{1}{m}\left(\sum_{j=1}^{m} y_{ij}\right)^2}{2} \alpha_i - (k_i - 1)\log \alpha_i + s_i \alpha_i - (k_{i0} - 1)\log \alpha_{i0} + s_{i0}\alpha_{i0}, \\
\text{if } \eta_i = 1 \\
-\frac{m}{2}\log \alpha_i - \frac{1}{2}\log \alpha_{i0} + \frac{1}{2}\log(\alpha_{i0} + m\alpha_i) + \frac{1}{2}\left(\mu_{i0}^2 \alpha_{i0} + \alpha_i \sum_{j=1}^{m} y_{ij}^2 - \frac{\left(\mu_{i0}\alpha_{i0} + \alpha_i \sum_{j=1}^{m} y_{ij}\right)^2}{\alpha_{i0} + m\alpha_i} \right) \\
-(k_i - 1)\log \alpha_i + s_i \alpha_i - (k_{i0} - 1)\log \alpha_{i0} + s_{i0}\alpha_{i0}, \text{if } \eta_i = 0
\end{cases}
\end{aligned} \tag{2.22}
$$

Since α_i and α_{i0} are positive variables, logarithm can be taken on them. The gradient of

the cost function $J_2(\alpha_i, \alpha_{i0})$ is:

$$\frac{\partial J_2(\alpha_i,\alpha_{i0})}{\partial \log \alpha_i} = \begin{cases} -\frac{m}{2} + \frac{1}{2} + \frac{1}{2}[\sum_{j=1}^{m} {y_{ij}}^2 - \frac{1}{m}(\sum_{j=1}^{m} y_{ij})^2]\alpha_i - (k_i - 1) + s_i\alpha_i & if \quad \eta_i = 1 \\ -\frac{m}{2} + \frac{m\alpha_i}{2(\alpha_{i0}+m\alpha_i)} + \frac{1}{2}\sum_{j=1}^{m} {y_{ij}}^2\alpha_i - (k_i - 1) + s_i\alpha_i & if \quad \eta_i = 0 \\ -\frac{2(\mu_{i0}\alpha_{i0}+\sum_{j=1}^{m} y_{ij}\alpha_i)(\alpha_{i0}+m\alpha_i)\sum_{j=1}^{m} y_{ij}\alpha_i - (\mu_{i0}\alpha_{i0}+\sum_{j=1}^{m} y_{ij}\alpha_i)^2 m\alpha_i}{2(\alpha_{i0}+m\alpha_i)^2} & \end{cases} \tag{2.23}$$

$$\frac{\partial J_2(\alpha_i,\alpha_{i0})}{\partial \log \alpha_{i0}} = \begin{cases} -(k_{i0} - 1) + s_{i0}\alpha_{i0} & if \quad \eta_i = 1 \\ -\frac{1}{2} + \frac{\alpha_{i0}}{2(\alpha_{i0}+m\alpha_i)} + \frac{1}{2}{\mu_{i0}}^2\alpha_{i0} - (k_{i0} - 1) + s_{i0}\alpha_{i0} & if \quad \eta_i = 0 \\ -\frac{2(\mu_{i0}\alpha_{i0}+\sum_{j=1}^{m} y_{ij}\alpha_i)(\alpha_{i0}+m\alpha_i)\mu_{i0}\alpha_{i0} - (\mu_{i0}\alpha_{i0}+\sum_{j=1}^{m} y_{ij}\alpha_i)^2\alpha_{i0}}{2(\alpha_{i0}+m\alpha_i)^2} & \end{cases} \tag{2.24}$$

Since it is difficult to get the analytical solution of α_i and α_{i0}, numerical optimization method (e.g., Newton's method, etc.) is used to find the solution of Equation (2.21). The variance σ_{ii}^2 and $\sigma_{ii,0}^2$ can be obtained by taking inverse of α_i and α_{i0}, respectively. After calculating σ_{ii}^2 and $\sigma_{ii,0}^2$ for each measurement, the covariance matrix Σ and Σ_0 can be constructed.

The posterior distribution given by Equation (2.20) is complex in general so that it cannot be directly applied in the three-layered optimization framework. An approximation of the posterior distribution is a key to simplify the calculation in the hierarchical Bayesian approach. MacKay[64] introduced a method called Laplace Approximation which can approximate posterior using a normal distribution. To approximate the posterior distribution by a normal distribution, the logarithm of the posterior distribution is approximated by its second order Taylor expansion around the most probable estimation, $\Theta^{MP} = (\log \alpha_i^{MP}, \log \alpha_{i0}^{MP})$,

and the posterior distribution can be approximated by:

$$\begin{aligned}
&\log P(\log\alpha_i, \log\alpha_{i0}|\eta_i, Y_i^R) \approx \log P(\log\alpha_i, \log\alpha_{i0}|\eta_i, Y_i^R)|_{\log\alpha_i^{MP}, \log\alpha_{i0}^{MP}} \\
&+\nabla \log P(\log\alpha_i, \log\alpha_{i0}|\eta_i, Y_i^R)|_{\log\alpha_i^{MP}, \log\alpha_{i0}^{MP}} \\
&+\tfrac{1}{2} z_i^T \nabla\nabla \log P(\log\alpha_i, \log\alpha_{i0}|\eta_i, Y_i^R)|_{\log\alpha_i^{MP}, \log\alpha_{i0}^{MP}} z_i
\end{aligned} \tag{2.25}$$

where $z_i = [\log\alpha_i - \log\alpha_i^{MP}, \log\alpha_{i0} - \log\alpha_{i0}^{MP}]^T$. Since $log\alpha_i^{MP}$ and $log\alpha_{i0}^{MP}$ correspond to a maximum of the logarithm of the posterior distribution, the second term on the right hand side of Equation (2.25) equals to zero. Using Laplace Approximation, the posterior distribution can be approximated by a normal distribution as following:

$$\begin{aligned}
&P(\log\alpha_i, \log\alpha_{i0}|\eta_i, Y_i^R) \approx P(\log\alpha_i^{MP}, \log\alpha_{i0}^{MP}|\eta_i, Y_i^R) \exp(-\tfrac{1}{2} {z_i}^T Q_i z_i) \\
&= (2\pi)^{-1/2} \sqrt{\det Q_i} \times \exp(-\tfrac{1}{2} z_i^T Q_i z_i)
\end{aligned} \tag{2.26}$$

where Q_i is the Hessian matrix of the cost function J_2 evaluated at $log\alpha_i^{MP}$ and $log\alpha_{i0}^{MP}$:

$$Q_i = -\nabla\nabla \log P(\log\alpha_i, \log\alpha_{i0}|\eta, D)|_{log{\alpha_i}^{MP}, log{\alpha_{i0}}^{MP}} \tag{2.27}$$

The Hessian matrix Q_i can be calculated as:

$$Q_i = \begin{pmatrix} Q_{i,11} & Q_{i,12} \\ Q_{i,21} & Q_{i,22} \end{pmatrix} = \begin{pmatrix} \frac{\partial^2 J_2}{\partial \log{\alpha_i}^2} & \frac{\partial^2 J_2}{\partial \log\alpha_i \partial \log\alpha_{i0}} \\ \frac{\partial^2 J_2}{\partial \log\alpha_{i0} \partial \log\alpha_i} & \frac{\partial^2 J_2}{\partial \log{\alpha_{i0}}^2} \end{pmatrix} \tag{2.28}$$

2.3.3 Third Layer: Inference of the Indicator η_i

In the above derivations, it is assumed that the gross error indicators are known. In the third layer, the objective is to identify the indicators. Applying Bayes rule and separating the posterior corresponding to each measurement, the posterior distribution is obtained as following:

$$P(\eta_i|Y_i^R) = \frac{P(Y_i^R|\eta_i)P(\eta_i)}{P(Y_i^R)} \propto P(Y_i^R|\eta_i)P(\eta_i) \tag{2.29}$$

For priors, it is assumed that each instrument has a probability p_i to contain a gross error, then the probability of η_i given p_i can be expressed as:

$$P(\eta_i|p_i) = {p_i}^{\eta_i}(1-p_i)^{1-\eta_i} \tag{2.30}$$

and the prior for p_i is set to be a Beta distribution:

$$P(p_i) = \frac{\Gamma(r_i+\beta_i)}{\Gamma(r_i)\Gamma(\beta_i)}{p_i}^{r_i-1}(1-p_i)^{\beta_i-1} \tag{2.31}$$

Then, by integrating out p_i, the prior distribution for η_i is obtained:

$$\begin{aligned} P(\eta_i) &= \int_0^1 P(\eta_i|p_i)P(p_i)dp_i \\ &= \int_0^1 \tfrac{\Gamma(r_i+\beta_i)}{\Gamma(r_i)\Gamma(\beta_i)}{p_i}^{\eta_i+r_i-1}(1-p_i)^{1-\eta_i+\beta_i-1}dp_i \\ &= \tfrac{\Gamma(r_i+\beta_i)}{\Gamma(r_i)\Gamma(\beta_i)}\tfrac{\Gamma(r_i+\eta_i)\Gamma(1-\eta_i+\beta_i)}{\Gamma(r_i+\beta_i+1)} \end{aligned} \tag{2.32}$$

The likelihood in the third layer is equal to the evidence in the second layer in Equation (2.15). Since the problem is divided into two cases according to whether there is a gross error or not in the second layer, the likelihood in the third layer can be handled in two cases by substituting Equation (2.18), Equation (2.19) and Equation (2.26) in Equation (2.15). However, for simplicity, the likelihood is written in a general form as following:

$$P(Y_i^R|\eta_i) = \frac{P(Y_i^R|\alpha_i,\alpha_{i0},\eta_i)P(\alpha_i,\alpha_{i0}|\eta_i)}{P(\log\alpha_i,\log\alpha_{i0}|\eta_i,Y_i^R)} \tag{2.33}$$

Since the left hand side is not relevant to α_i and α_{i0}, the right hand side has no relationship with α_i and α_{i0}, which means that the values of α_i and α_{i0} have no influence on the value of the likelihood. The MAP of α_i and α_{i0} is taken to simplify the calculation:

$$\begin{aligned} P(Y_i^R|\eta_i) &= \tfrac{P(Y_i^R|\alpha_i,\alpha_{i0},\eta_i)P(\alpha_i,\alpha_{i0}|\eta_i)}{P(\log\alpha_i,\log\alpha_{i0}|\eta_i,Y_i^R)}\big|_{\alpha_i^{MP},\alpha_{i0}^{MP}} \\ &\approx \tfrac{P(Y_i^R|\alpha_i,\alpha_{i0},\eta_i)P(\alpha_i,\alpha_{i0}|\eta_i)}{\sqrt{\det Q_i}}\big|_{\alpha_i^{MP},\alpha_{i0}^{MP}} \end{aligned} \tag{2.34}$$

After the above derivations, $P(\eta_i = 1|Y_i^R)$ and $P(\eta_i = 0|Y_i^R)$ are both calculated. They are further compared to determine the value of η_i. The indicator matrix η can be obtained after the value of the indicator for each measurement is decided.

2.3.4 Simultaneous Gross Error Detection and Data Reconciliation Procedure

The implementation procedure of the hierarchical Bayesian approach is outlined as **Algorithm 1**.

Algorithm 1 Bayesian Method for Simultaneous Gross Error Detection and Data Reconciliation

input: Sample data D, and selected initials for indicator matrix η

initialize: Variance of the random error: $\sigma_{ii}^{(0)} = MAD/0.6745$,
hyperparameters: a large value for $\sigma_{ii,0}^{2(0)}$ and the reconciled data for $\mu_0^{(0)}$

while *the estimations of the parameters do not change within tolerance* **do**

Step 1. In the first layer, maximize $P(x^{(k)}, \delta^{(k)}|D, \Sigma^{(k-1)}, \Sigma_0^{(k-1)}, \eta^{(k-1)})$ to updatethe MAP estimates of x and δ, $x^{(k)}$ and $\delta^{(k)}$ using Equations (2.12) and (2.13).

Step 2. Update $\mu_0^{(k)}$ as the estimates of x, i.e. $\mu_0^{(k)} = x^{(k)}$.

Step 3. In the second layer, maximize $P(\alpha_i^{(k)}, \alpha_{i0}^{(k)}|\eta_i^{(k-1)}, Y_i^R)$ for each measurement to update the MAP estimates of hyperparameters, $\alpha_i^{(k)}$ and $\alpha_{i0}^{(k)}$.The variance can be obtained by taking an inverse of α_i and α_{i0}.

Step 4. In the third layer, evaluate the posterior probability of each measurement, $P(\eta_i = 1|Y_i^R)$ and $P(\eta_i = 0|Y_i^R)$. Compare the values of them. If the value of $P(\eta_i = 1|Y_i^R)$ is larger, set $\eta_i^{(k)} = 1$, otherwise, set $\eta_i^{(k)} = 0$.

Step 5. Update the estimated values of $\Sigma^{(k)}$, $\Sigma_0^{(k)}$ and $\eta^{(k)}$ and use them in the next iteration.

end while

return: Estimations of different parameters $\hat{x}$, $\hat{\delta}$, $\hat{\Sigma}$, $\hat{\Sigma}_0$ and $\hat{\eta}$

The principle of the initial value selection is discussed as following. $\sigma_{ii}^{(0)} = MAD/0.6745$ is utilized to calculate the robust variance. This equation is commonly used in robust regression. The constant 0.6745 makes the estimate of σ_{ii}^2 unbiased for the normal distribution. MAD is the median absolute deviation of the residuals; a large value is set for $\sigma_{ii,0}^{2(0)}$ to reduce

the influence of not setting an accurate initial value for $\mu_{i0}^{(0)}$. μ_0 is the mean value in the hyperprior for x.

In **Algorithm 1**, Step 1 to 5 will be repeated iteratively until no further improvements (the estimations of the parameters do not change) are gained. The flow chart of **Algorithm 1** is shown in Figure 2.1.

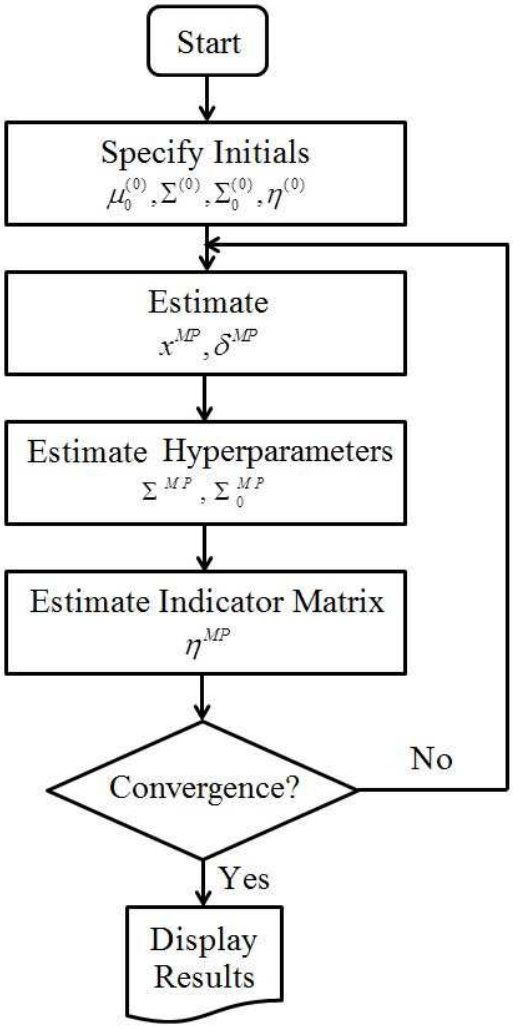

Figure 2.1: Flow chart of **Algorithm 1**

While **Algorithm 1** can be directly applied for gross error identification, it may lead to too many mispredictions. To improve the performance of the proposed simultaneous gross error detection and data reconciliation approach, a serial strategy is introduced in the next section.

2.4 Serial Strategy for Improved Performance

Algorithm 1 may lead to many mispredictions, which is mainly due to the smearing effect [1]. All the variables are related through the constraints according to the network of the system. A gross error in one measurement may influence other measurements, so that the probability $P(\eta_i = 1|Y_i^R)$ can be larger than $P(\eta_i = 0|Y_i^R)$ for a process measurement without gross error. There are many factors influencing the degree of smearing, such as the level of redundancy, the size of the standard deviations of the random error and the magnitudes of the gross errors [1, 72].

Furthermore, simultaneous gross error estimation and data reconciliation cannot be solved for an arbitrary set of gross error candidates due to the existence of equivalent sets [73]. The concept of equivalent sets is defined as follows: if two sets of gross errors have the same effect in data reconciliation, they are regarded as equivalent sets, which means that when simulating either one, they both lead to the same objective function value of data reconciliation. Equivalent sets exist when candidate streams are in the same loop in an augmented graph consisting of the original graph representing the flowsheet with the addition of environmental node. The environment node is an additional node of the flowsheet so that all process feeds and products can connect to it. It is impossible to distinguish the equivalent sets and this leads to the conditions of exact detectability in simultaneous gross error detection and data reconciliation problem. There are mainly two rules for this detectability problem [73]:

(1) The maximum number of gross errors that can be simulated in an open system is equal to the number of process units (blocks in the diagram).

(2) A set of gross errors can be exactly detected only if no subset of these variables forms a loop with an additional stream. In other words, a set of gross errors can be exactly detected only if the corresponding set of columns of the incidence matrix A does not form a linearly dependent set with any other additional column.

To address the above issues and improve the performance of **Algorithm 1**, a serial

strategy is adopted. The serial strategy identifies gross errors in a sequential mode. This strategy is based on the assumption that for any system, the probability of containing k gross errors is larger than the probability of containing $k+1$ gross errors. This strategy can detect the minimum possible number of gross errors and solve data reconciliation problem and estimation problem with all suspects. The strategy is outlined as **Algorithm 2** [73]:

Algorithm 2: Serial Strategy for Simultaneous Multiple Gross Error Detection and Data Reconciliation

---

Input: Sample data D

Initialize: Create two lists: one is for gross error candidates (GEC) and another is for the final gross errors (FGE). Set them empty at first. Set the initial values for η_i to be all $1s$

Step 1. Run **Algorithm 1** once to get the gross error candidates.

if *there are r variables in suspect* ($r > 0$)

go to step 2.

else

declare no gross error and stop.

end if-else

Step 2. Put all r variables detected in step 1 in GEC.

if *GEC and FGE have same elements*

erase them in GEC.

end if

while *GEC is not empty* **do**

Step 3. Run **Algorithm 1** with the initial values to be all the members in FGE and onemember of the GEC at a time. If there are r variables in GEC, then **Algorithm 1** is taken r times.

Step 4. Calculate the ratio $\frac{P(\eta_i=1|Y_i^R)}{P(\eta_i=0|Y_i^R)}$. For each run find the value of the ratio correspondingto the simulated member in GEC. Compare these values and determine which memberof the GEC leads to the largest value of ratio

and get the corresponding gross errorcandidates. Add that variable to the. FGE Empty set GEC.

Step 5. Add the gross error candidates obtained in step 4 into the GEC. If any members inthe GEC are in the same loop with the members in the FGE, erase the member in theGEC with the smallest ratio and also eliminate the member which is already in the FGE.

end while

Step 6. Determine all equivalent sets.

return: Estimations of different parameters x, δ, Σ, Σ_0 and η.

If there are equivalent sets for the gross errors, the equivalent sets are also returned.

The flow chart of **Algorithm 2** is shown in Figure 2.2.

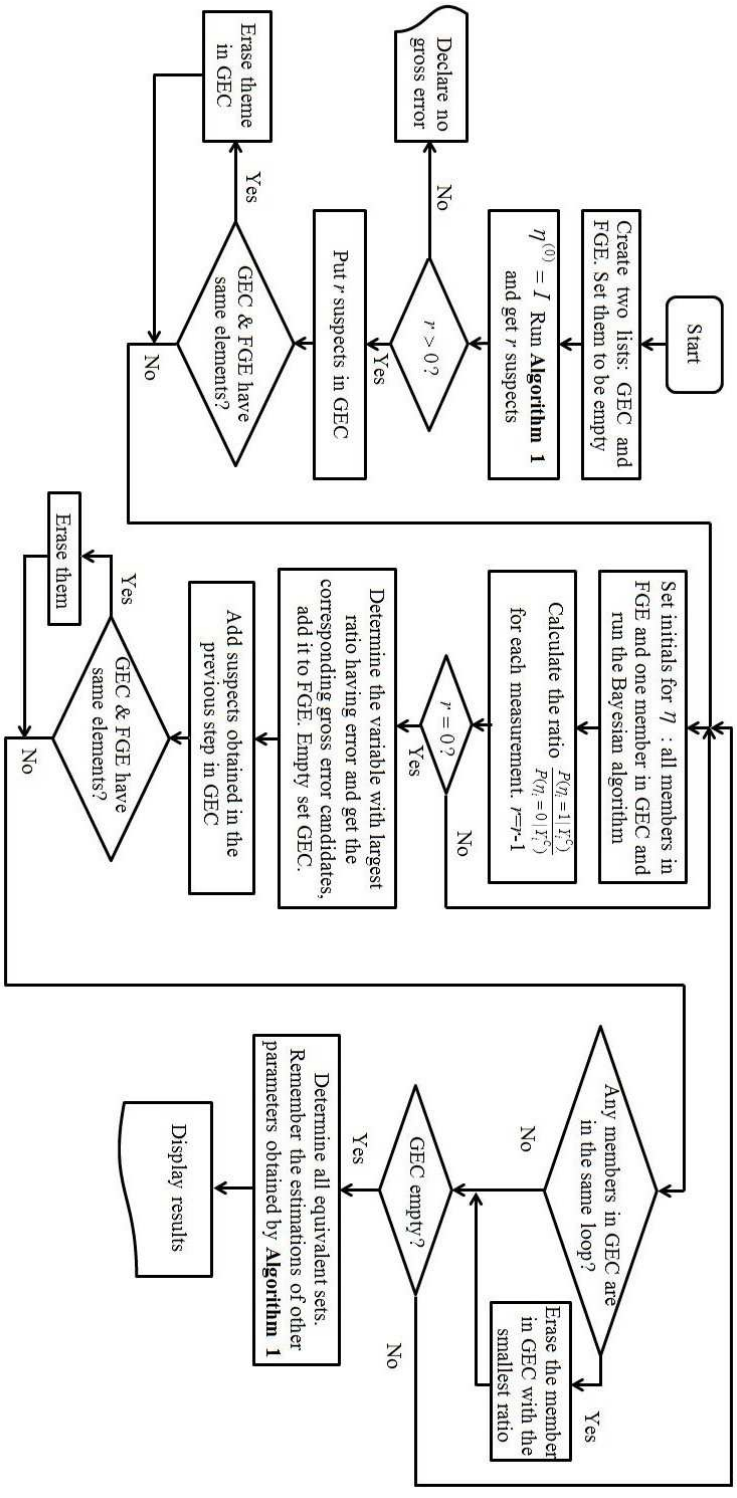

Figure 2.2: Flow chart of **Algorithm 2**

2.5 Simulation Study

2.5.1 Linear Case

In this section, simulated data-sets are used to study the effectiveness of the proposed Bayesian approach for simultaneous gross error detection and data reconciliation. The process network shown in Figure 2.3 is considered. There are 4 units and 7 flow rates.

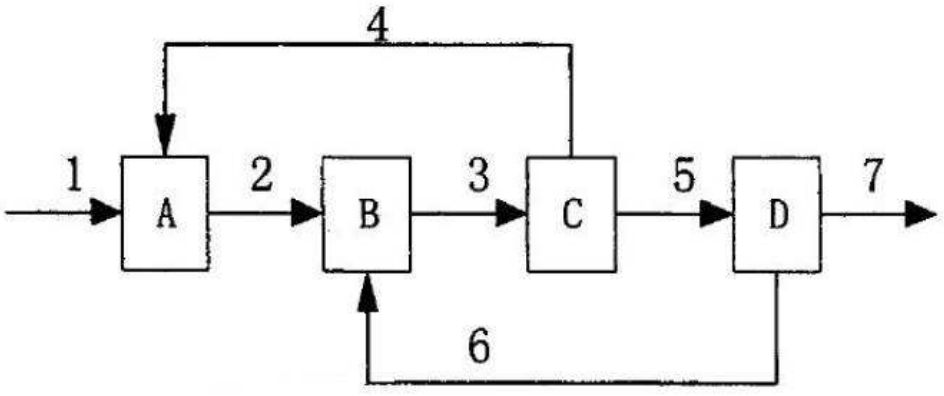

Figure 2.3: Diagram of process network

From the above process network, the flow rates satisfy the following material balance:

$$x_1 - x_2 + x_4 = 0$$
$$x_2 - x_3 + x_6 = 0$$
$$x_3 - x_4 - x_5 = 0$$
$$x_5 - x_6 - x_7 = 0$$

All the variables are assumed to be measured and the above equations can be further

written as $Ax = 0$, where $x = [x_1, x_2, ..., x_7]^T$ and the incidence matrix A is:

$$A = \begin{bmatrix} 1 & -1 & 0 & 1 & 0 & 0 & 0 \\ 0 & 1 & -1 & 0 & 0 & 1 & 0 \\ 0 & 0 & 1 & -1 & -1 & 0 & 0 \\ 0 & 0 & 0 & 0 & 1 & -1 & -1 \end{bmatrix}$$

The data are generated randomly using MATLAB. The vector of the correct values of the flow rates is set as $x = \begin{bmatrix} 1 & 2 & 3 & 1 & 2 & 1 & 1 \end{bmatrix}^T$. In order to avoid confusion between the gross errors and the noise (random error), the value of the covariance matrix Σ cannot be too large.

2.5.1.1 Case 1: Single Gross Error

In this case, only one gross error is introduced in the first measurement x_1 and the magnitude of the gross error is set to $\delta_1 = 2$. Since there are no gross errors in other measurements, the magnitudes of other gross errors are set to zeros.

The results with two different standard deviations(variance) of the measurements are compared:

(1) $\Sigma = 0.0016I$, , where I is identity matrix, the standard deviations are around $1.3\% - 4\%$ of the measurements.

(2) $\Sigma = 0.1I$, the standard deviations are around $11\% - 32\%$ of the measurements.

A set of simulated measurement data with the two different standard deviations are plotted in Figure 2.4 and Figure 2.5, respectively.

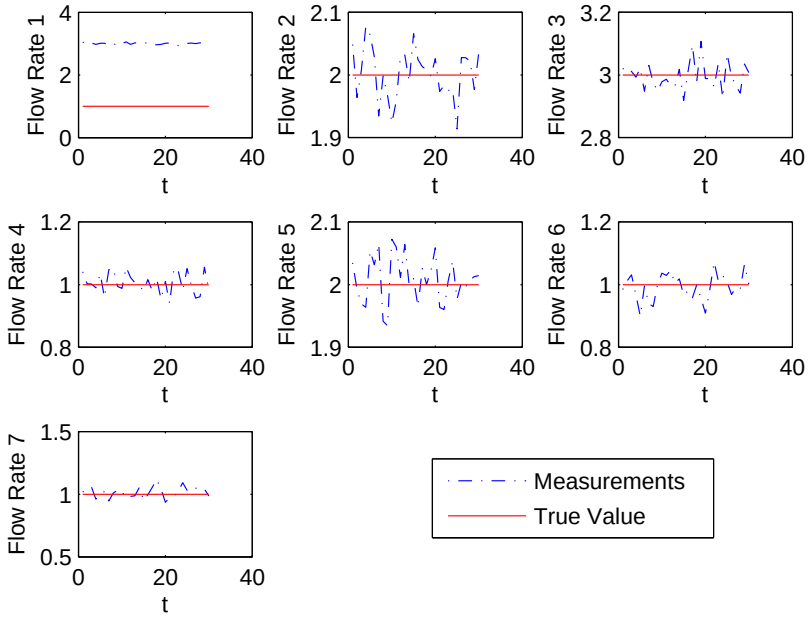

Figure 2.4: Data plot with gross error in the first measurement, $\Sigma = 0.0016I$

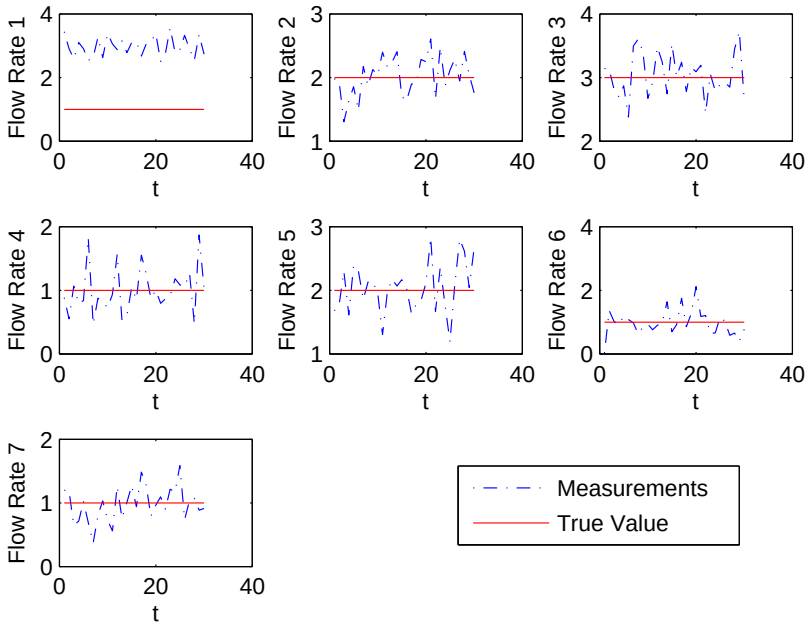

Figure 2.5: Data plot with gross error in the first measurement, $\Sigma = 0.1I$

To evaluate the performance of the proposed method, 50 sets of simulated measurement

data are generated and used for gross error detection and data reconciliation. With **Algorithm 2**, Figure 2.6-2.8 show the histograms of the estimated value of x, the estimated value of δ and the estimated value of the standard deviation σ with $\Sigma = 0.0016I$, respectively. Figure 2.9-2.11 show the histograms of the estimated value of x, the estimated value of δ (for both cases $\delta_1 = 2$, $\delta_2 = \delta_3 = \delta_4 = \delta_5 = \delta_6 = \delta_7 = 0$) and the estimated value of the standard deviation σ with $\Sigma = 0.1I$, respectively.

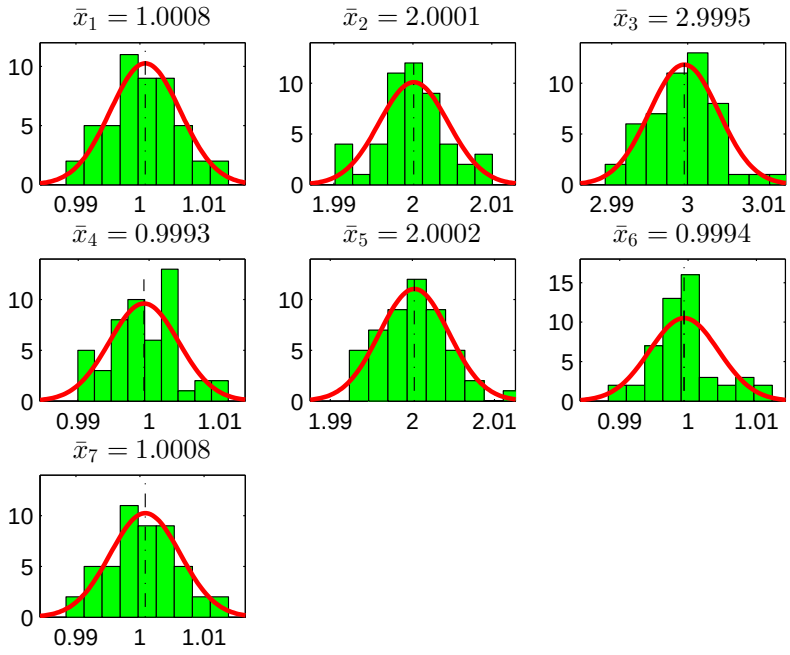

Figure 2.6: Histogram of the estimated value of x, $\Sigma = 0.0016I$ (50 Runs)

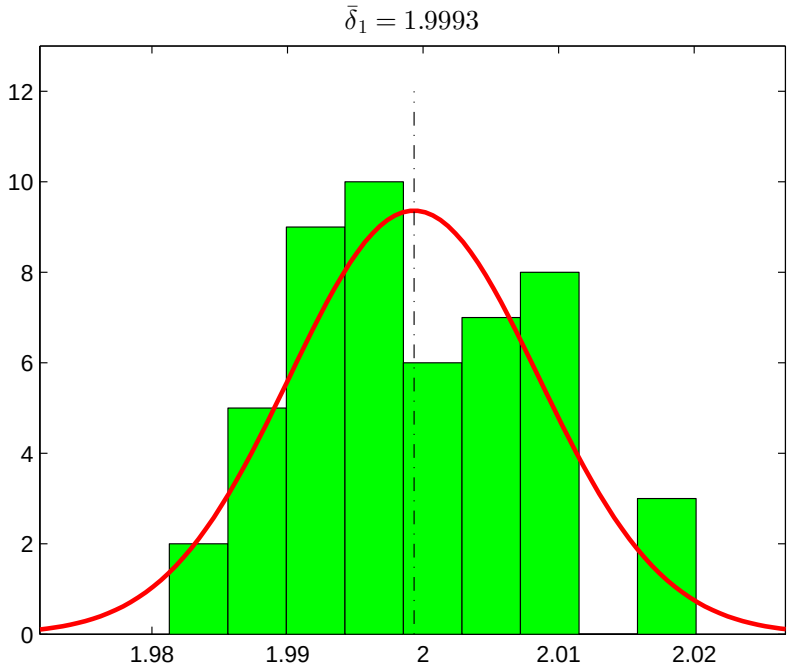

Figure 2.7: Histogram of the estimated value of δ_1, $\Sigma = 0.0016I$ (50 Runs)

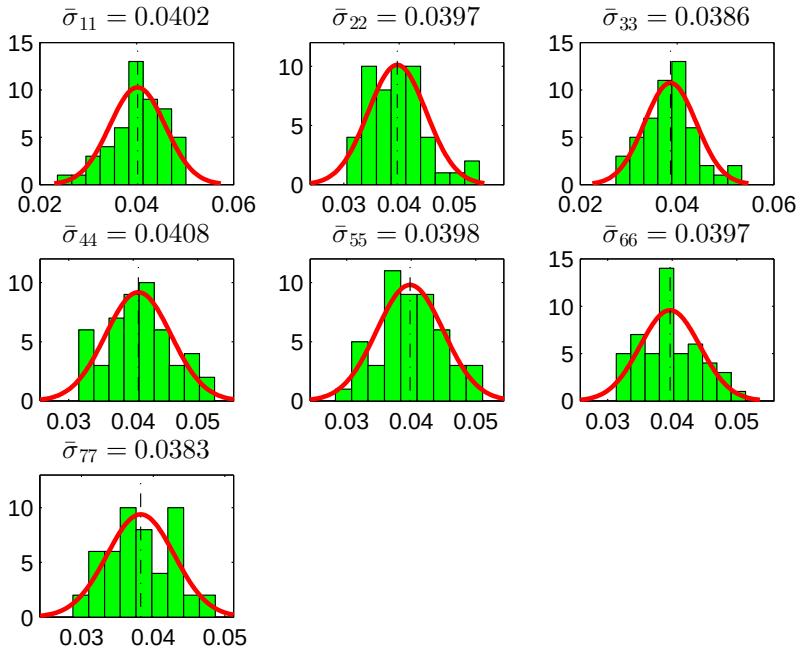

Figure 2.8: Histogram of the estimated value of σ, $\Sigma = 0.0016I$ (50 Runs)

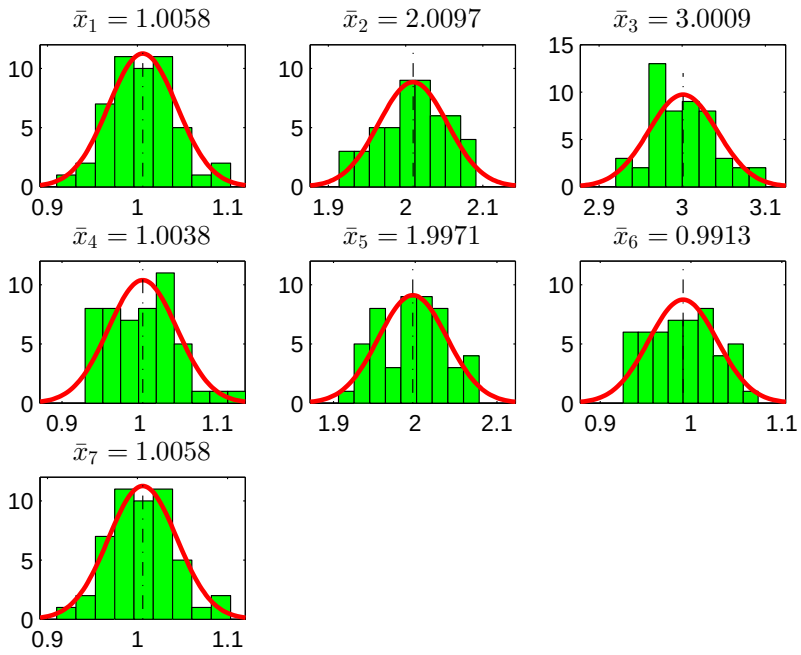

Figure 2.9: Histogram of estimated value of x, $\Sigma = 0.1I$ (50 Runs)

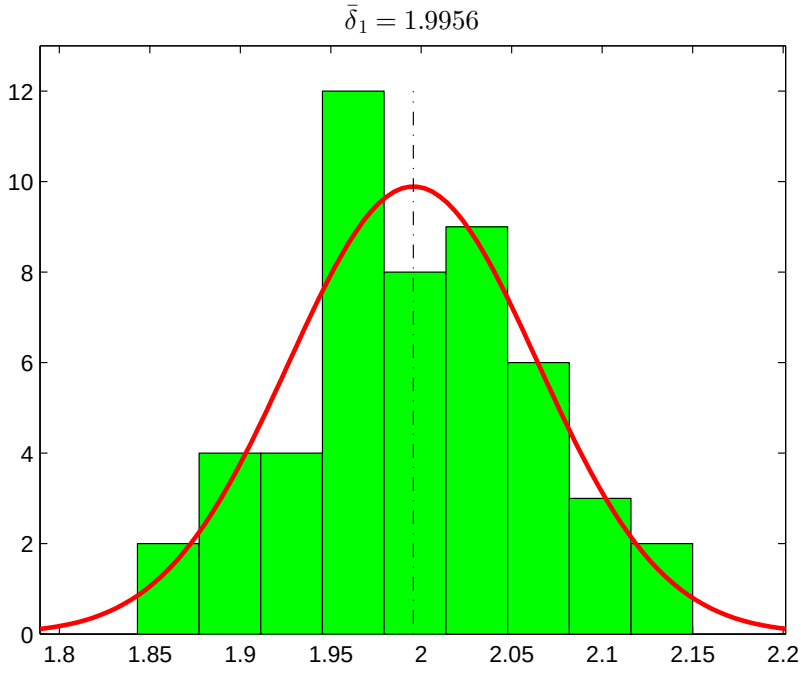

Figure 2.10: Histogram of the estimated value of δ_1, $\Sigma = 0.1I$ (50 Runs)

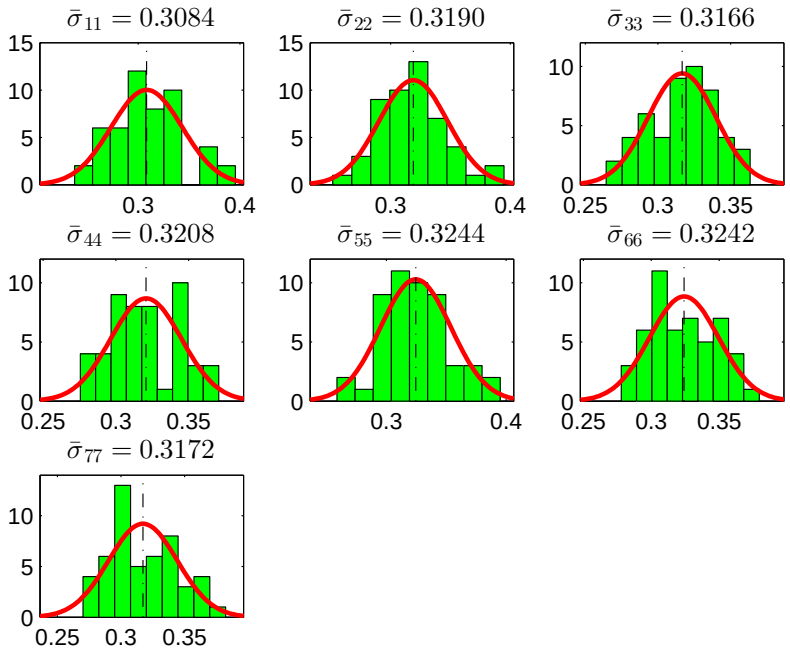

Figure 2.11: Histogram of the estimated value of σ, $\Sigma = 0.1I$ (50 Runs)

The performances of **Algorithm 1** and **Algorithm 2** are compared for all the cases of one gross error introduced. For each case, one of the seven measurements contains one gross error and the simulation is performed for 50 runs using **Algorithm 1** and **Algorithm 2**, respectively.

A performance measure−−correct rate is defined for performance evaluation:

$$\text{Correct Rate} = \frac{\text{Number of Runs that All the Gross Errors are Correctly Identified}}{\text{Total Number of Runs}}$$

Table 2.1 displays the correct rates of **Algorithm 1** and **Algorithm 2**. The results with different standard deviations of measurements are also compared.

Table 2.1: Comparison of correct rates (50 runs)

Measurement number	Correct Rate (**Algorithm 1**, $\Sigma = 0.1I$)	Correct Rate (**Algorithm 2**, $\Sigma = 0.0016I$)	Correct Rate (**Algorithm 2**, $\Sigma = 0.1I$)
1	48/50=96%	50/50=100%	50/50=100%
2	46/50=92%	50/50=100%	49/50=98%
3	23/50=46%	50/50=100%	48/50=96%
4	35/50=70%	50/50=100%	50/50=100%
5	46/50=92%	50/50=100%	49/50=98%
6	34/50=68%	50/50=100%	48/50=96%
7	49/50=98%	50/50=100%	50/50=100%

It can be seen from Table 2.1 that **Algorithm 1** has more mispredictions than **Algorithm 2**. Since in this case only single gross error is considered, according to the flowsheet there is no equivalent set for each case. The mispredictions may be caused by smearing effect. The confusion between the random error and the gross error may lead to the mispredictions (the magnitude δ of the gross error is only slightly larger than the 3σ). **Algorithm 2** enhances the correct rate of gross error detection and estimation. It is worth mentioning that the existing methods generally handle small standard deviations. For example, the standard deviations of the measurements are chosen to be 2% of each measurement by Bagajewicz and Jiang[74]. The proposed method in this chapter can deal with much larger standard deviations. The proposed approach also works well with small standard deviation as expected. **Algorithm 2** leads to 100% correct rate for $\Sigma = 0.0016I$. Even though the standard deviations are increased to $13\% - 32\%$ of the measurements, the correct rate shows that **Algorithm 2** is still efficient to detect the gross error. Since the proposed method can handle large standard deviation in the data, only $\Sigma = 0.1I$ is considered in the rest of the case studies.

2.5.1.2 Case 2: Multiple Gross Errors without Equivalent Sets

In this case, multiple gross errors in the data are investigated. First, the case that no equivalent set exists in the gross errors is studied. **Algorithm 2** is illustrated using the

simulation example under different scenarios. Table 2.2 and 2.3 below show the results in each steps following the procedure of the serial strategy. The gross error initial values for **Algorithm 1** are shown in the second column of the tables. The third column of the tables provides the estimations of the magnitudes of the gross errors. The values of the ratio $\frac{P(\eta_i=1|Y_i^R)}{P(\eta_i=0|Y_i^R)}$ are listed in the fourth column. The last column shows the variables as gross error candidates flagged by **Algorithm 1**.

Table 2.2: **Algorithm 2** with gross error in x_2(magnitude: 3) and x_7 (magnitude: 1)

Step Number	Gross Error Initials	Magnitude of Gross Error Estimated	Ratio	Variables flagged by **Algorithm 1**
step 1	All			2, 6
step 2	GEC: 2, 6			FGE: Empty
step 3	2		1.8×10^{17}	2, 7
	6		3.2×10^{3}	1,2,3,4,5,6
step 4	FGE: 2			
step 5	GEC: 7			
step 3	2,7		46.8	2, 7
step 4	FGE: 2,7	2 (magnitude: 3.0)		
		7 (magnitude: 1.0)		
step 5	GEC: Empty			
step 6	Equivalent sets: none			

Table 2.2 shows the solution procedure for two gross errors in x_2 and x_7 with magnitudes $\delta_2 = 3$ and $\delta_7 = 1$, respectively. In the first step, the initial values for indicator η_i are set to be all $1s$, and the gross errors candidates flagged by **Algorithm 1** are 2 and 6. In the second step, the flagged gross error candidates (2 and 6) are put into GEC. In the third step, **Algorithm 1** is run twice since there are two elements in the GEC. The initial values of indicator η_i are set as $\eta_2 = 1$ (others are set to zero) for the first run and $\eta_6 = 1$ (others are set to be zero) for the second run. In the fourth step, the ratio $\frac{P(\eta_2=1|Y_2^R)}{P(\eta_2=0|Y_2^R)}$ and $\frac{P(\eta_6=1|Y_6^R)}{P(\eta_6=0|Y_6^R)}$ are calculated for the two runs in step 3 and compare them. The run with initial $\eta_2 = 1$ has a larger ratio, so element 2 in GEC is identified as a variable with gross error (i.e., the second measurement is detected to contain a gross error). Element 2 is added to the FGE. The GEC is set empty. In the fifth step, the gross error candidates corresponding to element

2 are obtained, which are 2 and 7 and put them in the GEC. Since 2 is already in the FGE, it is eliminated in the GEC and GEC has only one element 7 at this time. The GEC is not empty so the algorithm goes to step 3; **Algorithm 1** is taken with initials to be all the members in the FGE (2) and one member of GEC (7). The gross error candidates flagged by **Algorithm 1** are 2 and 7. In the second step 5, the GEC is empty and the algorithm is stopped. Even though the gross error in the seventh measurement is not flagged by the **Algorithm 1** in step 1, the gross errors are still successfully identified. The number of iterations that is needed to detect all the gross errors in **Algorithm 2** is 2 which is the same as the number of gross error introduced. Using **Algorithm 2**, the gross errors are exactly detected. Then the magnitudes of the gross errors can be estimated. After the gross errors are successfully detected and the magnitudes of the gross errors are estimated, the correct values of x and the covariance matrix Σ of the random errors can be estimated.

The final estimated values are:

$$\hat{x} = \begin{bmatrix} 0.9749 & 2.0105 & 3.0604 & 1.0356 & 2.0248 & 1.0499 & 0.9749 \end{bmatrix}^T,$$

$\hat{\delta}_2 = 3.0$, $\hat{\delta}_7 = 1.0$, $\hat{\delta}_1 = \hat{\delta}_3 = \hat{\delta}_4 = \hat{\delta}_5 = \hat{\delta}_6 = 0$,

$\hat{\sigma}^2_{11} = 0.0918$, $\hat{\sigma}^2_{22} = 0.1085$, $\hat{\sigma}^2_{33} = 0.1109$, $\hat{\sigma}^2_{44} = 0.1117$, $\hat{\sigma}^2_{55} = 0.0919$, $\hat{\sigma}^2_{66} = 0.0878$,

$\hat{\sigma}^2_{77} = 0.0845$.

Table 2.3: **Algorithm 2** with gross error in x_1 (magnitude: 2), x_2(magnitude: 3) and x_5 (magnitude: 4)

Step Number	Gross Error Initials	Magnitude of Gross Error Estimated	Ratio	Variables flagged by **Algorithm 1**
step 1	All			2,3,5,7
step 2	GEC: 2,3,5,7			FGE: Empty
step 3	2		7.1×10^{13}	1,2,3,4,5,6,7
	3		8.8×10^{21}	2,3,4,5,6,7
	5		2.2×10^{23}	1,2,3,4,5,6,7
	7		8.1×10^{13}	1,2,3,4,5,6,7
step 4	FGE: 5			
step 5	GEC: 1,2,3,6,7			
step 3	5,1		80.0	1,2,3,4,5,6,7
	5,2		1.3×10^{18}	1,2,5
	5,3		1.2×10^{10}	1,2,3,4,5,6,7
	5,6		1.3×10^{10}	1,2,4,5,6,7
	5,7		8.5×10^{6}	2,3,5,6,7
step 4	FGE: 2,5			
step 5	GEC: 1			
step 3	1,2,5		8.9×10^{6}	1,2,5
step 4	FGE: 1,2,5	1 (magnitude: 1.9)		
		2 (magnitude: 3.1)		
		5 (magnitude: 3.9)		
step 5	GEC: Empty			
step 6	Equivalent sets: none			

In Table 2.3, three biases are considered with $\delta_1 = 2$, $\delta_2 = 3$ and $\delta_5 = 4$. The procedure is similar to Table 2.2. Since the number of gross errors introduced is larger than the above cases, **Algorithm 2** takes 1 more iteration to identify all the gross errors successfully.

The final estimated values are:

$\hat{x} = \begin{bmatrix} 1.0092 & 1.9142 & 2.9036 & 0.9050 & 1.9986 & 0.9894 & 1.0092 \end{bmatrix}^T$,

$\hat{\delta}_1 = 1.9$, $\hat{\delta}_2 = 3.1$, $\hat{\delta}_5 = 3.9$, $\hat{\delta}_3 = \hat{\delta}_4 = \hat{\delta}_6 = \hat{\delta}_7 = 0$,

$\hat{\sigma}^2_{11} = 0.0721$, $\hat{\sigma}^2_{22} = 0.1150$, $\hat{\sigma}^2_{33} = 0.0935$, $\hat{\sigma}^2_{44} = 0.0838$, $\hat{\sigma}^2_{55} = 0.0973$, $\hat{\sigma}^2_{66} = 0.1180$,

$\hat{\sigma}^2_{77} = 0.1168$.

In Table 2.2 and Table 2.3, the number of the gross errors introduced is less than the number of the units in the process network and none of them form a loop with an additional variable, which means that the gross errors introduced satisfy the condition of exact

detectability.

2.5.1.3 Case 3: Multiple Gross Errors with Equivalent Sets

In this case, multiple gross errors are investigated under the situation that equivalent sets exist. Here, two biases are introduced as $\delta_2 = 3$ and $\delta_3 = 4$. In the first step, the initial values for indicator η_i are set to be all $1s$ and the gross errors candidates flagged by **Algorithm 1** are 3 and 4. Since there are two suspects, it proceeds to step 2. In the second step, the flagged gross error candidates 3 and 4 are put into GEC. In the third step, **Algorithm 1** is run twice since there are two elements in the GEC. The initial values of indicator η_i are different for different runs, that is, $\eta_3 = 1$ (others are set to be zero) for the first run and $\eta_4 = 1$ (others are set to be zero) for the second run. In the fourth step, the ratio $\frac{P(\eta_3=1|Y_3^R)}{P(\eta_3=0|Y_3^R)}$ and $\frac{P(\eta_4=1|Y_4^R)}{P(\eta_4=0|Y_4^R)}$ are calculated for the two runs in step 3 and compare them. The run with initial $\eta_4 = 1$ has the largest ratio, so element 4 in GEC is determined to be the final gross errors, which means that the fourth measurement is detected to contain a gross error. Element 4 is added in the FGE. The GEC is set empty. In the fifth step, the gross error candidates corresponding to element 4 are obtained, which are 3 and 4 and put them in the GEC. Since 4 is already in the FGE, it is eliminated in the GEC and GEC has only one element 3 at this time. The GEC is not empty so the algorithm goes to step 3; **Algorithm 1** is taken with initials to be all the members in the FGE (4) and one member of GEC (3). The gross error candidates flagged by **Algorithm 1** are 3 and 4. In the second step 5, the GEC is empty and the algorithm is stopped. Since the second measurement and the third measurement form a loop with an additional stream 4, the gross errors introduced violate the second condition of exact detectability. It is difficult to identify the gross errors exactly in this case, but the equivalent sets are detected, as shown in Table 2.4.

Table 2.4: **Algorithm 2** with gross error in x_2 (magnitude: 3) and x_3(magnitude: 4)

Step Number	Gross Error Initials	Magnitude of Gross Error Simulated	Ratio	Variables flagged by **Algorithm 1**
step 1	All			3,4
step 2	GEC: 3,4			FGE: Empty
step 3	3		8.3×10^9	2,3,4
	4		7.6×10^{18}	3,4
step 4	FGE: 4			
step 5	GEC: 3			
step 3	3,4		23.9	3,4
step 4	FGE: 3,4	3 (magnitude: 0.9) 4 (magnitude: -3.2)		
step 5	GEC: Empty			
step 6	Equivalent sets: 2(3.2), 3(4.1) and 2(-0.9),4(-4.1)			

2.5.2 Nonlinear Case

The nonlinear programming problem in the first layer for both examples is solved in GAMS with solver CONOPT.

2.5.2.1 Case 1: Example from Pai and Fisher

This problem from Pai and Fisher [75] consists of 8 variables, 5 of them are measured and 3 of them are unmeasured. There are 6 nonlinear constraints which are shown as follows:

$$0.5x_1^2 - 0.7x_2 + x_3u_1 + x_2^2u_1u_2 + 2x_3u_3^2 - 255.8 = 0$$

$$x_1 - 2x_2 + 3x_1x_3 - 2x_2u_1 - x_2u_2u_3 + 111.2 = 0$$

$$x_3u_1 - x_1 + 3x_2 + x_1u_2 - x_3\sqrt{u_3} - 33.57 = 0$$

$$x_4 - x_1 - x_3^2 + u_2 + 3u_3 = 0$$

$$x_5 - 2x_3u_2u_3 = 0$$

$$2x_1 + x_2x_3u_1 + u_2 - u_3 - 126.6 = 0$$

The exact values of the 8 variables are:

$$x_{exact} = [4.5124, 5, 5819, 1.9260, 1.4560, 4.8545]^T$$
$$u_{exact} = [11.070, 0.61467, 2.0504]^T$$

In this example, the effectiveness of the proposed simultaneous gross error detection and data reconciliation algorithm (**Algorithm 1**) is demonstrated and the results are compared with the results of Tjoa and Biegler [16]. Following the same procedure provided by Tjoa and Biegle, the data are generated with the mean equal to the exact values and Gaussian noise level is 0.1. The algorithm is tested for 100 runs. 20% of all measured variables are assumed to be shifted and the effect of location of gross errors is tested in three different situations. In situation 1, 5 blocks with 20 gross errors in each block are added in sequence from x_1 to x_5. In situation 2, all the measured variables are added with gross errors in every fifth run and no gross errors in other runs. In situation 3, one gross error is added for each run in sequence from x_1 to x_5 in rotation. The magnitudes of gross errors are +0.4, +1, and +4, respectively.

For the case that the magnitude of gross errors is +0.4 (only 4σ), it is easy for the algorithm to be confused between the random error and gross error. The results are shown and compared in Table 2.5.

Table 2.5: Results of **Algorithm 1** for gross error detection ($\delta = +0.4$)

Situation	x_1		x_2		x_3		x_4		x_5	
	R	W	R	W	R	W	R	W	R	W
1 (**Algorithm 1**)	5	2	20	6	20	-	20	2	20	5
1 (Tjoa)	8	3	19	-	20	-	9	-	17	1
2 (**Algorithm 1**)	8	-	20	1	20	-	15	-	20	-
2 (Tjoa)	-	-	20	-	20	2	-	-	20	1
3 (**Algorithm 1**)	3	2	20	8	20	-	20	2	20	-
3 (Tjoa)	4	-	18	-	20	1	9	-	14	2

Note: R =Right; W= Wrong.

In Table 2.5, the number of a gross error correctly detected and the number of false alarm of a gross error for each variables are listed. From these numbers, we can see that

the number of a gross error correctly detected obtained by **Algorithm 1** is larger than Tjoa's method while the times of false alarm by **Algorithm 1** is also larger than Tjoa's method. This is because that the correctly detected number of gross error and the false alarm are intimately related. If the probability of false alarm is allowed to be larger, the correct detected number of gross error will increase. For **Algorithm 1**, we can balance them by setting some hyperparameters, such as the hyperparameters for the prior distribution of p_i. However, the results show that **Algorithm 1** is sufficient to detect the gross errors for the case that the magnitude of gross error is not easily distinguished from the random error.

Next, the case when the magnitude of gross errors is set as $\delta = 1$ is considered. This is a more typical case of gross error detection and the results are shown in Table 2.6.

Table 2.6: Results of **Algorithm 1** for gross error detection ($\delta = +1$)

Situation	x_1		x_2		x_3		x_4		x_5	
	R	W	R	W	R	W	R	W	R	W
1 (**Algorithm 1**)	20	2	20	-	20	1	20	1	20	2
1 (Tjoa)	19	-	20	1	20	-	19	1	20	2
2 (**Algorithm 1**)	10	-	20	-	20	-	19	-	20	-
2 (Tjoa)	12	-	20	-	20	1	20	1	17	1
3 (**Algorithm 1**)	20	1	20	2	20	2	20	2	20	1
3 (Tjoa)	20	2	20	-	20	-	19	-	20	1

Note: R =Right; W= Wrong.

In Table 2.6, the number of a gross error correctly detected increases compared with the case of $\delta = 0.4$ while the number of false alarm decreases. This means that **Algorithm 1** is more powerful for the case that the gross error can be distinguished from the random error. The performance of **Algorithm 1** is very close to Tjoa's method. Situation 3 will be used for the studying of estimations of the magnitudes δ of gross errors, the estimations of the variance σ^2 and the estimations of the values of both measured and unmeasured variables (x and u). The estimated values listed below are the means for 100 runs.

For the case that $\delta = +1$, the final estimated values are:

$\hat{x} = [4.5354, 5.5749, 1.9231, 1.4963, 4.8236]^T$

$\hat{u} = [11.1733, 0.6200, 2.1344]^T$

$\hat{\delta} = [0.9717, 0.9969, 0.9995, 1.0000, 0.9931]^T$

$\hat{\sigma}_{11}^2 = 0.0103, \hat{\sigma}_{22}^2 = 0.0101, \hat{\sigma}_{33}^2 = 0.0107, \hat{\sigma}_{44}^2 = 0.0095, \hat{\sigma}_{55}^2 = 0.0100$

For the case that $\delta = +4$, the final estimated values are:

$\hat{x} = [4.5439, 5.5539, 1.9228, 1.4094, 4.9022]^T$

$\hat{u} = [11.1428, 0.6128, 2.0728]^T$

$\hat{\delta} = [4.0102, 3.9862, 3.9975, 4.0028, 3.9951]^T$

$\hat{\sigma}_{11}^2 = 0.0102, \hat{\sigma}_{22}^2 = 0.0102, \hat{\sigma}_{33}^2 = 0.0100, \hat{\sigma}_{44}^2 = 0.0102, \hat{\sigma}_{55}^2 = 0.0104$

It is shown that for all the cases, the estimated values are very close to the exact values. From the results shown above, we can see that the proposed algorithms are good for gross error detection and data reconciliation problem. If further improvement is needed for the problem, the serial strategy introduced above can be taken for exact detection of the gross error.

Furthermore, the performance of **Algorithm 1** relies on the redundancy of the measurements. Since nonredundant variables can be adjusted only by the objective function not through the constraints. They may converge to the initial values (in the first layer). If the nonredundant variables contain gross errors, the reconciled data may be inaccurate and since the unmeasured variables are obtained through the constraints they may be influenced. The hyperparameter μ_0 is taken as the estimation of x and it is used in the third layer, so the performance of the gross error detection in the third layer may also be influenced. However, the redundancy of variables is related to both sensor network and the system constraints. Some existing methods can be applied to check the redundancy and the readers are referred to some related references [76, 77, 78].

2.5.2.2 Case 2: Example from Swartz

The second example for nonlinear system is first described by Swartz [78] for data reconciliation. The flow sheet of the process is shown in Figure 2.12. Standard deviations of the measurements for flow rate and temperature are 2% and 0.75 degree, respectively. The model is more complex than the first example. There are 16 measured variables, 14 unmeasured variables and 17 constraints. The constraints are obtained by considering mass and heat balances around the heat exchangers, splitting and mixing junctions. To see the effectiveness of gross error detection, 10 degree is added to measurement TA7 as a gross error. **Algorithm 1** can detect TA7 as a gross error and the final estimated values of both measured and unmeasured variables are shown in Table 2.7. The results are very close to the results obtained by Tjoa's method[16]. And the computation time depends on the number of iterations of **Algorithm 1** and the CONOPT solver. As an average, **Algorithm 1** finishes in around 4 seconds within 10 iterations.

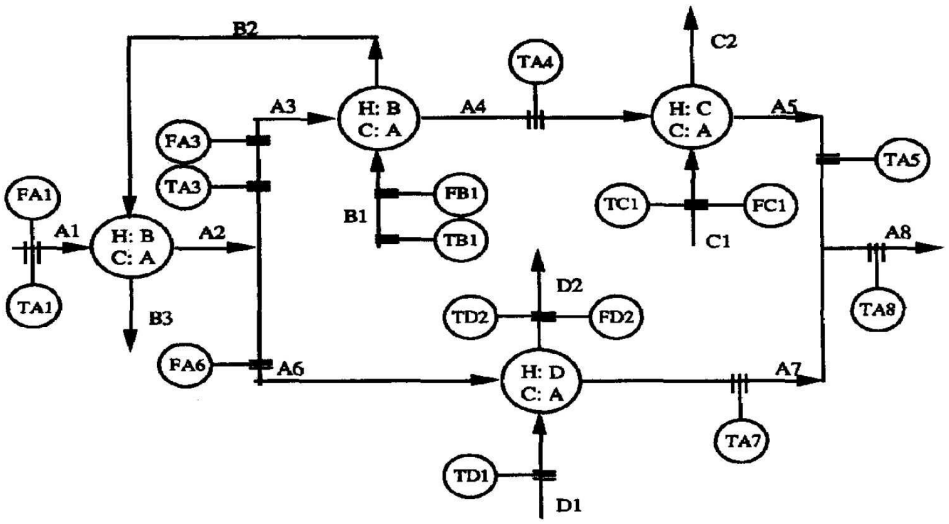

Figure 2.12: Flow sheet of the process for Swartz's example[16]

Table 2.7: Estimated variables for Swartz's example with TA7 as a gross error

Variable tagname	Estimates of variables (Tjoa)	Estimates of variables (**Algorithm 1**)	Estimated σ (**Algorithm 1**)
FA1	968.38	963.84	21.75
TA1	466.33	466.31	0.8301
FA2	968.38	963.84	-
TA2	481.79	478.01	-
FA3	406.71	408.39	9.0927
TA3	481.79	478.01	0.6939
FA4	406.71	408.39	-
TA4	530.09	530.08	0.5892
FA5	406.71	408.39	-
TA5	616.21	613.58	0.6807
FA6	561.71	555.45	9.7999
TA6	481.79	478.01	-
FA7	561.67	555.45	-
TA7	614.38	617.79	0.6912
FA8	968.38	963.84	-
TA8	615.15	611.77	0.9952
FB1	253.20	253.30	4.8389
TB1	618.11	618.22	0.7844
FB2	253.20	253.30	-
TB2	543.86	545.76	-
FB3	253.20	253.30	-
TB3	486.58	492.65	-
FC1	308.10	307.02	8.0189
TC1	694.99	695.49	0.8827
FC2	308.10	307.02	-
TC2	594.21	605.98	–
FD1	680.88	688.01	
TD1	667.86	668.84	0.8884
FD2	680.88	688.01	12.4112
TD2	558.33	564.28	0.6693

2.6 Conclusions

Gross error detection and data reconciliation problem is studied in this chapter. A unified framework is proposed to simultaneously estimate the true values of process variables x and u, the magnitudes of the gross errors δ, the covariance matrix Σ of the random error and the gross error indicator matrix η. In order to reduce the solution complexity of directly

solving the MAP problem, a hierarchical Bayesian framework is developed. The layered scheme allows us to obtain MAP estimates of the correct values of the measurements x, the magnitudes of the gross errors δ in the first layer, the covariance matrix Σ of the random error in the second layer and the gross error indicator matrix η in the third layer. To enhance the performance of the hierarchical Bayesian algorithm, the serial strategy is combined with the hierarchical Bayesian algorithm. The proposed method is not very sensitive to noise so that it can handle a large standard deviation of the noise. The proposed method is applicable to both linear and nonlinear cases. For linear case, the analytical forms of estimated values of the correct values of variables and magnitudes of gross errors are obtained. For nonlinear case, there is no need to do linearization or approximation in the proposed method.

The effectiveness of the proposed Bayesian approach and the serial strategies for simultaneous gross error detection and data reconciliation problem are demonstrated on simulated data-sets. In the linear case, it is shown that the serial strategy is able to improve the performance under this situation. The results show that if the gross errors are correctly detected, the estimations of other variables will be very close to the exact values.

Chapter 3

Robust Optimization Approximation for Joint Chance Constrained Optimization Problem

3.1 Introduction

In many optimization applications, it is assumed that the problem data are known and certain. However, uncertainties exist in almost every different realistic problem due to the random nature of the process data, measurement errors or other reasons. If the uncertainties are ignored while solving the optimization problem, it may lead to suboptimal or even infeasible solutions for practical applications. Thus, handling uncertainties in optimization problem becomes a crucial issue in both the academic and practical fields. Chance constraints and robust optimization are two popular ways to model and solve the optimization problems with uncertainty. Chance constraints quantify the uncertainty using probability distribution, which place a restriction on the probability of constraint satisfaction. On the other hand, robust optimization is a distribution-free approach to solving optimization problems with uncertainty. The main idea of robust optimization is to include the uncertainty in a given uncertainty set such that all the realizations in the uncertainty set will satisfy the constraints.

Chance constraint problem with a single constraint lying in the probability term is referred to as ICC, which has been studied and proved to be tractable with specific distributions and conditions [22, 23, 24]. However, if there are multiple constraints inside the probability term, which is known as JCC problem, the problem cannot be directly solved in general, and approaches should be developed to approximate JCC into tractable problems.

In this chapter, the application of the robust counterpart optimization to approximate the joint chance constrained problem is studied. First, the joint chance constraint is transformed into an individual chance constraint with the aid of the maximization operator. Then, the individual chance constraint is approximated by the robust optimization formulation through probability inequalities. Finally, different formulations of robust optimization are derived based on different types of uncertainty set. To improve the approximation and reduce the solution conservativeness, a two-layer optimization algorithm is proposed. The inner layer aims to reduce the size of the uncertainty set while satisfying the desired solution reliability, and the outer layer optimizes over a parameter t used for upper bounding the indicator function. The performance of the robust optimization approximation and the proposed improvement method is demonstrated through different examples.

The rest of this chapter is organized as follows. In Section 3.2, the joint chance constrained problem under investigation is presented with a general form. In Section 3.3, the joint chance constraints are approximated by uncertainty set induced robust counterpart optimization formulation based on different types of uncertainty set. In Section 3.4, a two-layer algorithm is proposed to improve the robust optimization approximation. An iterative algorithm is applied to select the appropriate set size in the inner layer. The outer layer performs optimization over the parameter t which is used in indicator function upper bounding. A norm optimization problem and a probabilistic transportation problem are studied to demonstrate the performance of the proposed method in Section 3.5. The chapter is concluded in Section 3.6.

3.2 Problem Statement

A general chance constrained optimization problem takes the following form:

$$\begin{aligned} \min_{x \in X} \quad & f(x) \\ \text{s.t.} \quad & P\{G(x,\xi) \leq 0\} \geq 1-\varepsilon \end{aligned} \tag{3.1}$$

where $G(x,\xi) = [g_1(x,\xi) \ \cdots \ g_n(x,\xi)]^T$, $\boldsymbol{\xi}$ is a random vector with support $\Xi \subseteq R^m$. The above constraint is an individual chance constraint with $n = 1$, and a joint chance constraint with $n > 1$.

In this chapter, the following linear joint chance constraint is considered

$$P\left(y_0^i + \sum_{k=1}^{m} y_k^i \xi_k \leq 0, i = 1,2,...,n\right) \geq 1-\varepsilon \tag{3.2}$$

The vector form representation of the joint chance constraint in (3.2) is as follows:

$$P\left(y_0^i + (\mathbf{y}^i)^T \boldsymbol{\xi} \leq 0, i = 1,2,...,n\right) \geq 1-\varepsilon \tag{3.3}$$

where $\mathbf{y}^i = [y_1^i \ y_2^i \ \cdots \ y_m^i]^T$, and $\boldsymbol{\xi} = [\xi_1 \ \xi_2 \ \cdots \ \xi_m]^T$. In this chapter, without loss of generality, it is assumed that the uncertain parameters ξ_k are normalized from random variable X. The normalization is $(X-\mu)/\sigma$ for unbounded distribution using the mean μ and standard deviation σ, or $(X - X_{min})/(X_{max} - X_{min})$ for bounded distribution using upper and lower bounds.

Robust optimization approximation for the joint chance constraint (3.3) will be derived in the subsequent section.

3.3 Robust Optimization Approximation

3.3.1 Approximation of JCC

Joint chance constraint (3.3) can be transformed into an individual chance constraint problem by introducing the maximization operator. The equivalent expression of (3.3) is

$$P\left(\max_i \left\{y_0^i + (\mathbf{y}^i)^T \boldsymbol{\xi}\right\} \leq 0\right) \geq 1 - \varepsilon \tag{3.4}$$

or

$$P\left(\max_i \left\{y_0^i + (\mathbf{y}^i)^T \boldsymbol{\xi}\right\} > 0\right) \leq \varepsilon \tag{3.5}$$

The general robust optimization approximation model for the joint chance constraint (3.3) can be further derived based on the above individual chance constraint, and the approximation is given by the following property.

Property 1. *An inner approximation of chance constraint (3.5) is given by*

$$\begin{cases} \phi + \sum_i \gamma^i \leq \varepsilon t \\ \phi \geq u_0 + \max_{\boldsymbol{\xi} \in U} \boldsymbol{\xi}^T \mathbf{u} \\ \phi \geq 0 \\ \gamma^i \geq v_0^i + \max_{\boldsymbol{\xi} \in U} \boldsymbol{\xi}^T \mathbf{v}^i \quad \forall i \\ \gamma^i \geq 0 \quad \forall i \\ u_0 = w_0 + t \\ \mathbf{u} = \mathbf{w} \\ v_0^i = \alpha_i y_0^i - w_0 \quad \forall i \\ \mathbf{v}^i = \alpha_i \mathbf{y}^i - \mathbf{w} \quad \forall i \end{cases} \tag{3.6}$$

where $t > 0$, $\alpha_i > 0$, $i = 1, 2, ..., n$, U *is the support of uncertainty for random vector* $\boldsymbol{\xi}$, $\mathbf{w} = [w_1\ w_2\ \cdots\ w_m]^T$, $\mathbf{u} = [u_1\ u_2\ \cdots\ u_m]^T$, $\mathbf{y}^i = [y_1^i\ y_2^i\ \cdots\ y_m^i]^T$ *and* $\mathbf{v}^i = [v_1^i\ v_2^i\ \cdots\ v_m^i]^T$.

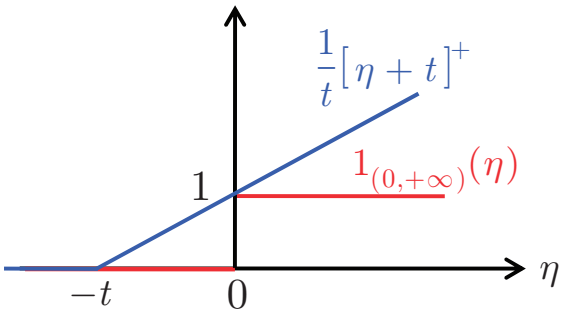

Figure 3.1: Illustration of the upper bound on the indicator function

Proof. The proof follows the idea introduced by Chen et al. [49]. First, Inequality (3.5) is equivalent to the following Inequality (3.7) by introducing auxiliary variable $\alpha_i > 0$, $i = 1, 2, .., n$

$$P\left(\max_i \left\{\alpha_i y_0^i + \alpha_i (\mathbf{y}^i)^T \boldsymbol{\xi}\right\} > 0\right) \leq \varepsilon \tag{3.7}$$

Define $\eta = \max_i \left\{\alpha_i y_0^i + \alpha_i (\mathbf{y}^i)^T \boldsymbol{\xi}\right\}$, Inequality (3.7) can be rewritten as

$$P\{\eta > 0\} \leq \varepsilon \tag{3.8}$$

The left hand side of Inequality (3.8) can be equivalently written as follows using indicator function,

$$P\{\eta > 0\} = E\left[1_{(0,+\infty)}(\eta)\right] \tag{3.9}$$

Apply an upper bound $\frac{1}{t}[\eta + t]^+$ (with $t > 0$, $[u]^+$ takes value u if u is positive and 0 otherwise) on the indicator function $1_{(0,+\infty)}(\eta)$ as shown in Figure 3.1, it is obtained that

$$P\{\eta > 0\} = E\left[1_{(0,+\infty)}(\eta)\right] \leq E\left\{\frac{1}{t}[\eta + t]^+\right\} = \frac{1}{t}E\left\{[\eta + t]^+\right\} \tag{3.10}$$

Applying the relation in Inequality (3.10) to Inequality (3.7),

$$P\left(\max_i \left\{\alpha_i y_0^i + \alpha_i (\mathbf{y}^i)^T \boldsymbol{\xi}\right\} > 0\right) \leq \frac{1}{t}E\left[\left(\max_i \left\{\alpha_i y_0^i + \alpha_i (\mathbf{y}^i)^T \boldsymbol{\xi}\right\} + t\right)^+\right] \tag{3.11}$$

Next, the right-hand-side of the above equation is further approximated with the Meilijson and Nadas inequality on the expected maximum [79] :

$$E\left[\left(\max_i X_i + t\right)^+\right] \leq E\left[(Y+t)^+\right] + \sum_i E\left[(X_i - Y)^+\right] \qquad for\ any\ r.v.\ Y \tag{3.12}$$

where X_i are random variables. Let $Y = w_0 + \mathbf{w}^T\boldsymbol{\xi}$, where $\mathbf{w} = [w_1\ w_2\ \cdots\ w_m]^T$, and apply the above inequality for the expectation term in Inequality (3.11),

$$\begin{aligned} &E\left[\left(\max_i \left\{\alpha_i y_0^i + \alpha_i (\mathbf{y}^i)^T\boldsymbol{\xi}\right\} + t\right)^+\right] \\ &\leq E\left[\left(w_0 + \mathbf{w}^T\boldsymbol{\xi} + t\right)^+\right] + \sum_i E\left[\left(\alpha_i y_0^i + \alpha_i (\mathbf{y}^i)^T\boldsymbol{\xi} - w_0 - \mathbf{w}^T\boldsymbol{\xi}\right)^+\right] \end{aligned} \tag{3.13}$$

Define $u_0 = w_0 + t$, $\mathbf{u} = \mathbf{w}$, $v_0^i = \alpha_i y_0^i - w_0$ and $\mathbf{v}^i = \alpha_i \mathbf{y}^i - \mathbf{w}$, Inequality (3.13) can be written as

$$\begin{aligned} &E\left[\left(\max_i \left\{\alpha_i y_0^i + \alpha_i (\mathbf{y}^i)^T\boldsymbol{\xi}\right\} + t\right)^+\right] \\ &\leq E\left[\left(u_0 + \mathbf{u}^T\boldsymbol{\xi}\right)^+\right] + \sum_i E\left[\left(v_0^i + (\mathbf{v}^i)^T\boldsymbol{\xi}\right)^+\right] \end{aligned} \tag{3.14}$$

which is equivalent to

$$\begin{aligned} &E\left[\left(\max_i \left\{\alpha_i y_0^i + \alpha_i (\mathbf{y}^i)^T\boldsymbol{\xi}\right\} + t\right)^+\right] \\ &\leq E\left[\left(u_0 + \boldsymbol{\xi}^T\mathbf{u}\right)^+\right] + \sum_i E\left[\left(v_0^i + \boldsymbol{\xi}^T\mathbf{v}^i\right)^+\right] \end{aligned} \tag{3.15}$$

As introduced by Chen and Sim [50], when U is the support of uncertainty, an upper bound of the expectation term in (3.15) is given by

$$E\left[\left(\mu_0 + \boldsymbol{\xi}^T\boldsymbol{\mu}\right)^+\right] \leq \left(\mu_0 + \max_{\boldsymbol{\xi}\in U} \boldsymbol{\xi}^T\boldsymbol{\mu}\right)^+ \tag{3.16}$$

Based on Inequality (3.15) and (3.16), the following relation holds

$$\begin{aligned} & E\left[\left(\max_i \left\{\alpha_i y_0^i + \alpha_i (\mathbf{y}^i)^T \boldsymbol{\xi}\right\} + t\right)^+\right] \\ & \leq (u_0 + \max_{\boldsymbol{\xi}\in U} \boldsymbol{\xi}^T \mathbf{u})^+ + \sum_i (v_0^i + \max_{\boldsymbol{\xi}\in U} \boldsymbol{\xi}^T \mathbf{v}^i)^+ \end{aligned} \tag{3.17}$$

and after applying Inequality (3.17) to Inequality (3.11),

$$\begin{aligned} & P\left(\max_i \left\{\alpha_i y_0^i + \alpha_i (\mathbf{y}^i)^T \boldsymbol{\xi}\right\} > 0\right) \\ & \leq \tfrac{1}{t}\left\{(u_0 + \max_{\boldsymbol{\xi}\in U} \boldsymbol{\xi}^T \mathbf{u})^+ + \sum_i (v_0^i + \max_{\boldsymbol{\xi}\in U} \boldsymbol{\xi}^T \mathbf{v}^i)^+\right\} \end{aligned} \tag{3.18}$$

So an inner approximation to $P\left(\max_i \left\{\alpha_i y_0^i + \alpha_i (\mathbf{y}^i)^T \boldsymbol{\xi}\right\} > 0\right) \leq \varepsilon$ is

$$\frac{1}{t}\left\{(u_0 + \max_{\boldsymbol{\xi}\in U} \boldsymbol{\xi}^T \mathbf{u})^+ + \sum_i (v_0^i + \max_{\boldsymbol{\xi}\in U} \boldsymbol{\xi}^T \mathbf{v}^i)^+\right\} \leq \varepsilon \tag{3.19}$$

which is further equivalent to

$$(u_0 + \max_{\boldsymbol{\xi}\in U} \boldsymbol{\xi}^T \mathbf{u})^+ + \sum_i (v_0^i + \max_{\boldsymbol{\xi}\in U} \boldsymbol{\xi}^T \mathbf{v}^i)^+ \leq \varepsilon t \tag{3.20}$$

Defining auxiliary variables $\phi = (u_0 + \max_{\boldsymbol{\xi}\in U} \boldsymbol{\xi}^T \mathbf{u})^+$ and $\gamma^i = (v_0^i + \max_{\boldsymbol{\xi}\in U} \boldsymbol{\xi}^T \mathbf{v}^i)^+$, Inequality (3.20) is simplified as

$$\phi + \sum_i \gamma^i \leq \varepsilon t \tag{3.21}$$

where the $(\cdot)^+$ terms can be further removed in the following equivalent formulation,

$$\begin{cases} \phi + \sum_i \gamma^i \leq \varepsilon t \\ \phi \geq u_0 + \max_{\boldsymbol{\xi}\in U} \boldsymbol{\xi}^T \mathbf{u} \\ \phi \geq 0 \\ \gamma^i \geq v_0^i + \max_{\boldsymbol{\xi}\in U} \boldsymbol{\xi}^T \mathbf{v}^i \quad \forall i \\ \gamma^i \geq 0 \quad \forall i \end{cases} \tag{3.22}$$

To summarize, a safe approximation to the chance constraint (3.5) is given by

$$\begin{cases} \phi + \sum_i \gamma^i \leq \varepsilon t \\ \phi \geq u_0 + \max_{\boldsymbol{\xi} \in U} \boldsymbol{\xi}^T \mathbf{u} \\ \phi \geq 0 \\ \gamma^i \geq v_0^i + \max_{\boldsymbol{\xi} \in U} \boldsymbol{\xi}^T \mathbf{v}^i \quad \forall i \\ \gamma^i \geq 0 \quad \forall i \\ u_0 = w_0 + t \\ \mathbf{u} = \mathbf{w} \\ v_0^i = \alpha_i y_0^i - w_0 \quad \forall i \\ \mathbf{v}^i = \alpha_i \mathbf{y}^i - \mathbf{w} \quad \forall i \end{cases} \tag{3.23}$$

□

In *Property 1*, probability bounds, in Inequality (3.10), Inequality (3.13) and Inequality (3.16), are used to approximate the original joint chance constraints. A convex piecewise linear function is used in Inequality (3.10) to upper bound the indicator function, which can keep the problem convex. In Inequality (3.13), the Meilijson and Nadas inequality shown in Inequality (3.11) are used to upper bound the expected maximum to eliminate the maximizing term. In Inequality (3.16), an upper bound on the expected term was used, which connects the approximation to uncertainty set induced robust optimization.

One of the major advantage of using these bounds is that finally the uncertainties are still in affine structure of the robust optimization formulation, which can be effectively solved. By adjusting the set size parameter Δ and the intercept parameter t with the proposed two-layer algorithm, the bounds can be further tightened and the solutions can be improved.

Based on *Property 1*, different formulations of uncertainty set induced robust counterpart optimization can be derived based on different types of uncertainty set U.

3.3.2 Robust Optimization Approximation Formulations

While the uncertainty set U covers the whole support of uncertainty distribution, it leads to the worst case scenario approximation for joint chance constraint (3.5). Correspondingly, any feasible solution of the robust optimization problem will be a feasible solution to the original joint chance constrained problem. However, the solution can be too conservative if the set U is designed to cover the full uncertainty space. To seek trade-off between conservativeness and robustness, the uncertainty set U can be designed based on the desired level of constraint satisfaction probability. Li et al. [48] investigated different types of uncertainty set for robust optimization, including box, ellipsoidal, polyhedral, interval+ellipsoidal (IE), and interval+polyhedral (IP), etc. They also developed different formulations of the robust counterpart corresponding to each type of uncertainty set.

For the following uncertain constraint

$$\sum_j \xi_j x_j \leq b, \tag{3.24}$$

the uncertainty set induced robust counterpart optimization constraint is

$$\max_{\xi \in U(\Delta)} \sum_j \xi_j x_j \leq b \tag{3.25}$$

For example, with box uncertainty set $U_{box} = \{\xi \,|\, |\xi_j| \leq \Delta, \forall j\}$, the robust counterpart optimization constraint (3.25) is equivalent to:

$$\Delta \sum_j |x_j| \leq b \tag{3.26}$$

where the absolute value operator can be further eliminated and the equivalent formulation is

$$\begin{cases} \Delta \sum_j p_j \leq b \\ -p_j \leq x_j \leq p_j \quad \forall j \end{cases} \tag{3.27}$$

The above robust counterpart optimization formulations can be applied to the robust optimization approximation model (3.6) for the joint chance constrained problem as shown in the following property.

Property 2. *For the joint chance constraint (3.3), with a box type uncertainty set defined as* $U_{box} = \{\xi \,|\, |\xi_k| \leq \Delta,\ k = 1, .., m\}$*, the corresponding robust optimization approximation model (3.6) is equivalent to*

$$\begin{cases} \phi + \sum_i \gamma^i \leq \varepsilon t \\ \phi \geq u_0 + \Delta \sum_k p_k \\ -p_k \leq u_k \leq p_k \quad \forall k \\ \phi \geq 0 \\ \gamma^i \geq v_0^i + \Delta \sum_k q_k^i \quad \forall i \\ -q_k^i \leq v_k^i \leq q_k^i \quad \forall i, k \\ \gamma^i \geq 0 \quad \forall i \\ u_0 = w_0 + t \\ \mathbf{u} = \mathbf{w} \\ v_0^i = \alpha_i y_0^i - w_0 \quad \forall i \\ \mathbf{v}^i = \alpha_i \mathbf{y}^i - \mathbf{w} \quad \forall i \end{cases} \tag{3.28}$$

where Δ *is the adjustable set size of the box, and* p_k *and* q_k^i *are the auxiliary variables.*

Following the same idea, the robust optimization approximation model (3.6) can be reformulated based on the type of uncertainty set following the derivation provided by Li et al. [48]. They are given in the following properties.

Property 3. *For the joint chance constraint (3.3), with a polyhedral type uncertainty set defined as* $U_{polyhedral} = \left\{ \xi \,\middle|\, \sum_{k=1}^{m} |\xi_k| \leq \Delta \right\}$*, the corresponding robust optimization approximation*

model (3.6) is equivalent to

$$\begin{cases} \phi + \sum_i \gamma^i \leq \varepsilon t \\ \phi \geq u_0 + \Delta z_0 \\ z_0 \geq p_k \quad \forall k \\ -p_k \leq u_k \leq p_k \quad \forall k \\ \phi \geq 0 \\ \gamma^i \geq v_0^i + \Delta z_i \quad \forall i \\ z_i \geq q_k^i \quad \forall i, k \\ -q_k^i \leq v_k^i \leq q_k^i \quad \forall i, k \\ \gamma^i \geq 0 \quad \forall i \\ u_0 = w_0 + t \\ \mathbf{u} = \mathbf{w} \\ v_0^i = \alpha_i y_0^i - w_0 \quad \forall i \\ \mathbf{v}^i = \alpha_i \mathbf{y}^i - \mathbf{w} \quad \forall i \end{cases} \tag{3.29}$$

Property 4. *For the joint chance constraint (3.3), with an ellipsoidal type uncertainty set defined as* $U_{ellipsoid} = \left\{ \xi \,\middle|\, \sum_{k=1}^{m} \xi_k^2 \leq \Delta^2 \right\}$*, the corresponding robust optimization approximation*

model (3.6) is equivalent to

$$\begin{cases} \phi + \sum_i \gamma^i \leq \varepsilon t \\ \phi \geq u_0 + \Delta \sqrt{\sum_k u_k^2} \\ \phi \geq 0 \\ \gamma^i \geq v_0^i + \Delta \sqrt{\sum_k \left(v_k^i\right)^2} \quad \forall i \\ \gamma^i \geq 0 \quad \forall i \\ u_0 = w_0 + t \\ \mathbf{u} = \mathbf{w} \\ v_0^i = \alpha_i y_0^i - w_0 \quad \forall i \\ \mathbf{v}^i = \alpha_i \mathbf{y}^i - \mathbf{w} \quad \forall i \end{cases} \tag{3.30}$$

Property 2-4 are appropriate for joint chance constraint under unbounded uncertainty distribution, since the uncertainty set size Δ can be sufficiently large (while the robust optimization problem is still feasible) to achieve the desired probability level of constraint satisfaction. The following two properties provide robust optimization approximations for joint chance constraint under bounded uncertainty distribution. without loss of generality, it is assumed that the uncertain parameters ξ_k distribute in the range [-1, 1].

Property 5. *For the joint chance constraint (3.3), with a interval+polyhedral type uncertainty set defined as* $U_{in+poly} = \left\{ \xi \left| \sum_{k=1}^{m} |\xi_k| \leq \Delta,\ |\xi_k| \leq 1,\ k = 1, ..m \right. \right\}$ *, the corresponding*

robust optimization approximation model (3.6) is equivalent to

$$
\begin{cases}
\phi + \sum_i \gamma^i \leq \varepsilon t \\
\phi \geq u_0 + \Delta z_0 + \sum_k s_k^0 \\
z_0 + s_k^0 \geq p_k \quad \forall k \\
-p_k \leq u_k \leq p_k \quad \forall k \\
z_0 \geq 0,\ s_k^0 \geq 0,\ \phi \geq 0 \\
\gamma^i \geq v_0^i + \Delta z_i + \sum_k s_k^i \quad \forall i \\
z_i + s_k^i \geq q_k^i \quad \forall i, k \\
-q_k^i \leq v_k^i \leq q_k^i \quad \forall i, k \\
z_i \geq 0,\ s_k^i \geq 0,\ \gamma^i \geq 0 \quad \forall i \\
u_0 = w_0 + t \\
\mathbf{u} = \mathbf{w} \\
v_0^i = \alpha_i y_0^i - w_0 \quad \forall i \\
\mathbf{v}^i = \alpha_i \mathbf{y}^i - \mathbf{w} \quad \forall i
\end{cases}
\tag{3.31}
$$

Property 6. *For the joint chance constraint (3.3), with a interval+ellipsoidal type uncertainty set defined as* $U_{in+ellip} = \left\{ \xi \,\middle|\, \sum_{k=1}^{m} \xi_k^2 \leq \Delta^2,\ |\xi_k| \leq 1, k = 1, ..., m \right\}$*, the corresponding*

robust optimization approximation model (3.6) is equivalent to

$$\begin{cases} \phi + \sum_i \gamma^i \le \varepsilon t \\ \phi \ge u_0 + \Delta \sqrt{\sum_k \left(r_k^0\right)^2} + \sum_k |u_k - r_k^0| \\ \phi \ge 0 \\ \gamma^i \ge v_0^i + \Delta \sqrt{\sum_k \left(r_k^i\right)^2} + \sum_k |v_k^i - r_k^i| \quad \forall i \\ \gamma^i \ge 0 \quad \forall i \\ u_0 = w_0 + t \\ \mathbf{u} = \mathbf{w} \\ v_0^i = \alpha_i y_0^i - w_0 \quad \forall i \\ \mathbf{v}^i = \alpha_i \mathbf{y}^i - \mathbf{w} \quad \forall i \end{cases} \tag{3.32}$$

Due to the bilinear terms involving variables α_i, the robust formulations based on the above five uncertainty sets are non-convex problems. However, with fixed value of α_i, the robust formulations based on box, polyhedral and interval+polyhedral uncertainty sets are linear optimization problem, and the robust formulations based on ellipsoidal and interval+ellipsoidal uncertainty sets are second order cone programming problem.

For fixed parameter t and Δ, the complete robust optimization approximation model and solution for the joint chance constraint problem (3.2) is given as

$$\begin{aligned} x_{RO}(t,\Delta) &= \arg\min_{x \in X} \{f(x), \text{s.t.(32)or(33)or(34)or(35)or(36)}\} \\ f_{RO}(t,\Delta) &= f(x_{RO}) \end{aligned} \tag{3.33}$$

With the robust solution, the probability of joint chance constraint satisfaction can be estimated with Monte Carlo sampling technique: if N samples are tested on the joint constraint, then the estimation is given by

$$p_{RO}^{satisfaction}(t,\Delta) = \frac{1}{N} \sum_{s=1}^{N} 1_{(0,\infty)} \left(\max_i \left\{ y_0^i + \left(\mathbf{y}^i\right)^T \boldsymbol{\xi}^{(s)} \right\} \le 0 \right) \tag{3.34}$$

For the robust optimization approximation problem with a fixed type of the uncertainty set, the relationships between the optimal objective value and the size of the uncertainty set, the probability of constraint satisfaction and the size of the uncertainty set are shown in the following example.

Example 1

Consider the following joint chance constrained problem:

$$\begin{aligned} \max \quad & 8x_1 + 12x_2 \\ s.t. \quad & P\left\{ \begin{array}{l} \tilde{a}_1 x_1 + \tilde{a}_2 x_2 \leq 140 \\ \tilde{a}_3 x_1 + \tilde{a}_4 x_2 \leq 72 \end{array} \right\} \geq 1 - \varepsilon \\ & x_1, x_2 \geq 0 \end{aligned} \tag{3.35}$$

There are uncertainties in the constraint coefficients, which are described as $\tilde{a}_1 = 10 + \xi_1$, $\tilde{a}_2 = 20 + 2\xi_2$, $\tilde{a}_3 = 6 + 0.6\xi_3$, and $\tilde{a}_4 = 8 + 0.8\xi_4$. It is assumed that ξ_1, ξ_2, ξ_3 and ξ_4 follow independent uniform distributions in the range $[-1, 1]$. The reliability level is set as $\varepsilon = 0.2$ (i.e., the desired probability of satisfaction is 0.8) and the corresponding joint chance constrained problem is studied.

To write the joint chance constraint in this example into the general form, it can be observed that the uncertainties in this example are in a linear structure. For a general formulation of the linear structured uncertainties, we have the following constraint representing each constraint in a joint chance constrained problem:

$$\begin{aligned} & \left(a_1^0 + a_1^1\xi_1 + \cdots + a_1^m\xi_m\right) x_1 + \left(a_2^0 + a_2^1\xi_1 + \cdots + a_2^m\xi_m\right) x_2 + \cdots \\ & + \left(a_p^0 + a_p^1\xi_1 + \cdots + a_p^m\xi_m\right) x_p \leq \left(b^0 + b^1\xi_1 + \cdots + b^m\xi_m\right) \end{aligned} \tag{3.36}$$

where a_j^k and b^k $(j = 1, ..., p,\ k = 0, ..., m)$ are known constants, and ξ_k $(k = 1, ..., m)$ are uncertain parameters, p and m are the number of decision variables and the number of uncertain parameters, respectively.

Constraint (3.36) can be rearranged as

$$\begin{aligned}&\left(a_1^0x_1+a_2^0x_2+\cdots+a_p^0x_p-b^0\right)+(a_1^1x_1+a_2^1x_2+\cdots+a_p^1x_p-b^1)\xi_1+\cdots\\&+(a_1^mx_1+a_2^mx_2+\cdots+a_p^mx_p-b^m)\xi_m\leq 0\end{aligned}\tag{3.37}$$

Define

$$\begin{aligned}y_0&=\sum_{j=1}^{p}a_j^0x_j-b^0\\y_k&=\sum_{j=1}^{p}a_j^kx_j-b^k,\ k=1,...,m\end{aligned}\tag{3.38}$$

Then constraint (3.37) becomes

$$y_0+\sum_{k=1}^{m}y_k\xi_k\leq 0\tag{3.39}$$

With the above procedure, the joint chance constraints with linear combination of uncertainties can be reformulated into the general form considered in this chapter (see Inequality (3.3)). In this example, the joint chance constraint can be reformulated as $P\left(\max_i\left\{y_0^i+(\mathbf{y}^i)^T\boldsymbol{\xi}\right\}>0\right)\leq\varepsilon$ with the following definitions:

$$\begin{aligned}y_0^1&=10x_1+20x_2-140\\y_0^2&=6x_1+8x_2-72\\y^1&=\begin{bmatrix}x_1&2x_2&0&0\end{bmatrix}^T\\y^2&=\begin{bmatrix}0&0&0.6x_1&0.8x_2\end{bmatrix}^T\end{aligned}\tag{3.40}$$

Since this problem contains bounded uncertainties, the robust counterpart optimization constraints can be formulated using the box, IP, and IE type of uncertainty set, respectively. Figure 3.2 shows the relationships between the objective value/probability of satisfaction and the set size. It is observed that the objective value decreases as the set size increases, which means that a larger set size leads to a more conservative robust optimization approximation. On the other hand, the probability of satisfaction (simulated with 100,000 samples) is higher

with a larger set size. There is a trade-off between the optimal objective value and the probability of constraint satisfaction. For all the three types of approximations, the solution of the robust optimization approximation can satisfy the desired target 0.8 with a set size value less than 1, which verifies that it is not necessary to design the uncertainty set U to cover the whole uncertainty space. Moreover, the box uncertainty set leads to the most conservative approximation among the three types and the IE uncertainty set provides the least conservative approximation.

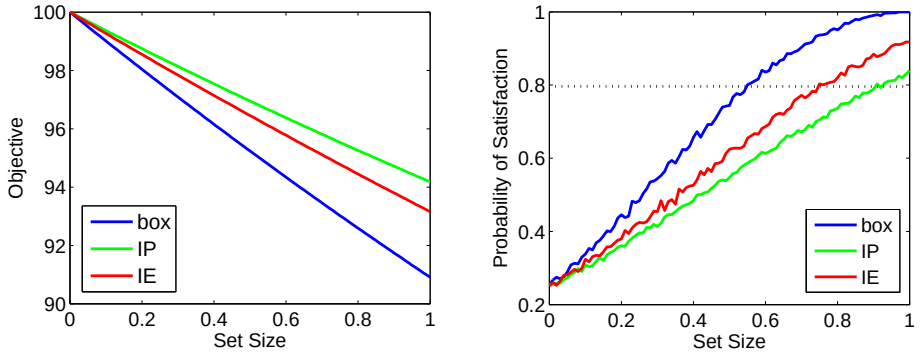

Figure 3.2: Robust optimization approximation with different uncertainty sets

The above robust optimization approximation framework contains several factors that affect the conservativeness of the approximation: the size of the uncertainty set Δ, the value of t and the values of α_i. Introducing α in the maximizing term in Inequality (3.7) is to add a weight on different constraints. Optimizing α is similar as optimizing ϵ_i ($\sum_i \epsilon_i \leq \epsilon$) for each individual constraint in Bonferroni's inequality approximation. It would improve the performance of the robust optimization approximation framework if α is treated as design variables rather than as parameters. However, if parameters α_i are considered as variables, the robust optimization approximation problem includes bilinear terms and become non-convex. To make the approximation problem tractable, the simplest way is to set $\alpha_i = 1, i = 1, 2, ..., n$, which is the similar idea as in Bonferroni's inequality approximation setting $\epsilon_i = \epsilon/n$. This chapter focuses on the optimization over the size of the uncertainty set Δ and the value of the parameter t. The influence of the selection of α will be discussed using example 2.

3.4 Improve the Robust Optimization Approximation

To improve the robust optimization approximation for the joint chance constrained problem, the optimal objective value should be improved while the robust solution satisfies the target reliability. This can be represented by the following optimization problem.

$$\begin{aligned} \min_{t,\Delta} \quad & f_{RO}(t,\Delta) \\ s.t. \quad & p_{RO}^{satisfaction}(t,\Delta) \geq 1-\varepsilon \end{aligned} \tag{3.41}$$

The distribution about the uncertainty is applied in calculating the simulated probability of satisfaction (explained in Equation (3.34)). The simulated probability of satisfaction is important in adjusting the set size and the value of t for the proposed two-layer algorithm which aims to find the best objective value that meets the probability of satisfaction requirement. This is the step where the comprehensive distribution information is applied.

Since the objective function and the constraint rely on the solution of the robust optimization problem, a two-layer algorithm is proposed for the above problem. In the inner layer, the set size Δ is adjusted with a fixed parameter t. In the outer layer, the value of t is optimized.

3.4.1 Optimization over Uncertainty Set Size Δ

The joint chance constrained problem has been approximated by the uncertainty set induced robust optimization with different formulations corresponding to different types of uncertainty set in Section 3.3. As shown in Example 1, for the same type of uncertainty set, when the set size increases (leading to a smaller feasible region for the robust optimization problem), the optimal objective value of the robust optimization problem will decrease (for a maximizing problem). That is, a larger set size leads to a more conservative solution for the chance constrained problem. In other words, to reduce the conservativeness, the set size should be as small as possible. However, a too small set size cannot cover enough informa-

tion about the uncertainties, which will violate the desired solution reliability of the original chance constrained problem. Uncertainty set size design is a crucial issue for the trade-off between conservativeness and robustness.

Table 3.1: Algorithm for optimization over the set size

Algorithm for set size optimization

Fix t, initialize the lower bound and the upper bound for the set size $[lb, ub] = [a, b]$,
set $size = 0.5(a + b)$
set reliability level ε
while $(|P_{sat} - (1 - \varepsilon)| > tolerance)$
    Solve robust optimization problem and evaluate the probability of
    satisfaction P_{sat}
    if $(P_{sat} < 1 - \varepsilon)$
        $lb = size$
    else$(P_{sat} > 1 - \varepsilon)$
        $ub = size$
    end
    $size = 0.5(lb + ub)$
end

Li and Floudas [56] proposed an iterative algorithm to select the proper uncertainty set size. There is a desired degree of constraint satisfaction in the joint chance constrained problem. The main idea of the iterative method is to reduce the gap between the desired satisfaction level and the true probability of satisfaction by adjusting the set size through iterations. In each iteration, the set size is adjusted based on solution validation. For the current robust solution, if the probability of constraint satisfaction is greater than the desired level, the set size is decreased, and if the probability of constraint satisfaction is less than the desired level, the set size will be increased. The adjustment is repeated until the gap between the desired satisfaction level and the actual probability of satisfaction is within a pre-defined tolerance. The algorithm is shown in Table 3.1.

Example 1 (continued)

The set size optimization algorithm is applied to design the size of the uncertainty set. The box uncertainty set based robust approximation model is applied here. The algorithm stops

after six iterations and it takes two seconds. Figure 3.3 shows the changes of the probability of constraint satisfaction, the optimal objective value and the set size with the iterations, respectively. The final solution satisfies the joint constraint with probability 0.8089. At the end of the iterative algorithm, a relatively small set size 0.5690 is found and the corresponding optimal objective value is 94.62, which is improved from value 80.0 of the first iteration.

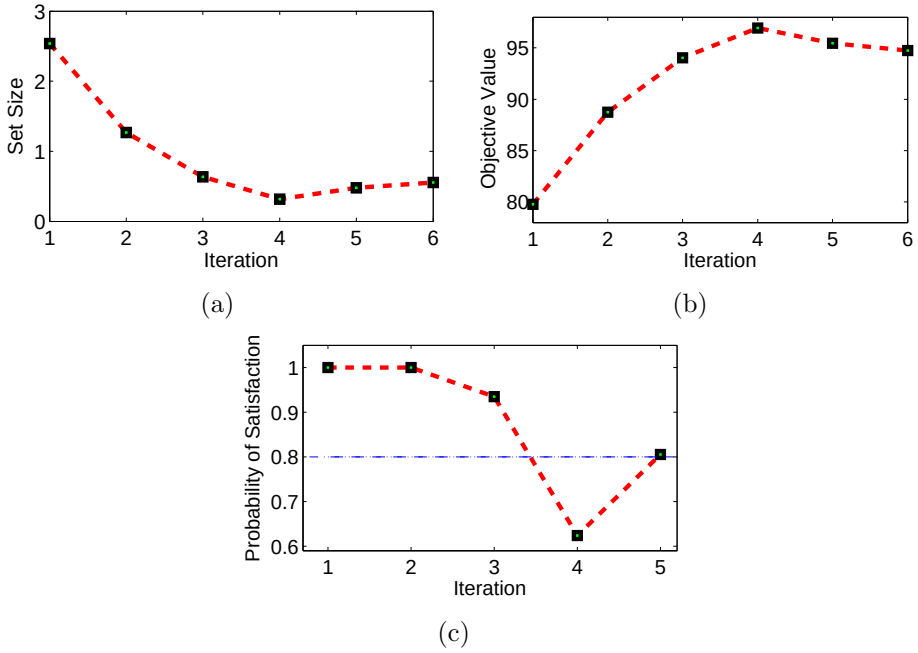

Figure 3.3: Iterative solution procedure for set size optimization

3.4.2 Optimization over the Parameter t

For the robust optimization approximation of the joint chance constraint problem proposed in section 3.3, some upper bounds on $P\left(\max_i \left\{\alpha_i y_0^i + \alpha_i (\mathbf{y}^i)^T \boldsymbol{\xi}\right\} > 0\right)$ are used to approximate the original joint chance constraint, which makes the approximation problem conservative. If we can make the upper bounds tighter by adjusting some of the parameters, the problem will be less conservative and the solution will become better. In Inequality (3.10), an upper bound is used to approximate the indicator function and a parameter t is introduced. As illustrated in Figure 3.1, parameter t controls the upper bounding function $\frac{1}{t}[(\eta + t)]^+$ of the indicator function $1_{(0,+\infty)}(\eta)$. If t varies, the difference between the upper bound and

the indicator function changes accordingly. The key point is to find the best value of t that makes the approximation least conservative. Example 2 is used to illustrate the above idea.

Example 2

This example is taken from Pagnoncelli et al. [30]. Two types of materials are blended to generate products A and B. The demands for product A and B are 7 and 4, respectively. The problem is formulated in (3.42). Parameter ω_1 and ω_2 are subject to uncertainties. It is assumed that they are independent continuous random variables following uniform distribution in $[1, 4]$ and $[1/3, 1]$ respectively. The objective is to minimize the total amount of the materials used.

$$\begin{aligned} \min \quad & x_1 + x_2 \\ \text{s.t.} \quad & P\left\{ \begin{array}{l} \omega_1 x_1 + x_2 \geq 7 \\ \omega_2 x_1 + x_2 \geq 4 \end{array} \right\} \geq 1 - \varepsilon \\ & x_1, x_2 \geq 0 \end{aligned} \tag{3.42}$$

Analytical solution is available for this problem. For $\varepsilon \in [0.5,\ 1]$

$$x_1^* = \frac{18}{9 + 8(1-\varepsilon)},\ x_2^* = \frac{2(9 + 28(1-\varepsilon))}{9 + 8(1-\varepsilon)} \tag{3.43}$$

For $\varepsilon \in [0,\ 0.5]$

$$x_1^* = \frac{9}{11 - 9(1-\varepsilon)},\ x_2^* = \frac{41 - 36(1-\varepsilon)}{11 - 9(1-\varepsilon)} \tag{3.44}$$

Our goal is to find the effect of t on the solution of robust optimization approximation. The reliability level ε is set as 0.5. Different values of t (i.e., 0.01, 0.5, 1, 2.5) are tested for different runs and the results are plotted in Figure 3.4. For each case, the set size varies from 0 to 1 and the robust optimization problem (3.28) (based on box uncertainty set) is solved and the solution is plotted. The true solutions under different ε are also plotted in Figure 3.4 for comparison.

Figure 3.4 shows the relationship between the probability of satisfaction and the optimal

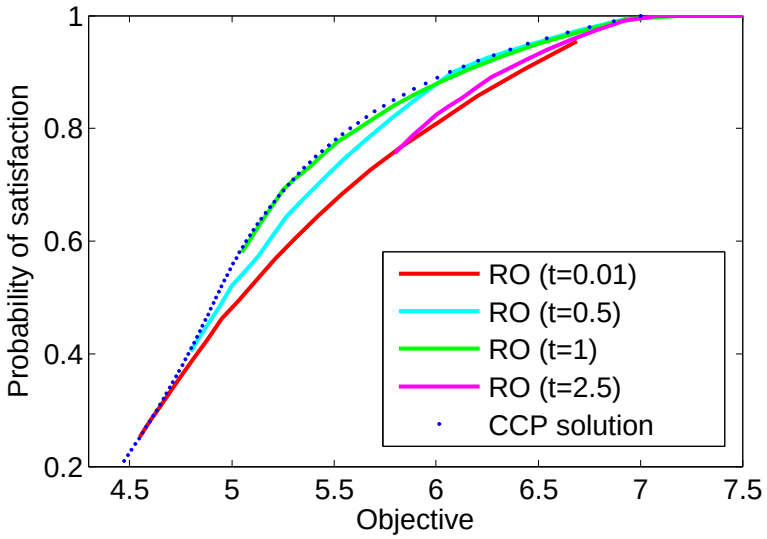

Figure 3.4: Effect of parameter t in the robust optimization approximation

objective value. The dotted line represents the analytical solution of the original chance constrained problem. The solid lines represent the robust approximations. It is shown that for different values of t, the conservativeness of the results are different. As t increases from 0, the line approaches to the target line until t equals 1 and then the line goes away from the target line as t increases from 1 to 5. The line for $t = 1$ almost coincides with the true solution curve, which means that the performance of the corresponding robust optimization approximation is closest to the true solution among the different t values tested.

The task here is to find the best value of t. For a joint chance constrained problem, the desired probability of satisfaction is specified by the user. So to find the line closest to the target line is to find the value of t which achieves the best possible objective value with the desired probability of constraint satisfaction. According to the above observation, the optimal objective of the robust model can be improved when t is adjusted (while satisfying the same probability level). Some scalar optimization algorithm, such as the golden section search algorithm can be applied to search the optimal value of t. The following algorithm is proposed to adjust the parameter t such that the probability is satisfied and the approximation is improved at the same time. The algorithm is summarized in Table 3.2.

The algorithm is taken for Example 2 with $\varepsilon = 0.5$ and the results are shown in Figure 3.5

Table 3.2: Algorithm for optimization over t

Algorithm for optimization over parameter t

Initialization $[lb, ub] = [lb_1, ub_1]$, set $k = 1$ and $\tau = \frac{\sqrt{5}-1}{2}$
$l = t_0 = lb_1 + (1-\tau)(ub_1 - lb_1), r = t_1 = lb_1 + \tau(ub_1 - lb_1)$
while$(ub_k - lb_k < tolerance)$
    Evaluate $f(l)$ and $f(r)$ using set size optimization
    algorithm with fixed set size l and r
    if $(f(r) < f(l))$
        $lb_{k+1} = l, ub_{k+1} = ub_k, l = r$
        $r = t_{k+1} = lb_{k+1} + \tau(ub_{k+1} - lb_{k+1})$
    else $(f(r) > f(l))$
        $lb_{k+1} = lb_k, ub_{k+1} = r, r = l$
        $l = t_{k+1} = lb_{k+1} + (1-\tau)(ub_{k+1} - lb_{k+1})$
    end
    $k = k + 1$
end

and Figure 3.6. Figure 3.5 shows the procedure of the outer layer of the algorithm proposed. The evolutions of the value of t, the current best objective value and the corresponding probability of satisfaction along the iterations are plotted separately. The objective value decreases (improves) as the algorithm goes on since the blending example is a minimization problem. The probability of satisfaction reaches the desired level (0.5 in the example) according to the adjustment of the set size in each iteration at the end of the algorithm. Figure 3.6 shows the changes of the probability of constraint satisfaction, the optimal objective value and the set size with the inner iterations for the final outer layer iteration. The probability of satisfaction converges to the desired satisfaction level 0.5 according to the adjustment of the uncertainty set size as the iteration goes on. At the end of the iterative algorithm, a relatively small set size is found and the corresponding optimal objective value is 4.95, which is improved (from 100 at the first iteration) and it is very close to the analytical objective value of 4.92.

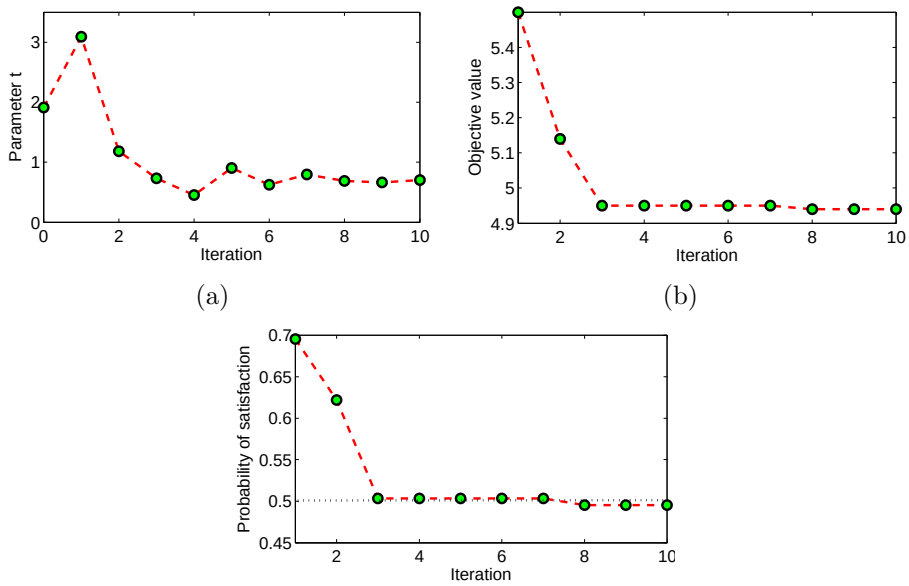

Figure 3.5: Solution procedure for the outer layer

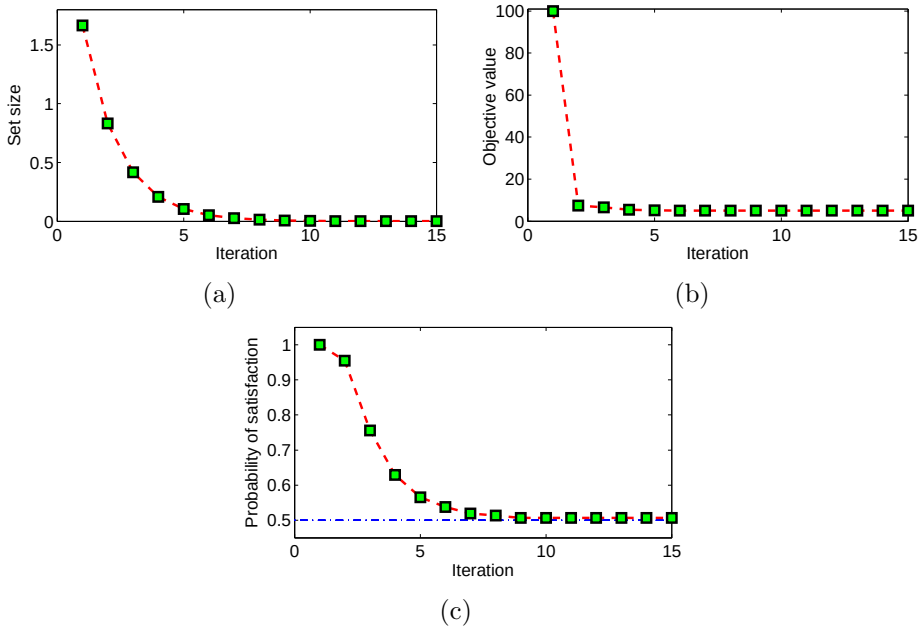

Figure 3.6: Solution procedure for the inner layer (at the last iteration of outer layer with t=0.7)

In this example, the effect of the selection of α_i is also tested. The two-layer algorithm is taken to solve the problem with different values of α_i, and the value of ϵ is set as 0.5. The results are summarized in Table 3.3.

Table 3.3: Results for different selections of α_i

α_1	α_2	α_1/α_2	Objective value
1	1	1	4.95
0.2	0.2	1	4.95
1	5	0.2	5.07
0.2	1	0.2	5.07
1	0.2	5	4.93
5	1	5	4.92

From the above table, the following observations can be obtained. First, the values of α_i will influence the solutions of the proposed robust formulation and the two-layer algorithm. Second, since α_i are the weights on different constraints, the proportions between different α_i rather than the absolute values of α_i are taking effects. For example, while the proportion α_1/α_2 is the same, and the optimal objective value obtained is the same even the values of α_1 and α_2 are different. So proper selection of the proportions between α_i can further improve the performance of the proposed method.

3.5 Case Studies

In this section, numerical studies are performed to further investigate the proposed method. The proposed optimization algorithms over set size Δ and parameter t are implemented in MATLAB. The robust problems are all formulated with box type uncertainty set. The norm optimization problem is a nonlinear problem and it is solved using IPOPT solver. The transportation problem is a linear problem and it is solved by CPLEX solver in GAMS 23.9.

3.5.1 Norm Optimization Problem

Consider the following norm optimization problem [36]:

$$\begin{aligned} \max \quad & \sum_{j=1}^{d} x_j \\ \text{s.t.} \quad & P\left\{\sum_{j=1}^{d} \zeta_{ij}^2 x_j^2 \leq 100, i = 1, ..., m\right\} \geq 1 - \varepsilon \\ & x_j \geq 0, j = 1, ..., d \end{aligned} \tag{3.45}$$

where $x = (x_1, ..., x_d)^T \in R^d$, $\zeta \in R^{d \times m}$, ζ_{ij} are independent and identically distributed random variables with standard normal distribution. The above norm optimization problem has an analytical solution. The optimal solution is $x_1 = \ldots = x_d = \frac{10}{\sqrt{F_{\chi_d^2}^{-1}\left[(1-\varepsilon)^{1/m}\right]}}$, where $F_{\chi_d^2}^{-1}$ is the inverse cumulative distribution function of chi-square distribution with d degrees of freedom. The joint probability of constraint satisfaction can be evaluated as $\left[F_{\chi_d^2}\left(\frac{100}{x_1^2}\right)\right]^m$.

Let $\xi_{ij} = \zeta_{ij}^2$, then ξ_{ij} is subject to chi-squared distribution with one degree of freedom, i.e., $\xi_{ij} \sim \chi_1^2$. Furthermore, we can introduce auxiliary variable z_j to replace x_j^2 and to make a linear chance constraint. The equivalent model is

$$\begin{aligned} \max \quad & \sum_{j=1}^{d} x_j \\ \text{s.t.} \quad & P\left\{\sum_{j=1}^{d} \xi_{ij} z_j \leq 100, i = 1, ..., m\right\} \geq 1 - \varepsilon \\ & x_j^2 \leq z_j, j = 1, ..., d \\ & x_j \geq 0, j = 1, ..., d \end{aligned} \tag{3.46}$$

The above problem can be solved using the proposed robust optimization approximation method. In this example, it is selected as $d = 10, m = 10$. For this example, it is found that solutions do not change as the value of t varies. Thus, for this example, the optimization over set size Δ is sufficient to find the optimal solution. The solutions obtained by robust optimization approximation and set size optimization converge to the true solutions determined analytically. For instance, it is set that $\varepsilon = 0.05$, $t = 1$ and the uncertainty set size

is changed from 1 to 4. The results obtained from the analytical solution and by robust optimization approximation are plotted in Figure 3.7 for comparison.

The result shown in Figure 3.7 shows that the solution obtained by the proposed robust optimization formulation coincide with the analytical solution, which implies that those bounding approximations are tight.

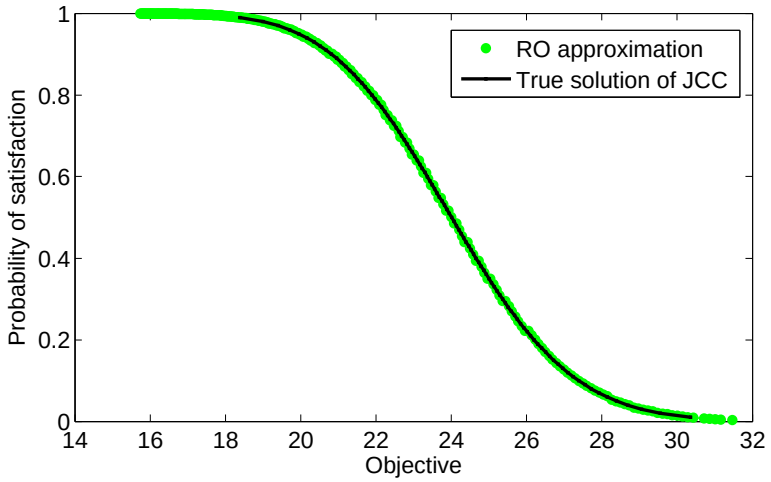

Figure 3.7: Fix the value of $t = 1$ and change set size from 1 to 4

Table 3.4: Results for norm optimization problem

	Optimal solution of JCC		Solution of RO approximation ($t = 1$)			
ε	Objective	Probability of satisfaction	Set size Δ	Objective	Probability of satisfaction	CPU time (sec)
0.05	19.9508	0.95	2.4931	19.9300	0.9522	7.28
0.2	21.8932	0.8	2.0731	21.8700	0.7992	6.18
0.5	24.0076	0.5	1.7235	23.9800	0.5012	8.22

For fixed $t = 1$, the solutions of several different reliability levels (ε is set as 0.05, 0.2 and 0.5) are reported in Table 3.4. In Table 3.4, the optimal solutions of the robust optimization approximation are obtained using only the inner layer (optimization over the set size), and the true optimal solutions are listed for comparison. The results show that for each value of ε the probability of constraint satisfaction (which can be evaluated analytically for this example) reaches the desired reliability. Furthermore, the final objective value of the proposed method is very close to the true optimal objective value, which implies that the proposed algorithm

can lead to the optimal solution of this problem.

3.5.2 Probabilistic Transportation Problem

The problem considered here is taken from Luedtke et al. [80]. The products are transported from suppliers to customers. There is a limited capacity M_i for each supplier and each customer has a demand b_j. The demand b_j is assumed to follow independent normal distribution $\mathcal{N}(1000, 10)$. The transportation cost of shipping a unit of product from supplier i to customer j is denoted by c_{ij}. The objective is to minimize the total cost of transportation. The transportation problem is formulated as a joint chance constrained problem in (3.47).

$$\begin{aligned} \min \quad & \sum_{i,j} c_{ij} x_{ij} \\ s.t. \quad & P\left\{ \sum_{i} x_{ij} \geq b_j, \forall j \right\} \geq 1 - \varepsilon \\ & \sum_{j} x_{ij} \leq M_i, \forall i \\ & x_{ij} \geq 0, \forall i, j \end{aligned} \tag{3.47}$$

Consider a case with 40 suppliers and 100 customers. The limited capacities M_i are all set as 2550. Different reliability levels are considered (ε is set as 0.05, 0.1, 0.15 and 0.5). The results are displayed in Table 3.5.

Table 3.5: Results for transportation problem

ε	t	Set size Δ	Objective value ($\times 10^5$)	Probability of satisfaction	Reliability upper bound	CPU time (sec)
0.05	0.9268	3.0156	1.2689	0.9547	0.0492	230.69
0.1	2.0007	2.4973	1.2675	0.8962	0.1000	224.86
0.15	1.8943	2.4511	1.2668	0.8539	0.1433	267.46
0.5	2.1072	2.1315	1.2638	0.5043	0.4997	313.16

The transportation problem is a cost minimization problem. It is shown from above results that as the allowed violation level ε increases, the required size of the box uncertainty set decreases and the corresponding total transportation cost decreases. The final value of

the parameter t varies for the different cases. The fifth column in Table 3.5 lists the simulated probabilities of constraint satisfaction (with 100,000 samples) for the robust solution obtained by the proposed method. The simulated probability of satisfaction is very close to the desired level for each case of ε, so the solution is not conservative. For this example, the solution reliability upper bound is also calculated (on the probability of constraint violation) using the methods introduced in Section 4 of [25]. When calculating the reliability upper bound, 90% confidence level is considered and 100000 samples are generated from the distribution of uncertainty. It is shown that they are all less than the corresponding target violation level, which means that the solutions obtained by the robust optimization approximation and the two-layer algorithm are reliable at the 90% confidence level.

3.6 Conclusion

This chapter investigates the robust optimization approximation method for solving joint chance constrained optimization problems. Different formulations of uncertainty set induced robust counterpart optimization are derived based on the type of the uncertainty set. To avoid a worst-case scenario approximation and improve the quality of robust solution while satisfying the target solution reliability, a two-layer algorithm is proposed. In the inner level, an iterative method is used for the set size design, with the objective of selecting the minimum possible set size that leads to the target probability of constraint satisfaction. In the outer layer, the parameter t (used for upper bounding the indicator function) is adjusted to improve the quality of the robust optimization approximation. The value of t is optimized with a golden section method. For each fixed value of t, an inner set size optimization problem is solved. The proposed method has the advantage that the robust optimization problem is tractable and the computational complexity only relies on the solution of multiple tractable robust optimization problems. The performance of the robust approximation algorithm is demonstrated in a norm optimization problem and a transportation problem. While calculating the simulated probability of constraint satisfaction, the distribution information

about the uncertainty is unrestricted. So the proposed method is applicable to general distributions. The proposed formulations can be applied to linear joint chance constraint with both continuous and integer variables. This can be seen from the derivations where no integrality restriction on variables is required.

The proposed framework can be directly applied or extended to address correlation in the joint chance constraint: 1) If the same uncertain parameter appears in multiple constraint of the JCC, the problem can be addressed using the proposed framework; 2) If there is correlation between different uncertain parameters appearing in the joint constraints, the proposed framework can be extended by applying robust optimization for single constraint under correlated uncertainty.

Chapter 4

Robust Optimization under Correlated Uncertainty: Formulations and Computational Study

4.1 Introduction

In Chapter 3, the importance of considering uncertainty in optimization has been discussed. With the advantages of distribution-free, simple formulation and tractability, robust optimization has been demonstrated to be an effective way to deal with uncertainty in optimization problem. Although considerable progress has been made in the area of robust optimization, in the existing methods, independence is generally assumed among uncertainties in the parameters. However, in practice, correlations may arise in the uncertainties. For instance, the price and demand of crude oil are correlated, which may affect the refinery planning decision making. As shown by the computational studies of this chapter, the traditional robust optimization methods that ignore the correlation may lead to a conservative solution. Hence, it is of great importance to consider the correlation among uncertainties in robust optimization.

In this chapter, novel results are presented for robust optimization under correlated un-

certainties. In Section 4.2, the robust optimization framework is proposed for correlated uncertainty within a single constraint. Based on five different types of uncertainty set, the corresponding robust counterpart optimization formulations are derived. Specifically, for unbounded and correlated uncertainties, box, polyhedral and ellipsoidal type of uncertainty sets are selected to derive the set-induced robust optimization formulations, and for bounded correlated uncertainties, "interval+polyhedral" and "interval+ellipsoidal" types of uncertainty set are applied to derive the set-induced robust optimization formulations. In Section 4.3, numerical examples are studied to investigate the proposed robust optimization framework for correlated uncertainty within a constraint. Different levels of the correlations are considered to demonstrate the necessity of incorporating uncertainty correlations into the traditional robust optimization approach. In Section 4.4, the proposed method is further applied to a production planning example. Moreover, in Section 4.5, the uncertainties are considered to be presence in multiple constraints and two types of uncertainty set, i.e., "constraint-wise" and "global" uncertainty set, are applied to formulate the robust optimization. Different assumptions about the correlations in uncertainties are studied and their influence in the robust formulation and solution is discussed. The chapter is concluded in Section 4.6.

4.2 Robust Counterpart Optimization Formulations

Consider the following linear optimization problem with uncertain constraint coefficients

$$\begin{aligned} &\max_{x \in X} \ cx \\ &s.t. \quad \tilde{a}^T x \leq b \end{aligned} \tag{4.1}$$

where $x \in R^n$ represents the decision variables, $\tilde{a}$ is an $n \times 1$ vector with entries $\tilde{a}_j$, $j = 1, \cdots, n$, i.e., $\tilde{a} = [\tilde{a}_1, ..., \tilde{a}_n]^T$, n is the number of decision variables. Without loss

of generality, the uncertainties in the coefficients can be modeled as

$$\tilde{a}_j = a_j + u_j, j = 1, ..., n \tag{4.2}$$

where a_j is the nominal (most expected) value of $\tilde{a}_j$, and u_j is the random part following a distribution with zero mean. Separating the deterministic part and the uncertain part, the constraint becomes

$$a^T x + u^T x \leq b \tag{4.3}$$

where $u = [u_1, ..., u_n]^T$. To ensure the constraint satisfaction under the worst-case scenario of an uncertainty set U, the constraint with uncertainty is rewritten as

$$a^T x + \max_{u \in U} u^T x \leq b \tag{4.4}$$

The above constraint (4.4) is the robust counterpart of the uncertain constraint (4.3). Its explicit expression depends on the uncertainty set U. Robust counterpart optimization problem of (4.1) can be obtained by replacing the uncertain constraint with its robust counterpart. In this work, five types of uncertainty set including box, ellipsoid, polyhedral, interval+ellipsoidal, and interval+polyhedral. The design of uncertainty set is related to the distribution of the uncertainty. If the uncertainty is subject to unbounded distribution, then the box, ellipsoidal and polyhedral type of uncertainty set is appropriate to be used in the robust optimization framework, where the size of the uncertainty set is not restricted. Instead, if the uncertainty is subject to bounded distribution, then the bounds information can be involved in the uncertainty set as intervals to avoid an unnecessarily large uncertainty set (which will lead to more conservative solution). Hence, the interval+ellipsoidal uncertainty set and the interval+polyhedral uncertainty set are appropriate for bounded uncertainty distribution. In the following subsections, explicit robust counterpart constraint formulations of (4.4) will be investigated based on different uncertainty sets.

4.2.1 Robust Formulations for Bounded Uncertainty Distribution

Property 7. ***(Box uncertainty set).*** *The robust counterpart optimization formulation for constraint (4.4) under the box type uncertainty set* $U_{box} = \{u \,|\, \|Mu\|_\infty \leq \Delta\}$ *is*

$$\begin{cases} a^T x + \Delta \sum_{k=1}^{n} y_k \leq b \\ -y_k \leq \sum_{j=1}^{n} m_{kj} x_j \leq y_k, \qquad \forall k = 1, ..., n \end{cases} \tag{4.5}$$

where m_{kj} *is the element of* $M^{-T} = \begin{pmatrix} m_{11} & ... & m_{1n} \\ ... & ... & ... \\ m_{n1} & ... & m_{nn} \end{pmatrix}$, M *is an invertible matrix and* M^{-T} *is the inverse transpose of* M.

Proof. Under the given uncertainty set, the inner maximization problem in constraint (4.4) is formulated as

$$\max_u \left\{ u^T x : \|Mu\|_\infty \leq \Delta \right\} \tag{4.6}$$

which can be further rewritten as

$$\max_u \left\{ u^T x : P_\infty u + p_\infty \in K_\infty \right\} \tag{4.7}$$

where $P_\infty = \begin{bmatrix} M_{n\times n} \\ 0_{1\times n} \end{bmatrix}, p_\infty = \begin{bmatrix} 0_{n\times 1} \\ \Delta \end{bmatrix}$, and $K_\infty = \{(\theta_{n\times 1}; t) | \|\theta\|_\infty \leq t\}$ is a norm cone. The inner maximization problem is a conic programming problem. Define dual variables $y = [w_{n\times 1}; \tau] \in K_\infty^*$, where K_∞^* is the dual cone of K_∞ and $K_\infty^* = \{(\theta_{n\times 1}; t) | \|\theta\|_1 \leq t\}$. Apply conic duality to problem (4.7), the problem can be formulated as:

$$\min_y \left\{ \Delta\tau : y \in K_\infty^*, M^T w = -x \right\} = \min_y \left\{ \Delta\tau : \|w\|_1 \leq \tau, M^T w = -x \right\} \tag{4.8}$$

Since the above is a minimization problem, τ can be replaced by its lower bound $\|w\|_1$

and the problem becomes

$$\min_{y} \left\{ \Delta \|w\|_1 : M^T w = -x \right\} \tag{4.9}$$

w can be further replaced by $w = -M^{-T}x$, and then the problem is reduced to

$$\min_{y} \left\{ \Delta \left\| -M^{-T}x \right\|_1 \right\} = \Delta \left\| M^{-T}x \right\|_1 \tag{4.10}$$

The inner maximization term is replaced by $\Delta \left\| M^{-T}x \right\|_1$ and the constraint with uncertainties becomes

$$a^T x + \Delta \left\| M^{-T}x \right\|_1 \leq b \tag{4.11}$$

Consider the element-wise representation of M^{-T}

$$M^{-T} = \begin{pmatrix} m_{11} & ... & m_{1n} \\ ... & ... & ... \\ m_{n1} & ... & m_{nn} \end{pmatrix}$$

Constraint (4.11) can be further written as

$$a^T x + \Delta \left\| \begin{pmatrix} \sum_{j=1}^{n} m_{1j}x_j \\ ... \\ \sum_{j=1}^{n} m_{nj}x_j \end{pmatrix} \right\|_1 \leq b \tag{4.12}$$

which is equivalent to

$$a^T x + \Delta \sum_{k=1}^{n} \left| \sum_{j=1}^{n} m_{kj}x_j \right| \leq b \tag{4.13}$$

Next, a new variable y_k is introduced to eliminate the absolute term, and the robust

counterpart of the constraint with box uncertainty set is

$$\begin{cases} a^T x + \Delta \sum_{k=1}^{n} y_k \leq b \\ -y_k \leq \sum_{j=1}^{n} m_{kj} x_j \leq y_k, \qquad \forall k = 1, ..., n \end{cases} \tag{4.14}$$

□

Remark 1. *If M is a diagonal matrix $Diag\{\hat{a}_1^{-1}, \ldots, \hat{a}_n^{-1}\}$, where $\hat{a}_j, j = 1, \cdots, n$ are the perturbation amplitudes, the robust counterpart constraint becomes*

$$\sum_{j=1}^{n} a_j x_j + \Delta \sum_{j=1}^{n} \hat{a}_j \left| x_j \right| \leq b \tag{4.15}$$

which is the same as the box type uncertainty set induced robust counterpart constraint presented by Li et al [48]. This represents the robust counterpart constraint without correlation consideration.

Remark 2. *The major motivation of the chapter is to incorporate correlation of uncertainties into the robust optimization formulation. Hence, the matrix M is selected based on the covariance matrix and it is assumed that the inevitability of M will hold. Specifically, if M is set as $M = \Sigma^{-1/2}$, where Σ is the covariance matrix of the uncertainties $\tilde{a}_1, \cdots, \tilde{a}_n$, then the correlations of the uncertainties are incorporated into the robust optimization formulation. This is illustrated later using a 2-dimensional example.*

Property 8. (Ellipsoidal uncertainty set). *The robust counterpart optimization model for constraint (4) under the ellipsoidal type uncertainty set $U_{ellipsoid} = \{u | \|Mu\|_2 \leq \Delta\}$ is*

$$a^T x + \Delta \sqrt{\sum_{k=1}^{n} \left(\sum_{j=1}^{n} m_{kj} x_j \right)^2} \leq b \tag{4.16}$$

where m_{kj} is the element of M^{-T}.

Proof. The inner maximization problem of (4.4) is formulated as

$$\max_{u} \left\{ u^T x : \|Mu\|_2 \leq \Delta \right\} \tag{4.17}$$

According to the definition of norm cone, the inner maximization problem can be rewritten as

$$\max_{u} \left\{ u^T x : P_2 u + p_2 \in K_2 \right\} \tag{4.18}$$

where $P_2 = \begin{bmatrix} M_{n\times n} \\ 0_{1\times n} \end{bmatrix}, p_2 = \begin{bmatrix} 0_{n\times 1} \\ \Delta \end{bmatrix}, K_2 = \{(\theta_{n\times 1}; t) | \|\theta\|_2 \leq t\}$. The inner maximization problem is a conic programming problem. Define dual variables $y = [w_{n\times 1}; \tau] \in K_2^*$, where K_2^* is the dual cone of K_2. Since is self-dual, $K_2^* = K_2 = \{(\theta_{n\times 1}; t) | \|\theta\|_2 \leq t\}$. Apply conic duality to problem (4.18), the problem can be formulated as:

$$\min_{y} \left\{ \Delta\tau : y \in K_2, M^T w = -x \right\} = \min_{y} \left\{ \Delta\tau : \|w\|_2 \leq \tau, M^T w = -x \right\} \tag{4.19}$$

Since the above is a minimization problem, τ can be replaced by its lower bound $\|w\|_2$ and the problem becomes

$$\min_{y} \left\{ \Delta\|w\|_2 : M^T w = -x \right\} \tag{4.20}$$

w can be further replaced by $w = -M^{-T}x$, and then the problem is reduced to

$$\min_{y} \left\{ \Delta \left\| -M^{-T}x \right\|_2 \right\} = \Delta \left\| M^{-T}x \right\|_2 \tag{4.21}$$

The inner maximization term is replaced by $\Delta \left\| M^{-T}x \right\|_2$ and the constraint with uncertainties becomes

$$a^T x + \Delta \left\| M^{-T}x \right\|_2 \leq b \tag{4.22}$$

Consider the element-wise representation of M^{-T}

$$M^{-T} = \begin{pmatrix} m_{11} & ... & m_{1n} \\ ... & ... & ... \\ m_{n1} & ... & m_{nn} \end{pmatrix}$$

Constraint (4.22) can be further written as

$$a^T x + \Delta \left\| \begin{pmatrix} \sum_{j=1}^{n} m_{1j} x_j \\ ... \\ \sum_{j=1}^{n} m_{nj} x_j \end{pmatrix} \right\|_2 \leq b \tag{4.23}$$

which is equivalent to

$$a^T x + \Delta \sqrt{\sum_{k=1}^{n} \left(\sum_{j=1}^{n} m_{kj} x_j \right)^2} \leq b \tag{4.24}$$

which is a second order conic programming (SOCP) problem. □

Remark 3. *If M is a diagonal matrix $Diag\{\hat{a}_1^{-1}, \ldots, \hat{a}_n^{-1}\}$, where $\hat{a}_j, j = 1, \cdots, n$ are the perturbations, the robust counterpart of the constraint becomes*

$$\sum_{j=1}^{n} a_j x_j + \Delta \sqrt{\sum_{j=1}^{n} \hat{a}_j^2 x_j^2} \leq b \tag{4.25}$$

which is the robust counterpart constraint without correlation modeling.

Remark 4. *If M is set as $M = \Sigma^{-1/2}$, where Σ is the covariance matrix of the uncertainties $\tilde{a}_1, ..., \tilde{a}_n$, it can be used to formulate the correlations of the uncertainties. The ellipsoidal uncertainty set can be represented as the following ellipsoidal*

$$U_{ellipsoid} = \{u \,|\, \|Mu\|_2 \leq \Delta\} = \left\{u \,\middle|\, u^T M^T M u \leq \Delta^2\right\} = \left\{u \,\middle|\, u^T \frac{\Sigma^{-1}}{\Delta^2} u \leq 1\right\} \tag{4.26}$$

For the ellipsoidal defined above, the center of the ellipsoidal is the origin; the lengths of the semi-axes of the ellipsoidal are given by $\sqrt{\lambda_i}\Delta$, where λ_i are the eigenvalues of Σ.

Property 9. (Polyhedral uncertainty set). *The robust counterpart optimization model for constraint (4.4) under the polyhedral type uncertainty set $U_{polyhedral} = \{u | \|Mu\|_1 \leq \Delta\}$ is*

$$\begin{cases} a^T x + \Delta\tau \leq b \\ -\tau \leq \sum_{j=1}^{n} m_{kj} x_j \leq \tau, \forall k = 1, .., n \end{cases} \tag{4.27}$$

where m_{kj} is the element of M^{-T}.

Proof. The inner maximization problem of (4.4) is formulated as

$$\max_u \left\{ u^T x : \|Mu\|_1 \leq \Delta \right\} \tag{4.28}$$

According to the definition of norm cone, the inner maximization problem can be rewritten as

$$\max_u \left\{ u^T x : P_1 u + p_1 \in K_1 \right\} \tag{4.29}$$

where $P_1 = \begin{bmatrix} M_{n\times n} \\ 0_{1\times n} \end{bmatrix}, p_1 = \begin{bmatrix} 0_{n\times 1} \\ \Delta \end{bmatrix}, K_1 = \{(\theta_{n\times 1}; t) | \|\theta\|_1 \leq t\}$. The inner maximization problem is a conic programming problem. Define dual variable $y = [w_{n\times 1}; \tau] \in K_1^*$, where K_1^* is the dual cone of K_1 and $K_1^* = K_\infty = \{(\theta_{n\times 1}; t) | \|\theta\|_\infty \leq t\}$. Apply conic duality to problem (4.29), the problem can be formulated as:

$$\min_y \left\{ \Delta\tau : y \in K_\infty, M^T w = -x \right\} = \min_y \left\{ \Delta\tau : \|w\|_\infty \leq \tau, M^T w = -x \right\} \tag{4.30}$$

Since the above is a minimization problem, τ can be replaced by its lower bound $\|w\|_\infty$ and the problem becomes

$$\min_y \left\{ \Delta \|w\|_\infty : M^T w = -x \right\} \tag{4.31}$$

Since w can be further replaced by $w = -M^{-T}x$, the problem is represented as

$$\min_{y} \left\{ \Delta \left\| -M^{-T}x \right\|_{\infty} \right\} = \Delta \left\| M^{-T}x \right\|_{\infty} \tag{4.32}$$

The inner maximization term is replaced by $\Delta \left\| M^{-T}x \right\|_{\infty}$ and the constraint with uncertainties becomes

$$a^T x + \Delta \left\| M^{-T}x \right\|_{\infty} \leq b \tag{4.33}$$

Consider element-wise representation of M^{-T}

$$M^{-T} = \begin{pmatrix} m_{11} & ... & m_{1n} \\ ... & ... & ... \\ m_{n1} & ... & m_{nn} \end{pmatrix}$$

Constraint (4.33) can be further written as

$$a^T x + \Delta \left\| \begin{pmatrix} \sum_{j=1}^{n} m_{1j}x_j \\ ... \\ \sum_{j=1}^{n} m_{nj}x_j \end{pmatrix} \right\|_{\infty} \leq b \tag{4.34}$$

which is equivalent to

$$a^T x + \Delta \max_{k} \left| \sum_{j=1}^{n} m_{kj}x_j \right| \leq b \tag{4.35}$$

Introduce a new variable τ to replace the maximization terms in constraint (4.35), the robust counterpart of the constraint with polyhedral uncertainty set is

$$\begin{cases} a^T x + \Delta\tau \leq b \\ \tau \geq \left| \sum_{j=1}^{n} m_{kj}x_j \right|, \forall k = 1, .., n \end{cases} \tag{4.36}$$

The absolute operator in (4.36) can be further eliminated and the above formulation is

equivalent to (4.27). □

Remark 5. *If M is a diagonal matrix $Diag\{\hat{a}_1^{-1}, \ldots, \hat{a}_n^{-1}\}$, where $\hat{a}_j, j = 1, \cdots, n$ are the perturbations, the robust counterpart of the constraint becomes*

$$\begin{cases} \sum_{j=1}^{n} a_j x_j + \Delta\tau \leq b \\ -\tau \leq \hat{a}_j x_j \leq \tau, \forall j \end{cases} \tag{4.37}$$

which represents the robust counterpart constraints without correlation modeling.

Remark 6. *If M is set as $\Sigma^{-1/2}$, where Σ is the covariance matrix of the uncertainties $\tilde{a}_1, \cdots, \tilde{a}_n$, it can be used to formulate the correlations of the uncertainties.*

4.2.2 Robust Formulations for Bounded Uncertainty Distribution

If the uncertainty u is subject to a bounded distribution, an interval set can be used to make sure the uncertainty lies in the bounds, which are modeled using matrix M_1 here. Correlation between uncertainties can be formulated in the polyhedral uncertainty set by matrix M_2. The interval+polyhedral uncertainty set is the intersection of the interval set and the polyhedral uncertainty set:

$$U_{in+poly} = \{u \,|\, \|M_1 u\|_\infty \leq 1, \|M_2 u\|_1 \leq \Delta\}$$

Property 10. (Interval+polyhedral uncertainty set). *The robust counterpart optimization model for constraint (4.4) under the interval+polyhedral type uncertainty set $U_{in+poly} = \{u \,|\, \|M_1 u\|_\infty \leq 1, \|M_2 u\|_1 \leq \Delta\}$ is*

$$\begin{cases} a^T x + \sum_{j=1}^{n} y_j + \Delta\tau \leq b \\ -y_j \leq m_j^{(1)}(x_j - z_j) \leq y_j, \forall j = 1, .., n \\ -\tau \leq \sum_{j=1}^{n} m_{kj}^{(2)} z_j \leq \tau, \forall k = 1, ..., n \end{cases} \tag{4.38}$$

where M_1 *is a diagonal matrix and* $m_j^{(1)}$ *is the diagonal element of* M_1^{-T}*, and* $m_{kj}^{(2)}$ *is the element of* ${M_2}^{-T} = \begin{pmatrix} m_{11}^{(2)} & ... & m_{1n}^{(2)} \\ ... & ... & ... \\ m_{n1}^{(2)} & ... & m_{nn}^{(2)} \end{pmatrix}$.

Proof. The inner maximization term in constraint (4.4) needs to be eliminated. The inner maximization problem is formulated as

$$\max_u \left\{ u^T x : \|M_1 u\|_\infty \leq 1, \|M_2 u\|_1 \leq \Delta \right\} \tag{4.39}$$

According to the definition of norm cone, the inner maximization problem can be rewritten as

$$\max_u \left\{ u^T x : P_\infty u + p_\infty \in K_\infty, P_1 u + p_1 \in K_1 \right\} \tag{4.40}$$

where

$$P_\infty = \begin{bmatrix} M_{1,n\times n} \\ 0_{1\times n} \end{bmatrix}, p_\infty = \begin{bmatrix} 0_{n\times 1} \\ 1 \end{bmatrix}, K_\infty = \{(\theta_{n\times 1}; t) | \|\theta\|_\infty \leq t\},$$

$$P_1 = \begin{bmatrix} M_{2,n\times n} \\ 0_{1\times n} \end{bmatrix}, p_1 = \begin{bmatrix} 0_{n\times 1} \\ \Delta \end{bmatrix}, K_1 = \{(\theta_{n\times 1}; t) | \|\theta\|_1 \leq t\}.$$

The inner maximization problem is a conic programming problem. Defining dual variables $y^1 = \left[w_{1(n\times 1)}; \tau_1\right] \in K_\infty^*$ and $y^2 = \left[w_{2(n\times 1)}; \tau_2\right] \in K_1^*$. K_∞^* is the dual cone of K_∞, and K_1^* is the dual cone of K_1, $K_1^* = K_\infty = \{(\theta_{n\times 1}; t) | \|\theta\|_\infty \leq t\}$. Applying conic duality to (4.40), the problem can be formulated as:

$$\begin{aligned} &\min_{y^1, y^2} \left\{ \tau_1 + \Delta\tau_2 : y^1 \in K_\infty^*, y^2 \in K_1^*, M_1^T w_1 + M_2^T w_2 = -x \right\} \\ =& \min_{y^1, y^2} \left\{ \tau_1 + \Delta\tau_2 : \|w_1\|_1 \leq \tau_1, \|w_2\|_\infty \leq \tau_2, M_1^T w_1 + M_2^T w_2 = -x \right\} \end{aligned} \tag{4.41}$$

Since the above is a minimization problem, τ_1, τ_2 can be replaced by its lower bound

$\|w_1\|_1$, $\|w_2\|_\infty$ and the problem becomes

$$\min_{y^1,y^2} \left\{ \|w_1\|_1 + \Delta \|w_2\|_\infty : M_1^T w_1 + M_2^T w_2 = -x \right\} \tag{4.42}$$

And w_2 can be further replaced by $w_2 = -M_2^{-T}(x + M_1^T w_1)$. The problem is represented as

$$\min_{w_1} \left\{ \|w_1\|_1 + \Delta \left\| M_2^{-T}(x + M_1^T w_1) \right\|_\infty \right\} \tag{4.43}$$

The inner maximization term is replaced by $\min_{w_1} \left\{ \|w_1\|_1 + \Delta \left\| M_2^{-T}(x + M_1^T w_1) \right\|_\infty \right\}$ and since the minimization term is on the left hand side of a "less or equal to" constraint, the minimization operator can be removed from the constraint

$$a^T x + \|w_1\|_1 + \Delta \left\| M_2^{-T}(x + M_1^T w_1) \right\|_\infty \leq b \tag{4.44}$$

Introduce an auxiliary variable $z = x + M_1^T w_1$, the constraint becomes

$$a^T x + \left\| M_1^{-T}(x - z) \right\|_1 + \Delta \left\| M_2^{-T} z \right\|_\infty \leq b \tag{4.45}$$

Consider element-wise representation of M_1^{-T} and M_2^{-T}

$$M_1^{-T} = \begin{pmatrix} m_1^{(1)} & ... & 0 \\ ... & ... & ... \\ 0 & ... & m_n^{(1)} \end{pmatrix}, \; M_2^{-T} = \begin{pmatrix} m_{11}^{(2)} & ... & m_{1n}^{(2)} \\ ... & ... & ... \\ m_{n1}^{(2)} & ... & m_{nn}^{(2)} \end{pmatrix}$$

Constraint (4.45) can be further written as

$$a^T x + \sum_{j=1}^{n} \left| m_j^{(1)}(x_j - z_j) \right| + \Delta \left\| \begin{pmatrix} \sum_{j=1}^{n} m_{1j}^{(2)} z_j \\ ... \\ \sum_{j=1}^{n} m_{nj}^{(2)} z_j \end{pmatrix} \right\|_\infty \leq b \tag{4.46}$$

which is equivalent to

$$a^T x + \sum_{j=1}^{n} \left| m_j^{(1)}(x_j - z_j) \right| + \Delta \max_k \left| \sum_{j=1}^{n} m_{kj}^{(2)} z_j \right| \leq b \tag{4.47}$$

Introduce a new variable y_j to eliminate the absolute term in the second term on the left hand side and a new variable τ to eliminate the maximization term

$$\begin{cases} a^T x + \sum\limits_{j=1}^{n} y_j + \Delta\tau \leq b \\ -y_j \leq m_j^{(1)}(x_j - z_j) \leq y_j, \forall j = 1, .., n \\ \tau \geq \left| \sum\limits_{j=1}^{n} m_{kj}^{(2)} z_j \right|, \forall k = 1, ..., n \end{cases} \tag{4.48}$$

After eliminating the absolute operator in (4.48), it is equivalent to (4.38). □

Remark 7. *If M_1 and M_2 are both diagonal and $M_1 = M_2 = Diag\{\hat{a}_1^{-1}, \ldots, \hat{a}_n^{-1}\}$, where $\hat{a}_j, j = 1, \cdots, n$ are the perturbations, the robust counterpart of the constraint becomes*

$$\begin{cases} a^T x + \sum\limits_{j=1}^{n} y_j + \Delta\tau \leq b \\ -y_j \leq \hat{a}_j(x_j - z_j) \leq y_j, \forall j = 1, .., n \\ -\tau \leq \hat{a}_j z_j \leq \tau, \forall j = 1, ..., n \end{cases} \tag{4.49}$$

which is the robust counterpart constraint without correlation consideration.

Remark 8. *If M_1 is diagonal matrix $Diag\{\hat{a}_1^{-1}, \ldots, \hat{a}_n^{-1}\}$, where $\hat{a}_j, j = 1, \cdots, n$ are the perturbations and M_2 is set as $M_2 = \Sigma^{-1/2}$, where Σ is the covariance matrix of the uncertainties $\tilde{a}_1, \cdots, \tilde{a}_n$, the robust optimization formulation (4.38) can be used to formulate the correlations of the uncertainties.*

Similar to the interval + polyhedral type of uncertainty set, the interval + ellipsoidal type of uncertainty set is also applicable to bounded uncertainty. An interval set can be used to make sure the uncertainty lies in the range in all dimensions and it is represented by matrix

M_1. Correlation between uncertainties can be formulated in the ellipsoidal uncertainty set by matrix M_2. The interval+ellipsoidal uncertainty set is the intersection of the interval set and the ellipsoidal uncertainty set $U_{in+ellip} = \{u \,|\|M_1 u\|_\infty \leq 1, \|M_2 u\|_2 \leq \Delta\}$.

Property 11. (Interval+ellipsoidal). *The robust counterpart optimization model for constraint (4.4) under the interval + ellipsoidal type uncertainty set given by:*

$$U_{in+ellip} = \{u \,|\|M_1 u\|_\infty \leq 1, \|M_2 u\|_2 \leq \Delta\}$$

is as follows:

$$\begin{cases} a^T x + \sum_{j=1}^{n} y_j + \Delta \sqrt{\sum_{k=1}^{n} \left(\sum_{j=1}^{n} m_{kj}^{(2)} z_j \right)^2} \leq b \\ -y_j \leq m_j^{(1)} (x_j - z_j) \leq y_j, \forall j = 1, .., n \end{cases} \tag{4.50}$$

where M_1 is a diagonal matrix and $m_j^{(1)}$ is the element of M_1^{-T}, and $m_{kj}^{(2)}$ is the element of ${M_2}^{-T}$.

Proof. The inner maximization term in constraint (4.4) needs to be eliminated. The inner maximization problem is formulated as

$$\max_u \left\{ u^T x : \|M_1 u\|_\infty \leq 1, \|M_2 u\|_1 \leq \Delta \right\} \tag{4.51}$$

According to the definition of norm cone, the inner maximization problem can be rewritten as

$$\max_u \left\{ u^T x : P_\infty u + p_\infty \in K_\infty, P_2 u + p_2 \in K_2 \right\} \tag{4.52}$$

where

$$P_\infty = \begin{bmatrix} M_{1,n\times n} \\ 0_{1\times n} \end{bmatrix}, p_\infty = \begin{bmatrix} 0_{n\times 1} \\ 1 \end{bmatrix}, K_\infty = \{(\theta_{n\times 1}; t) | \|\theta\|_\infty \leq t\},$$

$$P_2 = \begin{bmatrix} M_{2,n\times n} \\ 0_{1\times n} \end{bmatrix}, p_2 = \begin{bmatrix} 0_{n\times 1} \\ \Delta \end{bmatrix}, K_2 = \{(\theta_{n\times 1}; t) | \|\theta\|_2 \leq t\}$$

The inner maximization problem is a conic programming problem. Define dual variables $y^1 = \left[w_{1(n\times 1)}; \tau_1\right] \in K_\infty^*$ and $y^2 = \left[w_{2(n\times 1)}; \tau_2\right] \in K_2^*$. K_∞^* is the dual cone of K_∞, $K_\infty^* = K_1 = \{(\theta_{n\times 1}; t) | \|\theta\|_1 \leq t\}$ and K_2^* is the dual cone of K_2, . Apply conic duality to problem (4.52), the problem can be formulated as:

$$\begin{aligned} &\min_{y^1, y^2} \left\{\tau_1 + \Delta\tau_2 : y^1 \in K_\infty^*, y^2 \in K_2^*, M_1^T w_1 + M_2^T w_2 = -x\right\} \\ &= \min_{y^1, y^2} \left\{\tau_1 + \Delta\tau_2 : \|w_1\|_1 \leq \tau_1, \|w_2\|_2 \leq \tau_2, M_1^T w_1 + M_2^T w_2 = -x\right\} \end{aligned} \tag{4.53}$$

Since the above is a minimization problem, τ_1, τ_2 can be replaced by its lower bound $\|w_1\|_1$, $\|w_2\|_2$ and the problem becomes

$$\min_{y^1, y^2} \left\{\|w_1\|_1 + \Delta\|w_2\|_2 : M_1^T w_1 + M_2^T w_2 = -x\right\} \tag{4.54}$$

Since w_2 can be further replaced by $w_2 = -M_2^{-T}(x + M_1^T w_1)$, the problem is represented as

$$\min_{w_1} \left\{\|w_1\|_1 + \Delta\left\|M_2^{-T}(x + M_1^T w_1)\right\|_2\right\} \tag{4.55}$$

The inner maximization term is replaced by $\min_{w_1} \left\{\|w_1\|_1 + \Delta\left\|M_2^{-T}(x + M_1^T w_1)\right\|_2\right\}$ and since the minimization term is on the left hand side of a "less or equal to" constraint, the minimization operator can be removed from the constraint

$$a^T x + \|w_1\|_1 + \Delta\left\|M_2^{-T}(x + M_1^T w_1)\right\|_2 \leq b \tag{4.56}$$

Introduce an auxiliary variable $z = x + M_1^T w_1$, the constraint becomes

$$a^T x + \left\|M_1^{-T}(x - z)\right\|_1 + \Delta\left\|M_2^{-T} z\right\|_2 \leq b \tag{4.57}$$

Consider element-wise representation of M_1^{-T} and M_2^{-T}

$$M_1^{-T} = \begin{pmatrix} m_1^{(1)} & ... & 0 \\ ... & ... & ... \\ 0 & ... & m_n^{(1)} \end{pmatrix}, M_2^{-T} = \begin{pmatrix} m_{11}^{(2)} & ... & m_{1n}^{(2)} \\ ... & ... & ... \\ m_{n1}^{(2)} & ... & m_{nn}^{(2)} \end{pmatrix}$$

Constraint (4.57) can be further written as

$$a^T x + \sum_{j=1}^{n} \left| m_j^{(1)}(x_j - z_j) \right| + \Delta \left\| \begin{pmatrix} \sum_{j=1}^{n} m_{1j}^{(2)} z_j \\ ... \\ \sum_{j=1}^{n} m_{nj}^{(2)} z_j \end{pmatrix} \right\|_2 \leq b \tag{4.58}$$

which is equivalent to

$$a^T x + \sum_{j=1}^{n} \left| m_j^{(1)}(x_j - z_j) \right| + \Delta \sqrt{\sum_{k=1}^{n} \left| \sum_{j=1}^{n} m_{kj}^{(2)} z_j \right|^2} \leq b \tag{4.59}$$

Introduce a new variable y_j to eliminate the absolute term in the second term on the left hand side

$$\begin{cases} a^T x + \sum_{j=1}^{n} y_j + \Delta \sqrt{\sum_{k=1}^{n} \left(\sum_{j=1}^{n} m_{kj}^{(2)} z_j \right)^2} \leq b \\ -y_j \leq m_j^{(1)}(x_j - z_j) \leq y_j, \forall j = 1, .., n \end{cases} \tag{4.60}$$

□

Remark 9. *If M_1 and M_2 are both diagonal matrices $M_1 = M_2 = Diag\{\hat{a}_1^{-1}, \ldots, \hat{a}_n^{-1}\}$, where $\hat{a}_j, j = 1, \cdots, n$ are the perturbations, the robust counterpart of the constraint becomes*

$$\begin{cases} a^T x + \sum_{j=1}^{n} y_j + \Delta \sqrt{\sum_{j=1}^{n} \hat{a}_j^2 {z_j}^2} \leq b \\ -y_j \leq \hat{a}_j(x_j - z_j) \leq y_j, \forall j = 1, .., n \end{cases} \tag{4.61}$$

which is the robust optimization formulation without correlation consideration.

Remark 10. *If M_1 is set as $Diag\{\hat{a}_1^{-1}, \ldots, \hat{a}_n^{-1}\}$, where $\hat{a}_j, j = 1, \cdots, n$ are the perturbations and M_2 is set as $M_2 = \Sigma^{-1/2}$, where Σ is the covariance matrix of the uncertainties, it can be used to formulate the correlations of the uncertainties.*

4.2.3 Illustration of Uncertainty Sets

To illustrate the uncertainty set design for unbounded uncertainty distribution, consider the following constraint with uncertain parameters u_1 and u_2 in the constraint coefficients

$$(10 + u_1)x_1 + (20 + u_2)x_2 \leq 140 \tag{4.62}$$

Assume the uncertainty $u = [u_1, u_2]$ follows a multivariate Gaussian distribution with zero mean and covariance Σ (i.e., $u \sim \mathcal{N}(0, \Sigma)$), where

$$\Sigma = \begin{pmatrix} \sigma_{11}^2 & \sigma_{12} \\ \sigma_{21} & \sigma_{22}^2 \end{pmatrix} = \begin{pmatrix} 34 & -1.5 \\ -1.5 & 0.5 \end{pmatrix}$$

To incorporate the correlation into the uncertainty set definition, define

$$M = \Sigma^{-1/2} = \begin{pmatrix} 0.1740 & 0.0601 \\ 0.0601 & 1.5171 \end{pmatrix} \text{ and } M^{-T} = \begin{pmatrix} 5.8264 & -0.2310 \\ -0.2310 & 0.6683 \end{pmatrix}$$

Then, the box, ellipsoidal and polyhedral uncertainty set can be defined as following:

$$U_{box} = \{u \,||0.174u_1 + 0.0601u_2| \leq \Delta, |0.0601u_1 + 1.5171u_2| \leq \Delta\}$$

$$U_{ellip} = \left\{u \,\middle|0.0011u_1^2 + 0.2034u_1u_2 + 5.3135u_2^2 \leq \Delta^2\right\}$$

$$U_{polyhedral} = \{u \,||0.174u_1 + 0.0601u_2| + |0.0601u_1 + 1.5171u_2| \leq \Delta\}$$

Notice that for the ellipsoidal set, it centers at origin, and the lengths of the semi-axes of

0.658Δ and 5.8367Δ.

Figure 4.1 shows the three uncertainty sets, where the set sizes of box, ellipsoid and polyhedron are set as $\Delta = 1$. In the same figure, 1000 samples are drawn from the assumed multivariate Gaussian distribution $\mathcal{N}(0, \Sigma)$.

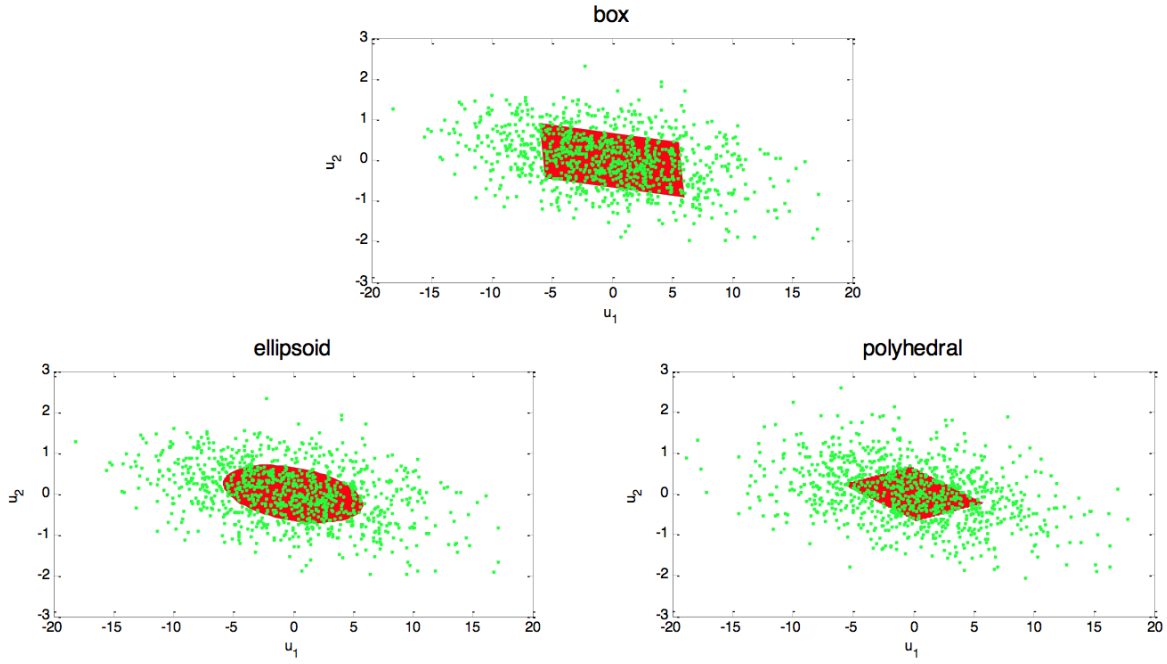

Figure 4.1: Visualization of uncertainty set for unbounded uncertainty in 2-dimensional space.

Since the uncertainty is assumed to follow a multivariate Gaussian distribution and according to the "3σ-rule" for Gaussian random variables, the samples will lie within the range around [-18, 18] and around [-2, 2] in the two dimensions, respectively. And with the definition of the three types of uncertainty set and set size , the uncertainty set will only cover part of the samples. Compared with uncertainty sets without considering correlations between uncertainties in Li et al. [48], the box, ellipsoidal and polyhedral uncertainty sets are distorted by the correlations.

To illustrate the bounded uncertainty distribution case, assume the uncertainty u follows a truncated multivariate Gaussian distribution with zero mean, covariance Σ, perturbations

$\hat{a}_1 = 3$ and $\hat{a}_2 = 0.25$, i.e., $u \sim \mathcal{N}(0, \Sigma)$, $u_1 \in \begin{bmatrix} -3 & 3 \end{bmatrix}$, $u_2 \in \begin{bmatrix} -0.25 & 0.25 \end{bmatrix}$, where

$$\Sigma = \begin{pmatrix} \sigma_{11}^2 & \sigma_{12} \\ \sigma_{21} & \sigma_{22}^2 \end{pmatrix} = \begin{pmatrix} 34 & -1.5 \\ -1.5 & 0.5 \end{pmatrix}$$

To incorporate the correlation into the uncertainty set definition, define

$$M_1 = \begin{pmatrix} \hat{a}_1^{-1} & 0 \\ 0 & \hat{a}_2^{-1} \end{pmatrix} = \begin{pmatrix} 0.33 & 0 \\ 0 & 4 \end{pmatrix}, \; M_2 = \Sigma^{-1/2} = \begin{pmatrix} 0.1740 & 0.0601 \\ 0.0601 & 1.5171 \end{pmatrix}$$

The interval+polyhedral and interval+ellipsoidal uncertainty sets are used for illustration of the bounded uncertainty. The definition of the two types of uncertainty set are given as

$$U_{in+ellip} = \left\{ u \,\middle|\, |u_1| \leq 3, |u_2| \leq 0.25, 0.0011u_1^2 + 0.2034u_1u_2 + 5.3135u_2^2 \leq \Delta^2 \right\}$$

$$U_{in+poly} = \{ u \,||u_1| \leq 3, |u_2| \leq 0.25, |0.174u_1 + 0.0601u_2| + |0.0601u_1 + 1.5171u_2| \leq \Delta \}$$

In Figure 4.2, the set size of box, ellipsoidal and polyhedral types of uncertainty set is set as $\Delta = 0.54$ and 1000 samples are drawn from the assumed truncated normal distribution $\mathcal{N}(0, \Sigma)$, $u_1 \in \begin{bmatrix} -3 & 3 \end{bmatrix}$, $u_2 \in \begin{bmatrix} -0.25 & 0.25 \end{bmatrix}$.

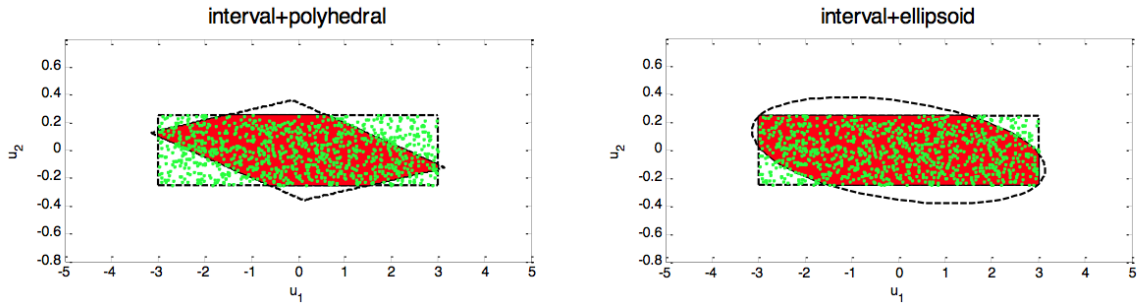

Figure 4.2: Visualization of uncertainty set for bounded uncertainty in 2-dimensional space.

As the assumption of the bounded uncertainty in this example, the samples lies within an rectangle representing the boundary of the uncertainty. Since the interval+polyhedral (inter-

val+ellipsoid) uncertainty set is defined by combination of interval and polyhedral(ellipsoid), the shape of the uncertainty set is the intersection of the rectangle reflecting the boundary of the uncertainty and a polyhedral (an ellipsoid) distorted by the correlations. Since the set size is set as $\Delta = 0.54$, and according to the definition of the uncertainty set, the intersection covers part of the samples.

4.3 Computational Study

In this section, computational studies are performed on the following numerical example to investigate the proposed robust optimization formulation under correlated uncertainty.

$$\begin{aligned} &\max\ 8x_1 + 12x_2 \\ &s.t.\ (10+u_1)x_1 + (20+u_2)x_2 \leq 140 \\ &\qquad 6x_1 + 8x_2 \leq 72 \\ &\qquad x_1, x_2 \geq 0 \end{aligned} \tag{4.63}$$

Two uncertainties u_1, u_2 exist in the first constraint. Both bounded and unbounded uncertainties are considered, and corresponding uncertainty sets are used for robust counterpart formulation. Based on different types of uncertainty set, the robust formulation optimization problems with different values of uncertainty set size are solved in GAMS 23.9. The robust formulations based on box, polyhedral and interval+polyhedral uncertainty sets lead to linear programming (LP) problem and the selected solver is CPLEX. Robust formulations based on ellipsoidal and interval+ellipsoidal uncertainty sets result in second order conic programming (SOCP) problem and are solved by BARON. After solving the optimization problems, the optimal objective value corresponding to different set size can be obtained. All the computations in this paper are performed on a desktop PC with an Intel i5-3570K core processor with 3.40 GHz CPU and 8GB RAM.

By changing the size of the uncertainty set, a series of robust solutions can be obtained

by solving the robust optimization problem. For each robust solution, the probability of constraint satisfaction is evaluated in MATLAB through the following steps. First, $N = 100000$ samples are generated from the assumed distribution of uncertainty; second, for a known robust solution, the number of times n that the uncertain constraint is satisfied is counted; finally, the simulated probability of constraint satisfaction is calculated as n/N.

In the subsequent computational studies, it is aimed to investigate: 1) the effect of the uncertainty set size on the robust solution and the probability of constraint satisfaction; 2) the effect of modeling (accurate) uncertainty correlation in the robust optimization framework. In order to demonstrate the importance of considering correlations in robust formulation, different covariance matrices with the same variance and different levels of correlation (from no correlation to exact correlation) are studied.

4.3.1 Unbounded Uncertainty Distribution

For unbounded uncertainty, assume the true uncertainty distribution is $u = \begin{pmatrix} u_1 \\ u_2 \end{pmatrix} \sim \mathcal{N}(0, \Sigma)$ with $\Sigma = \begin{pmatrix} 34 & -4 \\ -4 & 0.5 \end{pmatrix}$. The robust counterpart formulations based on box, ellipsoidal and polyhedral uncertainty set can be obtained by property 7, 8 and 9, respectively. If the covariance matrix used in robust formulation is the true covariance matrix in the assumption of the uncertainty i.e., $M = \Sigma^{-1/2}$, the box uncertainty set based robust counterpart of the constraint with uncertainty is

$$\begin{aligned} &10x_1 + 20x_2 + \Delta(y_1 + y_2) \leq 140 \\ &-y_1 \leq 5.7932x_1 - 0.6621x_2 \leq y_1 \\ &-y_2 \leq -0.6621x_1 + 0.2483x_2 \leq y_2 \end{aligned}$$

the ellipsoidal uncertainty set based robust counterpart of the constraint with uncertainty is

$$10x_1 + 20x_2 + \Delta\sqrt{34x_1^2 - 8x_1x_2 + 0.5x_2^2} \leq 140$$

and the polyhedral uncertainty set based robust counterpart of the constraint with uncertainty is

$$10x_1 + 20x_2 + \Delta\tau \leq 140$$
$$\tau \geq |5.7932x_1 - 0.6621x_2|$$
$$\tau \geq |-0.6621x_1 + 0.2483x_2|$$

Four different covariance matrices are considered when formulating the robust counterpart, i.e., $\Sigma_1 = \begin{pmatrix} 34 & 0 \\ 0 & 0.5 \end{pmatrix}$ (no correlation), $\Sigma_2 = \begin{pmatrix} 34 & -1.5 \\ -1.5 & 0.5 \end{pmatrix}$ (small correlation), $\Sigma_3 = \begin{pmatrix} 34 & -3.2 \\ -3.2 & 0.5 \end{pmatrix}$ (large correlation), $\Sigma_4 = \begin{pmatrix} 34 & -4 \\ -4 & 0.5 \end{pmatrix}$ (true correlation). The relationships between the simulation probability and objective, between the simulation probability and set size, and between the objective value and set size are shown in Figures 4.3-4.7 corresponding to different types of uncertainty set, respectively.

4.3.2 Uncertainty Set for Bounded Uncertainty

For bounded uncertainty, assume the uncertainty u follows a truncated normal distribution with zero mean, covariance $\Sigma = \begin{pmatrix} 34 & -4 \\ -4 & 0.5 \end{pmatrix}$, and bounds $u_1 \in \begin{bmatrix} -7 & 7 \end{bmatrix}$, $u_2 \in \begin{bmatrix} -1 & 1 \end{bmatrix}$. In the uncertainty set definitions, it is set that $M_1 = \begin{pmatrix} \hat{a}_1^{-1} & 0 \\ 0 & \hat{a}_2^{-1} \end{pmatrix} = \begin{pmatrix} 1/7 & 0 \\ 0 & 1 \end{pmatrix}$. The robust counterpart formulations can be obtained by property 10 and 11. If the covariance matrix used in robust formulation is the true covariance matrix Σ in the assumption of the uncertainty, the interval + polyhedral uncertainty set based robust counterpart of the

constraint with uncertainty is

$$
\begin{aligned}
&10x_1 + 20x_2 + \sum_{j=1}^{2} y_j + \Delta\tau \leq 140 \\
&-y_1 \leq 7(x_1 - z_1) \leq y_1 \\
&-y_2 \leq x_2 - z_2 \leq y_2 \\
&-\tau \leq 5.7932z_1 - 0.6621z_2 \leq \tau \\
&-\tau \leq -0.6621z_1 + 0.2483z_2 \leq \tau
\end{aligned}
$$

and the interval + ellipsoidal uncertainty set based robust counterpart of the constraint with uncertainty is

$$
\begin{aligned}
&10x_1 + 20x_2 + \sum_{j=1}^{2} y_j + \Delta\sqrt{34z_1^2 - 8z_1z_2 + 0.5z_2^2} \leq 140 \\
&-y_1 \leq 7(x_1 - z_1) \leq y_1 \\
&-y_2 \leq x_2 - z_2 \leq y_2
\end{aligned}
$$

The four different covariance matrices used in Section 4.3.1 were also used here to formulate robust optimization problem. The corresponding results are reported in Figure 4.6 and 4.7.

4.3.3 Discussion

Based on the results of the different types of uncertainty set and different covariance matrices for each type of uncertainty set, the following observations can be made. First, from the relationships between the probability of satisfaction and set size and between objective value and set size shown in Figure 4.3-4.7, it is observed that as the set size increases (e.g. box type, from 0 to 3.5), the probability of satisfaction increases (e.g., box type, from around 0.73 to 1), whereas the objective value becomes worse (i.e., decreases for a maximization problem). This observation shows the trade-off between the optimality and the solution reliability.

Second, as shown in Figure 4.3-4.7, the solutions obtained with different covariance ma-

trices vary from each other for all types of uncertainty set. The diagonal elements (variances) of the four covariance matrices are the same and the differences lie in the correlation of the uncertainties. The correlation level between the uncertainties were set as 0 (0), 0.36 (-1.5), 0.78 (-3.2), and 0.97 (-4), respectively. Notice that for a maximization problem, given a desired level of probability of satisfaction, a solution with larger objective value means less conservative solution and it is preferred. It is observed from Figure 4.3-4.7 that if the true correlation (off-diagonal element is -4) of the uncertainties is considered when formulating the robust counterpart, the result is the best (i.e., under the same probability level of constraint satisfaction, the optimal objective value is the largest). While the correlation used in robust counterpart formulation deviates more from the exact correlation of uncertainties, the result becomes worse (i.e., more conservative). And the result obtained by the robust formulation without considering correlation (off-diagonal element is 0) is the worst. For instance, as shown in Figure 4.3, given the desired level of probability of satisfaction as 0.9 (shown as pink dash line), the optimal objective value obtained from robust formulation with true correlation (off-diagonal element is -4) is 84.5 (shown as red dot), which is the best (largest for a maximum problem). While the optimal objective value obtained from robust formulation without considering correlation (off-diagonal element is 0) is 80 (shown as blue dot), which is the worst. As the correlation level considered in robust formulation deviates more from the true correlation (off-diagonal element -1.5 deviates more from -4 than -3.2), the optimal objective value becomes worse (from around 84 to around 82.5). This observation reflects the importance of considering accurate correlations in the robust formulation.

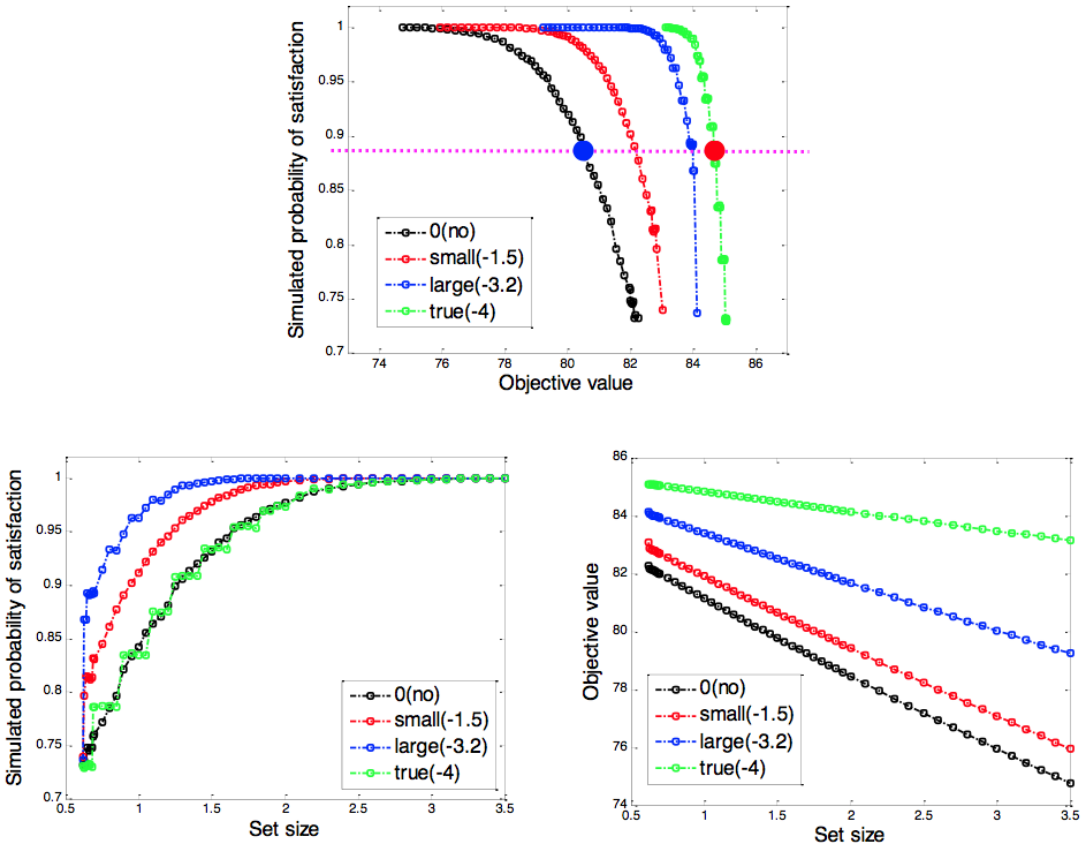

Figure 4.3: Box type uncertainty set induced robust optimization results.

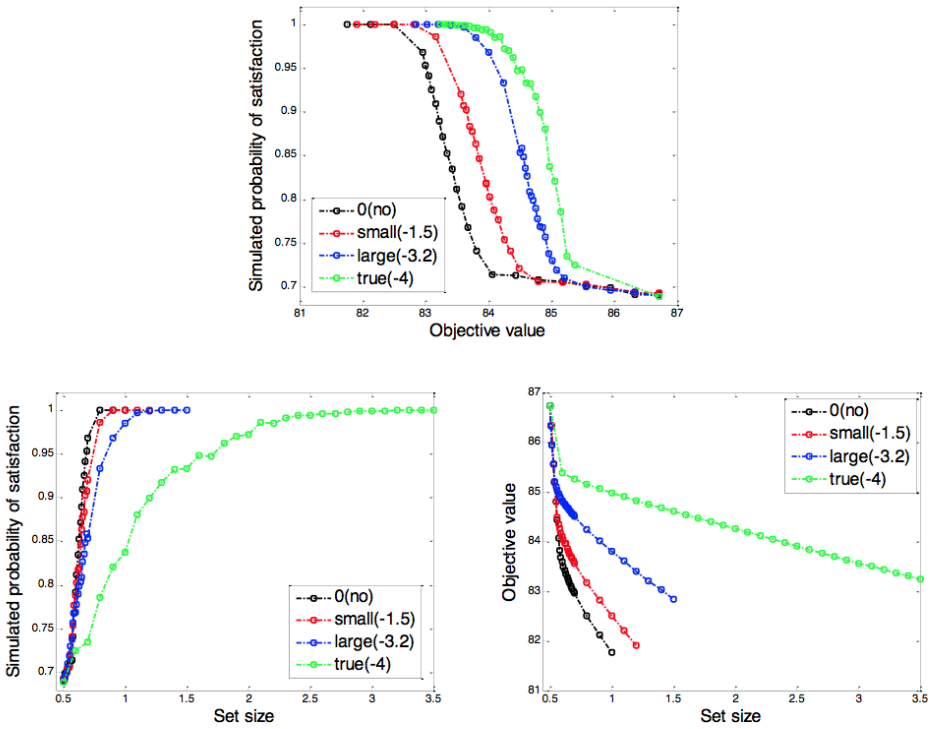

Figure 4.4: Robust optimization results (ellipsoidal set).

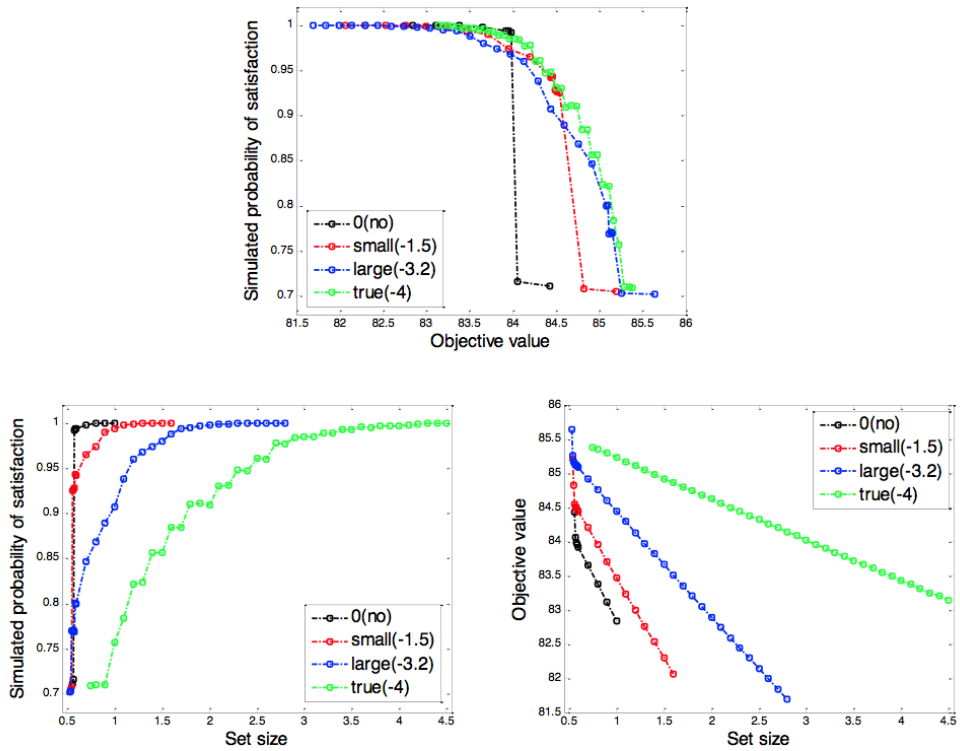

Figure 4.5: Robust optimization results (polyhedral set).

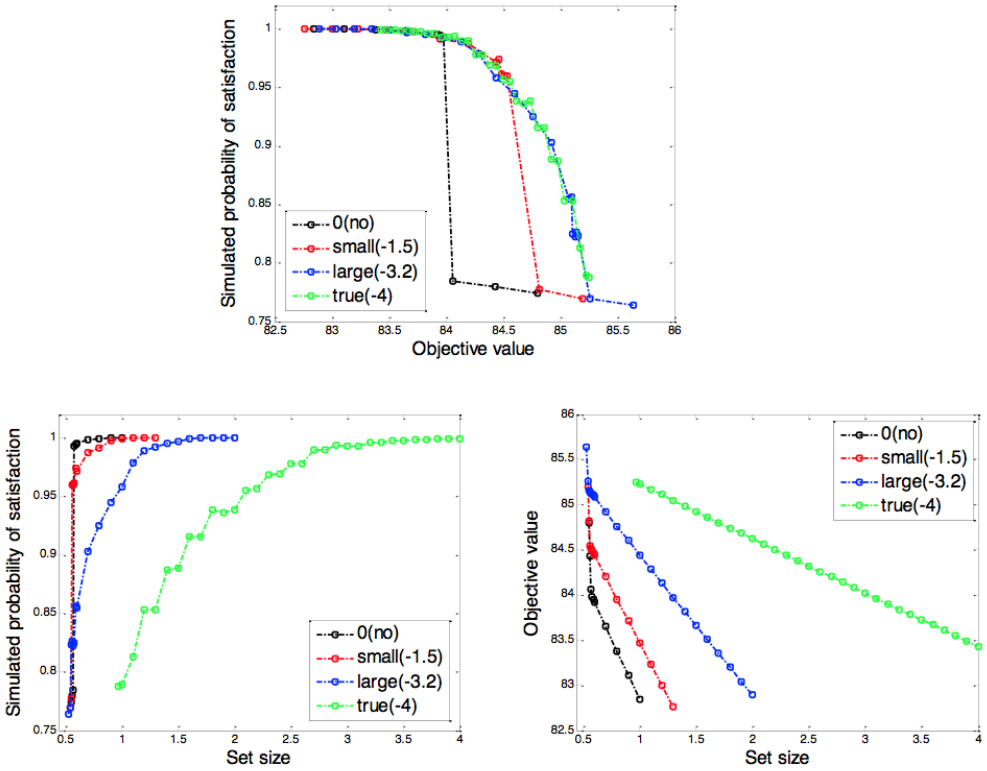

Figure 4.6: Robust optimization results (interval + polyhedral set).

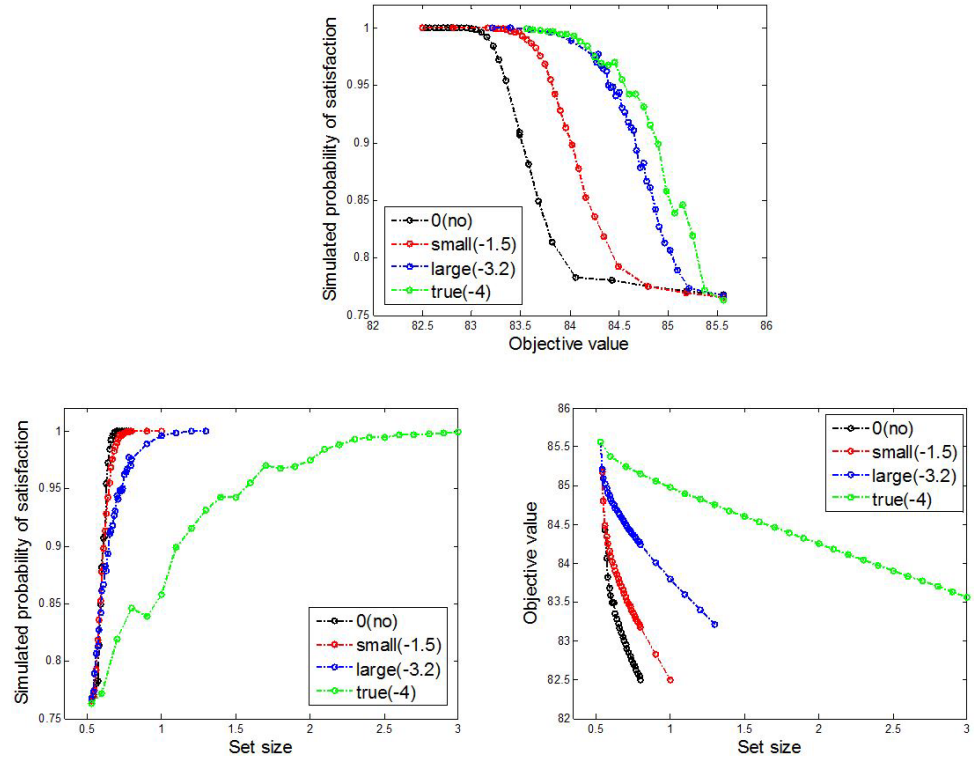

Figure 4.7: Robust optimization results (interval + ellipsoidal set).

Finally, for polyhedral and interval + polyhedral types of uncertainty set, there is a big jump of the probability of satisfaction around the set size 0.55 shown in Figure 4.5 and 4.6. This is caused by the change of the robust counterpart optimization solutions and this only happens when the correlation used for robust counterpart formulation is very different from the exact correlation of the uncertainties.

4.4 Production Planning Example

In this section, the robust optimization formulation under correlated uncertainties is applied to solve robust production planning problem introduced by Ravindran [81]. In this problem, a production plan needs to be made in a company for the coming year that is divided into 6 periods. In the first period, operations begin with an initial stock of 500 tons of the product, and the same amount of the product in storage is required at the end of the year. The objective is to maximize the sales. The following constraints are applied: the total cost is less than or equal to a given budget, the inventory material balances, the final stored product requirement, the production capacity limitations and the demand upper bounds. The production planning problem is formulated as a linear optimization model:

$$
\begin{aligned}
&\max \sum_j P_j z_j \\
&\text{s.t.} \sum_j C_j x_j + \sum_j V_j y_j \leq 400,000 \\
&\quad 500 + x_1 - (y_1 + z_1) = 0 \\
&\quad y_{j-1} + x_j - (y_j + z_j) = 0 \ \forall j = 2, ..., 6 \\
&\quad y_6 = 500 \\
&\quad x_j \leq U_j \ \forall j = 1, ..., 6 \\
&\quad z_j \leq D_j \ \forall j = 1, ..., 6 \\
&\quad x_j, y_j, z_j \geq 0 \ \forall j = 1, ..., 6
\end{aligned}
$$

where the symbols are explained as following and Table 4.1 displays the detailed parameter values:

j	index, period
P_j	parameter, price of product
C_j	parameter, production cost
V_j	parameter, storage cost
U_j	parameter, capacity limitation of production
D_j	parameter, market demand
x_j	variable, the amount of manufactured product during period j
y_j	variable, the amount of stored product at the end of period j
z_j	variable, the amount of sold product during period j

Table 4.1: Production planning problem data

j	P_j	C_j	V_j	U_j	D_j
1	180	20	2	1500	1100
2	180	25	2	2000	1500
3	250	30	2	2200	1800
4	270	40	2	3000	1600
5	300	50	2	2700	2300
6	320	60	2	2500	2500

Assume the production costs $\tilde{C}_j$ contain uncertainties and have a maximum of 50% perturbation around the nominal values listed in Table 4.1. It is assumed that the costs in different periods have correlations with each other. Assume the uncertain parameters $\tilde{C}_j$ are represented as $\tilde{C}_j = C_j + u_j$, where u_j follow a truncated multivariate Gaussian distribution, i.e., $u_j \in [-0.5C_j, 0.5C_j], u_j \sim \mathcal{N}(0, \Sigma)$. Considering the correlations of uncertainty (with known covariance matrix) in the robust optimization formulation and using "interval + polyhedral" type of uncertainty set, the robust counterpart constraints under correlated

uncertainty are written as

$$\begin{cases} \sum_j C_j x_j + \sum_j V_j y_j + \sum_j p_j + \Delta\tau \leq 400,000 \\ -p_j \leq m_j^{(1)}(x_j - q_j) \leq p_j, \forall j \\ -\tau \leq \sum_j m_{kj}^{(2)} q_j \leq \tau, \forall k \end{cases}$$

where $m_j^{(1)}$ are elements of the matrix M_1^{-T} representing the perturbation, i.e., $m_j^{(1)} = 0.5C_j$, $m_{kj}^{(2)}$ are elements of the matrix M_2^{-T} representing the correlations, and $M_2 = \Sigma^{-1/2}$. On the other hand, if we do not consider correlations (covariance matrix is unknown) and only consider perturbations in the robust optimization formulation and still select "interval + polyhedral" type of uncertainty set, the original constraint with uncertainty is written as

$$\begin{cases} \sum_j C_j x_j + \sum_j V_j y_j + \sum_j p_j + \Delta\tau \leq 400,000 \\ -p_j \leq m_j^{(1)}(x_j - q_j) \leq p_j, \forall j \\ -\tau \leq m_j^{(1)} q_j \leq \tau, \forall j \end{cases}$$

Both linear robust optimization problems were solved using CPLEX solver in GAMS 23.9. It only takes around 0.5 second to solve the robust optimization problem, which reflects the fact that the robust optimization method is efficient. Furthermore, the probabilities of constraint satisfaction are simulated using 100,000 samples in MATLAB. The relationships between the simulation probability and objective value for both cases (with and without considering correlations in robust optimization formulation) are shown in Figure 4.8.

It can be observed that for a given probability of satisfaction level, the robust optimization formulation considering correlations between uncertainties outperforms the robust optimization formulation considering independent perturbations. This is because a larger objective value is obtained from the correlated robust optimization model under the same level probability of constraint satisfaction. It can be concluded that if more information, such as the covariance matrix, is available for the uncertain parameters, considering them

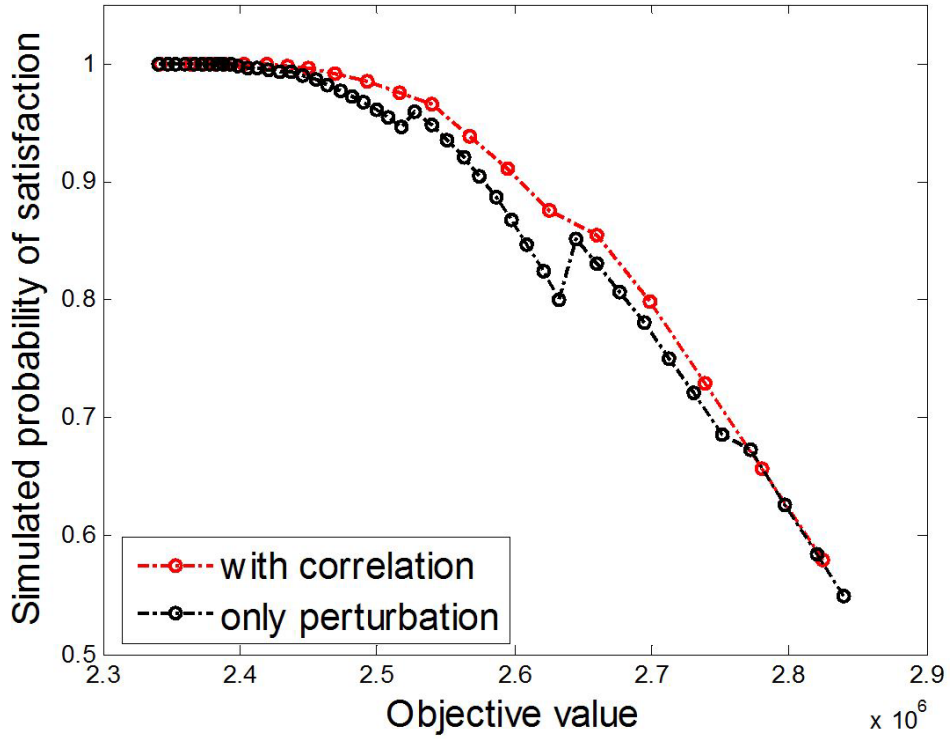

Figure 4.8: Objective value versus simulated probability of satisfaction.

in the formulation of the robust optimization problem can improve the performance of the robust optimization solution.

4.5 Comparison of Robust Optimization Formulations Based on Constraint-Wise and Global Uncertainty Set

In this section, linear optimization problems with parameter uncertainty are studied for multiple constraints and with out loss of generality, uncertainty is assumed to appear only in the constraints. The general form of the constraints used in Chapter 3 can be represented as follows:

$$y_0^i + (\mathbf{y}^i)^T \boldsymbol{\xi}^i \leq 0, i = 1, ..., n \tag{4.64}$$

where n is the number of constraints. In each constraint, the uncertainty vector can be written as $\boldsymbol{\xi}^i = (\xi_1^i, ..., \xi_{s_i}^i)^T$, where s_i is the number of uncertainties in the ith constraint. The structure of the uncertainty in different constraints is classified into three cases in this section:

1. Uncertainties in different constraints are exactly the same.
2. Uncertainties in different constraints are completely different.
3. Uncertainties in different constraints are partly the same.

Robust optimization formulations based on "constraint-wise" and "global" uncertainty set are considered. "Constraint-wise" uncertainty set is constructed for the uncertainties in each individual constraint, separately. Hence, the correlations of the uncertainties from different constraint cannot be captured in the uncertainty sets. When constructing the "global" uncertainty set, the uncertainties from all the constraints are collected together into one set with eliminating the repeated elements, and a unique uncertainty set is defined on the augmented set of uncertainties.

For the ith constraint, the "constraint-wise" uncertainty set is defined as follows:

$$U_{\boldsymbol{\xi}^i} = \left\{ \boldsymbol{\xi}^i \,\middle|\, \left\| M_{\boldsymbol{\xi}^i \times \boldsymbol{\xi}^i} \boldsymbol{\xi}^i \right\| \leq \Delta^i \right\} \tag{4.65}$$

where $\boldsymbol{\xi}^i$ is the uncertainty vector containing all the uncertainties in the ith constraint.

The "global" uncertainty set is defined as follows:

$$U_{\boldsymbol{\xi}} = \{ \boldsymbol{\xi} \,|\, \| M_{\boldsymbol{\xi} \times \boldsymbol{\xi}} \boldsymbol{\xi} \| \leq \Delta \} \tag{4.66}$$

where $\boldsymbol{\xi}$ is the augmented uncertainty vector for the uncertainties from all the constraints with eliminating the repeated ones.

4.5.1 Derivation of Robust Optimization Formulation

In this section, the robust optimization (RO) formulations are derived based on the two types of uncertainty set: "global" set for all the constraints together and "constraint-wise" set for each individual constraint. And the three cases of uncertainty structure listed above are considered. Since in the first case of uncertainty structure, it is obvious that RO formulations based on "constraint-wise" and "global" uncertainty set are the same, only the cases that uncertainties in different constraints are completely different and uncertainties in different constraints are partly the same are considered.

4.5.1.1 Different Constraints with Different Uncertainties

In this subsection, the case that uncertainties in different constraints are different is considered. The correlation between any two uncertainties are defined using the subscript $\xi_j^i \times \xi_{j'}^{i'}$.

The RO formulation based on the two types of uncertainty set can be obtained using Property 7-9 in Section 4.2.

a). RO formulation based on "global" uncertainty set is

$$y_0^i + \Delta \left\| M^{-T} \mathbf{y}_{aug}^i \right\|_* \leq 0, i = 1, ..., n \tag{4.67}$$

where $M^{-T} = \Sigma^{1/2}$, Σ is the covariance matrix for the augmented uncertainty vector $\boldsymbol{\xi} = (\boldsymbol{\xi}^1; ...; \boldsymbol{\xi}^n)$ and $\mathbf{y}_{aug}^i$ is the augmented vector corresponding to $\mathbf{y}^i$ containing n blocks with the ith block to be $\mathbf{y}^i$ and other blocks to be all zeros, i.e., $\mathbf{y}_{aug}^i = (0; ...0; \mathbf{y}^i; 0; ...; 0)$. $\|\cdot\|_*$ represents the dual norm for $\|\cdot\|$. Matrix M^{-T} can be written as

$$M^{-T} = \begin{bmatrix} M_{\boldsymbol{\xi}^1 \times \boldsymbol{\xi}^1} & ... & M_{\boldsymbol{\xi}^1 \times \boldsymbol{\xi}^n} \\ ... & ... & ... \\ M_{\boldsymbol{\xi}^n \times \boldsymbol{\xi}^1} & ... & M_{\boldsymbol{\xi}^n \times \boldsymbol{\xi}^n} \end{bmatrix}$$

b). RO formulation based on "constraint-wise" uncertainty set is

$$y_0^i + \Delta^i \left\| M_i^{-T} \mathbf{y}^i \right\|_* \leq 0, i = 1, ..., n \tag{4.68}$$

where $M_i^{-T} = \Sigma_i^{1/2}$, Σ_i is the covariance matrix for uncertainty $\boldsymbol{\xi}^i$ in the ith constraint, and $M_i^{-T} = M_{\boldsymbol{\xi}^i \times \boldsymbol{\xi}^i}$. For the "constraint-wise" uncertainty set, since matrix M_i^{-T} only contains the information about the uncertainty $\boldsymbol{\xi}_i$ in the ith constraint, the correlation of the uncertainty in different constraints has no influence on the formulation and the final results.

Three shapes of uncertainty set, i.e., box, ellipsoidal and polyhedral can be represented by infinite norm, 2-norm and 1-norm, respectively. For both "global" and "constraint-wise" uncertainty set, in order to illustrate, it can be denoted that $M^{-T}\mathbf{y} = (x_1, ..., x_N)^T$ with N to be the number of uncertainties. Write the norms in the RO formulation into explicit form with respect to different types of uncertainty set as follows:

Box uncertainty set: $U_{box} = \{u \,|\, \|Mu\|_\infty \leq \Delta\}$

$$\left\| M^{-T}\mathbf{y} \right\|_1 = \left\| (x_1, ..., x_N)^T \right\|_1 = \sum_{i=1}^{N} |x_i|$$

Ellipsoidal uncertainty set: $U_{ellipsoid} = \{u \,|\, \|Mu\|_2 \leq \Delta\}$

$$\left\| M^{-T}\mathbf{y} \right\|_2 = \left\| (x_1, ..., x_N)^T \right\|_2 = \sqrt{\sum_{i=1}^{N} {x_i}^2}$$

Polyhedral uncertainty set: $U_{polyhedral} = \{u \,|\, \|Mu\|_1 \leq \Delta\}$

$$\left\| M^{-T}\mathbf{y} \right\|_\infty = \left\| (x_1, ..., x_N)^T \right\|_\infty = \max_{i=1,...,N} |x_i|$$

Since

$$\left(\sum_{i=1}^{N} |x_i| \right)^2 = \sum_{i=1}^{N} x_i^2 + \sum_{i=1, i\neq j}^{N} \sum_{j=1}^{N} |x_i| \, |x_j| \geq \sum_{i=1}^{N} x_i^2$$

It can be obtained that $\left\|M^{-T}\mathbf{y}\right\|_1 \geq \left\|M^{-T}\mathbf{y}\right\|_2$. And it is obvious that $\left\|M^{-T}\mathbf{y}\right\|_2 \geq \left\|M^{-T}\mathbf{y}\right\|_\infty$. Then, it can be concluded that with the same uncertainty set size Δ, the RO formulation based on box uncertainty set is the most conservative since it has the highest protect level of the constraint, while polyhedral uncertainty set is the least conservative.

Next, different relationships of the uncertainties across different constraints are considered.

(I). Uncertainties in different constraints are independent

In this case, it is considered that the uncertainties in different constraints are independent, i.e., the elements in the matrices $M_{\boldsymbol{\xi}^i \times \boldsymbol{\xi}^j}, i \neq j$ are zeros. It can be obtained that

$$\left\|M^{-T}\mathbf{y}^i_{aug}\right\|_* = \left\| \begin{bmatrix} 0 \\ \dots \\ M_{\boldsymbol{\xi}^i \times \boldsymbol{\xi}^i}\mathbf{y}^i \\ \dots \\ 0 \end{bmatrix} \right\|_* = \left\|M_{\boldsymbol{\xi}^i \times \boldsymbol{\xi}^i}\mathbf{y}^i\right\|_* = \left\|M_i^{-T}\mathbf{y}^i\right\|_*$$

which implies that in this case, with same uncertainty set size Δ the RO formulation based on global uncertainty set represented in Eq.(4.67) is the same as the RO formulation based on constraint-wise uncertainty set in Equation(4.68) with box, ellipsoidal, polyhedral shapes of uncertainty set.

(II). Uncertainties in different constraints are correlated

In this case, the uncertainties in different constraints are considered to be correlated. First, the relationship between matrix M and covariance matrix Σ is explicitly written as follows:

$$\begin{pmatrix} m_{11} & \dots & m_{1N} \\ \dots & \dots & \dots \\ m_{N1} & \dots & m_{NN} \end{pmatrix} \begin{pmatrix} m_{11} & \dots & m_{1N} \\ \dots & \dots & \dots \\ m_{N1} & \dots & m_{NN} \end{pmatrix} = \begin{pmatrix} \sigma_{11}^2 & \dots & \sigma_{1N} \\ \dots & \dots & \dots \\ \sigma_{N1} & \dots & \sigma_{NN}^2 \end{pmatrix} = \Sigma$$

where $M^{-T} = \begin{pmatrix} m_{11} & ... & m_{1N} \\ ... & ... & ... \\ m_{N1} & ... & m_{NN} \end{pmatrix}$.

If uncertainties are independent, the off-diagonal elements of matrix Σ and matrix M^{-T} are zeros, and $\sigma_{ii} = m_{ii}^{'}, i = 1, ..., N$. If the uncertainties are correlated, it can be obtained that

$$\sigma_{ii}^2 = \sum_{j=1}^{N} m_{ij}^2 = m_{ii}^2 + \sum_{j \neq i} m_{ij}^2, i = 1, ..., N \tag{4.69}$$

It is obvious that the diagonal elements of matrix M^{-T} with independent uncertainties are always larger than those with correlated uncertainties, i.e.,

$$m_{ii}^{'} > m_{ii}, i = 1, ..., N \tag{4.70}$$

The relationship shown in (4.70) will be used for the following comparisons.

Box uncertainty set:

For the box uncertainty set, the norm part in "global" RO formulation is

$$\left\| M^{-T} \mathbf{y}_{aug}^i \right\|_1 = \left\| \begin{bmatrix} M_{\boldsymbol{\xi}^1 \times \boldsymbol{\xi}^i} \mathbf{y}^i \\ ... \\ M_{\boldsymbol{\xi}^i \times \boldsymbol{\xi}^i} \mathbf{y}^i \\ ... \\ M_{\boldsymbol{\xi}^n \times \boldsymbol{\xi}^i} \mathbf{y}^i \end{bmatrix} \right\|_1 = \left\| M_{\boldsymbol{\xi}^i \times \boldsymbol{\xi}^i} \mathbf{y}^i \right\|_1 + \sum_{j=1, j \neq i}^{N} \left\| M_{\boldsymbol{\xi}^j \times \boldsymbol{\xi}^i} \mathbf{y}^i \right\|_1 \tag{4.71}$$

Since in "constraint-wise" RO formulation, the uncertainties in different constraints can be regarded as independent, the term $\left\| M_{\boldsymbol{\xi}^i \times \boldsymbol{\xi}^i} \mathbf{y}^i \right\|_1$ in "constraint-wise" RO formulation shown in Equation(4.68) is always larger than the first term in (4.71), and the second term in (4.71) has nonnegative value. With the influence of both the two terms, there is no definite relationship of the conservativeness of constraint-wise and global RO formulation with box shape.

Ellipsoidal uncertainty set:

The norm part in global RO formulation can be explicitly written as

$$\left\|M^{-T}\mathbf{y}^i_{aug}\right\|_2 = \sqrt{(\mathbf{y}^i_{aug})^T\Sigma\mathbf{y}^i_{aug}} = \sqrt{\begin{bmatrix} 0 \\ \dots \\ \mathbf{y}^i \\ \dots \\ 0 \end{bmatrix}^T \begin{bmatrix} \Sigma_{\boldsymbol{\xi}^1\times\boldsymbol{\xi}^1} & \dots & \Sigma_{\boldsymbol{\xi}^1\times\boldsymbol{\xi}^i} & \dots & \Sigma_{\boldsymbol{\xi}^1\times\boldsymbol{\xi}^n} \\ \dots & \dots & \dots & \dots & \dots \\ \Sigma_{\boldsymbol{\xi}^i\times\boldsymbol{\xi}^1} & \dots & \Sigma_{\boldsymbol{\xi}^i\times\boldsymbol{\xi}^i} & \dots & \Sigma_{\boldsymbol{\xi}^i\times\boldsymbol{\xi}^n} \\ \dots & \dots & \dots & \dots & \dots \\ \Sigma_{\boldsymbol{\xi}^n\times\boldsymbol{\xi}^1} & \dots & \Sigma_{\boldsymbol{\xi}^n\times\boldsymbol{\xi}^i} & \dots & \Sigma_{\boldsymbol{\xi}^n\times\boldsymbol{\xi}^n} \end{bmatrix} \begin{bmatrix} 0 \\ \dots \\ \mathbf{y}^i \\ \dots \\ 0 \end{bmatrix}}$$

$$= \sqrt{\begin{bmatrix} (\mathbf{y}^i)^T\Sigma_{\boldsymbol{\xi}^i\times\boldsymbol{\xi}^1} \\ \dots \\ (\mathbf{y}^i)^T\Sigma_{\boldsymbol{\xi}^i\times\boldsymbol{\xi}^i} \\ \dots \\ (\mathbf{y}^i)^T\Sigma_{\boldsymbol{\xi}^i\times\boldsymbol{\xi}^n} \end{bmatrix}^T \begin{bmatrix} 0 \\ \dots \\ \mathbf{y}^i \\ \dots \\ 0 \end{bmatrix}} = \sqrt{(\mathbf{y}^i)^T\Sigma_{\boldsymbol{\xi}^i\times\boldsymbol{\xi}^i}\mathbf{y}^i} = \left\|{M_i}^{-T}\mathbf{y}^i\right\|_2$$

It can be concluded that for ellipsoidal shape uncertainty set, the "global" and "constraint-wise" formulation is the same although correlation exists in the uncertainties across different uncertainty.

Polyhedral uncertainty set:

The norm part in "global" RO formulation is as follows

$$\left\|M^{-T}\mathbf{y}^i_{aug}\right\|_\infty = \left\|\begin{bmatrix} M_{\boldsymbol{\xi}^1\times\boldsymbol{\xi}^i}\mathbf{y}^i \\ \dots \\ M_{\boldsymbol{\xi}^i\times\boldsymbol{\xi}^i}\mathbf{y}^i \\ \dots \\ M_{\boldsymbol{\xi}^n\times\boldsymbol{\xi}^i}\mathbf{y}^i \end{bmatrix}\right\|_\infty = \max_{j=1,\dots,n}\left\|M_{\boldsymbol{\xi}^j\times\boldsymbol{\xi}^i}\mathbf{y}^i\right\|_\infty \geq \left\|M_{\boldsymbol{\xi}^i\times\boldsymbol{\xi}^i}\mathbf{y}^i\right\|_\infty \tag{4.72}$$

When the " = " sign holds in (4.72), according to relation (4.70), the term $\left\|M_{\boldsymbol{\xi}^i\times\boldsymbol{\xi}^i}\mathbf{y}^i\right\|_\infty$ in "constraint-wise" RO formulation is always larger than that in (4.72) due to the independence

of uncertainties in different constraints in constraint-wise formulation. It can be concluded that the "global" formulation is less conservative than the "constraint-wise" formulation. If the " $=$ " does not hold in (4.72), there is no definite relationship of the conservativeness of "constraint-wise" and "global" RO formulations.

4.5.1.2 Different Constraints with Partly Same Uncertainties

Due to the definition of uncertainty set in this work, the matrix M is required to be invertible. When constructing the augmented uncertain vector, the repeated elements should be eliminated, so this case of uncertainty structure can be regarded as special cases in the case represented in subsection 4.5.1.1.

1. The unrepeated elements are independent

This case is actually equivalent as the case when the uncertainties in different constraints are completely different and the uncertainties are independent across constraints (**(I)** of section 4.5.1.1). In this case, the "global" RO formulation is the same as the "constraint-wise" RO formulation.

2. Only the distinguished elements are correlated

This case can be regarded as the case that uncertainties in different constraints are completely different when uncertainties are correlated among constraints (**(II)** of section 4.5.1.1). The conclusion is that the "global" and "constraint-wise" formulations are the same for ellipsoidal shape uncertainty set while for box and polyhedral shape, there is no definite relationship.

3. Correlations exist in the same constraints and across different constraints

This case is the most complicated one, not only the correlation across different constraints but also the correlation within the same constraint influence the final comparison results.

4.5.2 Illustrative Examples

4.5.2.1 Numerical Example (LHS Uncertainty)

The uncertainty exists on the left-hand-side (LHS) of the constraints and the case is that different multiple uncertainties appear in different constraints.

$$\begin{aligned} \max \quad & 8x_1 + 12x_2 \\ s.t. \quad & (10+\xi_1)x_1 + (20+\xi_2)x_2 \leq 140 \\ & (6+\xi_3)x_1 + (8+\xi_4)x_2 \leq 72 \\ & x_1, x_2 \geq 0 \end{aligned} \tag{4.73}$$

The uncertainties are assumed to follow normal distribution with zero mean, and the variance of the uncertainties are 4, 25, 16, and 9.

1. The conclusion in **(I)** of section 4.5.1.1 is tested by assuming that ξ_1 is independent with ξ_3 and ξ_4 and ξ_2 is independent with ξ_3 and ξ_4. Correlation between ξ_1 and ξ_2, and between ξ_3 and ξ_4 will not influence the results, a correlation of them is considered for generality. The correlation matrices for "global" and "constraint-wise" formulations are

$$R = \begin{bmatrix} 1 & 0.5 & 0 & 0 \\ 0.5 & 1 & 0 & 0 \\ 0 & 0 & 1 & 0.5 \\ 0 & 0 & 0.5 & 1 \end{bmatrix}, R_1 = \begin{bmatrix} 1 & 0.5 \\ 0.5 & 1 \end{bmatrix}, R_2 = \begin{bmatrix} 1 & 0.5 \\ 0.5 & 1 \end{bmatrix}$$

The relationship of set size and optimal objective value is plotted in Figure 4.9

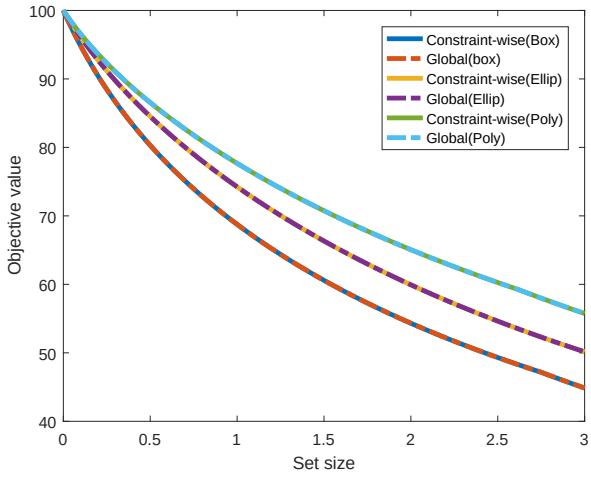

Figure 4.9: Set size vs. optimal objective value (**(I)** of section 1.1)

This figure can also be used to show the relationship of the RO formulations based on box, ellipsoidal, polyhedral shapes of uncertainty set. It can be observed that with the same set size, the objective value of the box formulation is the smallest and the objective value of the polyhedral formulation is the largest, which implies the conclusion that the RO formulation with box uncertainty set is the most conservative (smallest objective value for a maximization problem). For all the three shapes of uncertainty set, the lines for "constraint-wise" and "global" uncertainty set coincide, which means that when the uncertainties from different constraints are independent the RO formulations are the same.

2. The conclusion in **(II)** of section 4.5.1.1 is tested for box shape uncertainty set first. It is assumed that ξ_1 is correlated with both ξ_3 and ξ_4 and ξ_2 is correlated with both ξ_3 and ξ_4. In order to consider the influence of correlation from different constraints, it is assumed that ξ_1 is independent of ξ_2 and ξ_3 is independent of ξ_4. The correlation matrices for "global" and "constraint-wise" formulations are

$$R = \begin{bmatrix} 1 & 0 & 0.5 & -0.5 \\ 0 & 1 & -0.5 & 0.5 \\ 0.5 & -0.5 & 1 & 0 \\ -0.5 & 0.5 & 0 & 1 \end{bmatrix}, R_1 = \begin{bmatrix} 1 & 0 \\ 0 & 1 \end{bmatrix}, R_2 = \begin{bmatrix} 1 & 0 \\ 0 & 1 \end{bmatrix}$$

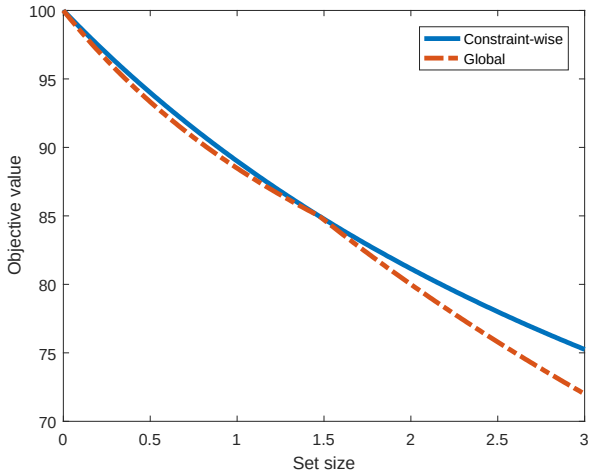

Figure 4.10: Set size vs. optimal objective value (**(II)** of section 4.5.1.1 box)

It can be observed that with the same set size, the objective value of the "constraint-wise" formulation is larger than the one of "global" formulation at most of the times, but when the set size is around 1.5, the two lines coincide, which means that there is no certain conclusion on the conservativeness of the RO formulation for the two types of uncertainty set with box shape under the condition that the uncertainties from different constraints are correlated.

3. The conclusion in **(II)** of section 4.5.1.1 is tested for ellipsoidal shape uncertainty set. The matrices are considered as the same as **case 2**.

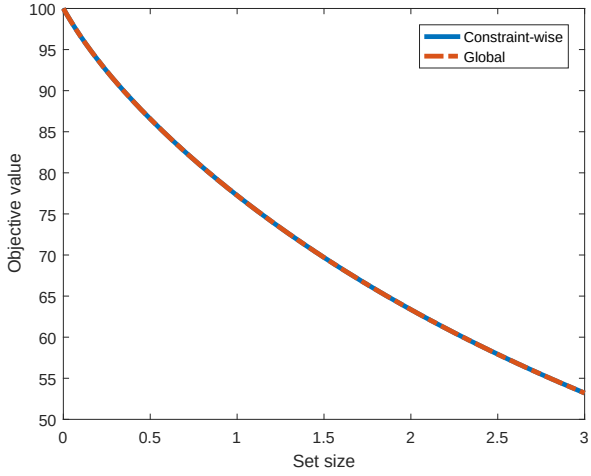

Figure 4.11: Set size vs. optimal objective value (**(II)** of section 4.5.1.1 ellipsoidal)

In this figure, the two lines coincide, which implies that the ellipsoid shape uncertainty

has the property that even when the uncertainties from different constraints are correlated, the "constraint-wise" and "global" RO formulation have the same results.

4. The conclusion in **(II)** of section 4.5.1.1 is tested for polyhedral shape uncertainty set. Two sets of assumption of the uncertainty structure are considered. First, correlations exist between ξ_1 and ξ_3, and between ξ_2 and ξ_4. The correlation matrices are shown as follows:

$$R = \begin{bmatrix} 1 & 0 & 0.5 & 0 \\ 0 & 1 & 0 & 0.5 \\ 0.5 & 0 & 1 & 0 \\ 0 & 0.5 & 0 & 1 \end{bmatrix}, R_1 = \begin{bmatrix} 1 & 0 \\ 0 & 1 \end{bmatrix}, R_2 = \begin{bmatrix} 1 & 0 \\ 0 & 1 \end{bmatrix}$$

The second assumption considers the same correlation matrices as **case 2**.

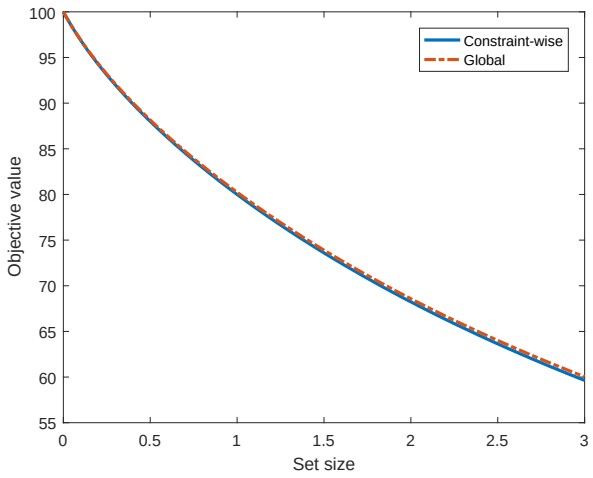

Figure 4.12: Set size vs. optimal objective value (**(II)** of section 4.5.1.1 polyhedral)

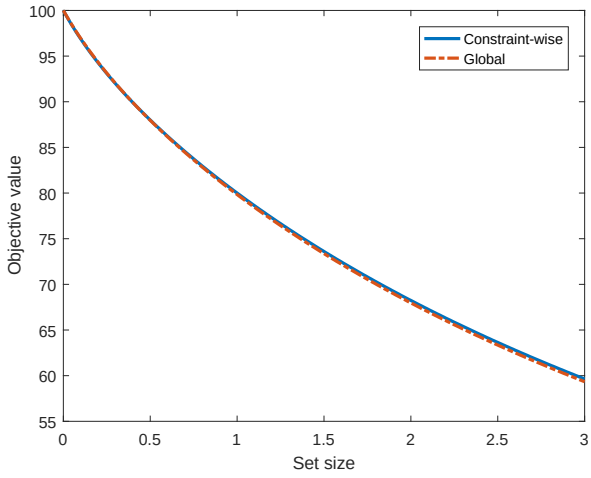

Figure 4.13: Set size vs. optimal objective value (**(II)** of section 4.5.1.1 polyhedral)

Figure 4.12 shows that "constraint-wise" formulation is more conservative, while Figure 4.13 shows that "global" formulation is more conservative. It implies that similar to the box shape uncertainty set, the results from the 'constraint-wise" and "global" uncertainty set are not certain for the case that the uncertainties from different constraints are correlated.

4.5.2.2 Numerical Example (Repeated Uncertainties)

In this example [82], uncertainty only appears on the right-hand-side (RHS) of the constraints. The numbers of uncertainties in different constraints can be different, and part of the uncertainties in each constraint can be the same.

$$\begin{aligned} \min \quad & x_1 + 2x_2 \\ s.t. \quad & x_1 + x_2 \geq \xi_1 + \xi_2 \\ & x_2 \geq \xi_2 \\ & 0 \leq x_1 \leq 2, 0 \leq x_2 \leq 5 \end{aligned} \tag{4.74}$$

ξ_1 and ξ_2 are assumed to follow normal distribution with mean 1 and 2, standard deviation 0.1 and 0.2. First, ξ_1 and ξ_2 are assumed to be independent (**case 1** in section 4.5.1.2). This case is the same as **(I)** of section 4.5.1.1, and the "global" and "constraint-wise" formulations

should be the same, which is demonstrated in Figure 4.14.

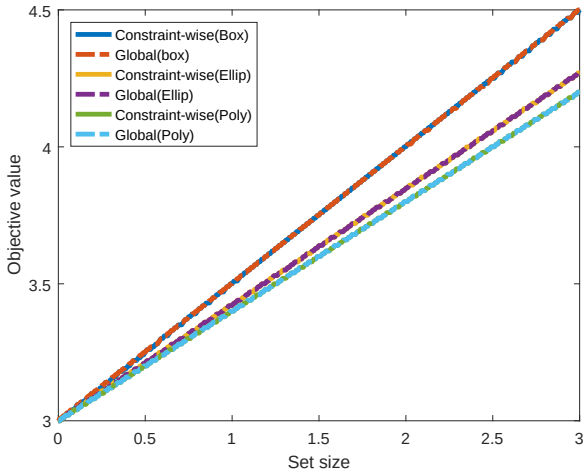

Figure 4.14: Set size vs. optimal objective value (**case 1** in section 4.5.1.2)

Second, ξ_1 and ξ_2 are considered to be correlated and this is the same as the third case in section 4.5.1.2, which is shown in Figure 4.15.

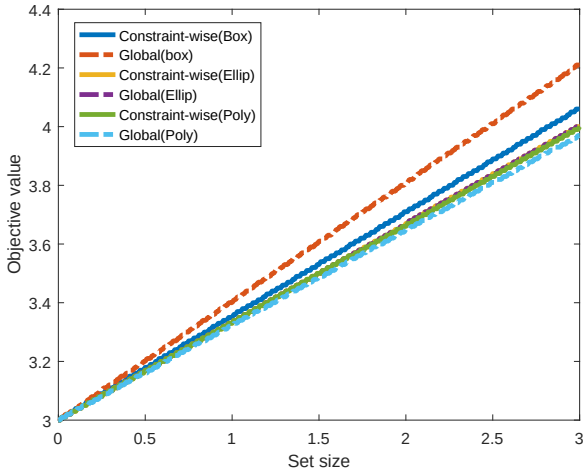

Figure 4.15: Set size vs. optimal objective value (**case 3** in section 4.5.1.2)

4.6 Conclusion

This chapter investigates robust optimization under correlated uncertainties. Specifically, correlated uncertainty within a single constraint is studied and the robust counterpart op-

timization formulations are derived based on five different types of uncertain set: box, ellipsoidal, polyhedral, interval+ellipsoidal, and interval+polyhedral. Computational studies and application example both demonstrate the advantage of modeling correlations in robust optimization framework. That is, less conservative solution can be obtained when more accurate correlation is incorporated into the robust optimization framework. Then, in Section 4.5, the RO formulations for multiple constraints with correlated uncertainties are considered and compared based on "constraint-wise" and "global" uncertainty set. Simple numerical examples are used to test the results with different conditions for the correlations between uncertainties. The conservativeness can be compared for specified conditions of correlation, e.g., when correlation only exist within the same constraints and the uncertainties from different constraints are independent. However, the conservativeness cannot be directly observed from the formulations for complicated correlation conditions. But the formulations can still give a hint on how to select a better uncertainty set in RO formulation.

Chapter 5

Nonlinear Robust Optimization for Process Design

5.1 Introduction

Robust optimization has become an active research area for considering uncertainty in optimization problems. Most of the available approaches in this area focus on linear programming, second-order cone programming and semi-definite programming problems. Chapter 3 and Chapter 4 study robust optimization for linear problems as well. However, nonlinearity reveals in most of the practical problems, for instance, many process design problems can be formulated as nonlinear optimization problems involving system parameters.

In this chapter, a novel nonlinear robust optimization framework is proposed to address general nonlinear problems under uncertainty. The proposed method is based on linearization with respect to uncertain parameter around multiple realizations and an iterative algorithm. The problems to be addressed can be classified as three categories. In the first case, the uncertain parameters are only involved in the inequality constraints, which is the simplest case of nonlinear optimization problems. It is commonly seen in process design or operations optimization problem with only static decisions. Here the objective is to find a robust decision that is feasible to all the possible uncertainty realizations in an uncertainty set. Lineariza-

tion can be directly applied to the nonlinear inequality constraint and robust counterpart optimization formulation is then applied. In the second case, the nonlinear optimization problem involves design variables and state variables coupled by equality constraints, and inequality constraints are enforced for some state variables. In such optimization problems, there will be equality constraints containing uncertain parameters and the traditional robust optimization method cannot be directly applied. However, the state variables can be determined after the design variables as well as the uncertain parameters are fixed. Using the Implicit Function Theorem, the state variables can be replaced by a function of uncertain parameters and design variables. Then the robust optimization formulation can be applied through linearization of the inequality constraints. Third, the nonlinear problem involves design variables, operation (control) variables and state variables. Generally, the design variables should be determined before the exact realizations of the uncertain parameters are available, but the operation (control) variables can actually adjust themselves with respect to the real values of the uncertain parameters during the process. For this type of problem, the operation (control) variables can be adjusted based on the realizations of the uncertainty. Correspondingly, a local affinely adjustable decision rule is adopted for the operation (control) variables (i.e., an affine function of the uncertain parameter). The decision rule will be applied in the nonlinear problem and the problem can be reduced to the second case. The corresponding adjustable robust optimization (ARO) for linear programs has been proposed by Ben-Tal and et al. [44]. The idea of ARO has been applied in scheduling problem of continuous industrial processes providing interruptible load [83] and multi-stage ARO for process scheduling under uncertainty has also been studied [84].

The rest of the chapter is organized as follows: In Section 5.2, the problems considered in this chapter are formally presented. In the Section 5.3, the robust counterpart formulations are derived for all the three classes of problems addressed in this chapter, respectively. In Section 5.4, the formulation based on linearization with respect to uncertain parameter around multiple realizations of uncertainty is provided. The iterative algorithm is also de-

scribed in this section. In Section 5.5, the proposed method is demonstrated through three different applications corresponding to each case of the problem and finally the chapter is concluded in last section.

5.2 Problem Statement

In this chapter, three categories of problems, classified according to the complexity, are considered. The simplest case only contains inequality constraints associated with uncertain parameters, which is expressed in (5.1) as follows:

$$\begin{aligned} \min_{u \in U} \quad & \phi(u) \\ s.t. \quad & G(u, s) \leq 0 \end{aligned} \tag{5.1}$$

where $s \in R^{N_s}$ represents uncertain parameters, $u \in R^{N_u}$ represents design variables which are constrained in a feasible set U, and N_s and N_u represent the number of the uncertain parameters and design variables, respectively. $G = (g_1, ..., g_m)^T \in R^m$, and m is the number of inequality constraints.

In the second case, state equations are involved in the formulation to represent the process model. The design variables and the state variables are coupled by the equality constraints, and uncertain parameters exist in equality constraints as well. The optimization problem is expressed as follows:

$$\begin{aligned} \min_{y, u \in U} \quad & \phi(y, u) \\ s.t. \quad & F(y, u, s) = 0 \\ & G(y, u, s) \leq 0 \end{aligned} \tag{5.2}$$

where $y \in R^{N_y}$ represents state variables, N_y represents the number of the state variables, and $F(y, u, s) = 0$ is known as the state equation. The size of the state variables y and the number of the state equations F should be equal so that the state variables can be determined by the design variables and uncertain parameters through the state equations. Throughout this

chapter, it is assumed that the function F and G are continuously differentiable. Function ϕ, F and G are general nonlinear functions.

In the final case, part of the variables, known as operation (control) variables, can be adjusted according to the realizations of the uncertain parameters during the process. The optimization problem is formulated as follows:

$$\begin{aligned} \min_{y,z,u\in U} \quad & \phi(y,z,u) \\ s.t. \quad & F(y,z,u,s)=0 \\ & G(y,z,u,s)\leq 0 \end{aligned} \tag{5.3}$$

where $z \in R^{N_z}$ represents operation (control) variables, N_z represents the number of the operation (control) variables.

5.3 Robust Optimization Formulation

In this section, the robust optimization formulation for the nonlinear optimization problem is developed. As the simplest case, the inequality-only constrained model (5.1) is considered first and then the results can be extended to the case with both equality and inequality constraints as shown in (5.2), as well as the general case involving operation (control) variables as expressed in (5.3). Defining an appropriate uncertainty set for the uncertain parameters is of great importance in robust optimization. Different robust counterpart formulations can be derived based on different types of uncertainty set [48]. The simplest type of uncertainty set is defined by p norm and the corresponding nonlinear robust optimization formulation has been derived [85], which is more suitable for unbounded uncertainty. However, for bounded uncertainty, constructing an uncertainty set which exceeds the bounded uncertain region is too conservative. It is more meaningful to define an uncertainty set considering the information of the bounded uncertainty region. While the uncertainty region is determined only by the bounds (i.e., interval) of each parameter, the corresponding robust optimization for-

mulations for linear optimization problem were derived by Li and et al. [48] for independent uncertainty and in Chapter 4, the robust optimization formulations for correlated uncertainties are derived. In this chapter, a more general type of uncertainty set is considered, which is defined as the intersection of two norm-induced uncertainty sets:

$$S_{intersect} = \left\{ s | \|M_1(s - s_1)\|_{p_1} \leq \Delta_1, \|M_2(s - s_2)\|_{p_2} \leq \Delta_2 \right\} \tag{5.4}$$

where M_1 and M_2 are invertible matrices representing information such as perturbation and correlation of the uncertainty, s_1 and s_2 are the center points of the two sets, p_1 and p_2 are norm parameters used in the two sets, and Δ_1 and Δ_2 are the set sizes.

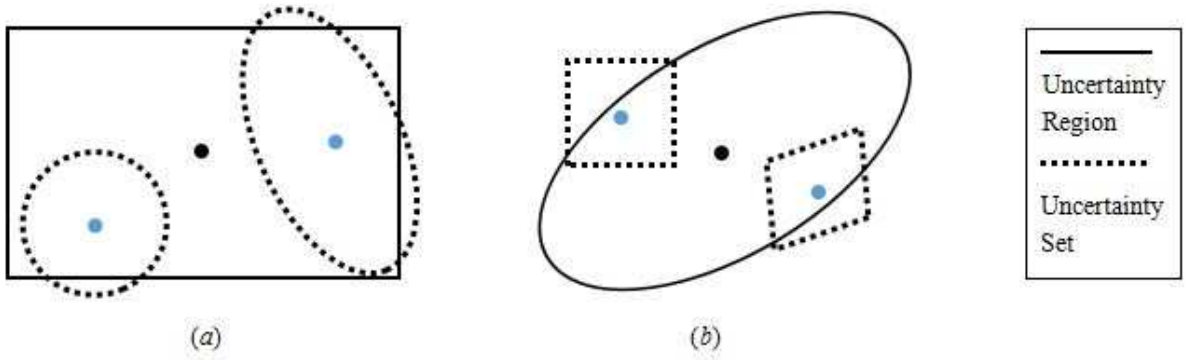

Figure 5.1: Illustration of the uncertainty set

Figure 5.1 illustrates the shape of the defined uncertainty set. The black and blue dots represent the center points of each set. The rectangle and ellipsoid in solid line in (a) and (b) are the confidence interval and joint confidence region. Confidence interval does not consider the correlations between different variables, while the joint confidence region does. Thus, the ellipsoid is rotated by the covariance matrix. The shapes in dash line are the other set selected by the designer. In Figure 5.1, ellipsoid type and box type set are selected in (a) and (b), respectively. If the designer would like to consider the correlations of different uncertainties, the covariance matrix can be incorporated in the uncertainty set as displayed on the right side of (a) and (b). The circle and rectangle on the left side of (a) and (b)

represent the selected sets without correlation information.

5.3.1 Inequality-Only Case

The main idea of robust optimization is to enforce the constraints to be satisfied for all the realizations of the uncertainty within the pre-defined uncertainty set $S_{intersect}$, which can be shown as:

$$G(u,s) \leq 0, \forall s \in S_{intersect} \tag{5.5}$$

which is equivalent to

$$\max_{s \in S_{intersect}} g_i(u,s) \leq 0, i = 1, ..., m \tag{5.6}$$

Before applying the robust optimization formulation, the nonlinear function g_i is linearized. Taking the first-order Taylor approximation in a small region around point s_*, it is obtained that

$$\begin{aligned} & g_i(u,s) \approx g_i(u,s_*) + (s-s_*)^T \nabla_s g_i(u,s_*) \\ & = g_i(u,s_*) - {s_*}^T \nabla_s g_i(u,s_*) + s^T \nabla_s g_i(u,s_*) \leq 0 \end{aligned} \tag{5.7}$$

where $\nabla_s g_i$ denotes the gradient of g_i with respect to s. The robust constraint (5.6) can be approximated as

$$\begin{aligned} & \max_{s \in S} g_i(u,s) \\ & \approx g_i(u,s_*) - {s_*}^T \nabla_s g_i(u,s_*) + \max_{s \in S_{intersect}} s^T \nabla_s g_i(u,s_*) \leq 0 \end{aligned} \tag{5.8}$$

Property 12. *With the uncertainty set defined by (5.4), the robust counterpart constraint (5.8) is equivalent to the following form:*

$$\begin{aligned} & g_i(u,s_*) - {s_*}^T \nabla_s g_i(u,s_*) \\ & + {s_1}^T \nabla_s g_i(u,s_*) + ({s_2}^T - {s_1}^T) r \\ & + \Delta_1 \left\| M_1^{-T} (r - \nabla_s g_i(u,s_1)) \right\|_{q_1} + \Delta_2 \left\| M_2^{-T} r \right\|_{q_2} \leq 0 \end{aligned} \tag{5.9}$$

Proof. Apply the uncertainty set in Equation (5.4), the inner maximization problem in (5.8)

can be formulated as

$$\max_{s} \left\{ \begin{array}{l} s^T \nabla_s g_i(u, s_*) : \\ \|M_1(s - s_1)\|_{p_1} \leq \Delta_1, \|M_2(s - s_2)\|_{p_2} \leq \Delta_2 \end{array} \right\} \tag{5.10}$$

The inner maximization problem is a conic programming problem. According to the definition of norm cone, write the inner maximization into the standard form of conic programming as follows:

$$\max_{s} \left\{ s^T \nabla_s g_i(u, s_*) : P_{p_1} s + p_{p_1} \in K_{p_1}, P_{p_2} s + p_{p_2} \in K_{p_2} \right\} \tag{5.11}$$

where $P_{p_1} = \left[\begin{array}{c} M_{1(n\times n)} \\ 0_{(1\times n)} \end{array} \right], p_{p_1} = \left[\begin{array}{c} -M_{1(n\times n)} s_{1(n\times 1)} \\ \Delta_1 \end{array} \right], K_{p_1} = \left\{ (\theta_{(n\times 1)}; t) | \|\theta\|_{p_1} \leq t \right\}$, and $P_{p_2} = \left[\begin{array}{c} M_{2(n\times n)} \\ 0_{(1\times n)} \end{array} \right], p_{p_2} = \left[\begin{array}{c} -M_{2(n\times n)} s_{2(n\times 1)} \\ \Delta_2 \end{array} \right], K_{p_2} = \left\{ (\theta_{(n\times 1)}; t) | \|\theta\|_{p_2} \leq t \right\}$.

Defining dual variables $y^1 = \left[w_{1(n\times 1)}; \tau_1 \right] \in K_{p_1}^*$ and $y^2 = \left[w_{2(n\times 1)}; \tau_2 \right] \in K_{p_2}^*$. $K_{p_1}^*$ is the dual cone of K_{p_1}, $K_{p_1}^* = K_{q_1} = \left\{ (\theta_{(n\times 1)}; t) | \|\theta\|_{q_1} \leq t \right\}$, and $K_{p_2}^*$ is the dual cone of K_{p_2}, $K_{p_2}^* = K_{q_2} = \left\{ (\theta_{(n\times 1)}; t) | \|\theta\|_{q_2} \leq t \right\}$. q_1 and q_2 are dual norm parameters, which satisfy $1/p_1 + 1/q_1 = 1$, $1/p_2 + 1/q_2 = 1$.

Applying conic duality, the problem can be formulated as the following minimization problem:

$$\begin{array}{l} \min\limits_{y^1, y^2} \left\{ \begin{array}{l} -{s_1}^T M_1^T w_1 + \Delta_1 \tau_1 - {s_2}^T M_2^T w_2 + \Delta_2 \tau_2 : \\ y^1 \in K_{p_1}^*, y^2 \in K_{p_2}^*, M_1^T w_1 + M_2^T w_2 = -\nabla_s g_i(u, s_*) \end{array} \right\} \\ = \min\limits_{y^1, y^2} \left\{ \begin{array}{l} -{s_1}^T M_1^T w_1 + \Delta_1 \tau_1 - {s_2}^T M_2^T w_2 + \Delta_2 \tau_2 : \\ \|w_1\|_{q_1} \leq \tau_1, \|w_2\|_{q_2} \leq \tau_2, M_1^T w_1 + M_2^T w_2 = -\nabla_s g_i(u, s_*) \end{array} \right\} \end{array} \tag{5.12}$$

Since the problem (5.12) is a minimization problem, τ_1 and τ_2 can be replaced by their

lower bounds $\|w_1\|_{q_1}$ and $\|w_2\|_{q_2}$, respectively. The problem (5.12) can be reformulated as

$$\min_{y^1,y^2} \left\{ \begin{array}{l} -{s_1}^T M_1^T w_1 + \Delta_1 \|w_1\|_{q_1} - {s_2}^T M_2^T w_2 + \Delta_2 \|w_2\|_{q_2} : \\ M_1^T w_1 + M_2^T w_2 = -\nabla_s g_i(u, s_*) \end{array} \right\} \tag{5.13}$$

And w_2 can be further replaced by $w_2 = -M_2^{-T}(\nabla_s g_i(u, s_*) + M_1^T w_1)$, then the problem is represented as

$$\begin{aligned} \min_{w_1} \Big\{ & -{s_1}^T M_1^T w_1 + \Delta_1 \|w_1\|_{q_1} + {s_2}^T (\nabla_s g_i(u, s_*) + M_1^T w_1) \\ & + \Delta_2 \big\| M_2^{-T} (\nabla_s g_i(u, s_*) + M_1^T w_1) \big\|_{q_2} \Big\} \end{aligned} \tag{5.14}$$

The inner maximization term is replaced by the minimization term above and since the minimization term is on the left hand side of a "less than or equal to" constraints, the minimization operator can be removed from the constraint, then the original constraint with uncertainty can be formulated as the following:

$$\begin{aligned} & g_i(u, s_*) - {s_*}^T \nabla_s g_i(u, s_*) \\ & -{s_1}^T M_1^T w_1 + {s_2}^T (\nabla_s g_i(u, s_*) + M_1^T w_1) \\ & + \Delta_1 \|w_1\|_{q_1} + \Delta_2 \big\| M_2^{-T} (\nabla_s g_i(u, s_*) + M_1^T w_1) \big\|_{q_2} \leq 0 \end{aligned} \tag{5.15}$$

Introducing an auxiliary variable $r = \nabla_s g_i(u, s_*) + M_1^T w_1$, constraint (5.9) can be obtained.

□

Combine all the constraints and the objective function, the robust optimization formulation for the original problem (5.1) can be represented as follows

$$\begin{aligned} \min_{u \in U} \quad & \phi(u) \\ s.t. \quad & g_i(u, s_*) - ({s_1}^T - {s_*}^T) \nabla_s g_i(u, s_*) + ({s_2}^T - {s_1}^T) r \\ & + \Delta_1 \big\| M_1^{-T} (r - \nabla_s g_i(u, s_1)) \big\|_{q_1} + \Delta_2 \big\| M_2^{-T} r \big\|_{q_2} \leq 0 \\ & i = 1, ..., m \end{aligned} \tag{5.16}$$

5.3.2 Equality-with-State-Variables Case

In the second case, state variables and equality constraints are involved in the nonlinear optimization problem. The state variables can be determined as a function of design variables and the uncertain parameters under the Implicit Function Theorem. First, $F_y(y,u,s)$ is defined as the partial Jacobian of $F(y,u,s)$ with respect to y, i.e.,

$$[F_y(y,u,s)]_{kl} = \frac{\partial F_k(y,u,s)}{\partial y_l}, k,l = 1,2,...,N_y \tag{5.17}$$

and F_s, G_y, G_s, y_s are defined similarly.

Property 13. *With the uncertainty set defined by (5.4), the robust formulation of problem (5.2) is obtained as follows:*

$$\min_{y,u\in U} \quad \phi(y,u)$$

$$s.t. \quad F(y,u,s_*) = 0 \tag{5.18a}$$

$$F_y y_s + F_s = 0 \tag{5.18b}$$

$$\begin{aligned} & g_i(y,u,s_*) + ({s_1}^T - {s_*}^T)(G_y y_s + G_s)^T e_i + ({s_2}^T - {s_1}^T) r \\ & + \Delta_1 \left\| M_1^{-T}(r - (G_y y_s + G_s)^T e_i) \right\|_{q_1} + \Delta_2 \left\| M_2^{-T} r \right\|_{q_2} \le 0 \\ & i = 1,...,m \end{aligned} \tag{5.18c}$$

where e_i is the ith column of the identity matrix, and F_y, F_s, G_y, and G_s take value at s_*.

Proof. The state variable y can be implicitly defined as a function $y(u,s)$ through the state equation $F(y,u,s) = 0$. Applying the implicit function $y(u,s)$ in the inequality constraint, it is obtained that

$$G(u,s) = G(y(u,s),u,s) \tag{5.19}$$

Differentiating both sides of the equation $F(y(u,s),u,s) = 0$ with respect to s leads to the matrix equation

$$F_y(y,u,s)y_s + F_s(y,u,s) = 0 \tag{5.20}$$

Notice that $y(u,s)$ is an implicit function, and it is not necessary to get an explicit expression of y_s. y_s is treated as variable in the formulation. Differentiating $G(u,s)$ with respect to s, it can be represented that

$$G_s(u,s) = G_y(y,u,s)y_s + G_s(y,u,s) \tag{5.21}$$

For each individual inequality constraint i, the derivative is obtained as

$$\nabla_s g_i(u,s)^T = e_i^T G_s(u,s) = e_i^T[G_y(y,u,s)y_s + G_s(y,u,s)] \tag{5.22}$$

Substituting Equation (5.22) into the robust optimization formulation for inequality constraints shown in Equation (5.9) and combining it with the constraint shown in Equation (5.20), the robust optimization (5.18) is obtained. □

5.3.3 General Case

In the general case, the problem (5.3) is considered with a new type of variables called operation (control) variables. Operation (control) variables can be adjusted to satisfy the design specifications during the operation of the process. In this case, since only the design variables remain fixed and the operation (control) variables are properly manipulated for the realizations of the uncertain parameters, the final design will be less conservative. In robust optimization framework, formulations with adjustable variables are referred to as adjustable robust counterpart (ARC). However, ARC is computationally intractable in most cases. In this chapter, the affine adjustable robust optimization algorithm proposed by Ben-Tal et al. [44] is applied to represent the relationship between the operation (control) variables and the uncertain parameters using an affine function, which is shown as follows:

$$z = As + b \tag{5.23}$$

where A is an N_z by N_s matrix, and b is a vector of dimension N_z.

It is worth pointing out that the above affine decision rule is reasonable because it is applied to the small uncertainty set around a selected point. In this local region, the nonlinear constraints are linearized and the operational variable decision rule is assumed to be affine function of the uncertain parameters.

Property 14. *With the uncertainty set defined by (5.4) and the affine function of the operation (control) variables with respect to the uncertain parameter in (5.23), the robust optimization formulation of problem (5.3) is obtained as follows:*

$$\begin{aligned}
\min_{y,z,u\in U} \quad & \phi(y,z,u) \\
s.t. \quad & F(y,z,u,s_*) = 0 && \text{(5.24a)} \\
& F_y y_s + F_z A + F_s = 0 && \text{(5.24b)} \\
& \begin{aligned} & g_i(y,z,u,s_*) + ({s_1}^T - {s_*}^T)(G_y y_s + G_z A + G_s)^T e_i + ({s_2}^T - {s_1}^T) r \\ & + \Delta_1 \left\| M_1^{-T}(r - (G_y y_s + G_z A + G_s)^T e_i) \right\|_{q_1} + \Delta_2 \left\| M_2^{-T} r \right\|_{q_2} \le 0 \\ & i = 1, ..., m \\ & z = As + b \end{aligned} && \text{(5.24c)}
\end{aligned}$$

where F_z, G_z are defined similarly as in Equation (5.17)*, and F_y, F_z, F_s, G_y, G_z, and G_s take value at s_*.*

Proof. The explicit affine function of the operation (control) variables z is represented as $z(s)$. The state equation $F(y,z,u,s)$ also involves the operation (control) variables. However, after substituting the explicit function $z(s)$, only state variables and design variables remain in the state equation. Similar to Equation (5.19), it can be obtained that

$$G(u,s) = G(y(z(s),u,s),u,s) \tag{5.25}$$

Differentiate both sides of the state equation $F(y(z(s),u,s),u,s) = 0$ with respect to the

uncertainty s, the following equation is obtained:

$$F_y(y,z,u,s)y_s + F_z(y,z,u,s)A + F_s(y,z,u,s) = 0 \tag{5.26}$$

where A is the derivative of function $z(s)$ with respect to s according to the affine function in Equation (5.23). And differentiating $G(u,s)$ with respect to s, it can be written that

$$G_s(u,s) = G_y(y,z,u,s)y_s + G_z(y,z,u,s)A + G_s(y,z,u,s) \tag{5.27}$$

The derivative form for each individual inequality constraint i can be expressed as

$$\nabla_s g_i(u,s)^T = e_i^T G_s(u,s) = e_i^T[G_y(y,z,u,s)y_s + G_z(y,z,u,s)A + G_s(y,z,u,s)] \tag{5.28}$$

Substituting Equation (5.28) into Equation (5.9), and including the equality constraint in Equation (5.26) and Equation (5.23), the robust optimization for the general case in (5.24) is obtained. □

5.4 Iterative Algorithm

Due to the limitation of the first-order Taylor linearization that it is effective only in a small range around a single point, the robust optimization formulation derived in the third section works well only under uncertainty with small perturbation. If the perturbation is large, the so-called "piecewise" linearization will be taken. The first-order Taylor expansion will be applied around multiple realizations of the uncertain parameter. The robust optimization formulation for the inequality-only case is summarized in (5.29)

$$\begin{aligned} \min_{u\in U} \quad & \phi(u) \\ \text{s.t.} \quad & \text{extending (5.9) with index } j \\ & \forall j, i = 1, ..., m \end{aligned} \tag{5.29}$$

In (5.16), the nonlinear functions are linearized around a single point, while in the "piecewise" linearization robust optimization formulation the functions are linearized around different points represented by index j. Therefore, the parameters and variables (s_*, s_1, s_2, r, Δ_1, Δ_2, q_1, q_2, M_1, M_2) associated with the points should also be extended with index j in (5.29).

Similarly to (5.29), the robust optimization formulation for the equality-with-state-variable case using "piecewise" linearization is shown as follows:

$$\begin{aligned}
\min_{y_m, u\in U} \quad & \phi(y_m, u) \\
\text{s.t.} \quad & \text{extending} \quad (5.18a), \forall j \\
& \text{extending} \quad (5.18b), \forall j \\
& \text{extending} \quad (5.18c), \forall j, i = 1, ..., m \\
& y^j \leq y_m, \forall j
\end{aligned} \tag{5.30}$$

Not only the parameters and variables involved in (5.29) but also the state variable y as well as the derivatives with respect to y are extended with index j in (5.30).

And the robust optimization formulation with "piecewise" linearization for the general case is expressed in the following form:

$$\begin{aligned}
\min_{y_m, z_m, u\in U} \quad & \phi(y_m, z_m, u) \\
\text{s.t.} \quad & \text{extending} \quad (5.24a), \forall j \\
& \text{extending} \quad (5.24b), \forall j \\
& \text{extending} \quad (5.24c), \forall j, i = 1, ..., m \\
& y^j \leq y_m, \forall j \\
& z^j = A^j s_*^j + b^j, \forall j \\
& z^j \leq z_m, \forall j
\end{aligned} \tag{5.31}$$

The control variable z and the derivatives associated with z are extended with index j as well in (5.31).

All the constraints and corresponding variables in mdoel (5.16), (5.18) and (5.24) are

extended with respect to the multiple points around which the "piecewise" linearization is taken. The design variable u remains the same for all the points. As shown in (5.30) and (5.31), if the state variables and operation (control) variables exist in the objective function, they are replaced by their maximum y_m and z_m among all the multiple points.

In the proposed nonlinear robust optimization framework, the "piecewise" linearization is taken around multiple realizations of the uncertain parameter. An important issue is how to select proper points. In this chapter, an iterative algorithm is applied to solve the problem. The algorithm is shown in Figure 5.2.

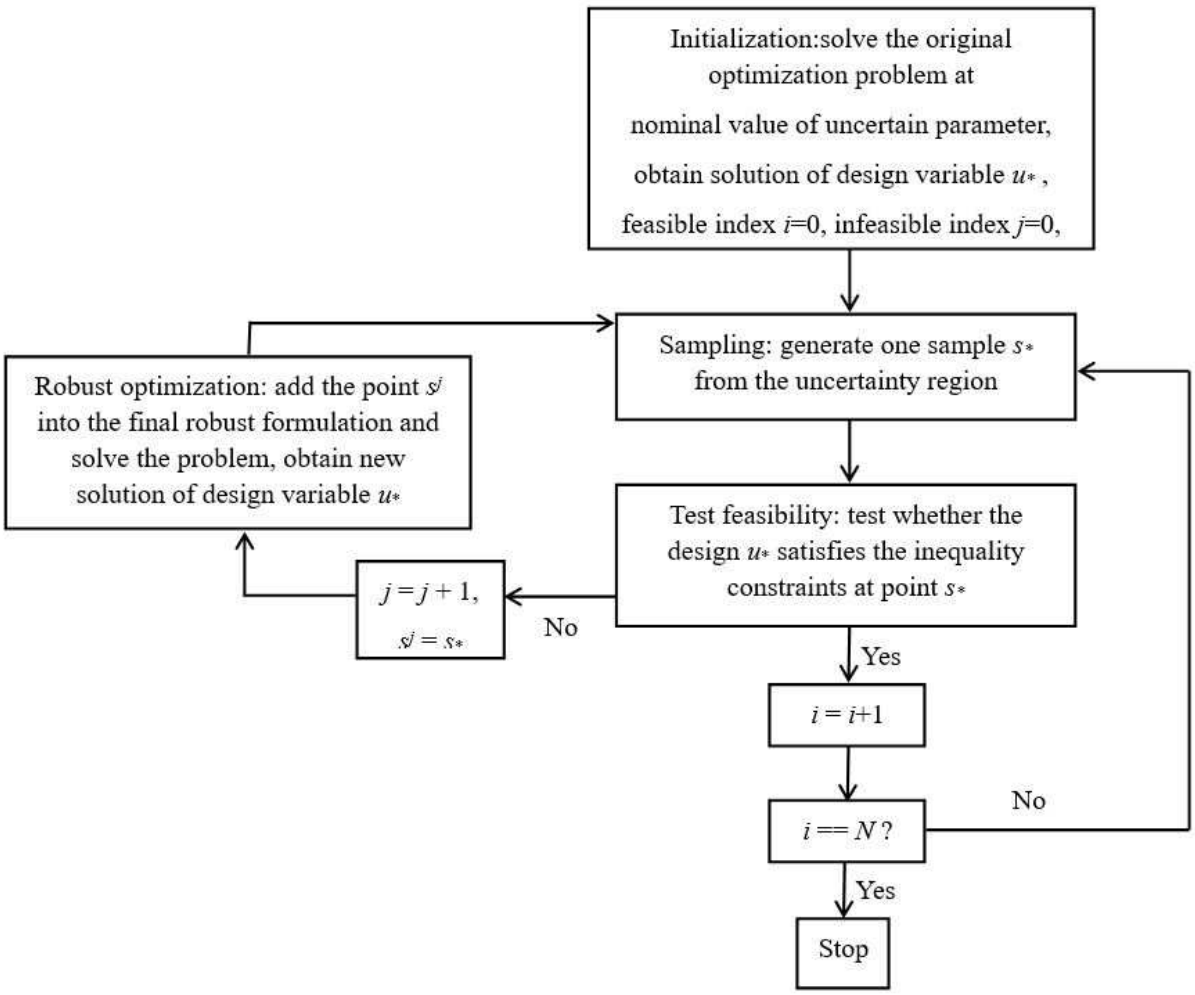

Figure 5.2: The iterative algorithm for solving the problem

In each iteration of the proposed iterative algorithm, there are mainly three steps. First,

a single point is randomly generated within the uncertainty region, and it is assumed that the uncertain parameter is uniformly distributed in the uncertainty region. The second step is called feasibility test, and in this step, whether the design variables obtained in the previous iteration are feasible for the process under the generated realization of the uncertain parameter is tested. The third step in each iteration is to solve the robust optimization problem (formulation (5.29), (5.30), and (5.31) corresponding to three cases) with all the points selected for "piecewise" linearization.

5.4.1 Feasibility Test

Next, the details for the feasibility test step are discussed. For the general case, in order to test the feasibility of the design variables, the following problem is solved

$$\begin{aligned} \min_{y,z} \quad & t \\ s.t. \quad & F(y, z, u_*, s_*) = 0 \\ & g_i(y, z, u_*, s_*) \leq t, i = 1, ..., m \end{aligned} \tag{5.32}$$

In the above formulation, t is a slack variable added to each inequality constraint, s_* is the randomly generated realization of the uncertainty, and u_* is the design variable fixed as the value obtained in the previous iteration. The slack variable is minimized, and if the value t is larger than 0 the design is not feasible at the current realization of the uncertain parameter and the corresponding point is selected for "piecewise" linearization, otherwise, the design is feasible and a new point should be generated. There are infinite number of points in the uncertainty region, but only up to N number of samples are generated in each iteration. This number reflects how much the uncertainty region is covered by the samples. Larger number of samples represents the region better; however, they will increase the computation burden.

For the equality-with-state-variable case, formulation (5.32) can still be used for feasibility test (by eliminating the control variables). Furthermore, another strategy can be applied to

test the feasibility. Since the number of state variables and the number of state equations are the same, with fixed design variable and uncertain parameter, the state variable can be directly obtained by solving the state equations $F(y, u, s) = 0$. Then, the state variable, design variable, and uncertain parameter are substituted into each inequality constraint $g_i(y, u, s) \leq 0$. If any of the inequality constraints is violated, the design is infeasible under the current realization of the uncertainty. For the inequality-only case, there is no need to solve (5.32), and the design variable and uncertain parameter are directly substituted into the inequality constraints to test the feasibility.

5.4.2 Illustrative Example

For an illustration, let us consider a simple optimization with only one inequality constraint and one uncertain parameter as follows:

$$\begin{aligned} \min \quad & (x_1 - 2)^2 + (x_2 - 0.2)^2 \\ s.t. \quad & (4.8 - 5\sin(\pi\sqrt{t})/(1 + t^2))x_1^2 - x_2 \leq 0, \forall t \in [0, 0.5] \\ & x_1 \in [-1, 1], x_2 \in [0, 0.2] \end{aligned} \tag{5.33}$$

The nominal value of t is 0.25, which means that the perturbation of the uncertainty is 25%. First, the example is used to show the iterative algorithm step by step. The set sizes of uncertainty set in all the iteration are set as 0.01. Initially, problem (5.33) is solved at the nominal value $t = 0.25$, and it is obtained that $u_* = x_* = [1, 0.2]$. Then, the samples are uniformly generated within the range $[0, 0.5]$. In the first iteration, a point $s_* = t_* = 0.0266$ is selected since the left-hand-side (LHS) of the constraint $(4.8-5sin(\pi\sqrt{t_*})/(1+t_*^2))x_{1*}-x_{2*}$ is calculated as 2.1491 which violates the "$\leq$" constraint. Next, setting $s_1 = s_* = 0.0266$, and solving the corresponding robust optimization problem, the design u_* is updated as $u_* = [0.2688, 0.2]$. In the second iteration, the selected point is $s_* = 0.0122$ with 0.0238 as the value of LHS. With $s_1 = 0.0266$ and $s_2 = s_* = 0.0122$, solving the robust optimization problem, the updated design is $u_* = [0.2305, 0.2]$. In the third iteration, point $s_* = 0.0036$ is selected

with 0.0054 as the value of LHS. With the three points together, the design obtained by solving robust optimization is $u_* = [0.1969, 0.2]$. In the next iteration, $N = 1000000$ samples are generated, but none of the samples violates the constraints with design $u_* = [0.1969, 0.2]$, and the algorithm stops. The final solution obtained in this run is $u_* = [0.1969, 0.2]$. The reason a large number N is used is that this problem is simple and the computational time for each step is very short. In order to cover more space of the uncertainty using the samples, a large number N is used. Figure 5.3 shows the shape of the function of the uncertainty t and the points selected for "piecewise" linearization in each iteration.

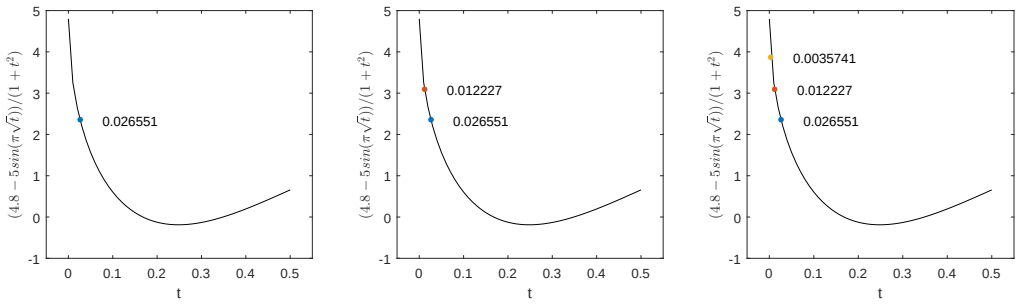

Figure 5.3: Points used for linearization in each iteration

In the proposed algorithm, the set size Δ can be selected by the decision maker. In the general robust optimization framework, the set size can influence the robustness of the solution in that larger size leads to more robust solution while the objective value may get worse. Next, the influence of different set sizes (0.01, 0.05, 0.1) on the results of the nonlinear robust optimization method is studied, and the results are summarized in Table 5.1. "Ave", "Max", "Min", "Obj", and "Num" represents average value, maximum value, minmum value, objective value, and number of points used for "piecewise" linearization, respectively. Monte Carlo simulation with 100 runs are taken for each set size case.

Table 5.1: Results for illustrative example

Size	Obj			Num		
Δ	Ave	Max	Min	Ave	Max	Min
0.01	3.3397	3.6007	3.2152	3.82	7	1
0.05	3.4667	3.8440	3.2214	2.6	4	1
0.1	3.4932	3.844	3.2178	2.07	3	1

It can be observed that as the set size increases, the objective value gets worse (larger for a minimization problem), while the number of points used for "piecewise" linearization decreases. The relationship between the number of points and the objective value is also studied. Since the number of points is not large for all different set size cases, the average objective value is calculated corresponding to each possible number of points used for linearization and the results are plotted in Figure 5.4.

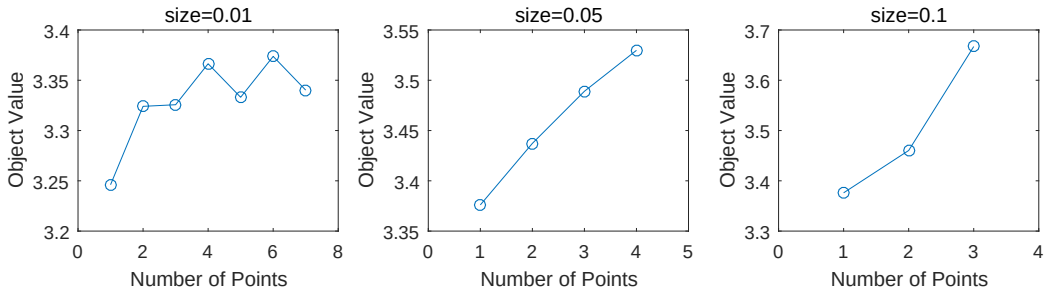

Figure 5.4: Relationship between the objective value and the number of points used for "piecewise" linearization for illustrative example

It can be seen that approximately, with fixed set size, the trend is that when the number of points used for linearization increases, the objective value gets worse. This is because that if more points are used for "piecewise" linearization, the robust formulation will be more conservative.

5.4.3 Discussion about the Iterative Algorithm

In the proposed iterative algorithm, two nonlinear optimization problems are solved in the second step (feasibility test) and the third step (robust optimization). In the feasibility test step, the problem is required to be solved for the global solution, because that the local solution may cause missed detection of the infeasible point. While in the robust optimization step, local solution is accepted, since the goal of this step is to find a design to be robust under the uncertainty with a lower objective function value. A global solution in this step can lead to better objective value, e.g., lower cost, but will increase the computational burden. In the algorithm, the first step (sampling) and the feasibility test step together find the

infeasible points with respect to the current design. If the pre-decided number N is selected to be large enough, the sampled points can cover almost the entire uncertain region and the design passing the feasibility test step for all the N points can be regarded as the robust design for the entire uncertain region. The algorithm converges when the robust design for the entire uncertain region is found. However, since the samples are randomly generated, there is no guarantee for the optimality regarding the objective function value (design cost) of the final robust design for a single run.

Most of the computation time is spent on the feasibility test step due to the global solution requirement and the computation time is affected by different aspects. First, as the number N increases, the computation time will certainly increase. Second, the fact that larger number of the points were kept for final linearization leads to longer computation time, since this number implies the times of repeats of the three steps in the iterative algorithm. Third, the order of the points among the N sampled points that are found to be infeasible will influence the computation time as well. For instance, the time when the $5th$ point is found to be infeasible is shorter than the time when the $55th$ point is infeasible, since the order of the points implies the times that the feasibility test step is taken. However, the last two aspects cannot be controlled due to the randomness of the sampling points.

The sampling and feasibility test step are actually taken to find the infeasible points of the current design and in the literature there are some available methods to deal with this kind of problem, including vertex search methods [86, 87, 88], active set with mixed-integer optimization strategies [89], and global optimization with mixed-integer optimization strategies [90]. All these methods are deterministic methods, but they still have certain drawbacks. The vertex search methods assume that the infeasible points correspond to vertices, and this will influence the reliability of the solution. Moreover, it involves enumeration of the vertices and if the dimension of the uncertainty is high the computation burden is also high. The other two methods are applied by solving a mixed-integer nonlinear optimization problem. The main step in the active set strategy is to find all the active sets of the constraints to

fix the integer values and reduce the problem to multiple nonlinear optimization problems. The active set strategy can guarantee global optimality for only certain types of problems. The global optimization strategy is based on αBB algorithm and includes multiple steps in the whole strategy, which makes the algorithm complicated. However, it can be a future research direction to improve the deterministic strategies and combine it with the iterative algorithm proposed in this chapter to avoid the randomness issue.

5.5 Example Problems

In this section, three optimal design problems corresponding to the three categories of problems considered in this chapter are studied to test the effectiveness of the proposed methodology. The optimal heat exchanger design problem only contains inequality constraints and the optimal reactor design problem contains both inequality and equality constraints associated with uncertain parameters. The final example is the reactor and heat exchanger network problem which contains inequality as well as equality constraints and also the operation (control) variables which can be adjusted with respect to the realizations of uncertain parameter. In the simulation, the samples are generated in MATLAB. All the optimization problems are solved in GAMS 23.9. For the feasibility test step, in the second example, it is accomplished in MATLAB by solving the state equation, and in the third example, problem (5.32) is solved using BARON. The robust optimization formulations in the iterative algorithm are all NLP problems and solved using local solver such as CONOPT, IPOPT.

5.5.1 Heat Exchanger Network

Figure 5.5 shows the diagram of the heat exchanger network problem. Three hot streams with different known inlet temperatures $T_{Hj,in}, j = 1, 2, 3$ are used to heat one cold stream from $100°F$ to $500°F$. The goal is to minimize the overall total area of the heat exchangers.

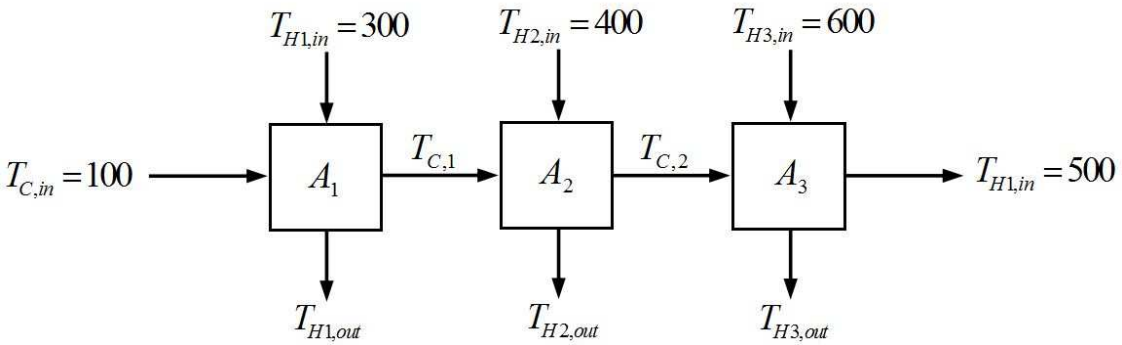

Figure 5.5: Heat exchanger network

The mathematical model for this problem can be written as [91]

$$
\begin{aligned}
&\min(A_1 + A_2 + A_3) \\
&s.t. \\
&T_{C,1} + T_{H1,out} - T_{C,in} - T_{H1,in} \leq 0, \\
&-T_{C,1} + T_{C,2} + T_{H2,out} - T_{H1,in} \leq 0, \\
&T_{H3,out} - T_{C,2} - T_{H3,in} + T_{C,out} \leq 0, \\
&A_1 - A_1 T_{H1,out} + \tfrac{FC_p}{U_1} T_{C,1} - \tfrac{FC_p}{U_1} T_{C,in} \leq 0, \\
&A_2 T_{C,1} - A_2 T_{H2,out} - \tfrac{FC_p}{U_2} T_{C,1} + \tfrac{FC_p}{U_2} T_{C,2} \leq 0, \\
&A_3 T_{C,2} - A_3 T_{H3,out} - \tfrac{FC_p}{U_3} T_{C,2} + \tfrac{FC_p}{U_3} T_{C,out} \leq 0, \\
&100 \leq A_1 \leq 10000, 1000 \leq A_2, A_3 \leq 10000, \\
&10 \leq T_{C,1}, T_{C,2} \leq 1000, \\
&10 \leq T_{H1,out}, T_{H2,out}, T_{H3,out} \leq 1000,
\end{aligned}
\tag{5.34}
$$

Only inequality constraints exist in the formulation of this problem. The known paramter is $FC_p = 10^5$,and the uncertain parameter are the heat transfer coefficient, i.e., $s = (U_1, U_2, U_3)$. The nominal value of the uncertain parameter is $\hat{s} = (\hat{U_1}, \hat{U_2}, \hat{U_3}) = (120, 80, 40)$. The perturbation of the uncertainty is assumed to be 30%, i.e., $U_i = \hat{U}_i + 30\%\hat{U}_i\xi, i = 1, 2, 3$, where ξ is the random variable lying in the range $[-1 \quad 1]$.

The uncertainty set was defined in Equation(5.4), for the sampled point of uncertainty

in the jth iteration, with $M_1^j = M_2^j = I$(identity matrix), $s_1^j = \hat{s}$ (nominal value), $s_2^j = s_*^j$ (sampled point), $p_1^j = p_2^j = \infty$, and $\Delta_2^j = 0.3$ representing the perturbation of the uncertainty. The uncertainty set $S_{intersect}$ is explicitly written as Equation(5.35), which is the intersection of a designed box type uncertainty set with the same set size Δ for all the sampled points and the interval representing the lower and upper bound of the uncertainty:

$$S_{intersect}^j = \left\{ s \middle| \left\| s - s_*^j \right\|_\infty \leq \Delta, \|s - \hat{s}\|_\infty \leq 0.3 \right\}, \quad \forall j \tag{5.35}$$

The uncertainty set will reduce to the interval set when the designed box type uncertainty set is completely covered by the interval set. This usually happens since the set size Δ cannot be too large in order to ensure the effectiveness of the first-order Taylor approximation around each sampled point.

Different sizes (0.01, 0.05, 0.1 and 0.2) are used in this example. Since the points used for "piece-wise" linearization in each iteration are randomly selected, the results for different runs will be different. Therefore, Monte Carlo simulations with 100 runs are applied for each set size. As discussed in the previous section, in each iteration, at most N samples are used for the feasibility test. If all the N samples pass the feasibility test, the algorithm is forced to stop. The number N is set as 1000 in this example.

For each set size, the relationship between the objective value and the number of points used for "piecewise" linearization is plotted in Figure 5.6.

From Figure 5.6, it can be observed that for most of the runs, as the number of the points used for "piecewise" linearization increases, the corresponding objective value also increases. However, the relevance level is different for different set size. For the case with set size 0.05, the relationship is quite prominent, while for other cases, it is not very obvious. This observation is similar as in the illustrative example.

The average value (Ave), the maximum value (Max), and the minimum value (Min) of the objective value (Obj) and the number of points (Num) used for "piecewise" linearization

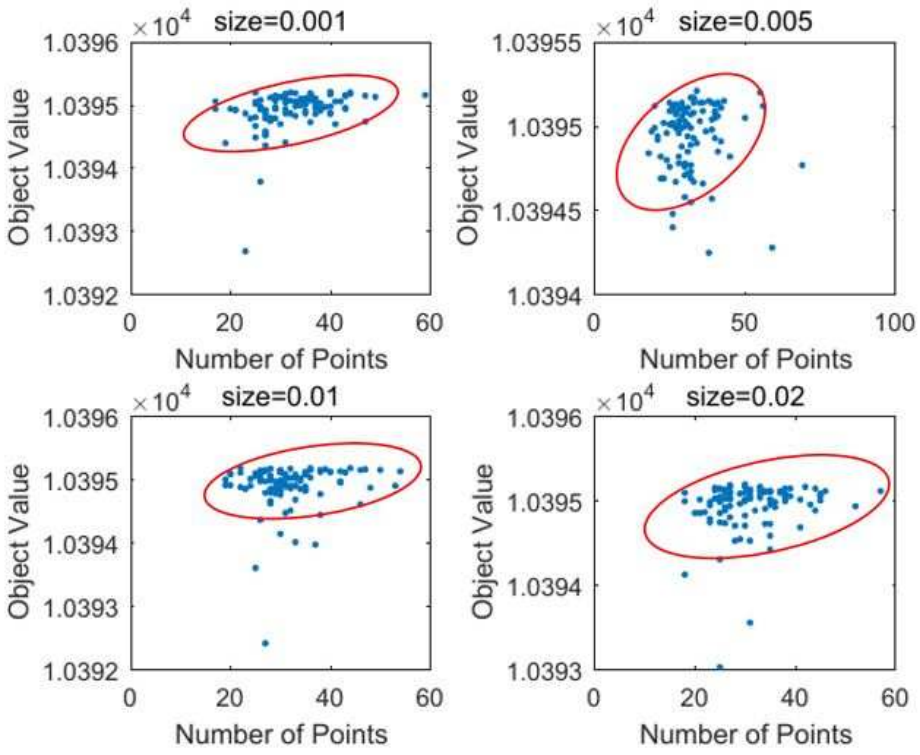

Figure 5.6: Relationship between the objective value and the number of points used for "piecewise" linearization for heat exchanger example

among 100 Monte Carlo runs are listed in Table 5.2.

Table 5.2: Results for heat exchanger example

Size	Obj			Num		
Δ	Ave	Max	Min	Ave	Max	Min
0.01	10395	10395	10393	32.68	59	17
0.05	10395	10395	10394	32.38	69	18
0.1	10395	10395	10392	31.92	54	19
0.2	10395	10395	10393	31.33	57	18

From Table 5.2, it can be observed that the average value, the maximum value, and the minimum value of the objective value for different set size Δ are almost the same, which implies that changing the set size has no influence on the final results in this example. For each set size, although the minimum case and the maximum case of the points used for linearization are quite different, there is only slight difference in the average value. This implies that in this example the number of points used for linearization does not affect the

final results significantly. For the iterative algorithm, as long as no point within 1000 samples fails in the feasibility test, the solution converges to the similar results.

The objective value obtained by linearization around only the nominal point is obtained as 7556.7[85], which is smaller than the solutions obtained by the "piecewise" linearization method. This is because that using multiple points for linearization will introduce conservatism.

Another important issue is the robustness of the solutions, and it is evaluated by testing the feasibility of the design under different points of uncertain parameter. 10,000 samples of the uncertain parameter are generated from the uncertain space to test the robustness of the solution for both the "piecewise" linearization formulation and the "single-point" linearization (only around nominal point). The solutions from all the 100 Monte Carlo runs for different set sizes are tested. The number of samples violating the constraints is counted for each case, and results are summarized in Table 5.3.

Table 5.3: Results of robustness for heat exchanger example

Size Δ	# of runs with no violation	Min # of violations	Max # of violations	Ave # of violations
0.001	44	1	7	1.875
0.005	44	1	8	2.2143
0.01	44	1	7	2
0.02	44	1	5	1.8929

From the second column of Table 5.3, it can be seen that for all set sizes, nearly 50% out of 100 Monte Carlo runs satisfy the constraints with all the samples. The fourth and fifth columns of Table 5.3 show the maximum number and the average number of samples under which the design violates the constraints. The maximum number among all the sizes is 8 and the average numbers are all around 2 (out of 10,000 samples). This shows great robustness of the design with respect to the uncertainty. However, the solution obtained by the "single-point" linearization causes 8726 samples to violate the constraints, which is significantly worse than the results of the "piecewise" linearization method. This is because that the first-order Taylor approximation is only effective in a small range, and when the

perturbation (30% in this example) of the uncertainty is large, the "single-point" linearization cannot provide robust solution under the uncertainty.

5.5.2 Reactor-Separator System

A reactor design problem is shown in Figure 5.7 [92, 93].

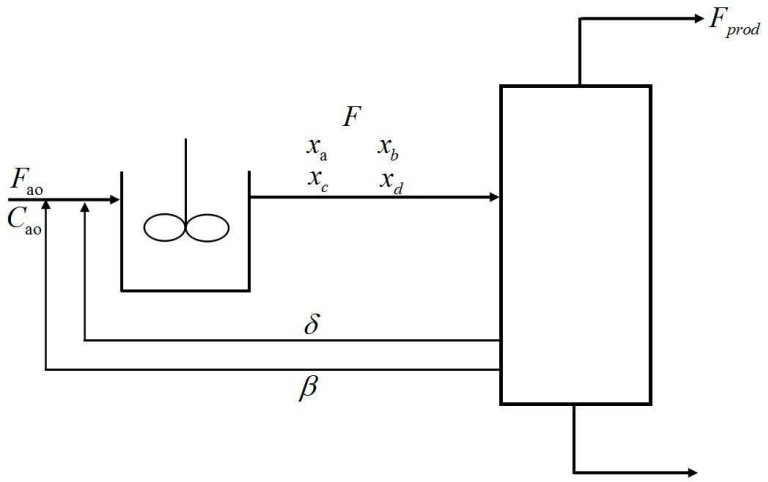

Figure 5.7: Reactor-separator flow sheet

The purpose of the system is to convert reactant A to product C via the following reaction system which consists of four first-order elementary reactions.

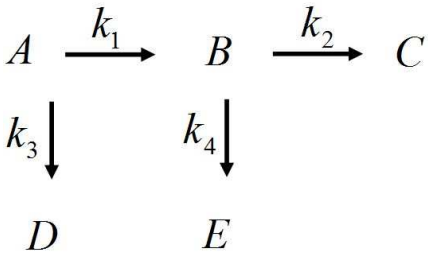

The uncertain parameters considered in this example are the reaction rates k_i, $i = 1, ..., 4$ with units of $time^{-1}$, i.e., $s = (k_1, k_2, k_3, k_4)^T$. Three variables are regarded as design variables, the volume V of the reactor (m^3), the fraction δ of species A and B that is recycled back to the reactor, and the fraction β of species D and E that are recycled back to the reactor, i.e., $u = (V, \delta, \beta)^T$. There are six state variables. They are the flow rate F out of the

reactor ($mol/time$), and the mole fractions of each species x_a, x_b, x_c, x_d, x_e at the reactor outlet, i.e., $y = (F, x_a, x_b, x_c, x_d, x_e)^T$. The final goal of the optimal design is to minimize the total cost, and the following optimization problem is formulated:

$$
\begin{aligned}
&\min 10V^2 + 5F \\
&s.t. \\
&F_{a0} - x_a F(1-\delta) - c_{a0} V(k_1 + k_3)x_a = 0 \\
&- x_b F(1-\delta) + c_{a0} V(k_1 x_a - (k_2 + k_4)x_b) = 0 \\
&- x_c F + c_{a0} V k_2 x_b = 0 \\
&- x_d F(1-\beta) + c_{a0} V k_3 x_a = 0 \\
&- x_e F(1-\beta) + c_{a0} V k_4 x_b = 0 \\
&x_a + x_b + x_c + x_d + x_e = 1 \\
&x_c F \geq 40 \\
&0 \leq \delta \leq 1, 0 \leq \beta \leq 1
\end{aligned}
\tag{5.36}
$$

In the above formulation, uncertain parameters exist in equality constraints. The inlet flow rate $F_{a0} = 100 mol/time$ and the concentration of species A at the inlet (the molar concentration throughout the entire system as well) $c_{a0} = 10 mol/m^3$ are the known parameters. The detailed information including the nominal value and the variation about the uncertain parameters can be found in the paper written by Rooney and Biegler [92]. Two types of uncertainty region which can be referred to as individual confidence region and joint confidence region are considered in this example. The uncertainty sets defined by Equation(5.4) are constructed for both types of the confidence region which are represented in Equation(5.37) and Equation(5.38), respectively:

$$
S^j_{intersect} = \left\{ s \middle| \left\| s - s^j_* \right\|_\infty \leq \Delta, \left\| s - \hat{s} \right\|_\infty \leq t_{1-(\alpha/2),n-p}\sigma \right\}, \forall j \tag{5.37}
$$

where σ is the standard derivation of the uncertain parameter, $t_{1-(\alpha/2),n-p}$ is the value of the

Student-t distribution, α is the desired confidence level, p is the number of uncertain parameters, and n is the number of data points used in the estimation problem. The individual confidence region is a box set.

$$S^j_{intersect} = \left\{ \begin{array}{l} s \,|\|s - s^j_*\|_\infty \leq \Delta, \\ \left\|\Sigma^{-1/2}(s - \hat{s})\right\|_2 \leq (pF_{1-\alpha,n-p})^{1/2} \end{array} \right\}, \forall j \tag{5.38}$$

where Σ is the covariance matrix of the uncertain parameters, and $F_{1-\alpha,n-p}$ is the value of the F-distribution. The joint confidence region is an ellipsoidal set.

The solutions obtained by the "single-point" linearization are shown in Table 5.4 [93].

Table 5.4: "Single-point" linearization [93]

Set type	V (m^3)	δ	β	Cost
Box	20.71	0.992	0.000	6632
Ellip.	19.57	0.978	0.000	5983

In this example, the influence of set size Δ is also studied. $\Delta = 0.005, 0.01, 0.02, 0.05$ for individual confidence region and $\Delta = 0.005, 0.01, 0.02$ for joint confidence region are considered. For each set size, Monte Carlo simulations with 100 runs are taken. The results for individual confidence region and joint confidence region are listed in Table 5.5 and Table 5.6, respectively. "Ave", "Min", "Max", "Obj", and "Num" are defined in the same way as in the heat exchanger example.

Table 5.5: Results for reactor-separator example (individual confidence region)

Size	Obj			Num		
Δ	Ave	Max	Min	Ave	Max	Min
0.005	6393.1	6645	6221	3.68	5	1
0.01	6388.3	6672	6171	2.64	4	1
0.02	6375.5	6681	6108	1.86	3	1
0.05	6403.1	6769	6133	1.8	3	1

Table 5.6: Results for reactor-separator example (joint confidence region)

Size	Obj			Num		
Δ	Ave	Max	Min	Ave	Max	Min
0.005	6195.1	6490	5865	2.04	3	1
0.01	6182.8	6674	5800	1.41	2	1
0.02	6290.2	6616	5922	1	1	1

From Table 5.5 and Table 5.6, it can be seen that for both the individual confidence region and joint confidence region, as the set size increases, the number of points needed for linearization decreases. However, the average of the objective value does not have the monotonic trend, and as the size increases it decreases first and then increases. The best results according to the average of objective value for the individual confidence region case is obtained at size 0.02, and for the joint confidence region case it is obtained at size 0.01. This is because that if the set size is too large, the linearization around each selected point is not accurate. From the optimal objective value point of view, the results show that the size Δ can be optimized to obtain better results.

Comparing the results in Table 5.5 and Table 5.6 with Table 5.4, it can be observed that for the individual confidence region case, the maximum objective value (6769) obtained by the "piecewise" linearization among all the set size cases is only slightly larger than the objective value (6632) by "single-point" linearization. Furthermore, the largest average value (6403.1) among all the set size cases is apparently smaller than the results in the literature. However, for the joint confidence region case, the objective value (5983) in the "single-point" linearization is better than the results obtained by "piecewise" linearization.

The robustness of the solutions is tested using 100 samples. The simulation results are plotted in Figure 5.8 and Figure 5.9. The design used for plotting the results corresponds to the design leading to the average objective value.

For the individual confidence region case, there is no sample violating the constraints for both the "piecewise" linearization method with all the set sizes and the "single-point" linearization method. While for the joint conficence region case, the number of samples

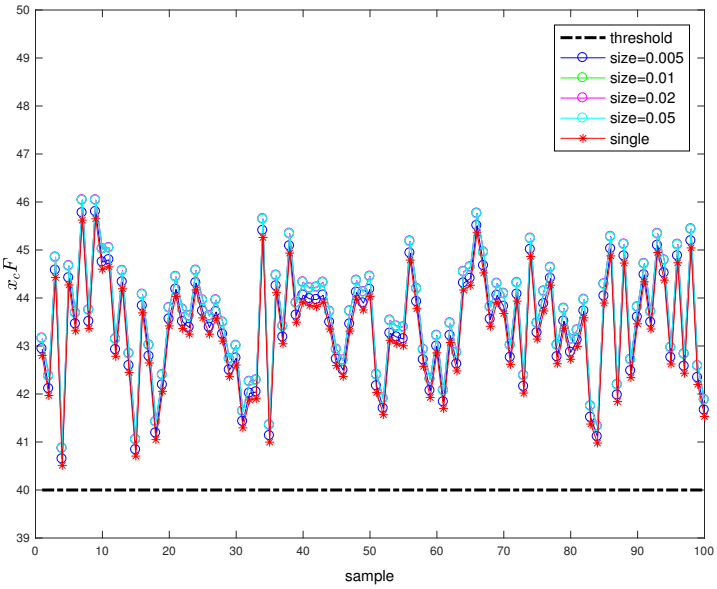

Figure 5.8: Simulation results for individual confidence region

violating the constraints by the "single-point" linearization method is 12. The numbers of violation point for "piecewise" linearization method with different set sizes are still all zero. Although in the joint confidence region case, the objective for the "single-point" linearization is better than the one for "piecewise" linearization, the robustness is worse.

For the constraints, the less conservative solutions have the corresponding curve which is closer to the threshold. In Figure 5.8, the lines for size 0.01, 0.02, and 0.05 coincide and they are slightly more conservative than the results for size 0.005. In Figure 5.9, as the size increases, the results become more conservative with respect to the constraints. This observation can be another aspect which is useful for selection of the set size.

5.5.3 Reactor and Heat Exchanger Network

In this example, a reactor and heat exchanger system shown in Fig.5.10 is studied.

The reaction is the first-order exothermic reaction using material A to generate product B. The optimal design of the reactor volume V and the area of the heat exchanger A need to be determined to guarantee a minimum of 90% conversion of the reactant, i.e., $u = (V, A)$. The commercial design objective is to minimize the total plant cost consisting

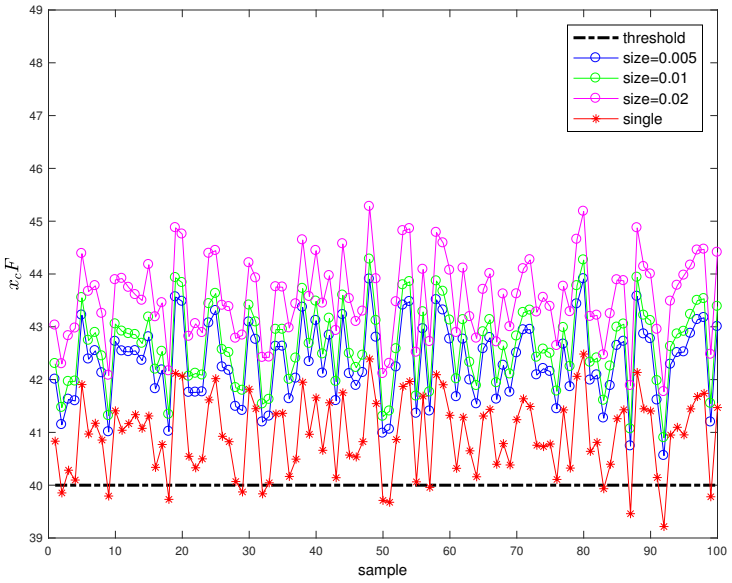

Figure 5.9: Simulation results for joint confidence region

of the investment and operating cost. In this problem, the flow rates F_1 and F_w can be manipulated for the realizations of the uncertain parameters, and they are classified as the operation (control) variables, i.e., $z = (F_1, F_w)$. The parameters considered to contain uncertainty are the Arrhenius rate constant k_0 and the feed flow rate F_0, i.e., $s = (k_0, F_0)$. The statistical data for these uncertain parameters are given in Table 5.7. The values for the known parameters are provided in Table 5.8.

Table 5.7: Uncertain parameters

Parameter	$F_0(kmol \cdot h^{-1})$	$k_0(h^{-1})$
nominal value	45.36	12
positive deviation	22.68	1.2
negative deviation	22.68	1.2

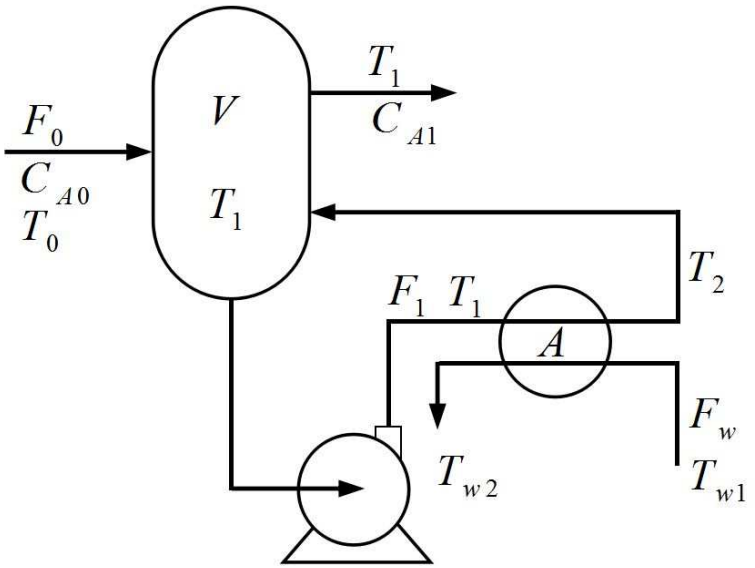

Figure 5.10: Reactor-cooler system

Table 5.8: Parameter values

Parameters	Values
concentration of A in the feed stream C_{A0}	32.04 $kmol/m^3$
feed temperature T_0	333 K
cooling water inlet temperature T_{w1}	300 K
overall heat transfer coefficient U	1635 $kJ/(m^2 \cdot h \cdot K)$
ratio of activation energy to perfect gas constant E/R	555.6 K
molar heat of reaction $-\Delta H_R$	23260 $kJ/kmol$
reactant heat capacity c_p	167.4 $kJ/(kg \cdot K)$
cooling water heat capacity c_{pw}	4.184 $kJ/(kg \cdot K)$

Defining $x_A = (C_{A0} - C_{A1})/C_{A0}$, the design problem can be formulated as the following

nonlinear programming problem:

$$
\begin{aligned}
\min \quad & 691.2V^{0.7} + 873.6A^{0.6} + 1.76F_w + 7.056F_1 \\
s.t. \quad & F_0 x_A - k_0 \exp\left(-(E/RT_1)\right) C_{A0}(1 - x_A)V = 0 \\
& F_0 c_p(T_0 - T_1) - F_1 c_p(T_1 - T_2) + (-\Delta H_R)F_0 x_A = 0 \\
& F_1 c_p(T_1 - T_2) = AU\Delta T_{\ln} \\
& \Delta T_{\ln} = \tfrac{(T_1 - T_{w2}) - (T_2 - T_{w1})}{\ln((T_1 - T_{w2})/(T_2 - T_{w1}))} \\
& F_1 c_p(T_1 - T_2) = F_w c_{pw}(T_{w2} - T_{w1}) \\
& 311 \le T_1 \le 389 \\
& 311 \le T_2 \le 389 \\
& 300 \le T_{w2} \le 380 \\
& T_1 - T_2 \ge 0 \\
& T_{w2} - T_{w1} \ge 0 \\
& T_1 - T_{w2} \ge 11.1 \\
& T_2 - T_{w1} \ge 11.1 \\
& x_A \ge 0.9
\end{aligned}
\tag{5.39}
$$

The uncertainty set is represented in Equation(5.40), for the sampled point of uncertainty in the jth iteration, with $M_1^j = I$, $M_2^j = [(22.68/45.36)^{-1} \quad 0; \quad 0 \quad (1.2/12)^{-1}] = [2 \quad 0; \quad 0 \quad 10]$ representing the perturbations of the uncertainty, $s_1^j = \hat{s}$ (nominal value), $s_2^j = s_*^j$ (sampled point), $p_1^j = p_2^j = \infty$, $\Delta_2^j = \Delta$ which is the set size designed by the decision maker, and $\Delta_2^j = 1$.

$$
S_{intersect}^j = \left\{ s \middle| \left\| s - s_*^j \right\|_\infty \le \Delta, \left\| \begin{pmatrix} 2 & 0 \\ 0 & 10 \end{pmatrix} (s - \hat{s}) \right\|_\infty \le 1 \right\}, \quad \forall j \tag{5.40}
$$

Set sizes 0.01, 0.03, 0.05 are considered in this example. Number N is set as 1000. Monte Carlo simulations with 100 runs are taken for each set size, and the results are shown in Table 5.9.

Table 5.9: Results for reactor and heat exchanger example

Size	Obj			Num		
Δ	Ave (10^4)	Max (10^4)	Min (10^3)	Ave	Max	Min
0.01	1.1477	1.9098	9.2688	7.31	36	1
0.03	1.1322	1.3233	9.3092	7.18	48	1
0.05	1.1577	1.3593	9.2109	8.80	47	2

Table 5.9 shows that the difference between the maximum and minimum objective value is large. This is because the difference of the number points used for linearization is also very large. The influence of the set size in this example is similar to the reactor network example in the sense that there is a middle point of the set size corresponding to which the solution is better. The feasibility is tested using 100 samples with the design corresponding to the minimum, maximum, and average objective value respectively, and the numbers of violations for the three designs are all zeros.

In order to demonstrate the advantage of considering manipulation of control variables with respect to the realizations of uncertain parameter, the formulation regarding F_1 and F_w as design variables is also studied, i.e., $u = (V, A, F_1, F_w)$. The design F_1 and F_w will remain unchanged for all the realizations of uncertainty. In this case, only set size 0.01 is considered for comparison. The results compared with the formulation with consideration of control are shown in Table 5.10.

Table 5.10: Results for comparison of considering and not considering control variables

Formulation	Obj			Num		
	Ave (10^4)	Max (10^4)	Min (10^3)	Ave	Max	Min
With Control	1.1477	1.9098	9.2688	7.31	36	1
Without Control	1.5550	9.7521	9.8075	17.2	43	1

It can be seen that the number of points used for linearization and the objective value for the case without control variables are both larger than the case considering control variables in the formulation. This is because that if the control variables are manipulated according to the realizations of uncertainty, more information about the uncertainty is considered in the formulation. Then, the solutions are less conservative than the case that the control

variables also remain unchanged.

To compare the results in the aspect of feasibility, the design solutions obtained from the formulation without control variable corresponding to the minimum, maximum, and average objective value are also tested using the same 100 samples as the case considering control variables, and the numbers of violations for the three designs are all zeros. The comparison of the two formulations with design corresponding to average objective value is plotted in Figure 5.11.

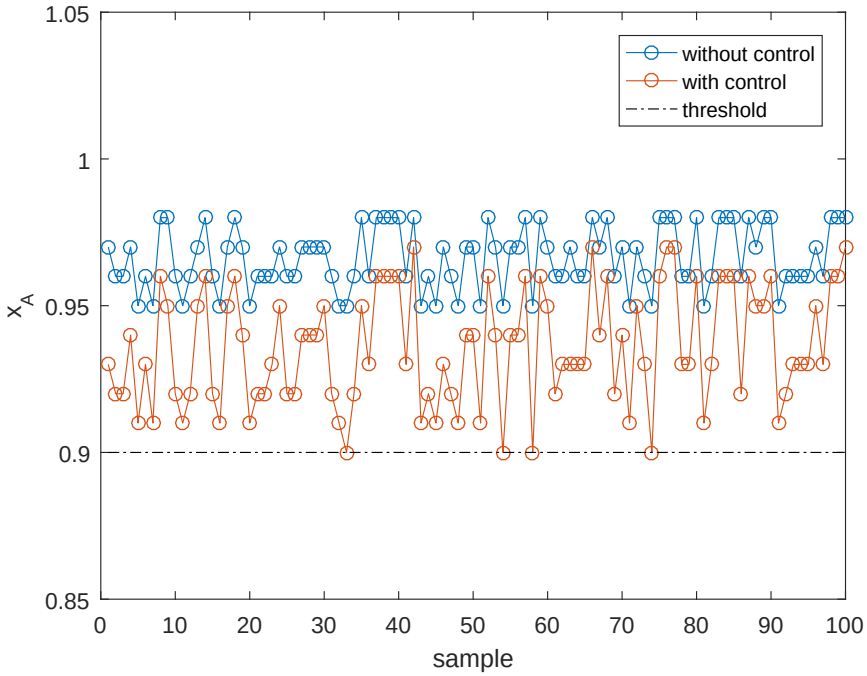

Figure 5.11: Comparison of the feasibiliby for considering and not considering control variables

Figure 5.11 shows that the curve corresponding to the case without control variables is above the one for the case considering control variables, which implies that the solutions obtained without considering control variables are more conservative.

Another issue known as price of robustness is also compared for the two formulations. The price of robustness is calculated based on the cost (objective value) of the "ideal" case where the realizations of uncertain parameter are known in advance of the design decision.

100 samples of the uncertainty are used to calculate the price of robustness, and the results are summarized in Table 5.11. The designs corresponding to the minimum, maximum, and average objective value are tested.

Table 5.11: Results for comparison of price of robustness

	Min		Max		Ave		Ideal
	With	Without	With	Without	With	Without	
Mean (Cost 10^4)	0.8020	0.9810	0.8767	9.7521	0.9667	1.5206	0.5021
Price of Robustness	0.60	0.95	0.75	18.42	0.93	2.03	

It can be observed that the price of robustness of the formulation considering control variables are all smaller than the solutions without control variables, which shows that manipulating the control variables with respect to the realizations of the uncertain parameter reduces the conservatism of the robust optimization formulation. Although in general the information of the uncertain parameter is not available at the beginning of the design, if it is available during the process, considering it in the formulation can improve the final results significantly.

5.6 Conclusion

In this chapter, a novel nonlinear robust optimization framework is proposed to solve the nonlinear process design problems. The robust counterpart formulation is derived based on a general type of uncertainty set defined by the intersection of two uncertainty sets. In order to deal with uncertainty with larger perturbation, "piecewise" linearization is taken around multiple realizations of the uncertain parameter and an iterative algorithm is applied to solve the problem. The framework is applicable to the optimization problems with only inequality constraints as well as the problems with equality constraints associated with uncertain parameter. Furthermore, the control variables which can be manipulated under the realizations of uncertainty are also considered in the robust optimization formulation based on an affine relationship between the control variables and the uncertain parameters. Three

application examples including the optimal design of a heat exchanger system, a reactor-separator system and a reactor-cooler system are studied to demonstrate the effectiveness of the proposed methodology. The proposed method has higher level of robustness than the "single-point" linearization method. In addition, while the results have the similar robustness level, the proposed method leads to less conservative robust solution. By comparing the results obtained from the formulation considering control variables and that obtained from not considering control variables, it is demonstrated that with consideration of the control variable, the solutions become less conservative.

Chapter 6

Economic Optimization of Water Flow Network in SAGD Operations

6.1 Introduction

This chapter focuses on economic optimization of the water flow network in SAGD operations under steady state. Uncertainties always exist in model parameters in any optimization problem, for instance, the demand of the steam for a steam generator cannot be known in advance and the prediction of it may not be accurate, and the uncertainties can also arise from the parameter estimation. Lack of considering uncertainties in optimization problem may cause suboptimal or even infeasible solutions of the real process. In this chapter, both deterministic formulation and formulation with uncertain model parameters of the optimization problems are considered. The background information of SAGD process and the objective of this chapter are introduced in Section 6.2. Section 6.3 considers a long-term planning problem for the steam distribution to different well pads starting at different times. The process models for different units are built based on the efficiency, e.g., the model of steam generators is built based on steam quality, and the model of well pads is built based on steam-to-oil-ratio (SOR) and water-to-oil-ratio (WOR). The efficiencies can be obtained using different techniques, such as soft sensor, empirical formulas or from historical data. In

Section 6.3, the capacity of the oil produced in the wells is predicted using empirical formulas from the literature. The formulas are based on the operation conditions in the reservoir, and since there will be environment disturbances, the prediction will contain some uncertainties. In Section 6.3, the uncertainty is considered in the predicted oil production rate capacity and quantify the uncertainty in the optimization problem through joint chance constraint (JCC). In order to solve the optimization problem with JCC, the proposed method in Chapter 3 is used to approximate the JCC to deterministic formulation.

6.2 Problem Statement

SAGD is known as steam assisted gravity drainage. The majority resources of Alberta oil sands are in deep underground and extracted by SAGD technique. In a typical SAGD process, two horizontal wells are drilled in parallel. Steam is injected to the upper injection well to generate a high-temperature vapor chamber where the surrounding bitumen can be heated, and the viscosity of it is reduced to let it be drained by gravity to the lower production well. The mixture of oil and water is pumped out to the ground and is sent to the separator. After the separation, the oil is transported to upgrader for further treatment and the produced water is sent to water treatment plants for purification and then is generated to become steam for injection to the well. The produced water and steam in SAGD process form a cycle. A brief overview of SAGD process is shown in Figure 6.1.

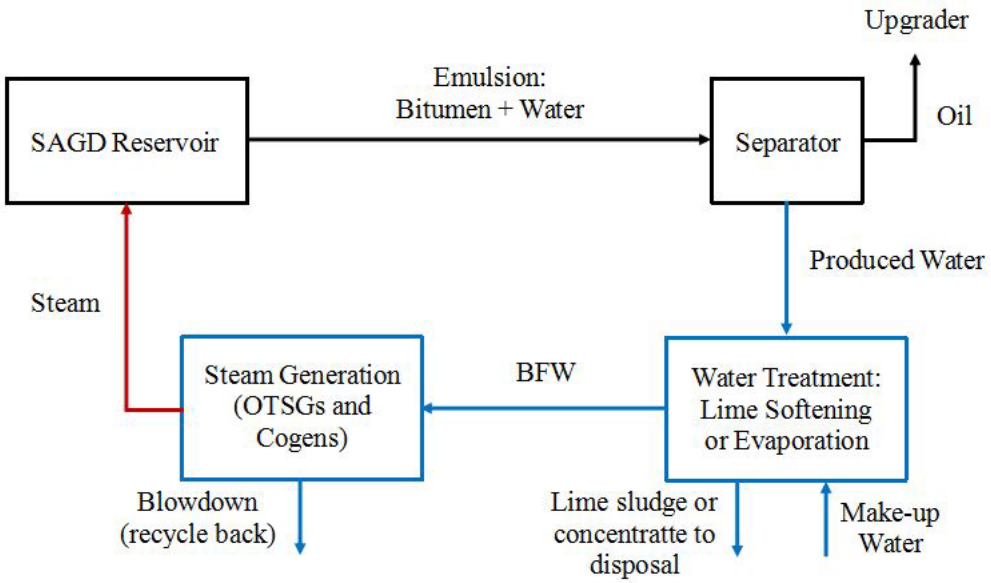

Figure 6.1: Overview of general SAGD process

In the current SAGD process, there normally exist five phases of operations: Start-up, ramp-up, chamber spread, ramp-down and blow down, which is displayed in Figure 6.2. In different stages of operations, the oil production rate as well as the requirement of the steam injection rate is different.

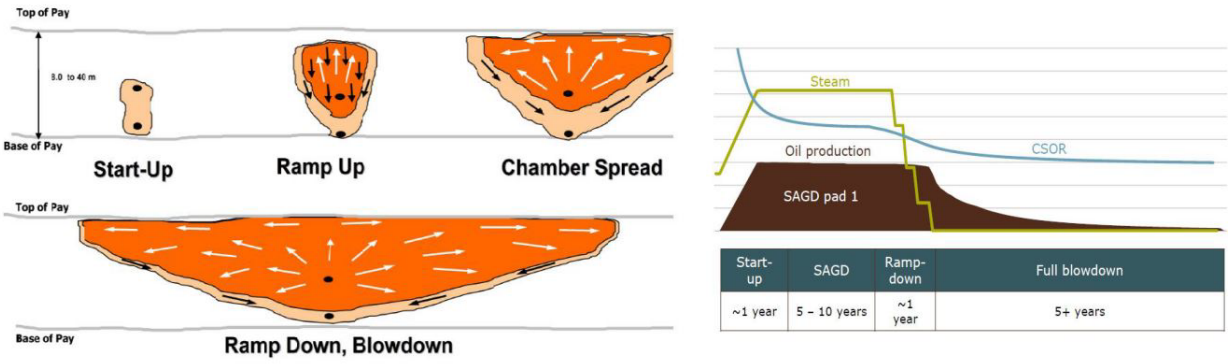

Figure 6.2: SAGD stages[94, 95]

At the initial conditions of reservoir, the oil is not able to be drained due to the high viscosity and lack of mobile water. In the start-up stage, the thermal and/or hydraulic communication between the injection well and production well is established and the mixture

of oil and water can be pumped out from the production well. There are different techniques for start-up stage, such as water dilation, steam dilation, solvent soak and steam circulation. The techniques can be selected based on the reservoir quality and presence of thief zones. In general, the start-up phase lasts one year approximately.

After establishment of the communication between injection well and production well by start-up stage, steam is continuously injected into the injection well at constant pressure and the mixture of oil and water is continuously removed from the production well at constant temperature in the ramp-up stage. In this stage, the SAGD chamber grows vertically until it reaches the reservoir top which may be a thick shale or some lower permeability facies, and at the same time the oil production rate peaks.

In the chamber spread phase, the SAGD chamber grows laterally and due to the widening of the chamber, overburden heat losses increas to consume more heat energy from injected steam. Thus, the oil production rates decline with steady steam rates, and if we want to keep steady oil rates, the steam rates should be increased. Ramp-up and chamber spread are the two major stages to produce oil and generally they will persist five to ten years.

The ideal transition from chamber spread stage to ramp-down stage is made by injection of the mixture of gas and steam. In this stage, the individual chambers of the well pairs on a pad will coalesce with each other and become one common SAGD chamber across the entire pad. Steam injection will be reduced during this stage and the pressure in SAGD chamber is supported by the injection of gas. Since this is a transitional stage, it only lasts nearly one year.

The final operation stage of SAGD process is blow-down. In this stage, the injection of steam stops while the gas is injected to maintain the pressure, and with declining production rate the bitumen production continues until the rate reaches an uneconomic point. One of the main purposes of ramp-down and blow-down stages is to reduce the CSOR (cumulative steam to oil ratio) of the well pairs. A full blow-down stage usually takes more than five years.

Optimizing the consumption of the water as well as the generation of steam is of great importance to the commercial target. In the long term process operations, the steam is distributed to different well pads starting at different times. Since the well pads are operated at different stages, the requirement of steam injection differs and it is necessary to build an optimal plan of steam generation and distribution to reduce waste of the steam as well as the cost of steam generation while producing as much oil as possible. Optimizations are the powerful techniques utilized in this chapter to achieve the commercial goals.

The water treatment and steam generation network is shown in Figure 6.3. According to the functionality of the units, they can be classified as PW (produced water) tank, WP (water treatment) plant, BFW (boiler feed water) tank and SG (steam generator). The details about the units are discussed in the following subsections.

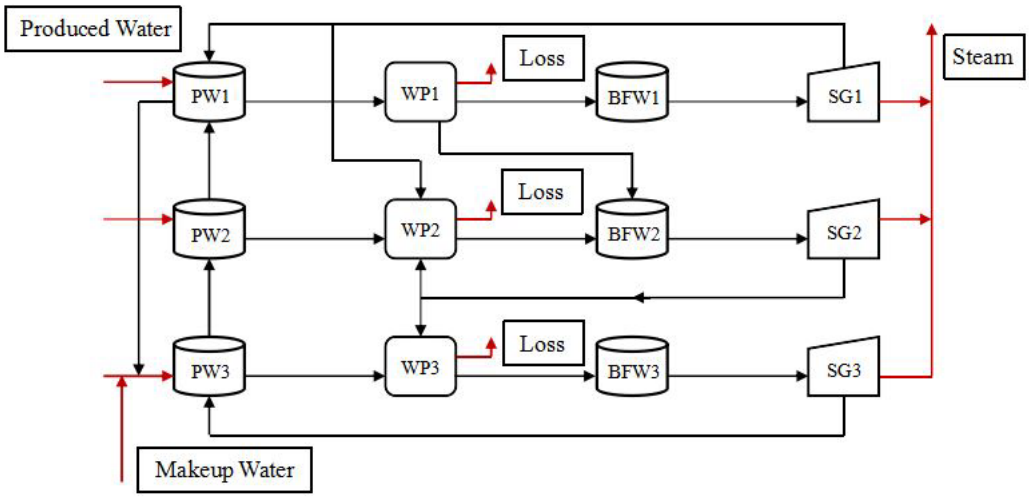

Figure 6.3: Water treatment and steam generation network

6.2.1 Water Treatment Plants

De-oiled water obtained by separating produced water from bitumen contains soluble contaminants including silica, hardness (calcium,magnesium, iron, etc.), total dissolved solids, organic carbon and dissolved oxyen. The contaminants in de-oiled water is removed in the water treatment plants with different methods.

Warm lime softening (WLS) is a traditional process to remove silica and hardness via physical-chemical treatment. Followed by a filtration system, WLS removes silica and hardness with addition of certain chemical compounds and produces insoluble sludge which can be separated from the treated water by the filter. Finally, filtered water is transported to WAC (weak acid cation) tanks where the majority of hardness is removed using weak acid cation resins. Water with very high amounts of total dissolved solids (TDS>7000 ppm) cannot be treated by WLS, however; it is cheaper to operate due to less requirement of energy compared to evaporators.

Evaporation is an alternative technique for water treatment, which convert the water content in the mixture into water vapor to separate the impurities. This process can handle water with high amounts of total dissolved solids and the output treated water has high quality. The only disadvantage is that it consumes more energy than WLS.

6.2.2 Steam Generators

After treatment, water is used for steam generation generally using two types of steam generators: OTSG (one through steam generator) and co-generator.

In OTSGs, pressurized water is fed into hot tubes at one end and superheated steam is produced at the other end. The advantage of OTSGs is that they can handle water with high levels of total dissolved solids (TDS) and silica. Steam produced by OTSGs has $70 - 80\%$ quality and a series of vapor-liquid separators are needed to separate the water from the steam to produce 100% quality steam for injection to the reservoir.

Co-generator or heat recovery steam generator (HRSG) can generate electricity using excess heat from hot gas steam during the steam generation. Startup and shutdown in Co-generator are slower than in OTSGs.

6.2.3 Tanks

Tanks are installed followed by water treatment and steam generator units for temporal storage of the water. PW tanks and BFW tanks are placed upstream of water treatment plants and steam generators, respectively. In long term problem, the dynamics in the tanks can be ignored and they are reduced to connectors for different streams.

6.3 Long-Term Planning

In this section, the long-term planning problem for distribution of steam to well pads starting at different times is addressed. First, the deterministic formulation of the optimization problem is studied and then, the uncertainty in oil production rate capacity is considered and formulated by JCC. Robust optimization is applied to approximate the JCC. The solutions obtained from deterministic and uncertain formulations are compared.

6.3.1 Deterministic Formulation

In the long-term planning problem, the models for water treatment plants, steam generators and well pads are considered. Due to the long time period considered, the dynamics in buffer tanks is not taken into consideration while the status (on/off) of steam generators can be optimized. Operation conditions, e.g., lower and upper limitation of each unit, need to be satisfied. The optimization model is formulated in the following subsections.

6.3.1.1 Plant Models

The input of water treatment plants is water with contaminants and the useful output is the purified water while the contaminants are the loss which is usually difficult to measure. The model of water treatment plants can be built through the treatment efficiency of the plants such that the output of purified water is the total input of water multiplying by the

efficiency:

$$\sum_{(i,j)\in Pair} F_{i,j}^t = \eta_i^{WP} \times \sum_{(j,i)\in Pair} F_{j,i}^t \qquad i \in U_{WP}, t = 0, ..., H \tag{6.1}$$

where $F_{i,j}^t$ is the flowrate from unit i to unit j at time t, and η is the efficiency. The set $Pair$ contains all the possible connections between two units. H is the total time horizon. The purified water is injected into the steam generators and steam is produced. Since the steam quality is not 100%, the water is separated from steam and recycled back, which is known as blowdown. The steam generators follow mass balance:

$$\sum_{(j,i)\in Pair} F_{j,i}^t = \sum_{(i,j)\in Pair} F_{i,j}^t \qquad i \in U_{SG}, t = 0, ..., H \tag{6.2}$$

The steam generated can be modeled through the steam quality:

$$\sum_{(i,j)\in Pair, j\in U_{Well}} F_{i,j}^t = \eta_i^{SG} \times \sum_{(j,i)\in Pair} F_{j,i}^t \qquad i \in U_{SG}, t = 0, ..., H \tag{6.3}$$

The real process of well pads is complicated and a rough model is utilized in this chapter to approximate the behaviour of the well pads in different operation stages using SOR and WOR. The SOR and WOR can be predicted using historical data and empirical formulas. The steam injected to each well pad is

$$\sum_{(j,i)\in Pair, j\in U_{SG}} F_{j,i}^t = SOR_i^t \times Oil_i^t \qquad i \in U_{Well}, t = 0, ..., H \tag{6.4}$$

The produced water pumped out from the well pad is

$$Water_i^t = WOR_i^t \times Oil_i^t \qquad i \in U_{Well}, t = 0, ..., H \tag{6.5}$$

Since the dynamics of the buffer tanks are not considered for long-time period optimization, the model for the tanks is reduced as a connector following mass balance that the total input equals to the total output. The inputs of PW tanks include makeup water, produced

water from the wells, and the streams from other units. The makeup water is used as an compensation when the produced water is not adequate due to loss in the reservoir and in the separation step. The model for PW tanks is shown as follows:

$$M_i^t + \sum_{(j,i)\in Pair} F_{j,i}^t = \sum_{(i,j)\in Pair} F_{i,j}^t \qquad i \in U_{PW}, t = 0, ..., H \tag{6.6}$$

where M_i^t is the amount of makeup water used in PW tank i at time t. The model for BFW tanks is simpler:

$$\sum_{(j,i)\in Pair} F_{j,i}^t = \sum_{(i,j)\in Pair} F_{i,j}^t \qquad i \in U_{BFW}, t = 0, ..., H \tag{6.7}$$

6.3.1.2 Status of Steam Generators

In the long-term planning problem, it is necessary to consider the on/off status of each steam generator since if the steam required by the well pads is not intensive, some of the steam generators can be shut down to save energy and during the shut-down time, the steam generators can be cleaned or maintained, or sometimes due to the malfunctioning of certain steam generator, it must be shut down. The operation status and switch of a steam generator are formulated in the following equations:

$$ST_i^{t+1} = ST_i^t + SW_i^t - 2ST_i^t \times SW_i^t \qquad i \in U_{SG}, t = 0, ..., H \tag{6.8}$$

where ST_i^t and SW_i^t are the status (on/off) and switch condition of SG i at time t, respectively.

6.3.1.3 Operation Conditions

The water treatment plant has a maximum capability of treating the water and it is defined on the total input of water, which is shown in (6.9):

$$\sum_{(j,i)\in Pair} F_{j,i}^{t} \leq Ca_{i}^{up} \qquad i \in U_{WP}, t = 0, ..., H \tag{6.9}$$

Similarly, the steam generators also have a maximum ability to generate steam. Moreover, due to safety consideration, it also has a lower production condition:

$$Ca_{i}^{lo} \times ST_{i}^{t} \leq \sum_{(j,i)\in Pair} F_{j,i}^{t} \leq Ca_{i}^{up} \times ST_{i}^{t} \qquad i \in U_{SG}, t = 0, ..., H \tag{6.10}$$

The oil production for each well pad should satisfy lower and upper bounds:

$$Oil_{i}^{lo,t} \leq Oil_{i}^{t} \leq Oil_{i}^{up,t} \qquad i \in U_{Well}, t = 0, ..., H \tag{6.11}$$

where $Oil_{i}^{lo,t}$ and $Oil_{i}^{up,t}$ are the lower and upper bound of oil production rate Oil_{i}^{t}. In this section, the lower bound of the oil production is assumed to be 90% of the full capacity, i.e., $Oil_{i}^{lo,t} = 0.9 \times Oil_{i}^{up,t}$.

Due to the loss of water in the reservoir and separation step, the amount of water produced from the well is larger than the amount of water distributed to the PW tanks:

$$\sum_{i\in U_{PW}} \sum_{(j,i)\in Pair, j\in U_{Well}} F_{j,i}^{t} \leq \sum_{j\in U_{Well}} Water_{j}^{t} \qquad t = 0, ..., H \tag{6.12}$$

6.3.1.4 Objective Function

The objective function of the long-term planning problem consists of three parts. First, the total production of oil is maximized. Second, the total usage of make-up water is minimized. Finally, since frequently switching the steam generators will cause additional cost, the total

number of switches should be minimized.

$$\max \sum_{t=1}^{H} \sum_{i \in U_{Well}} Oil_i^t - \sum_{t=1}^{H} \sum_{i \in U_{PW}} M_i^t - \sum_{t=1}^{H} \sum_{i \in U_{SG}} SW_i^t \tag{6.13}$$

An additional penalty term of the loss of the produced water can also be minimized by deducting the term $\sum_{t=1}^{H} (\sum_{i \in U_{PW}} \sum_{(j,i) \in Pair, j \in U_{Well}} F_{j,i}^t - \sum_{j \in U_{Well}} Water_j^t)$ in the objective function.

6.3.1.5 Prediction of Oil Production Capacity and SOR

A crucial part in the long term planning problem is to predict the oil production rate and theoretical methods in the literature can be used for the prediction. The models utilized in this chapter are for the rising steam chamber (ramp-up) stage and the lateral-spreading steam chamber (chamber spread) stage, and the transition between the two stages. The prediction model during the rising period from Butler et al. [96] is shown as follows:

$$q_r = \frac{4\gamma}{3} \left(\frac{9}{4} \frac{\beta}{\gamma^2} \right)^{2/3} (\varphi \Delta S_0)^{1/3} \left(\frac{kg\alpha}{m\nu_s} \right)^{2/3} t^{1/3} \tag{6.14}$$

Due to the depletion, the oil rate will decline in the chamber spread stage and the model from Butler et al. [96] can be expressed as:

$$q_d = 2\sqrt{\frac{akg\alpha \Delta S_0 h}{m\nu_s}} - 2\frac{t^2}{w^2} \frac{(kg\alpha/m\nu_s)^{3/2}}{(b\varphi \Delta S_0 h)^{1/2}} \tag{6.15}$$

The description and value of the parameters in the above two equation are listed in Table 6.1. ΔS_0 which is the displaceable oil saturation, is the only one that varies with time and it is estimated using (6.16) which was developed by Cardwell and Parsons [97]:

$$\Delta S_0 = S_0 - 0.43 \left(\frac{\nu_s \varphi h}{kgt} \right)^{0.4} \tag{6.16}$$

There is also an intermediate stage between the ramp-up stage and the chamber stage when the steam chamber reaches the top of the reservoir and begins to grow laterally. Neither

the model in (6.14) nor the model in (6.15) can represent the transition stage well. Guo et al. [98] proposed a weighting method based on the model in (6.14) and (6.15) which is shown as follows:

$$q_t^{oil} = y_d q_d + y_r q_r \tag{6.17}$$

where the weighting factor y_r decreases from 1 to 0, while the weighting factor y_d increases from 0 to 1. The weighting factors are modeled by the Dose Response function in (6.18) and (6.19):

$$y_r = \frac{1}{1 + 10^{u_r(v_r - t)}} \tag{6.18}$$

$$y_d = \frac{1}{1 + 10^{u_d(v_d - t)}} \tag{6.19}$$

Table 6.1: Parameters used for oil rate prediction

Parameter	Description	Value
w(m)	Half well spacing	75
$k(\mu\text{m}^2)$	Effective permeability	2.5
$\alpha(\text{m}^2\text{s}^{-1})$	Reservoir thermal diffusivity	$7.06\times\ 10^{-7}$
m	Viscosity-temperature relation parameter	4
$\nu_s(\text{mm}^2\text{s}^{-1})$	Kinematic viscosity of oil at steam temperature	10
S_0	Initial oil saturation of the reservoir	0.8
φ	Porosity	0.35
h(m)	Effective drainage height	26.5
a	Empirical constant	1.93
b	Empirical constant	0.66
β	Empirical constant	0.264
γ	Shape factor of the rising steam chamber	0.132
u_r	Constant	-0.556
u_d	Constant	0.864
v_r	Constant	2.9
v_d	Constant	2.125

The predicted oil rate is plotted in Figure 6.4. It can be observed that at the beginning of the operation, the ramp-up stage model dominates in the combined model, while at the end of the operation the chamber spread model plays the important role, and in the intermediate stage both of the models describe the transition model partially. In [99], the authors directly

used the predicted oil rate in the optimization model to avoid nonlinearity in the prediction model, while in this chapter the predicted oil production rate acts as the capacity (upper bound) of the real oil production.

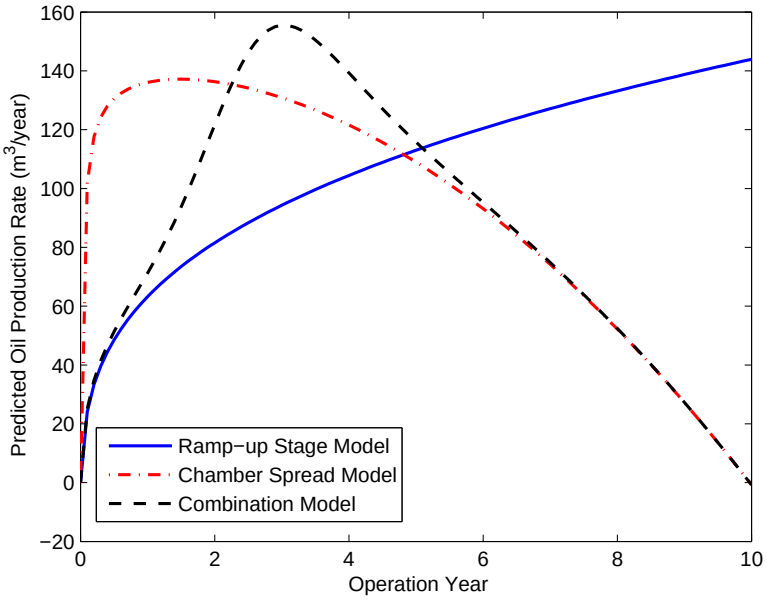

Figure 6.4: Predicted oil production rate

Butler et al. [96] also provided simple formulas for estimation of the oil-steam ratio as follows:

$$osr = \frac{1769\varphi\Delta S_0}{(T_S - T_R)\left(1 + 0.558\sqrt{t/h^2}\right)} \tag{6.20}$$

where the unit of t is day, $T_S = 467°F$ is the temperature in the steam chamber, and $T_R = 76°F$ is the initial temperature. SOR is calculated by taking the inverse of the oil-steam ratio and the plot of the predicted SOR is shown in Figure 6.5.

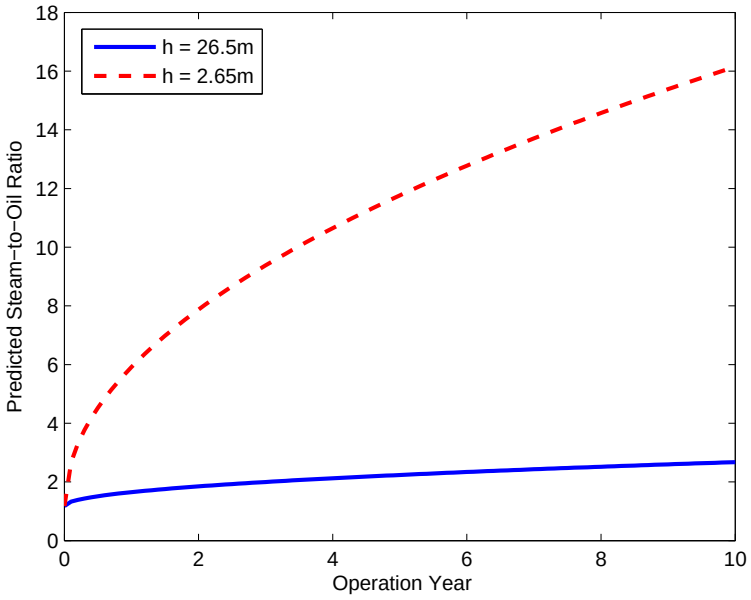

Figure 6.5: Predicted SOR

It can be observed that the thinner reservoir has larger SOR since the vertical heat losses from the heat input are larger. And as stated before, in chamber spread stage as the chamber widens heat losses increases, which leads to larger SOR.

The WOR used in this chapter is obtained from the open source of the company shown in reference [94].

6.3.1.6 Simulation Results

In this chapter, the total time horizon is assumed to be 15 years ($H = 15$) and the number of well pads is three. They are assumed to start working at the beginning of the time horizon, at the fourth year and at the sixth year, respectively. The blow down stage of the three pads starts in the seventh year, the tenth year and the twelfth year, respectively, which means that the steam injection stops in the given years since the predicted oil production rate declines more than 50% of the maximum rate. The profile of the oil production capability is predicted using (6.17). The problem is formulated as a mixed integer linear programming (MILP) problem and is sovled in GAMS 23.9 using solver CPLEX. The optimal objective

value is obtained as 125872.56.

Figure 6.6 displays the oil production rate, steam injection rate and the produced water rate in each year of each well pad. It can be observed that the oil production rate reaches the capacity. The steam injection to the three well pads stops in the seventh year, tenth year and twelfth year as given, respectively.

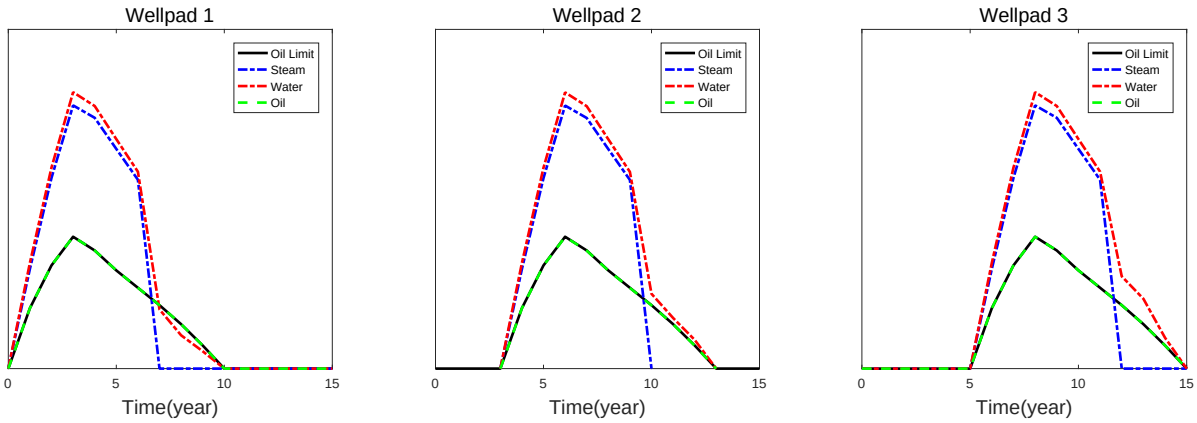

Figure 6.6: Oil production, steam injection and production water for each well pad

Figure 6.7 shows the statuses as well as the working conditions of the steam generators. The black dash lines are the upper and lower bounds of the steam generators. It can be seen that after twelfth year, the statuses of all the steam generators are off since the steam injection stops for all the three pads. Furthermore, it is not necessary for all the steam generators to be working all the time and the statuses of them can be optimized. As determined only from the sixth year to the ninth year, all the three well pads work, so most of the steam generators are open during these years. However, at the beginning and the end of the time horizon, there is only one well pad working and only a few steam generators are operational.

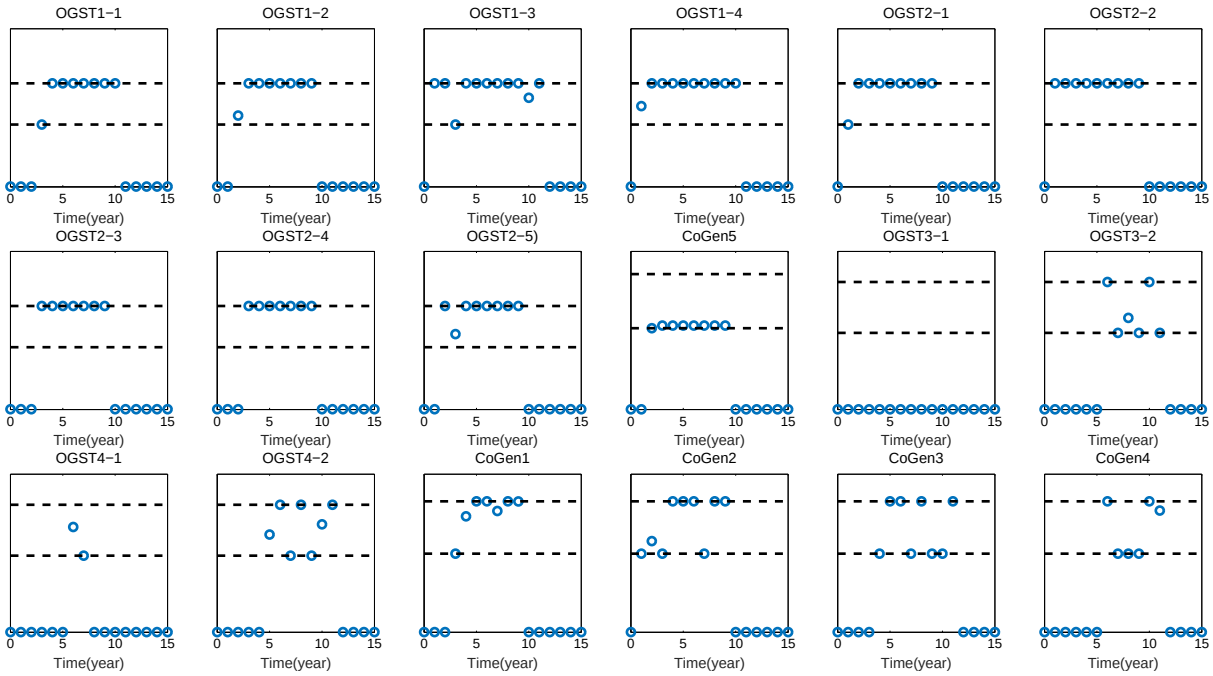

Figure 6.7: Statuses of steam generators

6.3.2 Optimization with Uncertainty

In the deterministic formulation, the capacity of the oil production rate is predicted using formulas which rely on the conditions in the reservoir. These conditions may not be satisfied perfectly during the operations. Moreover, the shape factor of the rising steam chamber γ is calculated by curve fitting in the formulas [98] which also involves uncertainties. In this section, instead of taking deterministic values, the capacity of oil production rate is considered to contain uncertainties. The uncertainties are quantified using joint chance constraints by setting a desired level of the probability of satisfying the constraints.

6.3.2.1 Formulation and Solution of Uncertain Optimization Problem

The capacity of the oil production rate is assumed to vary 5% around the nominal value, i.e., $Oil_i^{up,t} = \hat{O}il_i^{up,t} + 0.05\hat{O}il_i^{up,t}\xi$, where $\xi \in [-1 \quad 1]$ is uniformly distributed. Three JCCs are formulated corresponding to each well pad during the time when the well pad is working,

which is shown as follows:

For i representing the first well pad

$$P\left(0.9 \times Oil_i^{up,t} \leq Oil_i^t \leq Oil_i^{up,t}, t = 1, ..., 9\right) \geq 1 - \varepsilon \tag{6.21}$$

For i representing the second well pad

$$P\left(0.9 \times Oil_i^{up,t} \leq Oil_i^t \leq Oil_i^{up,t}, t = 4, ..., 12\right) \geq 1 - \varepsilon \tag{6.22}$$

For i representing the third well pad

$$P\left(0.9 \times Oil_i^{up,t} \leq Oil_i^t \leq Oil_i^{up,t}, t = 6, ..., 14\right) \geq 1 - \varepsilon \tag{6.23}$$

The JCCs are approximated using the proposed robust optimization framework in Chapter 3. The box type uncertainty set is utilized since it leads to linear form in the optimization formulation. The violation for each set of JCC is set as 0.1 in this section. The approximated optimization formulation is solved using the proposed two-layer algorithm. The weights for each constraints are all set as 1, and the uncertainty set size is optimized in the inner level to ensure that the probability of all the constraints being satisfied simultaneously is reached. One slight modification is made to optimize the variable controlling the upper bound of the approximations in Chapter 3. In Chapter 3, the variable is optimized in the outer using golden section algorithm. However, due to the exsitence of three sets of JCC in this section, the golden section method cannot be used and the genetic algorithm (GA) is utilized instead, since the objective of this problem is a black-box function.

6.3.2.2 Simulation Results

Using robust optimization based on box type uncertainty set to approximate the JCCs, the formulated optimization problem is still MILP. The robust optimization problem is solved

in GAMS 23.9 using solver CPLEX. The two-layer algorithm to optimizing the set size and the variable controlling the upper bound of approximation is implemented in MATLAB.

First, it is assumed that the uncertainties are mutually independent. Using GA, the optimal values for the upper bound of the approximation of the three sets of JCC are obtained as 0.8439, 0.6325, and 0.6969, respectively. Figure 6.8 shows the evolution of the objective value from GA, since the GA function in MATLAB is implemented for minimizing problem and the problem in this section is maximization, a negative sign is added to the objective function. It can be observed that GA converges to the best value of -119861, which means that the optimal objective value of the long term planning problem considering uncertainty in oil production capacity is 119861. The value is smaller than the one (125872.56) obtained from the deterministic formulation in Section 6.3.1.

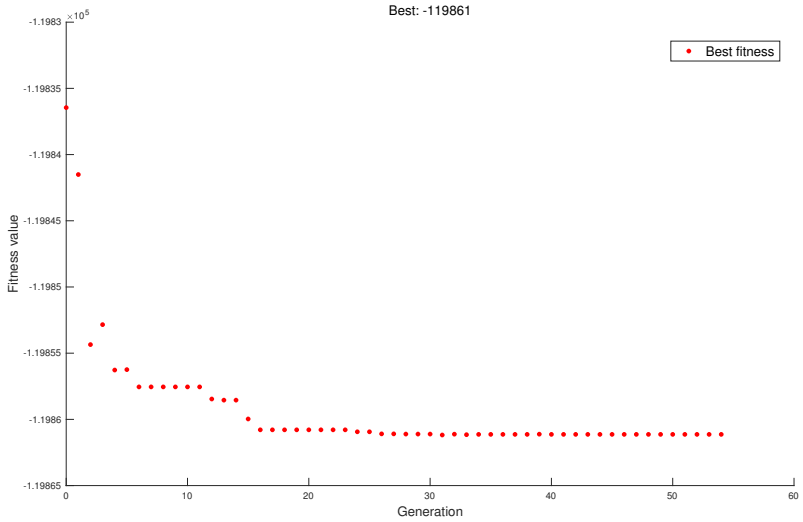

Figure 6.8: Objective value evolution in GA

With the fixed optimal value of variables that control the upper bound of the approximation, the set size is optimized using the iterative algorithm and Figure 6.9. (a), (b), (c) plots the evolution of objective value, probability of satisfaction, and set size, respectively. In some iterations, the robust optimization is infeasible and the objective is 0 which is not plotted in (a), and the corresponding probability of satisfaction is forced to be 1 in (b). Since the three JCCs have the same constraints inside except for the time index, the probability

of satisfaction and set size change are the same, and only one of the lines is plotted in (b) and (c).

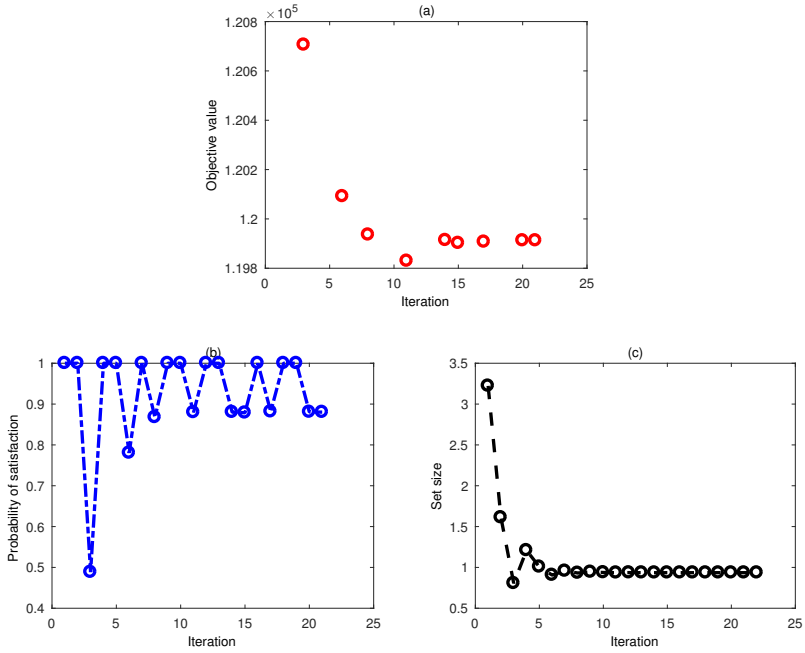

Figure 6.9: Prcedure for optimal set size selection

Similar as in Section 6.3.1, the oil rate production rate, steam injection rate and the produced water rate in each year of each well pad are displayed in Figure 6.10. The three black solid lines represent the oil production capacity with lower bound of perturbation, nominal value, and upper bound of perturbation. Since robust optimization always considers the worst case, the real oil production reaches the lowest level within the perturbation, i.e., $\hat{O}il_i^{up,t} - 0.05\hat{O}il_i^{up,t}$, which is the reason that the optimal objective of the optimization problem with uncertainty is worse than the one of the deterministic formulation.

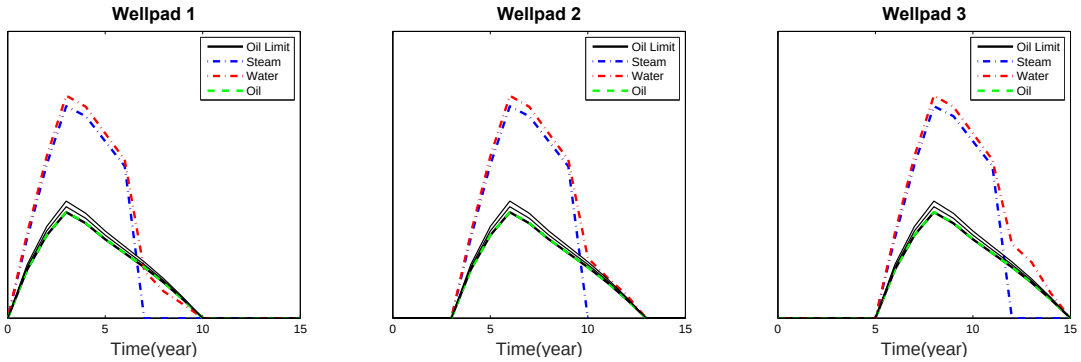

Figure 6.10: Oil production, steam injection and water production for each well pad

Figure 6.11 shows the statuses and the working conditions of the steam generators.

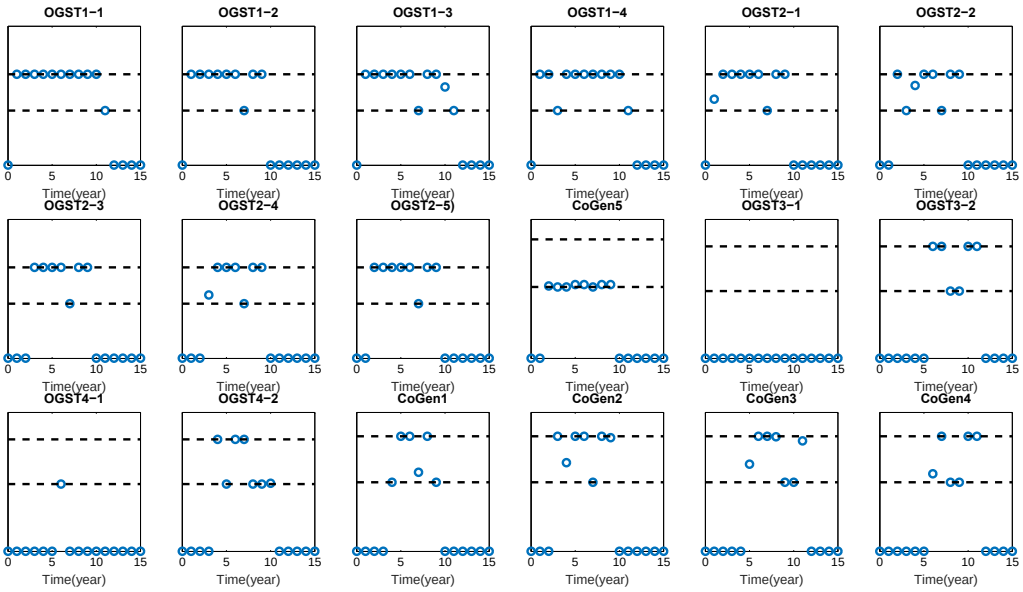

Figure 6.11: Statuses of steam generators

Second, it is assumed that there are correlations between the uncertainties and all the correlation coefficients are assumed to be 0.5. Using GA, the optimal values for the upper bound of the approximation of the three sets of JCC are obtained as 0.6321, 0.5997, and 0.6332, respectively. The optimal objective is 119947 which is a little larger than the one obtained from the independent uncertainty case (119861).

The probability of JCC satisfaction is estimated with Monte Carlo sampling technique

with 100,000 samples using Equation (3.34). Different assumptions of the correlation between the uncertainties are considered and the results are summarized in Table 6.2.

Table 6.2: Comparison of the probability of JCC satisfaction

Optimization Formulation	Correlation coefficients used for calculation of simulated probability					
	0 (independent)			0.5 (correlated)		
RO with correlation	0.8481	0.8411	0.8461	0.8925	0.8910	0.8926
RO without correlation	0.8920	0.8955	0.8886	0.9223	0.9230	0.9209
Deterministic	0.0021	0.0021	0.0017	0.1004	0.0996	0.1013

It can be observed that, for both assumptions of the correlation between the uncertainties the results obtained from deterministic formulation have very low probabilities of constraints satisfaction. If we assume that the uncertainties are mutually independent, the RO formulation without considering correlation can reach the desired level of probability of satisfaction (0.9), while with the solution from the RO formulation considering correlations, the joint probabilities of satisfaction are lower than the desired level. If the correlation coefficients between uncertainties are assumed to be 0.5, considering the exact correlations in RO formulation leads to the solution that satisfies the desired probability of constraints satisfaction. The joint probabilities of satisfaction exceed the desired level with the solution of RO formulation without considering correlations. It can be concluded that in this application, if there is no correlations in the uncertainties, then considering correlations in RO formulation will lead to the solutions that violate the probability of satisfaction. However, if there are correlations in the uncertainties and without considering them in RO formulation will make the solutions more conservative, which can also be observed from the objective value (119947 from RO with correlations and 119861 from RO without correlations). Thus, if the information of the correlations is not available it is safer to not incorporate correlations in RO formulation, while if the correlations are known, considering them in RO formulation can provide better results.

6.4 Conclusion

In this chapter, the economic optimization of steam generation and water distribution for SAGD process is studied. In the long term planning problem, the optimal distribution of the steam to the well pads which start working at different years is considered. The oil production rate capacity and SOR are predicted using empirical formulas from the literature. Due to the inaccuracy of the conditions in the reservoir, the predicted capacity may contain uncertainty. For each well pads, one set of JCC is constructed to model the uncertainty and there are three sets of JCCs in total. The proposed algorithm in Chapter 3 is applied to approximate JCC into tractable forms and the two-layer algorithm is used to improve the performance of the robust optimization approximation. The uncertainties are assumed into two cases: mutually independent and with correlation coefficients 0.5. The results from the RO formulation with and without considering correlations are compared with the aid of simulated joint probability of satisfaction. It is concluded that if the information of correlations is not available, it is safer to not consider them in RO formulation, while if it is available, it is better to incorporate the information in RO formulation.

Chapter 7

Concluding Remarks and Future Works

In this chapter, the conclusions from the previous chapters of the thesis are briefly summarized. Moreover, possible improvements of the methods discussed in this thesis and future works are introduced.

7.1 Concluding Remarks

With the aid of the development of modern computers, the collection and processing of a great volume of data become possible. Various information can be extracted from the data for multiple use including process control, optimization, process monitoring and process economic evaluation. Great benefits can be achieved by considering more information in the industrial applications. However, process data with errors will lead to inaccurate information of the process and using data with errors is hazardous for operation of the system.

Chapter 2 provides a unified framework based on Bayesian inference to detect the gross errors and reconcile the data to produce cleaned data. In this framework, gross errors are detected, the magnitudes of the gross errors and the covariance of random errors are estimated and the data are reconciled to satisfy the process model, e.g., mass balance and/or

energy balance. The framework is combined with serial gross error identification strategy with slight modifications. Instead of using statistical test, the probability ratio of a measurement containing gross error and not containing gross error is compared to generate a set of gross error candidates. The strategy can improve the effectiveness of the gross error detection technique. The developed framework is suitable for both linear and nonlinear system models, and the algorithms are tested using multiple examples. It can be observed that if there is only one gross error in the network, the proposed framework without the serial strategy is already efficient to detect the gross errors. While for multiple gross errors, due to the increasing of complexity in the network, the modified serial identification strategy is necessary and can be effective to detect the gross errors.

Optimization is a powerful technique to help operate the process, especially with some economic targets. Data is important in the optimization problems, for instance, process data can be used to build models for the optimization and the economic data such as the price and tax can be used to formulate the objective or the requirement in the optimization framework. Due to the nature of measured data, uncertainty inevitably exists in the data. The uncertain data may make the deterministic optimization solution fail since it can be suboptimal or infeasible due to the ignorance of the uncertainty in the data. In this thesis, optimization with uncertainty has been studied in various chapters.

Chapter 3 uses joint chance constraints to model the uncertainty in optimization problems and investigates the robust optimization approximation method for solving joint chance constrained problems. Different formulations of uncertainty set induced robust counterpart optimization are derived based on different types of the uncertainty set. To avoid a worst-case scenario approximation and improve the objective value by reaching the desired probability level of constraints satisfaction, a two-layer algorithm is implemented. In the inner level, an iterative method is used for the optimally selection of the uncertainty set size, whose goal is to select the minimum possible set size that leads to the target probability of constraint satisfaction. In the outer layer, the parameter used for upper bounding the indicator

function is adjusted by a golden section method to improve the quality of the robust optimization approximation by optimizing the objective value. The advantage and effectiveness of the proposed method has been demonstrated using multiple examples including a norm optimization problem and a transportation problem. The robust optimization problem is tractable and the computational complexity only relies on the solution of multiple tractable robust optimization problems. The probability information is only used for calculating the simulated probability of satisfaction. Thus, the algorithm is applicable to general distributions of the uncertainty. Furthermore, the proposed formulations can be applied to linear JCC with both continuous and discrete variables.

In Chapter 4, correlations in uncertainties are considered for the design of uncertainty set. Robust optimization formulations are derived based on different types of uncertain set: box, ellipsoidal, polyhedral, interval+ellipsoidal, and interval+polyhedral. Numerical examples are studied with different correlation levels to reveal the importance of incorporating correlation information into uncertainty set design. A production planning example is used to test the proposed method. Both the numerical studies and application example demonstrate the advantage of modeling correlations in robust optimization framework. That is, less conservative solution can be obtained when more accurate correlation is incorporated into the robust optimization framework. Then, in Section 4.5, a brief study of RO formulations for multiple constraints with correlated uncertainties is considered. The RO formulations are compared based on "constraint-wise" and "global" uncertainty set. Simple numerical examples are used to test the results with different correlation conditions between uncertainties. The brief study can still give a hint on how to select a better uncertainty set in RO formulation.

In Chapter 5, nonlinear process design problems are studied and a novel nonlinear robust optimization framework is developed. The robust counterpart formulation is derived based on a general type of uncertainty set defined by the intersection of two uncertainty sets. Three cases of optimization problems are considered including the optimization problems with

only inequality constraints as well as the problems with equality constraints associated with uncertain parameter. Furthermore, the control variables which can be manipulated under the realizations of uncertainty are also considered in the robust optimization formulation based on an affine relationship between the control variables and the uncertain parameters. In order to deal with uncertainty with larger perturbation, "piecewise" linearization is taken around multiple realizations of the uncertain parameter and an iterative algorithm is applied to select appropriate points for linearization. Three application examples including the optimal design of a heat exchanger system, a reactor-separator system and a reactor-cooler system are studied to demonstrate the effectiveness of the proposed methodology. The proposed method has higher level of robustness than the "single-point" linearization method. In addition, while the results have the similar robustness level, the proposed method leads to less conservative robust solution. This is because the "single-point" linearization utilizes first Taylor expansion around only one point and the performance of this method is only good when the perturbation of the uncertainty is small. Comparing the results obtained from the formulation considering control variables and that obtained from not considering control variables, it can be demonstrated that with consideration of the control variable, the solutions become less conservative.

In Chapter 6, the economic optimization of steam generation and water distribution is studied for SAGD process. The long term planning problem is considered to optimally distribute the steam to the well pads starting at different years. The oil production rate capacity is predicted using empirical formulas from literature. Due to the inaccuracy of the conditions in the reservoir, the predicted capacity may contain uncertainty, and multiple sets of JCC are used to model the uncertainty for each well pads. The proposed algorithm in Chapter 3 is applied to approximate JCC into tractable forms and the two-layer algorithm is used to improve the performance of the robust optimization approximation. Since there are multiple sets of JCC, when the outer layer optimizes the variable controlling the upper bound of the approximation, golden section is no longer available. Genetic algorithm is

used instead since it can handle multivariate optimization problem with black-box objective function.

7.2 Future Works

7.2.1 Data Rectification

In Figure 1.1, it can be seen that change point detection also belongs to data rectification since it acts as data segmentation to divide the data into different parts according to different steady states. The formulation is similar to the gross error detection and data reconciliation work (without indicator for gross errors) and it can also be solved using Bayesian inference technique. In practice, it is meaningful to assume the number of changes is unknown and needs to be determined.

7.2.2 Optimization with Uncertainty

In Chapter 3, the influence of the weights of each constraints on the quality of robust solution has been studied by comparing the results obtained using different combinations of the weights. However, it did not provide an algorithm to select the weights. The idea of risk allocation can be borrowed to optimally determine the weights and the quality of robust solutions can be further improved.

The uncertainty sets used in Chapter 3-6 have norm induced form. The uncertainty sets are symmetric and have simple form which has little room to incorporate more information of the uncertainty. Sometimes, the distribution of the uncertainty may not have regular shapes, e.g., mixture Gaussian distribution. In this case, asymmetric uncertainty set is useful to better capture the shape of the uncertain region. Due to the availability of historical data, the uncertainty set can be learnt from the process data.

7.2.3 Optimization Application in SAGD

In Chapter 6, the model for the well pads are built using simple linear model based on SOR and WOR. A more accurate model is needed to model the behaviour of the well pads to make the optimization result more reliable. Furthermore, the starting and ending time of different well pads are assumed to be known in Chapter 6. To be more practical, the starting and ending point should be considered as variables and can be determined under the optimization framework.

Large amount of historical data is available in practice, and the data can be used to built data-driven models for different units including water treatment plants and steam generators. The data-based model can be more accurate than the models used in Chapter 6, especially when the units have nonlinear behaviour. If the data-driven model has a nonlinear structure, and if the uncertainty in parameter estimation is considered, the proposed method in Chapter 5 can be applied.

Bibliography

[1] Narasimhan S, Cornelius J. Data reconciliation and gross error detection: An intelligent use of process data. Gulf Professional Publishing. 1999.

[2] Mah RSH, Mah RSH. Chemical process structures and information flows. Boston: Butterworths. 1990.

[3] Reilly PM, Carpani RE. Application of statistical theory of adjustment to material balances. In: Proceedings of the 13th Canadian Chemical Engineering Conference. Montreal, Quebec. 1963.

[4] Mah RSH, Tamhane AC. Detection of gross errors in process data. AIChE Journal. 1982;28(5):828-830.

[5] Crowe CM, Campos YA, Hrymak A. Reconciliation of process flow rates by matrix projection. Part I: linear case. AIChE Journal. 1983;29(6):881-888.

[6] Mah RSH, Stanley GM, Downing DM. Reconcillation and rectification of process flow and inventory data. Industrial and Engineering Chemistry Process Design and Development. 1976;15(1):175-183.

[7] Narasimhan S, Mah RSH. Generalized likelihood ratio method for gross error identification. AIChE Journal. 1987;33(9):1514-1521.

[8] Rollins DK, Davis JF. Unbiased estimation of gross errors in process measurements. AIChE journal. 1992;38(4):563-572.

[9] Tong H, Crowe CM. Detection of gross erros in data reconciliation by principal component analysis. AIChE Journal. 1995;41(7):1712-1722.

[10] Ripps DL. Adjustment of experimental data. In Chem. Eng. Prog. Symp. Ser. 1965;61(8).

[11] Serth RW, Heenan WA. Gross error detection and data reconciliation in steam metering systems. AIChE Journal. 1986;32(5):733-742.

[12] Rosenberg J, Mah RSH, Iordache C. Evaluation of schemes for detecting and identifying gross errors in process data. Industrial and Engineering Chemistry Research. 1987;26(3):555-564.

[13] Keller JY, Darouach M, Krzakala G. Fault detection of multiple biases or process leaks in linear steady state systems. Computers and chemical engineering. 1994;18(10):1001-1004.

[14] Sáchez M, Romagnoli J, Jiang Q, Bagajewicz M. Simultaneous estimation of biases and leaks in process plants. Computers and chemical engineering. 1999;23(7):841-857.

[15] Sáchez M, Romagnoli J. Use of orthogonal transformations in data classification-reconciliation. Computers and chemical engineering. 1996;20(5):483-493.

[16] Tjoa IB, Biegler LT. Simultaneous strategies for data reconciliation and gross error detection of nonlinear systems. Computers and chemical engineering. 1991;15(10):679-690.

[17] Soderstrom TA, Himmelblau DM, Edgar TF. A mixed integer optimization approach for simultaneous data reconciliation and identification of measurement bias. Control Engineering Practice. 2001;9(8):869-876.

[18] Han SP. A globally convergent method for nonlinear programming. Journal of optimization theory and appoications. 1977;22(3):297-309

[19] Powell MJ. A fast algorithm for nonlinearly constrained optimization calculations. In Numerical analysis. Springer BErlin Heidelberg. 1978:144-157

[20] Chen HS, Stadtherr MA. Enhancements of the Han-Powell method for sucdessive quadratic programming. Comuputers and chemical engineering. 1984;8(3):229-234

[21] Charnes A, Cooper WW, Symonds GH. Cost horizons and certainty equivalents: an approach to stochastic programming of heating oil. Management Science. 1958;4(3):235-263.

[22] Alizadeh F, Goldfarb D. Second-order cone programming. Mathematical programming. 2003;95(1):3-51

[23] Lagoa CM. On the convexity of probabilistically constrained linear programs. Proceedings of the 38th IEEE Conference on Decision and Control. 1999;Vol.1:516-521.

[24] Calafiore GC, Campi MC. The scenario approach to robust control design.IEEE Transactions on Automatic Control. 2006;51(5):742-753

[25] Nemirovski A, Shapiro A. Convex approximations of chance constrained programs. SIAM Journal on Optimization. 2006;17(4):969-996

[26] Ahmed S, Shapiro A. Solving chance-constrained stochastic programs via sampling and integer programming. Tutorials in Operations Research,(Z.-L. Chen and S. Raghavan, eds.), INFORMS. 2008.

[27] Prkopa A. Stochastic programming.Springer. 1995.

[28] Luedtke JR. Integer programming approaches for some non-convex and stochastic optimization problems, Doctoral dissertation, Georgia Institute of Technology. 2007.

[29] Nemirovski A, Shapiro A. Scenario approximations of chance constraints.In Probabilistic and randomized methods for design under uncertainty, Springer, London. 2006:3-47.

[30] Pagnoncelli BK, Ahmed S. Shapiro, A. Sample average approximation method for chance constrained programming: theory and applications. Journal of optimization theory and applications. 2009;142(2):399-416.

[31] Luedtke J, Ahmed S. A sample approximation approach for optimization with probabilistic constraints. SIAM Journal on Optimization. 2008;19(2):674-699.

[32] Atlason J, Epelman MA, Henderson SG. Optimizing call center staffing using simulation and analytic center cutting-plane methods. Management Science. 2008;54(2):295-309.

[33] Chebyshev PL. On mean values. Complete collected works. 1867;2.

[34] Bernstein SN. On certain modifications of Chebyshevsinequality. DokladyAkademiiNauk SSSR. 1937;17(6):275-277.

[35] Hoeffding W. Probability inequalities for sums of bounded random variables. Journal of the American statistical association. 1963;58(301):13-30.

[36] Hong LJ, Yang Y, Zhang L. Sequential convex approximations to joint chance constrained programs: A Monte Carlo approach. Operations Research. 2011;59(3):617-630.

[37] Soyster AL. Technical note–convex programming with set-inclusive constraints and applications to inexact linear programming.Operations research. 1973;21(5):1154-1157.

[38] El Ghaoui L, Lebret H. Robust solutions to least-squares problems with uncertain data. SIAM Journal on Matrix Analysis and Applications. 1997;18(4):1035-1064.

[39] El Ghaoui L, Oustry F, Lebret H. Robust solutions to uncertain semidefinite programs. SIAM Journal on Optimization. 1998;9(1):33-52.

[40] Ben-Tal A, Nemirovski A. Robust convex optimization. Math. Oper Res. 1998;23(4):769-805.

[41] Ben-Tal A, Nemirovski A. Robust solutions of uncertain linear programs. Operations research letters. 1999;25(1):1-13.

[42] Ben-Tal A, Nemirovski A. Robust solutions of linear programming problems contaminated with uncertain data. Mathematical programming. 2000;88(3):411-424.

[43] Ben-Tal A, Nemirovski A. On polyhedral approximations of the second-order cone. Math Oper Res. 2001;26(2):193-205.

[44] Ben-Tal A, Goryashko A, Guslitzer E, Nemirovski A. Adjustable robust solutions of uncertain linear programs. Math Program. 2004;99(2):351-76.

[45] Bertsimas D, Sim M. The price of robustness. Operations research, 2004;52(1):35-53.

[46] Bertsimas D, Pachamanova D, Sim M. Robust linear optimization under general norms. Oper Res Lett. 2004;32(6):510-6.

[47] Chen X, Sim M, Sun P. A robust optimization perspective on stochastic programming. Oper Res. 2007;55(6):1058-71.

[48] Li Z, Ding R, Floudas CA. A comparative theoretical and computational study on robust counterpart optimization: I. Robust linear optimization and robust mixed integer linear optimization. Industrial & engineering chemistry research. 2011;50(18):10567-10603.

[49] Chen W, Sim M, Sun J, Teo CP. From CVaR to uncertainty set: Implications in joint chance-constrained optimization. Operations research. 2010;58(2):470-485.

[50] Chen, W, Sim M. Goal-driven optimization. Operations Research. 2009;57(2):342-357.

[51] Li Z, Ierapetritou MG. Robust optimization for process scheduling under uncertainty. Ind Eng Chem Res. 2008;47(12):4148-57.

[52] Lin X, Janak SL, Floudas CA. A new robust optimization approach for scheduling under uncertainty: I. Bounded uncertainty. Computers & chemical engineering. 2004;28(6):1069-1085.

[53] Janak SL, Lin X, Floudas CA. A new robust optimization approach for scheduling under uncertainty: II. Uncertainty with known probability distribution. Computers & chemical engineering. 2007;31(3):171-195.

[54] Verderame PM, Floudas CA. Operational planning of large-scale industrial batch plants under demand due date and amount uncertainty. I. Robust optimization framework. Ind Eng Chem Res. 2009;48(15):7214-31.

[55] Li Z, Tang Q, Floudas CA. A comparative theoretical and computational study on robust counterpart optimization: II. Probabilistic guarantees on constraint satisfaction. Industrial & engineering chemistry research. 2012;51(19):6769-6788.

[56] Li Z, Floudas CA. A Comparative Theoretical and Computational Study on Robust Counterpart Optimization: III. Improving the Quality of Robust Solutions. Industrial & Engineering Chemistry Research. 2014;53(33):13112-13124.

[57] Li Z, Li Z. Optimal Robust Optimization Approximation for Chance Constrained Optimization Problem. Computers & Chemical Engineering. 2015;74:89-99.

[58] Ben-Tal A, Nemirovski A, Roos C. Robust solutions of uncertain quadratic and conic-quadratic problems. SIAM Journal on Optimization. 2002;13(2):535-560.

[59] Ben-Tal A, El Ghaoui L, Lebret H. Robust semidefinite programming. Handbook on Semidefinite Programming. 1998;27.

[60] Diehl M, Bock HG, Kostina E. An approximation technique for robust nonlinear optimization. Mathematical Programming. 2006;107(1):213-230.

[61] Zhang Y. General robust-optimization formulation for nonlinear programming. Journal of Optimization Theory and Applications. 2007;132(1):111-124.

[62] Houska B, Diehl M. Nonlinear robust optimization via sequential convex bilevel programming. Mathematical Programming. 2013;142(1-2):539-577.

[63] Ben-Tal A, Den Hertog D, Vial, JP. Deriving robust counterparts of nonlinear uncertain inequalities. Mathematical programming. 2015;149(1-2):265-299.

[64] MacKay DJC. Bayesian interpolation. Neural computation. 1992;4(3):415-447.

[65] MacKay DJC. Probable networks and plausible predictions-a review of practical Bayesian methods for supervised neural networks. Network: Computation in Neural Systems. 1995;6(3):469-505.

[66] Molina R, Vega M, Mateos J, Katsaggelos AK. Variational posterior distribution approximation in Bayesian super resolution reconstruction of multispectral images. Applied and Computational Harmonic Analysis. 2008;24(2):251-267.

[67] Galatsanos NP, Mesarovic VZ, Molina R, Katsaggelos AK. Hierarchical Bayesian image restoration from partially known blurs. Image Processing, IEEE Transactions on. 2000;9(10):1784-1797.

[68] Kwok JTY. The evidence framework applied to support vector machines. Neural Networks, IEEE Transactions on. 2000;11(5):1162-1173.

[69] Suykens JAK, Gestel TV, Brabanter JD, Moor BD, Vandewalle J. Least Squares Support Vector Machines. River Edge, NJ: World Scientific. 2002.

[70] Khatibisepehr S, Huang B. A Bayesian approach to robust process identification with ARX models. AIChE Journal. 2013;59(3):845-859.

[71] Jiang Q, Bagajewicz MJ. On a strategy of serial identification with collective compensation for multiple gross error estimation in linear steady-state reconciliation. Industrial and engineering chemistry research. 1999;38(5):2119-2128.

[72] Iordache C, Mah RSH, Tamhane AC. Performance studies of the measurement test for detection of gross errors in process data. AIChE Journal. 1985;31(7):1187-1201.

[73] Bagajewicz MJ, Jiang Q. Gross error modeling and detection in plant linear dynamic reconciliation. Computers and chemical engineering. 1998;22(12):1789-1809.

[74] Bagajewicz MJ, Jiang Q. A mixed integer linear programming-based technique for the estimation of multiple gross errors in process measurements. Chemical Engineering Communications. 2000;177(1):139-155.

[75] Pai CCD, Fisher GD. Application of Broyden's method to reconciliation of nonlinearly constrained data. AIChE Journal. 1988;34:873-876

[76] Tamhane AC, Mah RSH. Data reconciliation and gross error detection in chemical process networks. Technometrics. 1985;27(4):409-422

[77] Crowe CM. Reconciliation of process flow rates by matrix projection. Part II: the nonlinear case. AIChE Journal. 1986;32(4):616-623

[78] Swartz CLE. Data reconciliation for generalized flowsheet applications. In proceedings of the paper presented at American Chemical Society National Meeting, Dallas, TX

[79] Meilijson I, Ndas A. Convex majorization with an application to the length of critical paths. Journal of Applied Probability. 1979;671-677.

[80] Luedtke J, Ahmed S, Nemhauser GL. An integer programming approach for linear programs with probabilistic constraints. Mathematical Programming. 2010;122(2):247-272.

[81] Ravindran AR. Operations Research Methodologies. New York: CRC Press; 2008.

[82] Zhang Y, Monder D, Forbes JF. Real-time optimization under parametric uncertainty: a probability constrained approach. Journal of Process control. 2002;12(3):373-389.

[83] Zhang Q, Morari MF, Grossmann IE, Sundaramoorthy A, Pinto JM. An adjustable robust optimization approach to scheduling of continuous industrial processes providing interruptible load. Computers & Chemical Engineering. 2016;86:106-119.

[84] Lappas NH, Gounaris, CE. Multi-stage Adjustable Robust Optimization for Process Scheduling under Uncertainty. AIChE Journal. 2016;62(5):1646-1667.

[85] Zhang Y. General robust-optimization formulation for nonlinear programming. Journal of Optimization Theory and Applications. 2007;132(1):111-124.

[86] Halemane KP, Grossmann IE. Optimal process design under uncertainty. AIChE Journal. 1983;29(3):425-433.

[87] Swaney RE, Grossmann IE. An index for operational flexibility in chemical process design. Part I: Formulation and theory. AIChE Journal. 1985;31(4):621-630.

[88] Swaney RE, Grossmann IE. An index for operational flexibility in chemical process design. Part II: Computational algorithms. AIChE Journal. 1985;31(4):631-641.

[89] Grossmann IE, Floudas CA. Active constraint strategy for flexibility analysis in chemical processes. Computers & Chemical Engineering. 1987;11(6):675-693.

[90] Floudas CA, Gümüş ZH, Ierapetritou MG. Global optimization in design under uncertainty: feasibility test and flexibility index problems. Industrial & Engineering Chemistry Research. 2001;40(20):4267-4282.

[91] Andrei N. Nonlinear Optimization Applications Using the GAMS Technology. Springer,2013

[92] Rooney WC, Biegler LT. Design for model parameter uncertainty using nonlinear confidence regions. AIChE Journal. 2001;47(8):1794-1804.

[93] Hale ET, Zhang Y. Case studies for a first-order robust nonlinear programming formulation. Journal of Optimization Theory and Applications. 2007;134(1):27-45.

[94] https://www.cenovus.com/operations/docs/christinalake/phase-h/1a/1a-5.pdf

[95] https://www.cenovus.com/invest/docs/FC-Field-Tour-Handout.pdf

[96] Butler M. GravDrain's Black Book: Thermal Recovery of Oil and Bitumen. Calgary: GravDrain Inc., 2000

[97] Cardwell WT, Parsons RL. Gravity drainage theory. Petrol Trans AIME. 1949;179:199-211.

[98] Guo J, Zan C, Ma DS, Shi L. Oil production rate predictions for steam assisted gravity drainage based on high-pressure experiments. Sci.China Technol.Sci. 2013;56(2):324-334.

[99] Shahandeh H, Rahim S, Li Z. Strategic optimization of the oil sands development with SAGD: Drainage area arrangement and development planning. Journal of Petroleum Science and Engineering. 2016;137:172-184.